ALMA MATER STUDIORUM - UNIVERSITÀ DI BOLOGNA

SCUOLA DI INGEGNERIA E ARCHITETTURA

CIVIL, CHEMICAL, ENVIRONMENTAL AND MATERIALS ENGINEERING DEPARTMENT

TWO YEAR MASTER IN CIVIL ENGINEERING

MASTER THESIS

EFFECT OF ACTIVE MINERAL OR HYDRATED LIME FILLERS ON AGEING AND MOISTURE OF BITUMINOUS MIXTURES

MSc CANDIDATE

Gianluca Guardigli

SUPERVISOR

Dr. Claudio Lantieri

CO-SUPERVISOR

Dr. Aikaterini Varveri

Dr. Ruxin Jing

Prof. Dr. Valeria Vignali

Academic Year 2018/2019

Session III

ABSTRACT

Bitumen aging has been recognized as one of the main reasons for the gradual deterioration of asphalt pavements. The hardening of the binder due to ageing leads to the embrittlement of the overall asphalt mixture and a greater susceptibility to traffic and damage caused by the environment. During the service life of pavement, the presence of moisture may accelerate this aging process. Damage from moisture or water in asphalt mixtures causes a loss of strength and durability and could increase in rigidity which leads to a more fragile behaviour of the materials causes the failure of the adhesive on the surface of the binder-aggregate and/or the cohesive failure inside the binder or mastics. The performance and mechanical behaviour of asphalt mixes are mainly dependent on the response of bituminous binders and mastics. The aging process of bitumen in the field is in fact not only a function of the type of bitumen itself, but rather, additional effects attributed to the mineral phase and the design parameters of the asphalt mixture have been identified.

This thesis attempts to provide a deeper understanding of the effect of mineral fillers on the aging of bitumen with and without the presence of moisture in the mixture. More specifically, a chemical and mechanical performance characterization of mineral fillers containing hydrated lime was carried out, deepening the issue of degradation and carbonation in limestone following oxidative aging. Six different mineral fillers have been used in this research; the fillers differed with respect to the amount of active hydrated lime. The mixtures of bitumen-mineral fillers were prepared according to a single design protocol. The resulting mastics together with the neat bitumen were subjected to accelerated aging in the laboratory by means of the Pressure Aging Vessel (PAV). The ageing protocols differed with regard to the gas that was used and the presence of humidity.

After each conditioning protocol, the samples were tested by using Dynamic Shear Rheometer (DSR) and Fourier Transfer Infrared spectrometer (FTIR). DSR was used to determine the rheological properties of materials, such as relaxation, fatigue and stiffness. In the post-processing analysis, the construction of master curves based on the time-temperature superposition principle allowed to describe the viscoelastic behaviour on a wide range of frequencies. FTIR was used to study the chemical composition of fillers and mastics before and after conditioning. The FTIR measurements were further used to develop a methodology that enables the quantification of the degradation of hydrated lime due to moisture and ageing effects.

The rheological evaluation of the resulting materials and the derivation of the aging indices revealed the overall capacity of the mineral fillers, especially with the presence of a not excessive quantity of hydrated lime in the mineral filler, to mitigate the aging of the bitumen incorporated in the mastics. This mitigation is also found in the presence of moisture.

The chemical investigation of the materials showed that, in effect, the chemically active mineral fillers catalysed or inhibited the oxidation of the bitumen incorporated in the mastics. On the other hand, the bitumen present in the mastic, adhering to the mineral filler and isolating it from direct contact with the carbon dioxide present in the air, reduced the carbonation of the hydrated lime in calcium carbonate, maintaining its chemical properties after conditioning.

Furthermore, it has been possible to affirm that there is a linear relationship between a rheology property (i.e. relaxation and crossover modulus) and a chemical property (carbonyl content) after aging of PAV, and that the presence of moisture does not affect this linear relationship.

CONTENTS

CHAPTER 1 – INTRODUCTION

1.1 PROBLEM DEFINITION

Road infrastructure is one of the most important assets of society and contributes to its economic growth and general prosperity. Considering the constant increase in traffic and the transfer of goods, it is of enormous importance that road networks ensure a safe, rapid and continuous flow of transport, and at the same time, their development and the necessary maintenance impose the minimum possible financial burden for the society. Key features of the highway infrastructures are the adequate design and a longer life of the asphalt mixture applied. If respected, these aspects lead to adequate performance of the asphalt pavement and involve minimal effort and maintenance costs to achieve the expected duration. From the beginning and throughout its duration, an asphalt pavement is exposed to extreme conditions, both environmental and traffic-related. As a result, there is a gradual deterioration of its constituent materials, which usually results, over time, in damage to the overall asphalt pavement. It is therefore essential to gain a deep understanding about the influence of these environmental and traffic related factors on the performance of asphalt pavements which will allow the development of adequate design guidelines and durable constituent materials. Numerous studies have studied the sensitivity of asphalt mixtures to the harmful effects of climatic conditions and traffic load. In particular, the aging processes that occur during the service life of asphalt pavements lead to mixtures that are more fragile over time and therefore subject to cracks. Various aging mechanisms are identified in the literature, in particular physical hardening, loss of volatile components and oxidation. Among all, oxidation is considered the most important aging process that can alter the chemical and rheological properties of bitumen. The aging of bitumen occurs from the beginning in the production of the asphalt mixture and in the construction of the asphalt pavement and develops continuously during its service life in the field. Oxygen, moisture, extreme temperatures and ultraviolet (UV) radiation are some of the factors that significantly affect the aging of bitumen. A direct result of the process is the gradual change over time of the physico-chemical properties of bitumen, which leads to a rigid and fragile material. As a result, the overall brittle of the asphalt mixture increases. Although this may be useful with regard to resistance to certain modes of failure (eg rutting), the resulting embrittlement implies a high susceptibility to fatigue failure, thermal induction failure, moisture damage and loss of stones or cracks. Oxidative aging is a diffusion-driven phenomenon, which occurs due to photo oxidation and

thermal reaction between the components of bitumen and atmospheric oxygen. Oxygen diffuses into the bitumen, changes the chemical characteristics of the bitumen and, consequently, influences its physical properties. In general, the diffusion phenomenon is driven by internal thermal energy and is influenced by several parameters. A further fundamental element that will be analyzed, as it involves a loss of bituminous binder performance is the diffusion of moisture, which can influence the rheological and chemical properties of different types of bituminous binders (mastics). The intrusion of water into asphalt pavements is one of the main processes that reduce performance and reduce the life of the system. The complex mechanical response of the pavements is governed by the properties of asphalt mastics and substantially depends on the properties of the filler and the way they interact with the bitumen.

1.2 RESEARCH QUESTION

The following study therefore aims to study the chemical and rheological properties of asphalt mastics, composed by mineral filler with active components and bitumen and subjected to aging and moisture.

In particular, fillers with various percentages of hydrated lime were used, resulting to mastics with different chemical characteristics. A chemical study exclusively on fillers is performed to better understand the carbonation phenomena of hydrated lime following aging protocols.

A rheological related analysis is aimed at defining the performance increases of the bituminous mixtures containing mineral fillers, trying to establish the quantity of hydrated lime suitable for better performing in conditions of aging with presence of moisture.

1.3 OUTLINE OF THIS STUDY

The dissertation is divided into 7 chapters:

- Chapter 1:. An introduction to the problem under consideration and the objectives that want to be achieved.

- Chapter 2: provides a preliminary review of the literature on bitumen and filler properties, in particular with the presence of hydrated lime.

- Chapter 3: provides a literary review of the influence of aging and moisture in the performance of bituminous binders.

- Chapter 4: describes the experimental program in all phases, such as materials (bitumen and filler types), sample preparation and their conditioning protocols. This chapter also lists the test methods used. The DSR device helped to obtain rheological information. The FTIR device is able to detect changes in the chemical composition.

- Chapter 5: all filler results are shown in this chapter. A chemical evaluation is carried out between the different fillers, studying the degradation of calcium hydroxide, and the consequent formation of calcium carbonate.

- Chapter 6: all results on mastics are shown in this chapter. A chemical evaluation is carried out between the various mastics, studying oxidative aging plus moisture and making a comparison with the chemical results obtained in the fillers. A rheological evaluation is carried out with the relaxation tests, linear amplitude and frequency sweep test to define the relaxation properties of mastics, the viscoelastic characteristics for fatigue resistance and physical performance after aging.

- Chapter 7: Conclusions of this research work and recommendations for future studies are provided.

CHAPTER 2 – BITUMEN AND FILLER

2.1 BITUMEN

The bitumen is a heterogeneous organic compound, generally obtained from the distillation processes of crude oil. Being made up of the fractions with the highest boiling point of the latter, bitumen is traditionally obtained as the bottom product of the vacuum distillation tower, used to process the residue of a first distillation at atmospheric pressure. The material thus obtained can be directly used, after classification, for various civil and construction engineering applications, ranging from the creation of waterproofing membranes to the production of the most varied mixtures for road superstructures. When necessary, the distillation residue is also subjected to oxidation, extraction with solvents and / or mixing with other bitumen which vary considerably according to the production scheme of each refinery and which have the common purpose of modifying their suitably the chemical and rheological characteristics. Bitumen is a viscoelastic material therefore if it is subjected to short load times there is an elastic deformation, on the contrary if it is subject to long load times it behaves like a viscous substance giving rise to irreversible deformations. It is a thermoplastic material for which it occurs in a solid-brittle state at low temperatures, in a solid-semisolid state at room temperature, and in the liquid state at high temperatures. The different origin of the crude oil, as well as the various methods for refining, make the characteristics of the bitumen highly random. Since bitumen is marketed with specification values that are essentially physical and non-chemical, production is aimed at achieving these values.

2.1.1 CHEMICAL COMPOSITION

As said, the performance of a binder depends directly on the physical and rheological properties of the material, which in turn depend on the chemical and structural composition of the bitumen.

The chemical composition of bitumen is regarded as extremely complex. It is highly dependent on the source of the crude oil, from which bitumen originates, and the refinery process (Hunter et al. 2015). As a general rule, bitumen is predominantly composed of hydrocarbon molecules, as well as some heterocyclic species and functional groups (heteroatoms) containing sulfur, nitrogen and oxygen atoms. In addition, traces of metals such as nickel, vanadium, iron, calcium and magnesium, in the form of metallic salts, oxides or in porphyrin structures, can be found in its chemical structure (Hunter et al. 2015).

Table 2.1 presents the elemental composition of bitumen. The results are derived by elemental analyses performed on different bitumen, originating from a variety of sources, and reflect the actual state for the majority of the tested bitumen (Hunter et al. 2015).

Element	Wt (%)
Carbon	82-88
Hydrogen	8-11
Sulfur	0-6
Oxygen	0-1.5
Nitrogen	0-1

Table 2.0.1 - Elements of bitumen composition

It should be emphasized that the percentages indicated above may vary according to the crude oil of origin and / or the production process of the bitumen used, but are generally included in these ranges.

The complexity of the chemical analysis of bitumen lies in its internal composition identified in a mixture of hydrocarbons. These chemical compounds are formed exclusively of carbon and hydrogen (Figure 2.1) and, based on the proportions between these two elements and the molecular structure they form, they are divided into different series. The hydrocarbons that make up the oil can be divided according to the type of chains prevalent in them: paraffins (alkanes), naftenes (cycloalkanes), aromatics, resins and asphaltenes.

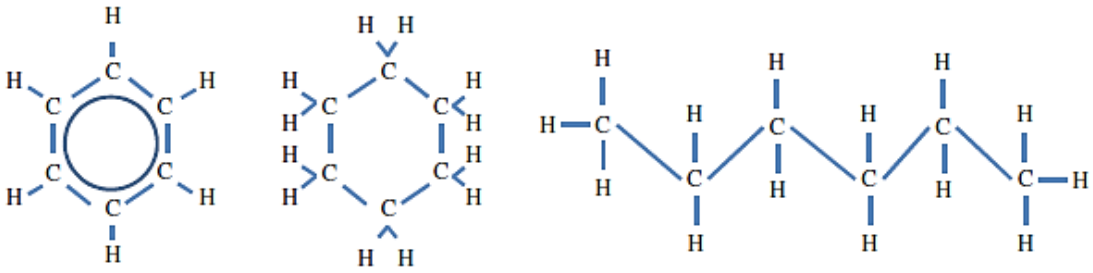

Figure 2.1 - Principal molecular structures in bitumen

Considering that in a single type of bitumen a vast number of different molecules with various chemical structures exist and that the chemical composition of bitumen is greatly affected by its origin and the implemented refinery process, it is impossible to completely separate and identify every single molecule present in its micro structure. For that reason, researchers had put efforts to separate bitumen into less complex and more homogeneous (generic) fractions and/or identify the chemical composition of bitumen by means of chemical functional groups, for research purposes.

Bitumen, indeed, is a substance made up of several different chemical compounds, having variable molecular weights. This complexity makes detailed chemical analysis unnecessary. The quantitative ratios between the various components are correspondingly determined by less complex fractionation methods; but which allow the bitumen to be divided into a few groups of molecules having similar properties and which can be framed in the colloidal schematization. According to the separation scheme used, they can be classified different tecniques, through these it is possible to identify two main groups constituting bitumen: the Asphaltenes and the Maltenes.

The subdivision of the Maltenic into fractions, resins and oils is of practical importance for the colloidal balance of the bitumen. Corbett proposed elution liquid chromatography - absorption in active alumina, with solvents that increased polarity and aroma; this test methodology is still a reference for the separation of Maltenic into Saturated, Aromatic and Resins by elution respectively in: n-heptane, benzene and double elution in 50/50 of benzene and methanol followed by trichlorethylene. It should be emphasized that Corbett did not use aromatic and resin terms, but rather "naphtene aromatics" and "polar aromatics" (Corbett, 1969). This classification gives rise to the name SARA, an acronym for Saturated - Aromatic - Resins – Asphaltenes. In Fig. 2.2, a schematic representation of the procedure proposed by Corbett is presented.

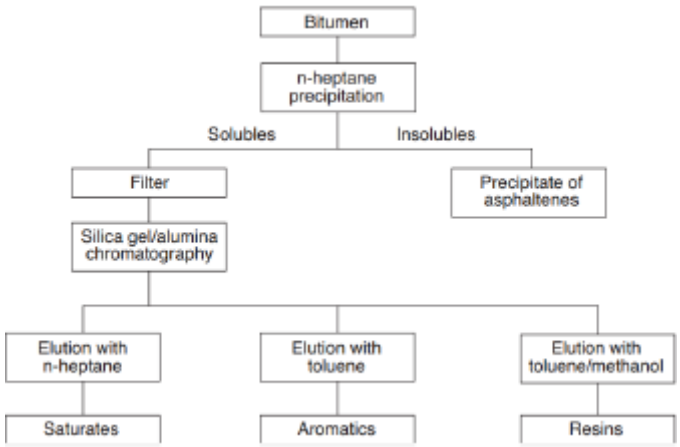

Figure 2.2 - Schematic representation of SARA fractions

Saturates are characterized as non-polar, viscous oils (Hunter et al. 2015). They may consist of straight and branched-chain hydrocarbons, saturated cyclic hydrocarbons (naphthenic hydrocarbons) and a small quantity of mono-ring aromatic hydrocarbons. The latter are dominated by attached saturated hydrocarbon side chains. In addition, sulphur can be found in the saturate fraction (Petersen 1984). Lesueur (2009) reported that, in this fraction, the ratio of

hydrogen over carbon is approximately equal to 2. In general, this fraction constitutes 5-20% of the total bitumen (Hunter et al. 2015).

Aromatics are viscous liquids and consist of non-polar carbon chains attached to unsaturated ring systems (Hunter et al. 2015). The heteroatoms sulphur, oxygen and nitrogen may also be part of the molecules (Petersen 1984). Aromatics constitute the major component of the bitumen's maltene phase, the dispersion medium for the peptized asphaltenes. In general terms, they account for 40-65% of the total bitumen. The hydrogen-to-carbon ratio fluctuates between 1.4 and 1.6 (Lesueur 2009).

The resins are soluble compounds in n-heptane, structurally very similar to the asphaltenes, dark brown in colour and solid or semi-solid consistency, approximately equal to the consistency of the entire bitumen. The resins are polar in nature and have significant adhesive properties, they perform the function of dispersing or peptizing agents for asphaltic macromolecular structures. They are co-solvents for oils and asphaltenes, mutually insoluble if they are not present in adequate concentrations. When the bitumen oxidizes, the resins acquire oxygen molecules and take on a structure similar to asphaltenes, therefore the proportion between resins and asphaltenes governs, to a large extent, the character of the bitumen. They constitute 10% to 25% by weight of bitumen.

Asphaltenes are amorphous solids consisting of complex mixtures of hydrocarbons, have an aromatic structure, that is, unsaturated cyclic, are black or brown in colour and insoluble in n-heptane. The characteristic that distinguishes them is the high polarity, which translates the presence of molecules in which the individual polar bonds are not placed perfectly symmetrically and therefore not in equilibrium. Asphaltenes have a great effect on the characteristics of bitumen even if they are present in bitumen only between 5% and 25% by weight. The increase in the asphaltene content results in a harder and more viscous bitumen, with a lower penetration value and a higher softening point.

2.1.2 FUNCTIONS OF THE BITUMEN COMPONENTS AND RHEOLOGICAL PROPERTY

Maltenic oils, resins and asphaltenes perform specific functions in the context of the physical behaviour of bitumen. It is important both their quality or type, and their respective concentration, and their respective chemical and physical interactions due to molecular structures.

Asphaltenes are mainly responsible for the viscous behaviour of the bitumen, its elasticity or plasticity as a function of temperature, its ability to resist mechanical stress and to settle quickly if poured hot on any surface forming a very adhesive film. Due to the lack of asphaltenes, bitumen shows a reduced consistency, is more susceptible to deformations induced by mechanical or thermal stresses and loses most of its adhesive properties.

Resins are the compounds that disperse the asphaltenes and at the same time also the maltenes. For this reason their presence and their quality, understood as chemical-physical reactivity, assume a fundamental importance in the balance of the bitumen constituents: the resins provide elasticity, flexibility, make the bitumen ductile and adhesive. Due to the lack of resins, the bitumen proves unstable, that is, it tends to separate the asphaltenes in the form of an agglomerate, leaving the oils to emerge.

Maltenic oils are the most fluid component of bitumen, therefore they influence its behaviour when hot, giving the surfaces to be treated fluently and therefore wettable. Due to the lack of maltenic oils, bitumen loses its fluidity characteristics even at medium-high temperatures, making it too hard and sticky to be worked and without sliding capacity.

The particular properties of bitumen with respect to mechanical stress have led to the attribution of a colloidal structure (Nellensteyn, 1923), a structure that responds to deformations as a function of the methods and time of application of mechanical stress. This behaviour is opposite to that typical of Newtonian fluids, and is present only in bitumen containing Asphaltenes; the colloidal nature of the bitumen was therefore associated with the presence of asphaltenes, or in more detail with the presence of asphaltenic nuclei surrounded by aromatic components with high molecular weight, the resins. It can be imagined that each Asphaltene is at the center of a structure, called "micelle", surrounded by resins (whose polar character decreases the more they are far from Asphaltene); the resins interact with the aromatics that make up the boundary of the structure, and can interface with saturated, the non-polar phase in which the micelle is immersed.

In the presence of sufficient quantities of resins, the Asphaltenes are totally solvated or peptized, therefore the micelles have good mobility in the bitumen and this corresponds to a Newtonian liquid type behaviour at high temperatures and a very viscous but not elastic fluid at low temperatures.

A bitumen having these characteristics is defined as SOL type. In the opposite case, in the absence of resins, the asphaltenes join together to form a continuous network where the lighter components merely fill the intermicellar voids. There is a non-Newtonian fluid type behaviour at high temperatures and an elastic solid at low temperatures, this bitumen is defined as a GEL type. In practice, most bitumen have intermediate characteristics between these two extreme structures. The behaviour of bitumen, whether it is viscoelastic, Newtonian or intermediate, is a function of temperature, but it is also directly dependent on the state of aggregation of the micelles, that is, on the relationship between asphaltenes, resins, aromatics and saturated. Intermediate bitumens have better elasticity and mechanical properties than SOL, while GEL-type bitumens have better mechanical resistance but do not have elastic properties (Petretto, 2012).

The character of a bitumen also depends on the fraction of saturated oils because these reduce the solvent power of the maltenes towards asphaltenes, therefore high saturated contents can lead to a flocculation of asphaltenes, with consequent growth of the gel character. If the asphaltenes are highly branched, their interaction with the resins is greater, and therefore they are less affected by the destabilizing effect of the saturated. From a qualitative point of view, the rheological properties of bitumen depend in some way on the content of asphaltenes. It can therefore be considered that at constant temperature the viscosity of a bitumen tends to increase as the concentration of asphaltenes increases. These bonds break at high temperature and the viscosity consequently decreases with increasing temperature. It can therefore be said that at low and intermediate temperatures, the rheology of bitumen is dominated by the degree of association of the asphaltenic agglomerates and by the relative presence in the system of other species that favor such associations. It is then assumed that, with the same asphaltenes, increasing the aromatic content and keeping the saturated / resins ratio constant, there is little effect on rheology and only a minimal reduction in deformability. On the contrary, by keeping the resin / aromatics ratio constant and increasing the saturates, the bitumen becomes softer. In general, it is assumed that increasing the resin content increases the hardness of the bitumen, i.e. reduces the penetration index and shear deformability and increases the viscosity (Petretto, 2012).

Since the overall behaviour of bitumen is determined by the compatibility and interactions between the different components in the mixture rather than by the relative quantity of this or that component, there are several synthetic composition parameters to be correlated with the rheological behaviour. The rheological study is fundamental to define the internal response of

materials to stress. Various tests are performed to define the rheological properties of the viscoelastic material, among which the most important are the phase angle and the complex shear modulus.

2.2 MINERAL FILLER

When bitumen is mixed with mineral fillers, the mix created is called mastic. Fillers provide added stiffness and stability to the mixtures, as well as controlling the void structure of the asphalt binder. Filler particles are defined according to EN 13043 as fine aggregates, most of which passes a 63 μm sieve that can be added to construction materials to provide certain properties. At least 70% filler must pass 63 μm sieve and 100% must pass the 2 mm size sieve (*Hunter 2015*) (Table 2.3).

Sieve size (μm)	Cumulative percentage passing by mass (%)
2000	100
125	85 to 100
63	70 to 100

Table 2.2 - Mineral fillers gradation requirements according to EN 13043

Fillers have several purposes in asphalt binders:

- To reduce the optimum content of the asphalt binder by filling the voids in the granular skeleton;
- To stabilize the mixture;
- To increase the post-compaction resistance of the mixtures;
- To improve the bond strength within the asphalt-aggregate system;
- To stiffen the asphalt binder and mixture;
- To increase the asphalt volume in the mixture.

2.2.1 DEFINITION OF MINERAL FILLERS

Wypych (1999) stated that filler can be defined as "*solid material capable of changing the physical and chemical properties of materials by surface interaction or its lack thereof and by its own physical characteristics*". This definition implies the existence of two ways in which fillers modify a system. Firstly, the ways in which the filler's shape, particle size and particle size distribution affect the system through filling of the liquid with solid particles (physical component). Secondly, the way in which interactions between the solid and liquid phases of the mixture affects the material (chemical component). The second interactions can vary from

strong chemical bonds or physical interactions leading to strongly reinforced materials, to almost no interaction at all (Aburkaba & Muniandy 2016).

There are several categories of fillers:

- The first category are fillers extracted from natural minerals (Andesite, Basalt, Caliche, Dolomite, Granite and Limestone) by mechanical sieving after the quarrying operation. These materials are generally referred to as Quarry Dust (QD), Washed Mining Sand (WMS), River Sand (RS) and Limestone (calcium carbonate) powder (LSP), the most common fillers used in HMA (Hot Mixed Asphalt).
- The second category of fillers is made up of post conditioning fillers or produced fillers (hydrated lime, fly ash and slag). This category refers to hydrated lime powder (HLP) and carbon black (CB). The use of these materials is specific for anti-stripping purposes.
- The third category refers to fillers with a combination of chemicals and natural minerals that undergo special processing before it is ready for use as an Ordinary Portland Cement (OPC). The most used filler in asphalt is limestone (calcium carbonate), which derives from the consolidation of microorganisms during the formation of the earth's crust. Limestone is the general term for rocks where calcite, a form of calcium carbonate, is the predominant mineral (Aburkaba and Muniandy 2016).

In general, fillers with high carbonate content such as limestone are easier to coat with binder than fillers with high silica content. This is due to the fact that siliceous aggregates contain high concentrations of hydroxyl groups with greater affinity for carboxylic acid and water. The carboxylic acid components present in the binder are absorbed by the surface of these particles, generating a binder-aggregate bond. However, these bonds with carboxylic acids are also subject to displacements in the presence of water. Such displacement is reduced when hydrated lime is used in the mixture (Hunter 2015).

2.2.2 PROPERTIES OF MINERAL FILLERS

In a literature review performed within the framework of the National Cooperative Highway Research Program (NCHRP) Project 9-45 (2010), they are indicated that the most commonly measured filler characteristics can be classified into two categories: physical-geometrical and chemical composition (Table 2.3).

Geometrical/physical property	Chemical property
Particles' Size and Size Distribution	Plasticity Index
Specific Gravity	Clay Content-Methylene Blue Test
Surface Area	pH Value of Diluted Suspension
Fractional Voids-Rigden Voids	Water Solubility/Susceptibility
Shape, Angularity and Texture	Elemental Analysis

Table 2.3 - Mineral filler properties

Aburkaba & Muniandy (2016) provided an extensive summary of the mineral filler's properties, their means of measurement and the corresponding standards. For each category a number of properties have been found to be important with regard to influence on mastic and mixture performance. The physical-geometrical (specific gravity, shape, angularity, and size distribution) as well as chemical (mineral) composition of fillers such as dioxides content can be important variables (Table 2.4).

Property	Means of measurement	Standard
Geometrical property		
Particles' Size Distribution	Air-Jet, Sedimentation, Laser Diffraction	EN 993-10 / BS ISO13320-1:1999
Particles' Morphology	Scanning Electron Microscopy (SEM)	-
Surface Area	Blaine test	EN 196-6
Physical/mechanical property		
Water Content	-	EN 1097
Particles' Density	-	EN 1097-7
Stiffening property		
Fractional Voids	Rigden Voids	EN 1097-4:1998
Delta ring and ball	-	EN 13179-1
Absorption	Bitumen Number	EN 13179-2
Loose Bulk Density in Kerosene	-	EN 1097-3
Chemical property		
Water Solubility	-	EN 1744-1:1998
Water Susceptibility	-	EN 1744-4:2001
Calcium Carbonate Content	X-Ray Fluorescence, Spectroscopy	EN 196-21/EN 495-2
Calcium Hydroxide Content	-	EN 495-2
Organic Content	Loss on Ignition of oal Fly Ash	EN 1744-1:1998
Organic Content	Loss on Ignition of Blast-Furnace Slags	EN 196-2:1994
Mineral Composition	Energy-Dispersive X-Ray (EDX) Spectroscopy	-
Harmful Fines	Methylene Blue Test	EN 933-9
Plasticity Index	-	BS1377:1990

Table 2.4 - Mineral filler geometrical, physical, mechanical, stiffening and chemical properties

The importance of physical-chemical interaction between the fillers and asphalt has been recognized for a long time and the dependency of mechanical properties of the mastics on the nature of the interaction has been shown in several studies.

2.2.3 EFFECTS OF MINERAL FILLERS ON MASTICS

Two major mechanisms are distinguished regarding the interaction of mineral matter and bitumen when the two materials are mixed together:

- Absorption of bitumen components into the mineral aggregates structure: absorption refers to the phenomenon according to which, the oily components of bitumen migrate into the porous structure of aggregates. Hence, the action of absorption is not a phenomenon limited on the interface of bitumen and aggregates but, rather, free space and volume, in the internal structure of aggregates, are required to accommodate the absorbed material. The absorption of bitumen oily components can lead to hardening of the material. It has been observed (Wu, 2009) that bitumen recovered from aged mastics is typically softer than neat aged bitumen, aged in identical conditions; a possible explanation for the latter is that the oily and / or less polar components of the bitumen have been absorbed into the mineral filler particles. These components, being protected from oxidation and evaporation, are easily recovered at the time of extraction, by virtue of their weak bonds with the aggregate surface, and give the recovered bitumen a softer nature.
- Adsorption of bitumen components on the mineral aggregates surface: Adsorption is a surface phenomenon and refers to the bonding of bitumen components on the surface of aggregates through the development of molecular forces (Wu 2009). The adsorption intensity of the bitumen components on the surface of the aggregates is (strongly) influenced by the interfacial area available for interactions. The chemical analysis (Plancher et al. 1977) of the adsorbed materials revealed that the residual material on the aggregate surface was composed of the oxygenated functional groups present in the bituminous microstructure (ketones, carboxylic acids, dicarboxylic anhydrides, quinolone and sulfoxides) as well as nitrogen. Based on their relative affinity with the surface of the aggregates, the various components have been classified as shown in the table.

Bitumen component	Relative affinity
Carboxylic Acids	High
Dicarboxylic Anhydrides	↑
2-Quinolone Types	
Sulfoxides	
Nitrogen	↓
Ketones	Low

Table 2.5 - Bitumen components relative affinity to aggregate surface

Plancher's research highlights two very important aspects. On the one hand, the importance of the specific surface of the aggregate particles in the adsorption mechanism and, on the other, the tendency of the functional chemical groups of bitumen, formed by oxidation, to absorb strongly on the surface of the mineral material. These two aspects, in most cases, constitute the main ways in which the results are interpreted when considering the effect of mineral fillers on the aging of bituminous mixtures. Lesueur el al. (2010) considered the properties of the filler related to its stiffening effect on the bitumen. In particular, the voids of the dry compacted filler (Rigden air voids) and delta Ring and Ball are measured. The voids of the dry compacted filler (EN 1097-4) (Fig 2.3) consists in measuring the density of a compacted specimen of the studied filler and divide it by the particle density of the filler. The ratio therefore gives the volume fraction of voids in the packed filler.

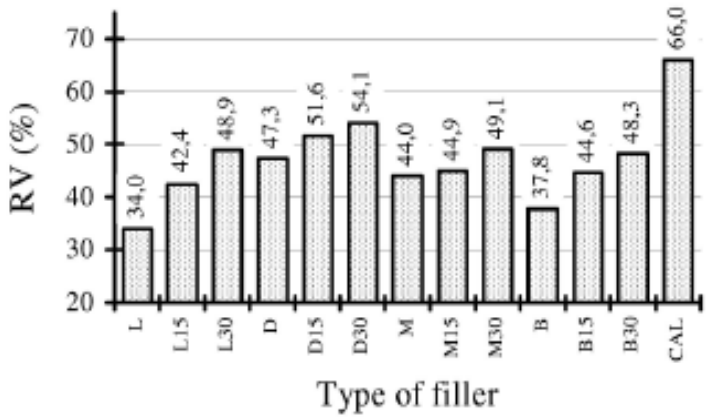

Figure 2.3 - Rigden air voids of several fillers and mixed fillers

The delta ring and ball test (EN 13179-1) consists in measuring the increase in softening temperature of a 70/100 bitumen after addition of 37.5vol. % of the studied filler. Mineral fillers typically have delta ring and balls between 8 and 25°C, 15°C being a common value (Fig. 2.4).

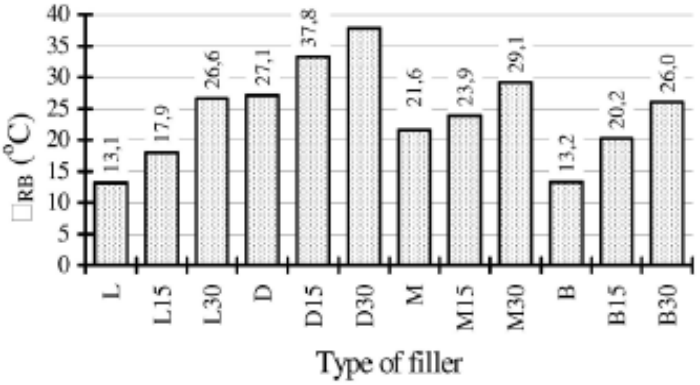

Figure 2.4 - Delta ring and ball of several fillers and mixed fillers

As just seen in the literature there are different visions and definitions of the stiffening or reinforcement mechanisms. Consistent definitions need to be established for the following reinforcement mechanisms.

- Volume-filling reinforcement, in which the reinforcement caused by the presence of rigid inclusions in a less rigid matrix;
- Physiochemical reinforcement, in which the stiffening caused by interfacial effects between asphalt and filler particles, including absorption, adsorption and selective absorption. The modified asphalt actually forms a rigid layer, which leads to a greater concentration of the net volume of rigid matter, which in turn leads to a greater rigidity of the mastic.
- Particle interaction reinforcement, this effect increases with increasing filler content, since the rigid matter comes into contact and forms a skeletal structure.

Other factors may influence the stiffness of asphalt mastics, including the shape of the particles, the agglomerates, the degree of dispersion and the dimensional distribution (Buttlar 1999).

The addition of mineral fillers to the asphalt binder is known to stiffen the asphalt binder, transforming it into a new material called mastic. It is known that this new material affects the workability of the asphalt mixture and, therefore, plays an important role in compaction and influences the overall performance of asphalt pavement mixtures. Numerous studies have been conducted on the effects of fillers on mastics and asphalt mixtures. The mechanical properties of the asphalt mixture are strongly dictated by the type and quantity of the mineral filler. The increase in the filler-bitumen ratio can positively affect the mechanical properties of the mixture. Furthermore, the physical properties (such as the aid of penetration and

softening point) of mastics strongly depend on the type and concentration of the mineral filler. Based on the results of the mastic, the temperature susceptibility of the mixture can be improved if a greater amount of filler-bitumen ratios is applied. In general, the type of filler and their quantity are essential parameters when designing the mixture in order to guarantee the performance of the mixture in the field. According to some studies (Muniandy et al 2012) the viscosity increases, the penetration decreases and the softening point increases with the increase of the size of the filler particles. In addition, the medium to coarse particle size of the filler appears to lead to better tear strength and fatigue failure properties than fine-sized particles. On the other hand, the type of filler influences the flaking and fatigue parameters, as well as the properties of the temperature.

Zhou et al (2017) assessed the effects of filler characteristics on asphalt mastic performance using Fourier transform infrared spectroscopy (FTIR) and DSR using complex modulus (G *), phase angle (δ) and rigidity scroll. Five limestone fillers were selected to produce asphalt mastics. The FTIR results showed that the interaction between asphalt and filler is a physical process without the production of new functional groups or compositions. Five fillers with different characteristics showed different effects on the high temperature properties of the asphalt mastic. Higher bitumen-filler ratios can improve the G* value of asphalt mastic.

Test temperatures, bitumen filler ratios and filler types have significant effects on G*. Kim et al (2002) described how the resistance of a micro-crack mastic development is strongly influenced by the dispersion of the mineral filler. Therefore, the cohesive strength of the mastic is not controlled only by asphalt binder, but by the combination and interaction of asphalt binder and mineral filler.

Kim (2003) also studied fundamental changes in material characteristics and fatigue behaviour due to the addition of fillers. For this study two types of filler were selected, limestone and hydrated lime. The evaluation of the properties of the linear viscoelastic material of binders and mastics identifies significant stiffening effects due to the fillers. Systems filled with hydrated lime generally show higher modulus than mixtures filled with limestone. Fillers offer better resistance to microcracking due to a lower rate of damage evolution and a greater ability to accumulate total damage.

Hydrated lime was more effective than limestone filler. Furthermore, this study indicates that the physical-chemical interaction between binder and filler depends on the type of materials. In summary, the importance of bitumen-filler mastics has been known for many years and

numerous studies have been conducted, trying to describe the characteristics of the fillers that best explain the behaviour of the resulting mastics.

2.3 ACTIVE FILLER WITH HYDRATED LIME

Hydrated lime is mainly composed of calcium hydroxide $Ca(OH)_2$. It is obtained by hydrating quicklime (essentially calcium oxide CaO) using specific equipments called hydrators. Quicklime is manufactured by burning limestone of very high purity (made of calcium carbonate $CaCO_3$) at temperatures around 900°C in dedicated kilns.

Hydrated lime generally comes in the form of a dry white powder (Figure 2.5) with a particle density close to 2.2Mg/m^3. Because of a high level of particle porosity (of order 50%), its apparent density typically ranges from 0.5 to 0.8Mg/m^3 as measured by EN 459-2.

Figure 2.5 – Hydrated lime

2.3.1 PROPERTIES OF HYDRATED LIME FILLER

Because of its mineral origin and powder form, hydrated lime is generally compared to mineral fillers in the asphalt industry. In this sense, hydrated lime can be evaluated using the specifications on aggregates for asphalt mixtures as detailed in Table 2.6.

Property	Standard	Unit	Hydrated lime
Particle density	EN 1097-7 / AASHTO T84	Mg/m^3	2,2
Voids in dry compacted filler	EN 1097-4 / NAPA IS-127	%	60-70
Delta Ring and Ball	EN 13179-1	°C	n,m,
Bitumen Number	EN 13179-2	ml/100g	70-120
Masss in Kerosene	EN 1097-3	Mg/m^3	0,3

Blaine specific surface	EN 196-6 - ASTM C 204	cm^2/g	>10000
Specific surface area	BET	cm^2/g	150000-200000
Methylene blue value	EN 933-9	g/kg	<1

Table 2.6 - Typical properties of hydrated lime

As discussed in sub-section 2.2.3 the standard mainly considers the properties of the filler related to its stiffening effect on the bitumen; in particular, the voids of the dry compacted filler (Rigden air voids) and delta Ring and Ball. The figure shows that when mixed fillers are concerned, Rigden air voids increase when the hydrated lime content increases, with typical values in the 45-50% range for 25wt.% hydrated lime in the mixed filler.

Several studies claim that the test cannot be performed on pure hydrated lime. As a matter of fact, the stiffening power of hydrated lime is so pronounced that the 37.5vol% mixture is not fluid enough to prepare the test sample. Only a reduction in the quantity specified in the European standard would allow to quantify the stiffening effect. For hydrated lime, the typical values are in the range 0.7-1.0, while they are 1.5-2.5 for mineral fillers. Consequently, when hydrated lime is used as a filler, it has been found that 15 and 30% by weight cause an increase in the ring ball value respectively from 2 to 10 °C and from 8 to 20 °C (Schellenberg and Eulitz, 1999).

Of special interest is the bitumen number (EN 131791-2), which consists in measuring the amount of water in ml that needs to be added to 100g of filler in order to reach a reference consistency defined by a penetration value of 5 to 7mm. The test is being used especially in the Netherlands (where it is also known as de Van der Baan number) and gives an information on the stiffening power of the filler, which is somewhat similar to the Rigden air voids value.

Mass in kerosene is also sometimes used to characterize fillers (EN 1097-3). It measures the so-called apparent density of 10g of filler in 25ml of kerosene, obtained by measuring the height of filler that sediment in kerosene after 6 hours.

Methylene blue value (EN 933-9) is not relevant for hydrated lime, because the test is intended to measure the amount of clayey materials in an aggregate. Still, the asphalt industry uses the test a lot to characterize fillers and there is no difficulty to perform it on hydrated lime. The value is normally inferior to 1g per kg for hydrated lime.

Although the Blaine method (EN 196-6) is intended for cements, it is sometimes used to characterize hydrated lime. This is generally not appropriate, because the high porosity of hydrated lime makes it impossible to run the test according to the required level of porosity,

which in turns strongly affects the repeatability of the method. Still, values can be obtained and they are usually higher than 10,000cm^2/g (= 1m^2/g) for standard hydrates.

2.3.2 CYCLE OF HYDRATED LIME

Burning limestone/chalk occurs at roughly 840°C. The reaction for the thermal decomposition of calcium carbonate is as follows:

$$CaCO_3 = CaO + CO_2$$

This chemical reaction produces quicklime. Quicklime's principal component is calcium oxide. Its quality often depends on a number of certain factors including physical properties, reactivity to water and chemical composition. Adding water to quicklime produces an exothermic reaction (gives out heat) and hydrated lime. The reaction for the hydration of quicklime is as follows:

$$CaO + H_2O = Ca(OH)_2$$

The recarbonation process is essentially the opposite of the calcining/burning process. Both quicklime and hydrated lime, when exposed to the air for long periods, begin to draw in carbon dioxide from the atmosphere. This therefore replaces the oxide component of the chemical and turns the lime roughly back to its original state, being limestone:

$$Ca(OH)_2 + CO_2 = CaCO_3 + H_2O$$

The Figure 2.6 summarizes the various phases of the lime cycle.

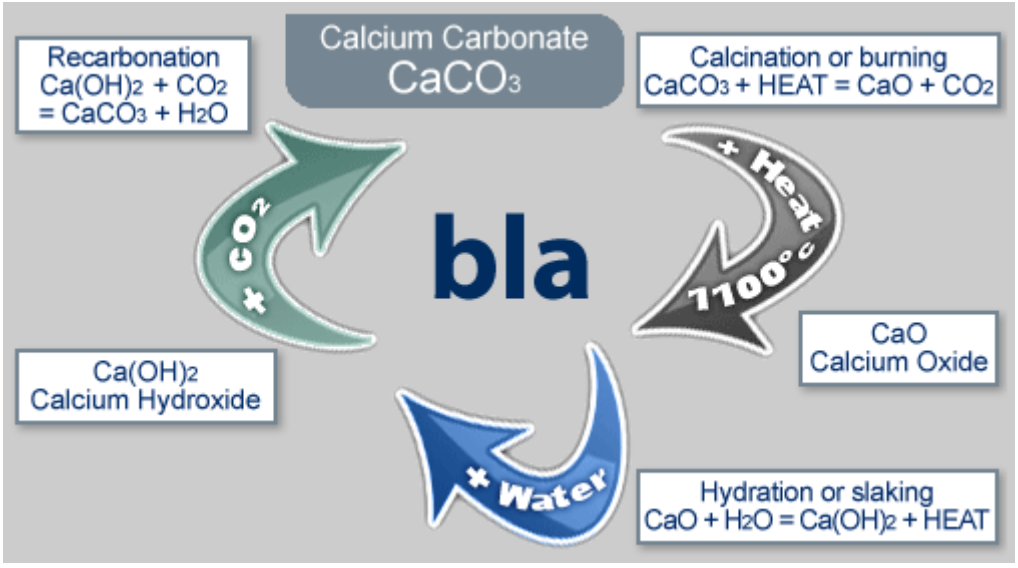

Figure 2.6 – Lyme cicle (British Lime Association)

The carbonation of lime-based materials has been widely explored in the decarbonisation processes of the energy and industrial sectors. However, their ability to capture carbon dioxide from the air under realistic environmental conditions in direct air capture technologies is less explored.

Erans et al. (2020) study the lime and hydrated lime samples exposed to ambient air for prolonged periods, as well as to environmental calcination/carbonation cycles, to evaluate their carbonation performance. Erans et al. (2020) show that moisture plays a key role in the carbonation of lime in environmental conditions. In addition, hydrated lime demonstrates greater weather resistance and higher conversions, with a carbonation conversion of 70% after 300 hours. The study performed indicated that lime-based materials are suitable for the capture of carbon dioxide from ambient air using cyclical processes, on a practical time scale, and that air humidity plays a key role.

2.3.3 EFFECT OF HYDRATED LIME ON ASPHALT MIXTURES

Hydrated lime is considered as a multifunctional additive that improves the properties and therefore the durability of bituminous materials: the ability of lime to improve the resistance of bituminous mixtures to moisture damage, reduce oxidative aging, improve the mechanical properties, and improve resistance to fatigue and rutting, has led to observed improvements in the field performance of lime-treated HMA pavements.

The available tests allow to evaluate the resistance of road materials with respect to the action of harmful agents such as water, freeze-thaw cycles, temperature and exposure to UV rays (aging) and/or traffic. The effects of hydrated lime in the mixes of bituminous conglomerate are therefore reported below:

- The resistance to moisture damage and frost;
- The resistance to chemical ageing;
- The mechanical properties, in particular modulus, strength, rutting resistance, fatigue and thermal cracking.

Resistance to moisture damage and frost

Moisture induced-damage and the effect of freeze-thaw cycles are common phenomena with asphalt mixtures. It generally materializes by the progressive loss of aggregate: the bitumen-aggregate bond gets weakened in the presence of water to the point that it becomes not strong enough to hold the aggregate. This is generally called aggregate stripping or ravelling when it

is limited to the surface (Caro et al. 2008). Ravelling is also one type of water damage that similarly yields to the loss of aggregate, but from the bottom layer of the material as a consequence of the traffic-induced water pressure in the binder course.

The terms "water susceptibility" and "water sensitivity" are often used to designate the loss of strength or other properties of asphalt pavement in the presence of moisture. The water susceptibility of asphalt pavement is controlled by:

- Aggregate properties
- Asphalt cement binder properties
- Mixture characteristics
- Climate
- Traffic
- Construction practices
- Pavement design considerations

It is usually the aggregate properties that dominate the water susceptibility properties of an asphalt pavement. Although asphalt cement properties may also affect water susceptibility, generally an aggregate related water susceptibility problem cannot be overcome by selecting an unmodified asphalt cement binder with superior antistripping properties. Problem pavements under high traffic levels normally experience more rapid premature distress than similar pavements under low traffic loading. Compacted mixtures with high air voids are generally more likely to experience stripping than pavements that are compacted to low air void contents.

If untreated, these damages can deteriorate into potholes. Frost and freeze-thaw cycles tend to enhance these detrimental effects, and a tough winter can directly generate potholes.

Several test methods are available to evaluate the frost and moisture resistance of bituminous mix mixtures; the most frequently used in literature are listed in the Table 2.7. The Lottman test (AASHTO T-283) was found to be one of the most effective among the tests in use.

Test method	Standard	Result
Hamburg Wheel Tracking	EN 12697-22B	Rut depth in mm
Indirect Tensile Strength	EN 12697-12A	ITS ratio in %
Duriez	EN 12697-12B	ITS ratio in %
Cantabro	EN 12697-17	Mass loss ratio

Saturation Ageing Tensile Stiffness	-	ITS ratio in %
Lottman	AASHTO T283	ITS ratio
Repeated Lottman	-	ITS ratio vs number of freeze-thaw cycle
Texas Freeze-Thaw Pedestal		Number of freeze-thaw cycles to failure
Retained tensile strenght	ASTM D4867	ITS ratio
Immersion/Compression	AASHTO T165	Compressive strenght ratio
Retained Marshall		Stability ratio
Texas Boil Test	ASTM D3625	% retained bitumen after boiling

Table 2.7 - Most used testing methods in order to evaluate the improvement of the moisture resistance of asphalt mixtures

In all cases, regardless of the test method, the data confirm that 0.5-2% by weight of hydrated lime compared to dry aggregates improves the resistance to moisture and frost of the mixes of bituminous conglomerate. At least 1% by weight is necessary to obtain benefits.

Resistance to chemical ageing

Hydrated lime was early observed to decrease bitumen chemical aging. The first observations of the anti-ageing effect of hydrated lime on bituminous materials date back from the late 1960's in USA, when C. V. Chachas with the Utah State Department Highways observed that control specimens of bitumen recovered from hydrated lime treated asphalt mixtures were softer than the reference materials. From then on, many laboratory studies and in the field confirmed the impact of hydrated lime on bitumen chemical ageing.

The effect of hydrated lime on the aging of bitumen can be described by a set of different factors:

- Hydrated lime-modified bitumens show a decreased ageing susceptibility; This is materialized by a slower increase in viscosity (or any other mechanical property) versus ageing time;
- In parallel, the rate of carbonyl formation slows down hydrated lime-modified bitumens. However, this effect was only found at ageing temperatures of 88°C and above, but was not found when low temperature ageing was studied (60°C);
- Sulfides, sulfoxides and ketones formation seem not to be significantly modified by hydrated lime;
- In all cases, asphaltenes content increases at a slower pace with hydrated lime modified than with non-modified bitumens;
- These effects are only seen with hydrated lime and not with limestone filler.

Some elements of interpretation of these observations, in terms of bitumen and hydrated lime interactions, are further discussed in sub-section 2.3.4.

Mechanical properties

When studying mastics, it becomes apparent that a mastic made with hydrated lime behaves in a distinct way than a mastic made with normal mineral filler. In fact, the delta Ring and Ball test described earlier is already a test on mastic showing that hydrated lime has a higher stiffening effect than normal mineral fillers.

Several studies confirmed that properties such as viscosity (or equivalently the complex modulus) are similarly increased when hydrated lime is used instead of regular mineral filler.

Still, bitumen does show a higher stiffening effect with hydrated lime than normal mineral fillers. As a rule of thumb, and taking an average asphalt mixture with 5% mineral filler and 5% bitumen, the substitution of 1% and 2% mineral filler by 1% and 2% hydrated lime respectively would be equivalent to using a bitumen with a R&B softening temperature higher by ~2.5 and ~8°C respectively. Note that the difference in R&B temperature range between 2 adjacent paving grades is about 5°C in the current European specifications. Therefore, the 2% hydrated lime substitution is on average similar to shifting the bitumen to the next harder grade. This can be quantified by means of the intrinsic viscosity [η] defined as:

$$[\eta] = \lim_{\Phi \to 0} \left(\frac{\eta(\Phi) - \eta_0}{\eta_0} \right)$$

Where η (Φ) is the viscosity of the mastic with a volume fraction of filler Φ and η_0 is the viscosity of the base bitumen. Using this parameter that quantifies the stiffening effect of a filler, it is shown that hydrated lime ([η] ~ 3-10) is about twice as stiffening as other mineral fillers ([η] ~ 2.5-5). However, temperature is a key issue here, and the above results only hold because the testing was performed at high temperatures. On the contrary, the low temperature studies show that hydrated lime is similar to other mineral fillers in terms of stiffening effect at low temperature. The switch from the low temperature region of normal stiffening to the high temperature region of high stiffening occurs close to room temperature.

The bituminous conglomerate has a viscoelastic behaviour, therefore it has mechanical properties that depend on the temperature and duration of the load. It follows that also the modulus, that is the ratio between the applied stress and the resulting deformation, depends on the temperature and duration (or frequency) of the load, and is generally expressed by the complex modulus. On the mix formulation standpoint, modulus is known to peak at an optimum bitumen content, to increase with the modulus of the binder and to decrease with the air void content. Modulus is of critical importance in the design of pavement layers, because it

governs the stress distribution inside each pavement layer. For given load and thickness, higher modulus means lower stresses in the layer. A limited number of studies give information about how hydrated lime affects the modulus of asphalt mixtures. A study (Witzcak et al. 2005) measured the dynamic modulus in tension-compression between -10°C and 54.4°C and frequencies ranging from 0.1 to 25 Hz for 17 mixture–lime percentage combinations across six different hot-mix formulas. The mixes were made with 4.2-5.2% of four different binders and contained 0, 1, 2, or 3% hydrated lime as a filler substitute (Figure 2.7).

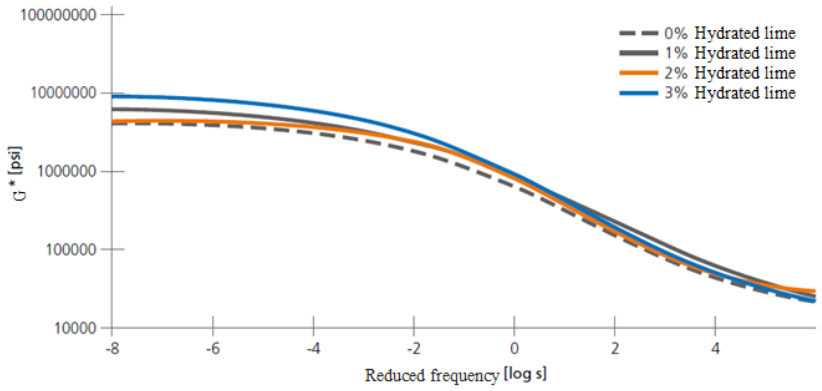

Figure 2.7 - Master curve (norm of the complex modulus versus reduced loading time) for four different binders

As a result, hydrated lime was seen to increase the modulus of asphalt mixtures by 8% up to 65% across the range of mixtures and hydrated lime contents at all temperatures and frequencies. Concerning the effect of hydrated lime concentration on the modulus, the published data do not give very conclusive results. As already mentioned, the Witczak study observed the highest stiffening with 2.5% hydrated lime. Other further studies (Aragao et al. 2008) (Baig et al. 1998) have provided different optimal percentages of hydrated lime in the mixture, in the first case 1.5%, in the second 4%. As a conclusion, hydrated lime does not always increase the modulus of asphalt mixtures. The optimum hydrated lime content in order to enhance this effect seem to be highly mixture dependent and published data give values ranging from 1.5 to 4%.

Strength is an engineering mechanical property of materials. It is the maximum stress applied to break the material. Strength is usually measured either in compression or in indirect tension for asphalt mixtures, and generally at controlled temperatures close to room temperature. In general, modulus and strength are somewhat related when measured in the same temperature and loading conditions, although one is an intrinsic property (modulus) and the other (strength) strongly depends on specimen shape and dimensions and is therefore not intrinsic.

Strength is known to peak at an optimum bitumen content, to increase with the modulus of the binder and to decrease with the air void content. The published data (Timoshenko, 1976) suggest that only about half of the mixtures exhibit an increase in strength when treated with hydrated lime, without any clear explanation: as a conclusion, hydrated lime does not always increase the strength of asphalt mixtures.

Rutting occurs when the traffic load over the asphalt mix exceeds its plastic limit, hence generating permanent deformation. Rutting is normally caused by low-speed loads at high temperatures. However, rutting remains a complex phenomenon, because the asphalt mixes deform in a viscoelastoplastic way under these conditions. On the mix formulation standpoint, rutting is known to be favoured by several factors such as high bitumen content, high sand content, round aggregate shape (like uncrushed gravel) or high binder deformability. Therefore, factors favouring the stiffening of the mixtures should also increase the rutting resistance. The published data (Verhasselt et al. 2001) clearly suggest that hydrated lime generally improves the rutting resistance when treated with hydrated lime. Comparing to modulus and strength data, this might confirm that the stiffening effect of hydrated lime is generally more pronounced at high temperature (where rutting is measured) than at lower temperature. Also, hydrated lime content higher than 1.5% are generally seen to be more effective in order to observe a significant effect.

Fatigue cracking occurs when the repeated traffic loads progressively damage the asphalt mixtures, generating cracks propagating from the bottom of the layer to the top. As a consequence, fatigue cracking is favoured by low thicknesses of the layer or bad adhesion between the successive layers, that both promote high flexural stresses at the bottom of the asphalt layers. On the mix formulation standpoint, fatigue resistance is known to be enhanced by a high bitumen content or the use of high-performance binders. Fatigue cracking is the main failure mode that is used in the design of pavement layers. More precisely, the bituminous layers are designed to be thick enough to insure that fatigue cracking won’t appear until the end of design life, which can go from 10 to 40 years. Some studies (Rhagava Charie & Jacob, 1984) (Little & Petersen, 2005) assert that hydrated lime improves fatigue strength: this is confirmed in 77% of cases, however the number of load applications is limited, below of 1 million cycles, therefore it is not appropriate to extrapolate from this data the useful life of a pavement, whose repeated loads are between 1 and 100 million.

Thermal cracking is especially seen in cold areas. In these regions, the low temperatures imposed on the bitumen, make it essentially perform in its glassy state where it becomes brittle. As a consequence, the thermal shrinkage occurring upon cooling develops stresses that can overcome the materials resistance, hence generating a large crack. On the mix formulation standpoint, and just like fatigue cracking, thermal resistance is known to be enhanced by a high bitumen content or the use of high-performance binders. A soft binder increases the cracking resistance. Some studies show that neither the failure temperature nor the thermal stresses were significantly different between the hydrated lime modified and the unmodified materials. So, hydrated lime is not expected to affect the low temperature fracture properties differently than other mineral fillers, as confirmed by the limited number of studies published on the absence of improvement of hydrated lime on the low temperature cracking of asphalt mixtures.

2.3.4 MECHANISMS OF HYDRATED LIME MODIFICATION OF ASPHALT MIXTURES

Hydrated lime has several effects, some having consequences in terms of adhesion, others in terms of ageing and yet some others in terms of mechanical properties. Therefore, it seems reasonable to conclude that hydrated lime is acting at different levels:

- Hydrated lime is modifying the aggregate surface;
- Hydrated lime is also reacting with the bitumen. There are chemical reactions between this basic compound and some of the acidic moieties naturally present in the bitumen. This aspect is referred to as the chemical effect on bitumen;
- Hydrated lime develops some physical interactions with the bitumen, arising from its porous structure. This will be referred to as the physical effect on bitumen.

For all of these reasons, the interactions between hydrated lime and the other components of the asphalt mixture are quite intense, explaining the improvement in properties as different as moisture damage resistance, ageing resistance and mechanical properties.

Effect on the aggregate

It is well known in asphalt science that siliceous aggregates have worst adhesive properties toward bitumen than limestone aggregates. Reasons for that are that both anionic and cationic surfactants naturally present in the bitumen strongly bond with calcium ions when only cationic surfactants strongly bond with silica atoms. As a consequence, anionic surfactants are easily displaced by water on siliceous aggregates. Therefore, one of the effects of hydrated

lime is to allow for the precipitation of calcium ions onto the aggregate surface, making it more favourable to bitumen. As a consequence, a surface treatment with almost no remaining hydrated lime particles already improves the bitumen-aggregate adhesion (Figure 2.8).

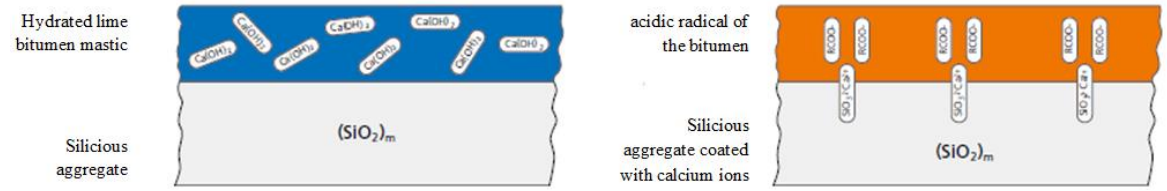

Figure 2.8 - The effect of hydrated lime on the aggregate surface

In addition, calcium carbonate can precipitate in the presence of water (at the manufacturing stage or in-situ upon rain exposure) and therefore create a higher surface roughness which is known to favour bitumen adhesion as well. Still, the surface modification effect is not the only mechanism. In fact, this mechanism would be almost inexistent with limestone aggregates. However, hydrated lime is known to improve the adhesion of the limestone aggregates as well. So, other mechanisms must operate, and especially those acting on the bitumen as described below.

Effect on the bitumen

As previously mentioned the chemical interaction between mineral fillers and bitumen had already been analyzed by Plancher in 1977. In this case, an in-depth analysis is made on the reaction of bitumen in the presence of hydrated lime: the materials treated with lime presented by Plancher have shown lower concentrations of carboxylic acids, dicarboxylic anhydrides and 2-quinolones, which are typically present in the heavier components of bitumen, asphaltenes; ketones remain more numerous and sulfoxides have varied significantly. Hydrated lime reacts with the bitumen acids, anhydrides and 2-quinolones: its presence therefore reduces the amount of ketones, anhydrides and especially of carboxylic acids responsible for aging.

Lime-bitumen chemical interactions have two effects:

- First, polar molecules neutralized by hydrated lime remain highly adsorbed on the hydrated lime particles. This prevents them from causing the chemical aging of the bitumen. The phenomenon is responsible for a slower aging kinetics.
- Secondly, neutralized polar molecules cannot move to the bitumen-aggregate interface, unlike the remaining non-acid surfactants. These are typically amine based and are not easily moved by water, unlike anionic surfactants. The effect is confirmed

by the observation that the hydrated lime in the bitumen improves the moisture resistance of the corresponding mixtures of bituminous conglomerate.

In conclusion, the chemical interactions between hydrated lime and acid fractions of bitumen contribute to the improvement of both resistance to aging and aggregate-bitumen adhesion. As described in a previous section, hydrated lime has higher dry porosity (Rigden air voids) than mineral fillers, with typical values ranging from 60 to 70% when mineral fillers have values closer to 30-34%. The difference comes from the higher porosity of the hydrated lime particles: For mineral filler, the porosity essentially comes from the voids between the particles. For hydrated lime, the porosity inside the particles sums up to the porosity between the particles, hence leading to a much higher value.

As described in a previous section, hydrated lime has higher dry porosity (Rigden air voids) than mineral fillers, with typical values ranging from 60 to 70% when mineral fillers have values closer to 30-34%. The difference comes from the higher porosity of the hydrated lime particles: For mineral filler, the porosity essentially comes from the voids between the particles. For hydrated lime, the porosity inside the particles sums up to the porosity between the particles, hence leading to a much higher value. Rigden air voids correlates very well with the stiffening power as measured by the delta Ring and Ball, therefore, the stiffening effect of hydrated lime at high temperature can be explained, at least partially, by the higher porosity as captured by the high Rigden air voids values. It can be concluded that the physical effect of hydrated lime essentially lies in its porosity which generates a higher stiffening effect than normal mineral fillers, as captured by the Rigden air void test. However, the high stiffening effect observed with hydrated lime at high temperature disappears below room temperature.

CHAPTER 3 – AGEING AND MOISTURE EFFECT ON BITUMINOUS MASTICS

3.1 MOISTURE

Moisture can cause many forms of premature damage in asphalt pavements, which entail substantial costs for the maintenance, repair and restoration of the infrastructure system. Several mechanisms can constantly degrade the properties of the material and affect the performance of asphalt mixtures (Varveri et al. 2015). This phenomenon is complex and involves thermodynamic, chemical, physical and mechanical processes.

According to Caro et al. (2008), thermodynamic theories, fracture mechanics, continuous damage mechanics and other analytical methodologies have been used to analyze the effect of moisture in asphalt mixtures. Some of the research areas that focus on understanding the fundamental phenomena that cause damage from moisture are the analysis of the contribution of the distribution and connectivity of the air voids, the transport of moisture and physical characteristics of the material and aggregates-binder adhesive bond.

3.1.1 TRANSPORT AND DIFFUSION

Three main ways of transporting moisture are described (Caro et al. 2008):

- Infiltration of surface waters (water permeability);
- Capillary increase of groundwater;
- Diffusion of water vapour.

The infiltration of water from the surface is the main source of moisture in the pavement and is directly related to rainfall, drainage conditions and material properties (Table 3.1). In addition, infiltration is strongly influenced by the permeability of asphalt mixtures. Several factors influence the permeability of a material, one of these is certainly the air-void content (Varveri et al. 2015).

Mixture	Correlation	Range of x in %	R2 value
Dense graded	ln (k) = 0,432x - 13,386	2-8	0,85
Stone mastic asphalt	ln (k) = 0,459x - 9,821	4-9	0,93
Porous asphalt	ln (k) = 0,209x - 7,017	12-20	0,9

Coarse graded 9,5 mm NMAS	$k = 0{,}0054x_{ip}^{4{,}9098}$	-	0,6925
Coarse graded 12,5 mm NMAS	$k = 0{,}0047x_{ip}^{4{,}8672}$	-	0,6423
Coarse graded 19 mm NMAS	$k = 0{,}0054x_{ip}^{4{,}9098}$	-	0,6925
Coarse graded 25 mm NMAS	$k = 0{,}6739x_{ip}^{3{,}7721}$	-	0,4964
Florida limestone	$k = 28{,}83PSP^{0{,}89}$	-	0,68
Georgia granite	$k = 4{,}35PSP1{,}181$	-	0,79

k=permeability, x=total air void content, x_{ip}=in-place air void content, PSP=pore size parameter of the mix

Table 3.1 - Correlations between permeability and air voids (Caro et al.2008).

However, field reports of pavements with severe moisture damage from regions with low rainfall levels suggest that vapour permeation and capillary rise in groundwater can be just as important ways of transporting moisture. Capillary increase is defined as the increase of a liquid above the zero pressure level due to a total upward force produced by the attraction of liquid molecules on a solid surface (Bowles 1984). In asphalt pavements, the capillary rise allows the water to be transported underground through the interconnected voids (Figure 3.1).

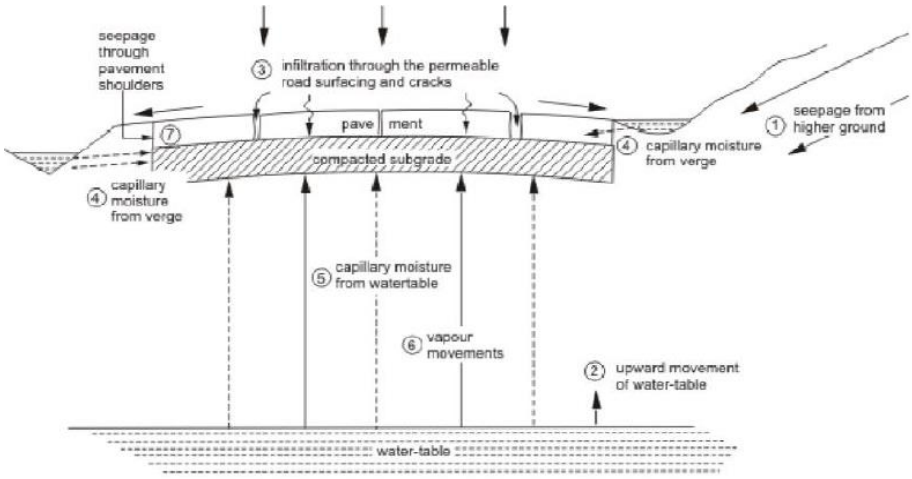

Figure 3.1 - Water transport

The way in which water can infiltrate the road pavement is strictly dependent on the permeability of the asphalt mixture. In general, moisture can be transported in a porous material in three different ways: diffusion, capillary flow, hydraulic flow, depending on the moisture content and driving potential. Diffusion occurs when particles of different substances mixed together create a flow of molecules from regions with higher concentration to regions with lower concentration. The concentration gradient guides the diffusion process.

This mechanism follows the dissolution process, in which the moisture molecules are absorbed by the bituminous material. The limit on the amount of chemicals that can be absorbed is called saturation. Moisture diffusion in bituminous materials is a long-term

process (Varveri et al. 2017). In general, the diffusion modality and the rapidity are strictly influenced by the properties of the material in contact and by their physical phase. Many factors influence diffusion: it depends on the specific characteristics of each material examined but also on external factors such as temperature. The following section describes the main factors that influence the typical diffusion of moisture in asphalt pavements.

3.1.2 FACTORS AFFECTING MOISTURE

The process of moisture transport in asphalt mixtures is influenced by many parameters, such as the microstructure of the mixture, the physico-chemical properties and the environmental conditions. Apeagyei et al. (2013) considered and discussed four main factors that influence the spread of moisture in asphalt concrete: type of aggregate, type of mineral filler, thickness of the sample, concentration of moisture. According to Varveri et al. (2017), other factors should be analyzed, such as temperature, air voids and bitumen.

Aggregates

The physical-chemical properties of the mineral aggregate strongly influence the processes of diffusion and transport of moisture in the asphalt mixture (Varveri et al. 2017). Arambula et al. (2010) conducted several experiments to measure the diffusion of water vapor on coarse aggregates, mixtures of fine aggregates and hot mix asphalt. Aggregates can be classified as hydrophilic or hydrophobic: hydrophilic aggregates such as granite tend to strip more easily than hydrophobic aggregates such as limestone. Mixtures with granite aggregates show moisture absorption profiles higher than those containing limestone aggregates, demonstrating the fact that the mineralogical and microstructural properties of the aggregates influence the diffusion of moisture and the transport processes. The studies show that the nature, origin, microstructure and mineralogy of the aggregates have a great impact on the moisture diffusion coefficient.

Fillers

The filler particles are added to the asphalt binder in order to increase its stiffness and improve the duration of fatigue up to permanent deformation (Kim et al. 2003). However, fillers can significantly change the diffusion characteristics of the binders. According to Varveri (2017), an increase in the filler content increases the rate of diffusion of moisture, while the type of filler has a significant impact on the overall diffusivity of the mastics. More detailed observations on the effects of mineral and active fillers with hydrated lime content will be addressed in the sub-section 3.1.5.

Thickness effect

The diffusion coefficient increases with increasing thickness, in particular for the calcareous aggregate mastic considered by Apeagyei et al. (2013) (Table 3.2).

Mastic type	Test method	n of specimen tested	Thickness (mm)	Moisture diffusion coefficient x 10^{-12} (m^2/s)
LA + LF	Dessicator jar	8	3,19±1,50	4,02±5,09
	Climatic chamber	3	3,37±1,04	2,59±0,22
LA + GF	Dessicator jar	6	2,63±1,08	1,33±0,74
	Climatic chamber	3	4,22±0,50	4,75±0,06
GA + LF	Dessicator jar	3	3,93±1,09	2,04±1,07
	Climatic chamber	3	3,37±0,27	2,87±0,01
GA + GF	Dessicator jar	3	4,32±0,71	2,17±0,48
	Climatic chamber	3	3,53±0,98	2,44±0,22

GA = granite aggregate, GF = granite filler, LA = limestone aggregate, LF= limestone filler

Table 3.2 - Moisture Diffusion Coefficient according to Apeagyei et al. (2013).

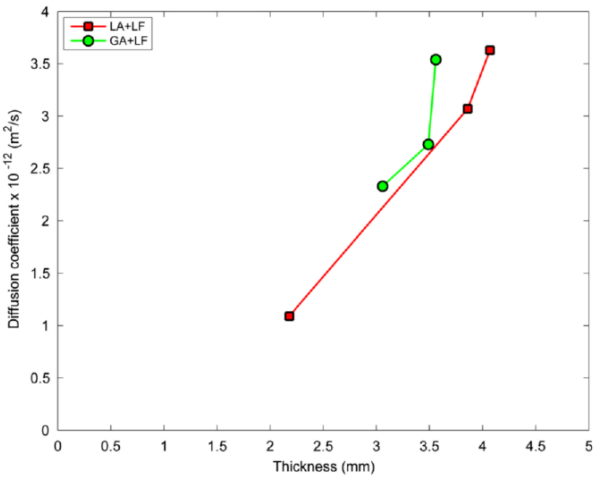

Figure 3.2 - Effects of aggregate type and specimen thickness on moisture diffusion coefficient

Figure 3.2 shows how the thickness of the sample influences the diffusion coefficient of bituminous binders containing the same limestone mineral filler (LF).

Moisture concentration

The dependence on the concentration of the diffusion of moisture in asphalt mastics (Apeagyei et al. 2013) was studied by tracing the diffusion coefficient against the absorption of equilibrium moisture for the various mastics considered. In all cases, the diffusion coefficient seems to decrease with increasing equilibrium moisture content.

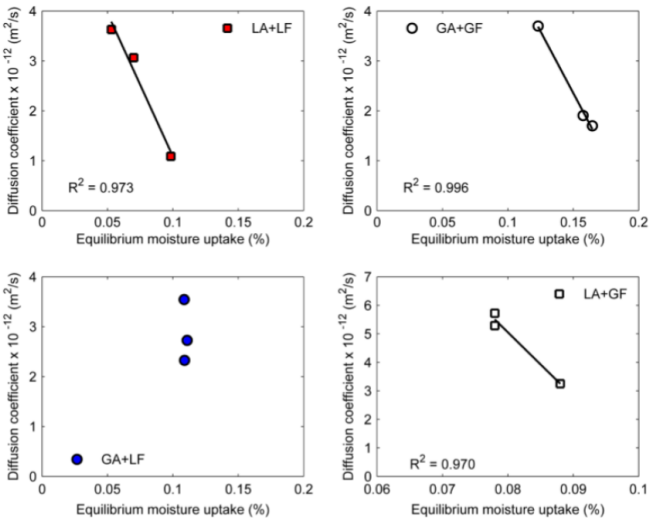

Figure 3.3 - Plots of diffusion coefficient against equilibrium moisture uptake for four different mastic types (Apeagyei et al. 2013).

The results in Figure 3.3 shown that the diffusion of moisture in the asphalt mastic depends on the concentration.

Temperature

As a general rule, diffusion increases as we increase temperature, because the diffusion rates enhances due to the higher velocity of the molecule (kinetic molecular theory).

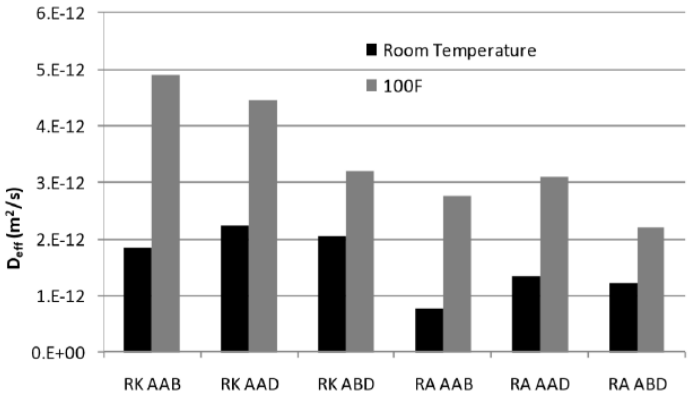

Figure 3.4 - Effective diffusivity on fine aggregate mixtures influenced by different temperatures Vasconcelos et al. (2011).

The results in Figure 3.4 (Vasconcelos et al. 2011) exhibit the influence of temperature on diffusion properties and it is easy to deduce that there is a correlation between temperature and moisture sorption.

Air voids

The air voids in the asphalt pavements facilitate the access of water and moisture to the mixes. Air voids offer points where water or moisture can easily flow through and move faster. The

higher the air void content in the pavement structure, the more permeable the system will be. The overall diffusivity of asphalt mixtures is a function of the air vacuum content and the void radius, which also induce damage to the pavement (Varveri et al, 2017).

Bitumen

The diffusion properties of moisture in bituminous materials are strongly influenced by the chemical composition. Filler particles can further modify the behaviour of bituminous binders subject to moisture conditioning. Bitumen types with high polarity have a strong affinity for polar molecules such as water. On the other hand, bitumen types with a lower polarity are not sensitive to water diffusion.

3.1.3 DAMAGE MECHANISM INDUCED BY MOISTURE

Two main mechanisms are linked to moisture damage in asphalt pavements: loss of cohesion and loss of adhesion (Figure 3.5). Cohesion is the internal strength of the asphalt binder (bitumen or mastic) due to intermolecular forces and is influenced by the rheological and chemical properties. Adhesion is the bond that keeps the binders attached to the aggregates.

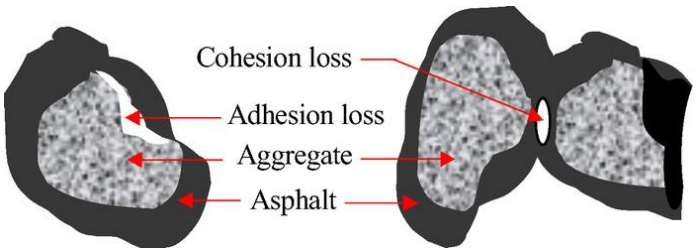

Figure 3.5 - Cohesive failure and adhesive failure stripping an aggregate from the mixture.

Moisture diffuses into the binding material through diffusion and softens it, reducing its cohesive strength and rigidity. Water can affect cohesion in several ways such as deterioration of the mastic due to saturation and swelling of the voids and can act as a solvent, reducing resistance and increasing permanent deformation.

Loss of adhesion can be described as the quantity of energy required to break the bond between asphalt binder and aggregate. Several factors influence the adhesion failure: Surface tension binder-aggregate, chemical composition of the system, viscosity of the binder, surface texture of the aggregate, porosity of the aggregate, moisture content and temperature of the aggregate during mixing phase.

3.1.4 DISTRESS MECHANISM IN ASPHALT PAVEMENTS DUE TO MOISTURE

Moisture damage can be defined as the loss of strength and durability in asphalt mixes due to the effects of moisture. A separation of the asphalt from the aggregate or the breaking of the asphalt texture in a mixture under the action of the load of cyclic traffic and the presence of moisture or water at the same time, is called stripping. This phenomenon, already described previously in sub-section 1.3.2, occurs due to the loss of adhesion between the binder and the aggregates in the presence of water. There are several stripping mechanisms: detachment, displacement, spontaneous emulsification, pore pressure, hydraulic abrasion.

3.1.5 EFFECTS OF ACTIVE FILLER ON THE MOISTURE SUSCEPTIBILITY

Kringos (et al. 2007) states that for small percentages of the presence of mineral filler the influence of the typology on the diffusion of moisture seems to be minimal (Fig. 3.6). However, as the presence of the filler in the mixture increases, the replacement of a mineral filler with an active one (hydrated lime) improves the sensitivity of the asphalt mixtures to moisture. This means that the application of mineral fillers implies longer times to reach the equilibrium moisture content, compared to limestone particles.

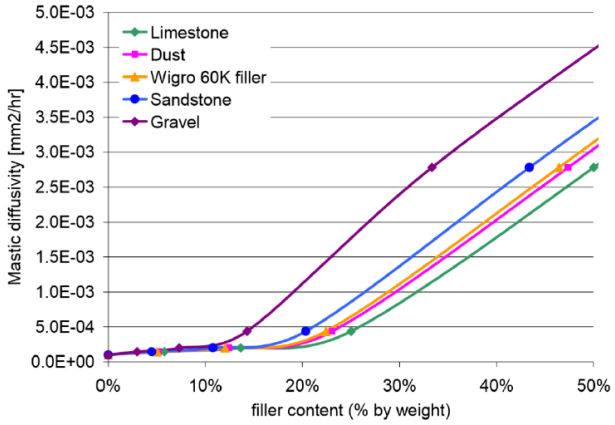

Figure 3.6 - Mastic diffusivity as a function of filler content for different fillers

The finite element analysis performed by Apeagyei et al. (2013) shows two different mastics (with granite filler and limestone filler) subject to moisture (Fig. 3.7).

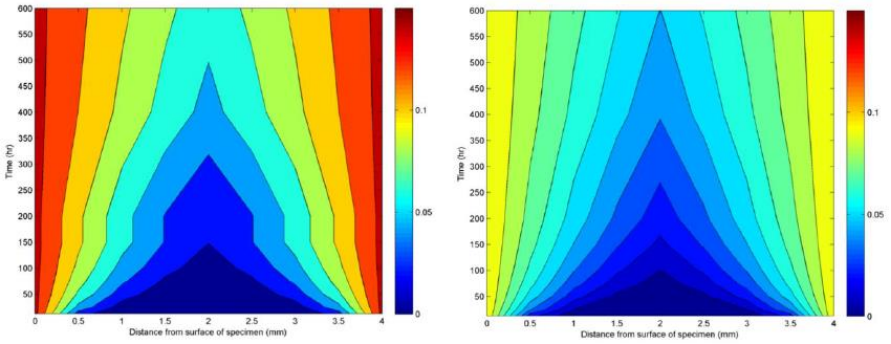

Figure 3.7 - Simulation of moisture diffusion in asphalt mastic containing granite filler (on the left) and limestone filler (on the right) (Apeagyei et al. 2013).

Equilibrium moisture uptake (saturation of the mastic) is relatively higher in mixtures containing granite fillers compared with limestone fillers mixtures. This means that granite mastics are able to absorb more moisture. In contrast, the diffusion coefficient of limestone mastics is higher than granite, meaning that limestone mixtures reach saturation faster than granite mastic.

3.2 AGEING

Aging of the binder represents one of the key factors that determine the useful life of a mixture of bituminous conglomerate. The aging process is strongly linked to the thermal susceptibility of bitumen as its structure is rather complex. It evolves with thermo-dependent processes resulting from molecular rearrangement which have not yet been fully understood and studied. In addition, the molecules can undergo irreversible evolutions due to chemical aging, which is generally considered to be the sum of oxidation and polymerization reactions, and to a lesser extent, the volatilization of lighter substances. In any case, it must be borne in mind that the susceptibility of a bitumen to chemical aging mainly depends on two predominant factors: from the crude oil of origin and from the production process (Read, 2003). Regardless of the process by which bitumen is produced, the aging phenomenon can be divided into two different types, as they occur at different times:

- Primary or short-term aging:
    - In the production phase of bituminous conglomerates;
    - During the transportation and paving phase of bituminous conglomerates.
- Secondary or long-term aging:
    - During the pavement service life.

In Fig. 3.8, the effect of STA and LTA on bitumen's rheology is presented through the ratio of its viscosity in the aged state over the fresh state.

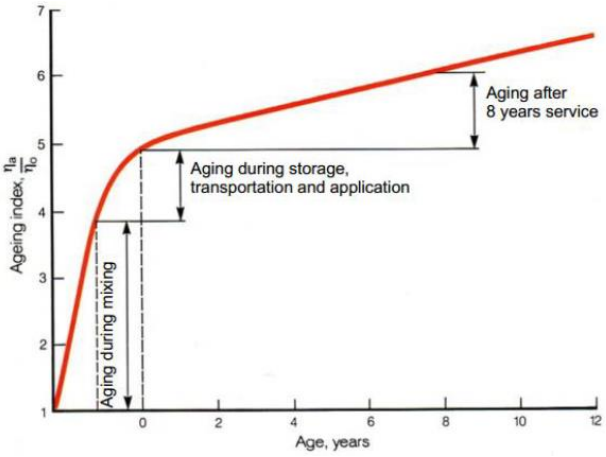

Figure 3.8 - The effect of STA and LTA on bitumen's rheology.

Primary aging, called "Short-Term Aging - STA" occurs at a variable temperature, depending on the type of bitumen used, a typical value is 160 ° C. The process is of short temporal duration, if compared to the long term one, it is generated during the mixing phase of the binder with the aggregates and the spreading and compaction process. Short-Term Aging is reproduced in the laboratory through the "Rolling Thin Film Oven Test - RTFOT" test (EN 12607 - ASTM D2872). The test consists in subjecting a thin layer of bitumen, ~ 1.25 mm, to a jet of hot air (163 ° C) for 75 minutes.

Secondary aging, defined in this case as "Long-Term Aging - LTA", is a process that can last for decades, as it develops throughout the service life of the road. The degree of aging depends on a set of factors that concur simultaneously and are sometimes hardly divisible. The position of the layer in the pavement structure has a significant influence, the surface ones are more subject to aging than the deep layers. In relation to what has just been said, a determining factor is represented by climatic conditions since UV rays and / or rigid winter temperatures considerably affect the evolution of aging. In addition to this, the physical characteristics of the layer, the mix design and consequently the porosity, are parameters to be taken into account when studying Long-Term Aging. The reproduction in the laboratory of this type of aging is very complex, the test most used is the "Pressure Aging Vessel Test - PAV" (EN 14769 - ASTM D6521), in which the bitumen is put under pressure and subjected to a jet of air at a variable temperature depending on the maximum achievable in situ. The goal is to reproduce an aging that could undergo the binder in about 4-8 years. Several

mechanisms have been identified that promote bitumen aging. Among the main ones we find the following.

Oxidation

Oxidation refers to the reaction of atmospheric oxygen with bitumen, leading to irreversible hardening of the material. The oxidation rate is a function of the composition of bitumen, temperature and time of exposure. Hardening of bitumen due to oxidation has been identified as the major cause of ageing. As mentioned before, oxidation is a mechanism responsible for both the STA and LTA of the binder.

Volatilization

Volatilization refers to the evaporation of the volatile components of bitumen and is mainly dependent on temperature and exposure conditions. The lighter fractions of bitumen tend to evaporate above their boiling temperature. Volatilization is a mechanism that is more significant during the mixing process of the asphalt mixture's constituents (STA), where high temperatures are involved.

Polymerization

Polymerization describes the process by which similar molecules form associations, leading to the configuration of large molecules. Consequently, the molecular weight increases, which translates into a progressive hardening of the material. At low temperatures, where the viscosity of the bitumen is high, the polymerization rate is considered low.

3.2.1 EFFECT OF OXIDATION ON THE CHEMICAL COMPOSITION OF BITUMEN

The mechanism of bitumen oxidation, deal with fractional changes (i.e. changes on SARA components) and molecular changes in the bitumen micro-structure

Compositional changes in bitumen during oxidative ageing can be described by the movement of components from the non-polar fractions to the more polar fractions, due to the formation of oxygen-containing functional groups in bitumen molecules. The aging causes a decrease in the content of aromatics and consequently an increase in the content of resins and a greater value of asphaltenes. In this opinion it is accepted that the aromatics generate resins which in turn produce asphaltenes while the saturated ones remain almost unchanged, this is due to their low thermal reactivity. Fig.3.9 graphically represents the fractional changes as a function of ageing time.

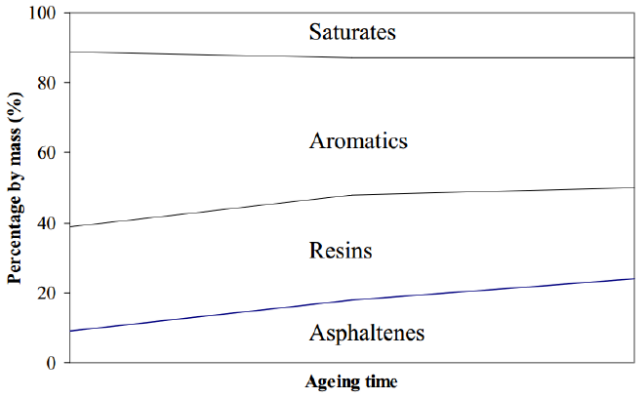

Figure 3.9 - Fractional changes of bitumen as a function of ageing time.

However, the relative changes in the mass percentages of the Corbett (SARA) fractions, when the different fractions are aged as a whole, provide little information with respect to the chemical reactions that occur within the fractions themselves and/or the susceptibility of the different fractions to oxidation (Petersen 2009). In an effort to gain additional chemical insight, Petersen et al. (1974) oxidized separately, the SARA fractions from a bitumen: based on the obtained results, they were able to demonstrate that reactivity with oxygen increases with increasing fraction polarity.

Changes on molecular level, that occur during oxidation of bitumen, are usually studied from the aspect of the formation of chemical functional groups in bitumen molecules. Upon oxidation the main occurring chemical functionalities are ketones and sulfoxides whereas dicarboxylic anhydrides and carboxylic acids are also formed. Ketones, dicarboxylic anhydrides and carboxylic acids are usually referred to as the carbonyls functional group (Wu 2009). In Fig. 3.10, the structural formulas of the functional groups formed during oxidative ageing are presented.

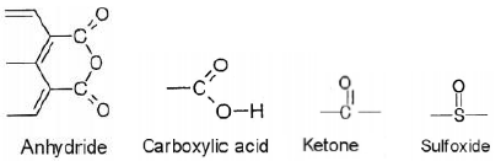

Figure 3.10 - Structural formulas of the functional groups formed during oxidative ageing

Sulfoxides, result from the oxidation of the sulphides present in the bitumen's molecules. At the initial oxidation spurt, the rate of formation of sulfoxides is much higher than the one of ketones. At this initial stage, oxygen reacts with hydrocarbons to form hyperoxides. There is a rapid reaction, characterized by the scavenger action of sulphides, according to which the latter react with hydroperoxides to form sulfoxides. However, when high temperatures are

involved during oxidation, the hydroperoxides may decompose, due to their thermal instability, and free radicals are formed which favour the formation of ketones. As a result, more ketones are formed at the expense of sulfoxides. The rate of sulfoxides formation over ketones is also highly dependent on the sulphur content of bitumen (Petersen 2009). By comparing the oxidation products formed in different bitumen and their oxidative hardening, the following observations were made: bitumen in which approximately the same amounts of ketones and sulfoxides were formed exhibited quite different age-hardening. On the other hand, bitumen which showed similar oxidative hardening, contained fairly different amounts of oxygenated products. These observations suggest that, the susceptibility of different bitumen to oxidative hardening may be more accurately described by the effect of the formation of oxygenated products on its components' compatibility rather than the actual amounts of ketones and sulfoxides formed.

3.2.2 BITUMINOUS BINDERS AGEING ASSESSMENT

The aging of the binder has effects not only on the chemical composition but also on the rheological behaviour of the bitumen; consequently, all rheological indices are used to study the aging problem. The extent of ageing of bitumen and/or bituminous mixtures is usually assessed by the degree of change of one or more physical properties upon ageing, expressed through the so-called Ageing Indices (AI).

$$AI = \frac{X_{aged}}{X_{unaged}}$$

where,

X_{Aged}=Physical property after ageing

X_{Unaged}=Physical property at the unaged stage.

The utilized physical property can vary between viscosity (η), or more fundamental properties such as the complex shear modulus (G*).

As pointed out in sub-section 3.2 oxidative ageing of bitumen leads to an increase of its polar functional groups (i.e. asphaltenes) with a simultaneous decrease of the naphthene aromatics and resins, while saturates show negligible chemical reactivity. The extent of ageing of the binder can be expressed through the Gaestel Index (IC):

$$IC = \frac{Asphaltenes + Saturates}{Aromatics + Resins}$$

More severe ageing is captured through an increase of the IC. Fourier transform infrared spectroscopy (FTIR) is a technique used in identifying changes in the chemical structure of bituminous binders with oxidative aging. A detailed description of the basic principles of this method is provided in Sub-Section 4.5.1. As mentioned above, sulfoxides (S=O) and carbonyls (i.e. ketones, dicarboxylic anhydrides and carboxylic acids, C=O) are the main products formed in the microstructure of bitumen after oxidative aging. The formation of these functional groups can be traced, through visible peaks, in the infrared spectrum obtained by FTIR, to specific wave numbers, i.e. sulfoxides at ~1030 cm^{-1} and carbonyls (ketones) at ~1700 cm^{-1} (Fig. 3.11).

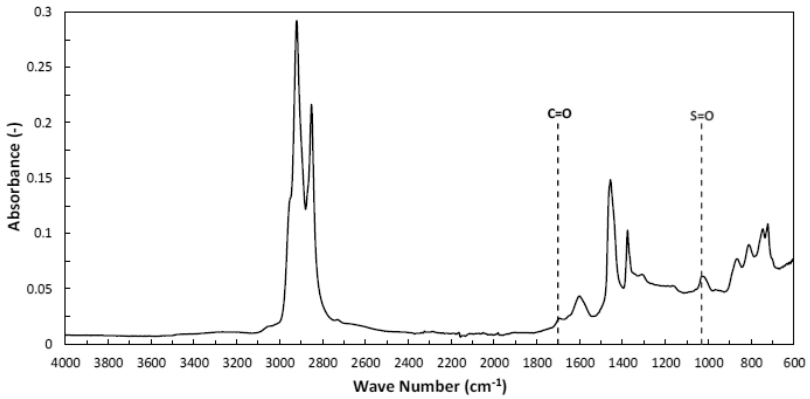

Figure 3.11 - Infrared spectrum, carbonyls and sulfoxides peaks.

From the analysis of the band areas around the aforementioned wave numbers, indices for carbonyls (CI) and sulfoxides (SI) can be derived which can describe the degree of oxidative aging of the bitumen examined. There are several approaches by which the analysis of the obtained spectra can be performed. It can be performed on original or normalized spectra. The quantitative analyzes of some functional groups can be performed by directly obtaining the value of the respective peak (maximum absorbance value) or by integrating the area, determined by predefined limit wave numbers, below the absorbance spectrum and around the peak of interest . Finally, the above values can be obtained by considering an absolute or tangential baseline (Hofko et al. 2017). Fig. 3.12 Schematically illustrates all the approaches mentioned above.

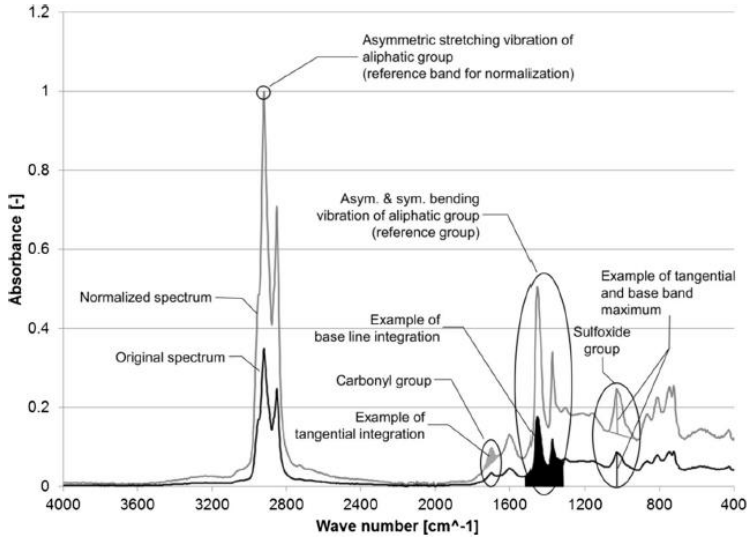

Figure 3.12 - Various approaches for infrared spectra analysis (Hofko et al. 2017).

As regards mastics, the derivation of CI and SI should be performed on normalized spectra, using the integration of areas and the absolute baseline approach, i.e. the IBN method.

$$IB_{n,i} = \int_{w_{l,i}}^{w_{u,i}} a_{norm}(w)dw$$

Where:

- $a_{norm}(w)$, normalized absorbance value at wavenumber w;
- $w_{u,i}$, upper wavenumber limit for structural group i;
- $w_{l,i}$, lower wavenumber limit for structural group i.

The structural groups i can be:

- The carbonyl group (C=O):1666–1746 cm^{-1}
- The sulfoxide group (S=O): 924–1066 cm^{-1}

3.3 COMBINATION OF MOISTURE AND AGEING

In the previous section, the phenomena of diffusion of moisture in the mixtures and oxidative aging have been described. In asphalt pavements, both air and water flow mainly through interconnected air voids and therefore the damage to moisture becomes more serious with the aging of the asphalt pavement. Therefore, it is important to consider aging when assessing the moisture sensitivity of the asphalt mixture. For this reason it is essential to carry out an analysis where these two actions take place in a combined way.

Some studies have investigated possible ways to couple the effect of aging and the damage of moisture on the asphalt mixture Das et al. (2015) has established the necessary formulations for the modeling of the finite elements (FE) for the diffusion process of oxygen and moisture. By integrating the morphology of the mixture, a framework has been proposed capable of capturing the combined effect of aging and damage from moisture. Such an FE model can help find trends and relationships that can aid in the development of the predictive model of pavement performance. Furthermore, from this, it is possible to understand the key parameters that are mainly responsible for the premature damage induced by aging with the moisture of the asphalt pavements. The micro-structural investigation carried out has shown strong indications that, depending on the bitumen and its conditioning, thin films soluble in water are formed due to aging. This means that aging and damage from moisture are strongly interconnected and this should therefore be considered in the design of the materials and in the prediction of its long-term performance.

Ma et al. (2011) performed an analysis of the damage from aging and moisture coupled directly to the materials: the effect of aging due to humidity and the mechanism of the asphalt binder during the service life of the pavement was simulated in laboratory. The pressure aging vessel (PAV) test that simulates the long-term aging of the binder during the service life of the pavement has been modified by adding 10 ml of water to capture the long-term aging effect moisture of the binder. Ma et al. (2011) concluded that different factors such as heat, oxygen, pressure, and water have mutual effect on the aging process of asphalt binder. The moisture condition together with heat and oxygen results in stiffer and more brittle binder and eventually leads to more low-temperature cracking propensity. Therefore, moisture plays a notable role in long-term aging of asphalt binder and has detrimental effect on the durability of asphalt pavements.

In the mastic, the filler can slow down the aging speed of asphalt acting like antioxidant. However, the age hardening continues to occur and moisture condition causes not only accelerated aging of the bitumen in the mastic but also accelerated degradation of the filler in the mastic. Thus, if mastic is used in severe moisture condition, a filler with well resistance to moisture aging should be considered. Therefore, PAV aging in the presence of water accelerates the aging process. Furthermore, there is a linear relationship between a physical property (rheology) and a chemical property (carbonyl content) after PAV aging, but water does not affect this linear relationship.

CHAPTER 4 - MATERIALS AND TESTING METHODS

4.1 BITUMEN

For the experimental study of this research, an unmodified bitumen was used, available in the TU Delft Pavement Engineering laboratory, supplied by Q8, Kuwait Petroleum Corporation. The bitumen density was assumed at 1.03 gr/cm^3. Originally bitumen (Fig. 4.1) was classified as bitumen with a degree of penetration of 70/100. The penetration test and the ring & ball test were carried out on it to actually check its classification.

Figure 4.1 – Can of bitumen 40/60 at TU Delft laboratory.

Penetration grade

The penetration test according to NEN –EN 1426 allows to classify the bitumen according to the scale of the degree of penetration. The preparation consists of heating 100 grams of bitumen, pouring it into a metal can, cooling to room temperature for 2 hours and placing the sample in a water bath at 25 °C for another 2 hours. Bitumen penetration is the measure of how a specific needle can guide in the sample. Three measurements were performed, in three different positions of the sample and with different needles (Table 4.1). During the test, the samples were kept in water to maintain the test temperature at the specified value (25 °C) for the duration of the measurements. Based on the results, bitumen was classified as bitumen with a degree of penetration of 40/60.

Measurement	Penetration at 25°C (dmm)	Average penetration (dmm)
1	49	
2	50	48.67
3	47	

Table 4.1 - Penetration test results

Softening point

The ring & ball test is performed to determine the bitumen softening point according to NEN-EN 1427. The bitumen samples are bound by a metal ring and a ball is placed on them. The systems are immersed in a 5 °C water bath. The heater under the bath raises the water temperature by 5 ° C / min. As soon as the bitumen touches the bottom plate (due to the softening of the material and the weight of the ball), the temperature is recorded. Mastoras (2019) tested two sets of samples and 4 measurements were recorded in total (Table 4.2). The results show an average softening point of 48.4 °C.

Measurement	Softening point (°C)	Average Softening point (°C)
1	48	48.38
2	48.2	
3	48.5	
4	48.8	

Table 4.2 - Ring & Ball test results according to Mastoras (2019).

4.2 FILLER

Six different mineral fillers were employed for the purpose of the present research. A brief description of each material and its purpose of use is provided below.

HYDRATED LIMESTONE

Hydrated lime is an active filler supplied by *Sibelco-Winterswijk*. 93.2% of it is calcium hydroxide $Ca(OH)_2$. Its features presented in Sub-Section 2.3.1.

WIGRO60K

Wigro60K has been provided by *Sibelco-Winterswijk* and constitutes the specified by the regulation mineral filler that is used in the production of PA mixtures in the Netherlands. This mineral filler is composed of limestone with the incorporation of 26.4wt% of hydrated lime. The specification for Wigro60K are reported in the Table 4.3.

ANALYSIS	UNIT OF MEASURE	VALUE	STANDARD
Particle's size distribution			*EN 993-10*
0.063 mm	% (mm/mm)	83	
0.125 mm	% (mm/mm)	95	
2.000 mm	% (mm/mm)	100	
Bitumen number	ml/100g	59	*EN 13179-2*
$Ca(OH)_2$	% (mm/mm)	26.4	

Mass loss at 110 °C	% (mm/mm)	0.4	*EN 1097-5*
Water Solubility	% (mm/mm)	6.1	*EN 1744-1*
Density	Mg/m^3	2.57	*EN 1097-7*
Fractional Voids (Ridgen)	% (v/v)	47	*EN 1097-4*

Table 4.3 – Specification of Wigro60K.

WIGRO50K+

Wigro50K+ was provided by *Sibelco-Winterswijk* and is composed of limestone with the incorporation of 13.3wt% of hydrated lime. Compared to the previous fillers, there is a lower presence of calcium hydroxide therefore that of calcium carbonate CaCO3 and calcium oxide CaO is higher. In essence, Wigro50K+ is the same material as Wigro 60K, with half percentage of hydrated lime. Specification are shown in the Table 4.4.

ANALYSIS	UNIT OF MEASURE	VALUE	STANDARD
Particle's size distribution			*EN 993-10*
0.063 mm	% (mm/mm)	81	
0.125 mm	% (mm/mm)	94	
2.000 mm	% (mm/mm)	100	
Bitumen number	ml/100g	49	*EN 13179-2*
$Ca(OH)_2$	% (mm/mm)	13.3	
Mass loss at 110 °C	% (mm/mm)	0.2	*EN 1097-5*
Water Solubility	% (mm/mm)	6.5	*EN 1744-1*
Density	Mg/m^3	2.65	*EN 1097-7*
Fractional Voids (Ridgen)	% (v/v)	41	*EN 1097-4*

Table 4.4 – Specification of Wigro50K+.

WIGRO50K

Wigro50K was provided by *Sibelco-Winterswijk* and is composed of limestone with the incorporation of 5.7wt% of hydrated lime: an even lower percentage of calcium hydroxide in limestone leads to a significant increase in calcium carbonate. Specification are shown in the Table 4.5.

ANALYSIS	UNIT OF MEASURE	VALUE	STANDARD
Particle's size distribution			*EN 993-10*
0.063 mm	% (mm/mm)	80	
0.125 mm	% (mm/mm)	93	
2.000 mm	% (mm/mm)	100	
Bitumen number	ml/100g	47	*EN 13179-2*

$Ca(OH)_2$	% (mm/mm)	5.7	
Mass loss at 110 °C	% (mm/mm)	0.3	*EN 1097-5*
Water Solubility	% (mm/mm)	5.8	*EN 1744-1*
Density	Mg/m^3	2.72	*EN 1097-7*
Fractional Voids (Ridgen)	% (v/v)	40	*EN 1097-4*

Table 4.5 - Specification of Wigro50K.

WIGRO

Wigro was provided by *Sibelco-Winterswijk* and is composed of limestone, or calcium carbonate ($CaCO_3$). In essence, Wigro is the same material as previous Wigro, in the absence of the hydrated lime. So, the effect of hydrated lime on ageing of bituminous mixtures can be evaluated, when its performance is compared to that of Wigro 60K, Wigro50K+ and Wigro50K. Specification are shown in the Table 4.6.

ANALYSIS	UNIT OF MEASURE	VALUE	STANDARD
Particle's size distribution			*EN 993-10*
0.063 mm	% (mm/mm)	85	
0.125 mm	% (mm/mm)	95	
2.000 mm	% (mm/mm)	100	
Bitumen number	ml/100g	44	*EN 13179-2*
$Ca(OH)_2$	% (mm/mm)	0	
Mass loss at 110 °C	% (mm/mm)	0.4	*EN 1097-5*
Water Solubility	% (mm/mm)	1.7	*EN 1744-1*
Density	Mg/m^3	2.78	*EN 1097-7*
Fractional Voids (Ridgen)	% (v/v)	38	*EN 1097-4*

Table 4.6 - Specification of Wigro.

QUARTZ

Silverbond M6 is a commercial filler provided by *Sibelco-Dessel*, which is exclusively comprised of quartz. Silverbond M6, hereafter designated simply as quartz, was included in the research due to its "inert" nature. It was hypothesized that, by virtue of its "inert" nature, no chemical interactions will occur between the mineral filler particles and bitumen during the ageing process. Having excluded the latter, quartz can be used to demonstrate any potential effect of the mineral fillers on the ageing of bituminous mixtures due to their physical presence in the mastics. Specification are shown in the Table 4.7.

ANALYSIS	UNIT OF MEASURE	VALUE	STANDARD
Particle's size distribution			*EN 993-10*
0.063 mm	% (mm/mm)	86	
0.125 mm	% (mm/mm)	95	
2.000 mm	% (mm/mm)	100	
Bitumen number	ml/100g	40	*EN 13179-2*
$Ca(OH)_2$	% (mm/mm)	0	
Mass loss at 110 °C	% (mm/mm)	0.12	*EN 1097-5*
Water Solubility	% (mm/mm)	-	*EN 1744-1*
Density	Mg/m^3	2.65	*EN 1097-7*
Fractional Voids (Ridgen)	% (v/v)	33.07	*EN 1097-4*

Table 4.7 - Specification of Quartz.

4.3 MATERIAL PREPARATIONS

Six different mastics and neat bitumen were prepared for testing. The necessary bitumen was first preheated to be processed and divided into five 350 g containers (one for each condition). Subsequently, each container is further heated separately for mixing with the fillers. The applied heating temperature and time, in the production process, were chosen in accordance with NEN-EN 12594. The norm specifies that the heating temperature of bitumen should be 80 to 90°C above its softening point and the duration of heating should not exceed 2 hours. Based on the softening point of the utilized bitumen (48.4°C), a heating temperature of 130°C was selected. The heating duration was limited to 1 hour as it was regarded sufficient for the bitumen to develop the necessary workability and for the mineral fillers to expel any moisture residue.

4.3.1 BITUMEN PREPARATION

In addition to the various mastics also neat bitumen samples were prepared for the purpose of the present research. It should be noted that it is of immense importance for this study that all materials (i.e. mastics and bitumen) undergo the same ageing. In order to avoid any undesired effects in the production phase that could lead to variant ageing level between the different materials, the preparation of bitumen was slightly modified to match the heating times of the mastics. More specifically, in the mastics production process, after the initial blending of the materials the composite was placed in the stove for 30 minutes at 130°C. As it is easily conceivable, this extra heating time may (slightly) contribute to the age-hardening of the mastics. For that reason, prior to sampling, bitumen was heated-up in the stove for a total of 1

hour and 30 minutes, instead of 1 hour, at 130°C, to compensate for the difference with the mastics. Analytically, the steps followed for the sampling of neat bitumen are listed below:

- Bitumen was heated-up in the stove for 1 hour at 130°C;
- After the initial heating-up, bitumen was manually blended for 5 minutes on a heating plate set at 130°C;
- The material was placed in the stove for another 30 minutes at 130°C, to match the age-hardening of the mastics;
- The bitumen was manually blended for 1 minute;
- Depending on the condition procedure the bitumen is poured into the silicon molds for subsequent tests or into the PAV plate for aging.

4.3.1 MASTICS PREPARATION

All mastics were prepared with a filler to bitumen mass ratio equal to 1 (f/b=1 by mass), following the standard Dutch mix design. The concentration of the mineral filler has an impact on the ageing of bituminous mixtures. In this study, this parameter was kept constant and, thus, the effect of the mineral matter on bitumen ageing due to variations in its content was not investigated. The production of mastics was performed according to the following steps:

- 50 g are poured into metal containers for each filler (Figure 4.2);

Figure 4.2 - The six different fillers used.

- Bitumen and the six different filler were heated-up in the stove for 1 hour at 130°C (Figure 4.3);

Figure 4.3 - The oven used.

- The appropriate amount of bitumen, that is 50 g to achieve the intended filler to bitumen ratio (f/b=1), was added to filler and the materials were manually stirred for 5 minutes. The applied stirring time ensured that a homogeneous blend was achieved while the workability of the mastic was kept at a tolerable level. The latter was enhanced by making use of a heating plate, set at 130°C, during blending of the materials.
- The initial blending was followed by placing the mastic in the stove for 30 minutes at 130°C. This step was added to enhance the bonding of the materials through application of heat.
- The mastic was manually re-stirred for 1 minute to regain any mineral filler particles that might had migrated towards the bottom of the can and could affect the homogeneity of the mixture (Figure 4.4).

Figure 4.4 - Stirring the bitumen with the filler on the heating plate.

- Depending on the condition procedure (Sub-Section 4.4) the mastic is poured into the silicon molds for subsequent tests or into the PAV plate for aging.

4.4 CONDITION PROCEDURE

In the following study we want to compare the performance of mastics with the phenomena of aging, diffusion of humidity and the combined effect. To satisfy the aging request, the standard aging protocol with PAV is used; as regards the diffusion of humidity without aging, PAV is used with the presence of water inside but with inert gas. Finally, to evaluate the combined effect of humidity and aging, the Standard PAV protocol is used with the addition of water for the diffusion of humidity. So, to compare the resistance to moisture and aging damage of the various mastics, five different conditions were adopted, one with the "fresh" materials and four through a conditioning process (Table 4.8)

Conditioning	Protocol
1	Fresh state
2	Standard PAV
3	Standard PAV + moisture
4	Nitrogen PAV
5	Nitrogen PAV + moisture

Table 4.8 – Condition procedure

4.4.1 FRESH STATE

Once the mixes of filler and bitumen are prepared and heated in the oven as indicated in Sub-Section 4.3 these are poured into silicone molds the size of 2 € coins and placed in the freezer at -25 °C for half an hour (Figure 4.5). Then the samples are removed from the molds and stored in a 10°C climate cell.

Figure 4.5 – Sample placed in the freezer.

4.4.2 AGEING CONDITIONING

PAV samples preparation

The PAV (Fig. 4.6) is an aging method that developed by the SHRP-A-002A research team, with the purpose to provide accelerated laboratory aging. The test is conducted in accordance with NEN-EN 14769. The norm, associated with the PAV aging, specifies that for aging temperatures of 90, 100 or 110 °C, 20 hours were found to be an appropriate aging duration.

Figure 4.6 – The Pressure Ageing Vessel.

In this study, the test was conducted at a temperature of 90° C and 2.1 MPa (~ 300 psi) of pressure for a duration of 20 hours. It should be noted that the aging time can be a parameter that could influence the effect of mineral fillers on the aging of bitumen. In this study this parameter was kept constant (i.e. 20 hours) and no time intervals were considered in the aging process. Mastics and neat bitumen are prepared as described in Section 4.3. Once the samples are created they are then poured into the PAV pan (Figure 4.7).

Figure 4.7 - Sample poured into the PAV pan.

During PAV ageing oxygen diffuses into the bituminous film. To allow for a comparison among the various materials, it is of immense importance that the geometry of the film, namely its thickness, is kept constant. NEN-EN 14769 specifies that 50 g of neat bitumen are

placed in the PAV pan. Knowing the bitumen mass, the bitumen density (value at Sub-Section 4.1) and the PAV pan diameter (Table 4.9), one can obtain a film thickness in the metal tray approximately equal to 0.315 cm, through trivial calculations.

Diameter (cm)	Thickness (cm)	Area (cm^2)
14	0,95	153,94

Table 4.9 - PAV pan dimensions.

$$t_i = \frac{4 \cdot m_i}{\rho_i \cdot \pi \cdot D_{pan}^2}$$

Where:

t_i = Thickness in the PAV pan of material (i) ([L]);
m_i = The mass of material (i) ([M]);
ρ_i = The density of material (i) ([M]/[V]);
D_{pan} = The diameter of the PAV pan ([L2]).

All mastics were prepared with a f/b=1 by mass. Knowing the mass and the density (from Table 4.3 to 4.7) of the individual mastic ingredients one can obtain their volume percentages in the final mastic blend. The density of the various mastics can be determined through equation:

$$\rho_{M,i} = \rho_b \cdot V_{b,i} + \rho_{f,i} \cdot V_{f,i}$$

Where:

$\rho_{M,i}$ = Density of mastic (i) ([M]/[V]);
ρ_b = Density of bitumen ([M]/[V])
$V_{b,i}$ = Volume percentage of bitumen in mastic (i);
$\rho_{f,i}$ = Density of mineral filler (i) ([M]/[V]);
$V_{f,i}$ = Volume percentage of mineral filler (i) in mastic (i).

The results are presented in Table 4.10:

Mastic	Density (gr/cm^3)
Mastic HYD	1,404
Mastic W60K	1,472
Mastic W50K+	1,483

Mastic W50K	1,495
Mastic W	1,503
Mastic QZ	1,481

Table 4.10 – Density of the mastics.

With the densities of the mastics known, solving the equation for the mass, with a predefined film thickness of 0.315 cm, the necessary amount of each mastic, that will lead to the desired material film thickness in the PAV pan (i.e. 0.315 cm) can be obtained (Table 4.11).

Mastic	Mass in the PAV pan (gr)
Mastic HYD	68,15
Mastic W60K	71,45
Mastic W50K+	71,98
Mastic W50K	72,56
Mastic W	72,95
Mastic QZ	71,88

Table 4.11 – Mastic mass to obtain the required thickness.

Figure 4.8 - Mastic samples in PAV dishes.

The completion of the accelerated aging method was followed by positioning the aged materials in the stove at 150 °C for 30 minutes, as suggested in NEN-EN 14769. This step is carried out so that the aged material becomes sufficiently fluid to allow the removal of boils through manual stirring. The aged materials were manually stirred for 1 minute, on a heating plate set at 170 °C, then poured into the silicone molds as for the "fresh" samples and cooled in the freezer at -25°C for 30 minutes.

All the samples obtained are stored in a 10°C climatic cell pending subsequent tests.

STANDARD PAV

The first aging condition is that of using the standard parameters for the PAV oven, in accordance with NEN-EN 14769.

For this it will be set with the following parameters:

- Temperature = 90°C;
- Pressure = 2.1 MPa (~ 300 psi);
- Time = 20 hours.

With this condition we will evaluate changes in the chemical and rheological properties of bitumen and mastics exclusively due to oxidative aging.

Plates containing only fillers are also inserted inside the PAV: in this way a chemical analysis can be carried out to study the degradation effect of hydrated lime due to aging.

MOISTURE PAV

The second condition consists in oxidative aging with the presence of moisture. At the PAV with Standard conditions a PAV pan containing 15 ml of water was included (Figure 4.9).

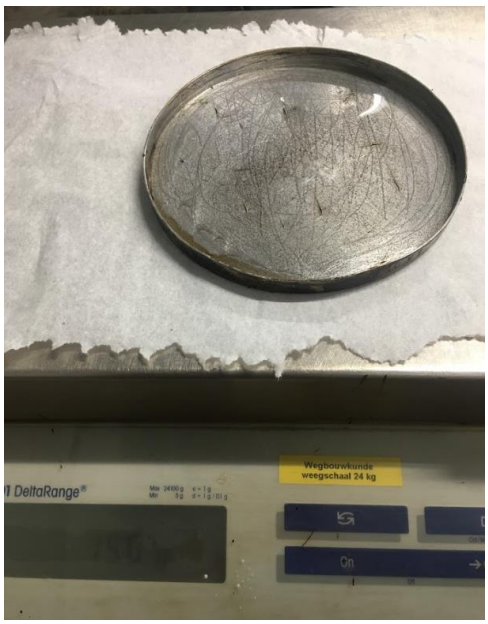

Figure 4.9 - PAV pan containing water for conditioning.

The presence of water inside the PAV must be assessed so as not to incur risks of overpressure and oversaturation. The volume of the PAV was calculated, by measuring the dimensions with the ruler and adding the volume of the cylinder and the two domes that make up the pressure oven:

$$V_{tot} = \frac{1}{2}\pi h(3r^3 + h^2) + \pi r^2 H$$

Where:

r: radius of the oven dome;
h: depth of the dome;
H: cylinder length.

Through a simple calculation software (*HW4 Software – Rotronic*), the parameters of Volume, Temperature and Pressure of the PAV have been inserted with the presence of 15 mL of water obtaining the relative moisture value inside the PAV and the partial pressure of the water (Table 4.12).

Parameters	**Values**
PAV Volume	47,16 L
PAV Temperature	90 °C
PAV Pressure	2,1 MPa
Water quantity	15 ml
ϱ air (PAV condition)	19,95 kg/m³
HR Moisture Relative	75%
Vapour Concentration	313,71 g/m³
Vapour partial pressure	0,0525 MPa

Table 4.12 - Parameters of the PAV for conditioning with 15 ml of water.

The quantity of water vapour present in the air is directly proportional to the pressure of water vapour (pressure of its vapour when the balance between the liquid phase and the gas phase is reached).

$$UR = \frac{Pv}{Ps} \cdot 100$$

Where:

Pv: partial pressure of the water vapour present in the air;
Ps: partial pressure of water-saturated vapour.

For the calculation of the partial pressure of the water vapour gas, the state equation of perfect gases is applied, considering temperature and volume remain constant, the equation becomes:

$$P_i = \frac{n_i}{n_{tot}} \cdot P_{tot}$$

Where:

$\frac{n_i}{n_{tot}}$: molar fraction of gas i;

P_{tot}: total pressure in the PAV.

75% relative humidity means that the air inside the PAV is not saturated. After 20 hours it was noted that the water in the pan had completely evaporated.

NITROGEN PAV

The third condition consists of non-oxidative aging due to the exclusive presence of nitrogen (N_2) inside the PAV. The oven time, temperature and pressure parameters are the same as in the previous conditions. The hardening of bitumen due to oxidation has been identified as the main cause of aging, for this reason aging with inert gas is presumed to cause more limited aging. However, in the absence of oxygen, the inhalation of nitrogen or other inert gas causes loss of consciousness. For this reason, in conditions of PAV with nitrogen it is necessary to proceed with caution, using sensors that record the level of oxygen and aerating the rooms.

NITROGEN PAV PLUS MOISTURE

The last condition combines the characteristics of the previous condition with inert gas N_2 with the presence of moisture through a 15 ml dish of water as for the second PAV condition. Also in this case at the end of the 20 hours a complete evaporation of the water was noticed.

4.5 TEST METHOD

At the end of each conditioning process, the samples were tested to investigate any changing in terms of chemistry (FTIR test) and rheology (DSR test).

4.5.1 FOURIER TRANSFORM INFRARED (FTIR) SPECTROSCOPY

Fourier transform infrared spectroscopy (FTIR) is one of the most used methods to characterize the chemical composition of materials. The method is based on the interaction between infrared radiation and existing bonds in a material, defining its chemical composition. From a technical point of view, an infrared light beam is loaded into the sample leading to vibrations and rotations of the molecular bonds at different frequencies (Van den Bergh 2011). FTIR spectroscopy uses the infrared spectrum, which forms part of the electromagnetic spectrum (Fig. 4.10) (Hagos 2008).

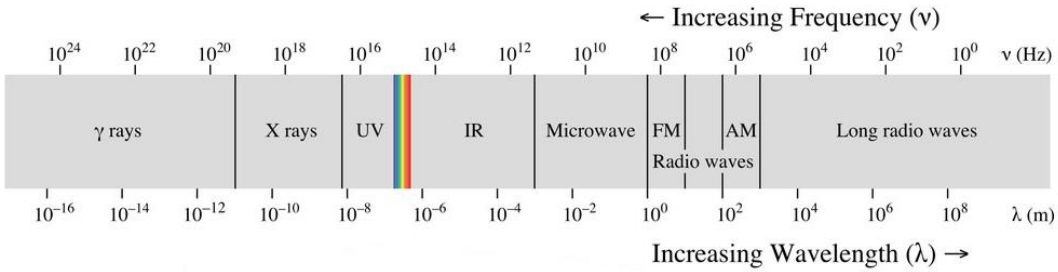

Figure 4.10 - Various regions of the electromagnetic spectrum.

As far as electromagnetic radiation is concerned, the velocity of propagation in the vacuum is constant, throughout the electromagnetic spectrum, and equal to the speed of light (c). Propagation can be conceived as a wave with a velocity defined as the product of the wavelength (λ) and frequency (v). The first (wavelength) is defined as the distance between two successive peaks while the second (frequency) is the number of cycles per second. The energy of an infrared photon is related to these two quantities through the Bohr equation, using the Planck constant (h). Equation shows that the photon energy is proportional to the frequency and wave number (Van den Bergh 2011).

$$E = h \cdot v = \frac{h \cdot c}{\lambda} = h \cdot c \cdot \bar{v}$$

Where,

E = The energy of photon (J);
h = Planck's constant ($6.626 \cdot 10^{-34}$ J·s);
v = The frequency (cycles/s);
c = The speed of light (2.997925·108 m/s);
λ = The wavelength (m);
$\bar{v}$ = The wave number (cm^{-1}).

The chemical composition of a material is described by the binding energy between its components. When infrared radiation is loaded into the material, different types of bonds will absorb different frequencies. This frequency is essentially the energy of a specific photon which brings the particular bond to a specific excited state (vibrations). Therefore, each molecule will have its own characteristic spectrum, which can be identified by the reflected or absorbed beam light (Van den Bergh 2011).

The interaction of infrared radiation should be conceived as a change in molecular dipoles resulting from rotations and vibrations of the atoms, the latter being very important for the identification of the types of functional groups present in the examined material. Three general modalities of atomic vibrations can be distinguished (Fig. 4.11) (Van den Bergh 2011):

- Stretching;
- In-plane Bending;
- Out-of-plane Bending.

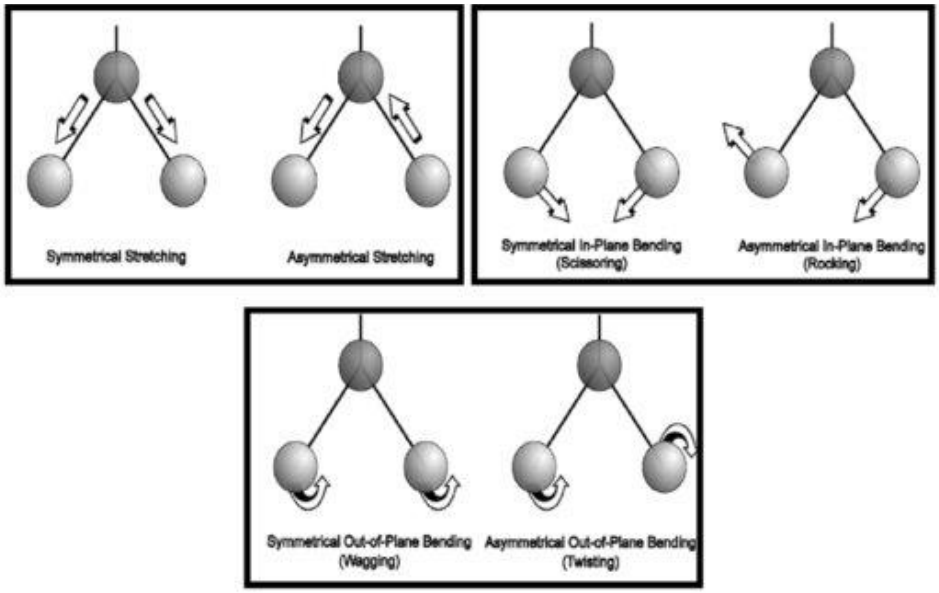

Figure 4.11 - Different types of stretching and bending vibrations (Van den Bergh 2011).

There are two general ways of measuring infrared spectroscopy: the transmittance of the beam through the sample and the reflection of the beam within the sample. The first is the oldest infrared method in which infrared radiation is sent through a sample and specific wavelengths are absorbed. However, for materials with extremely high absorption coefficients such as bitumen, there is an intrinsic problem that transmission is very low or impossible and therefore the signal-to-noise ratio is unacceptable low (Hofko et al. 2017). This method is now replaced by reflectance spectroscopy which is the second type of measurement reported. It remedies the previous method, since the radiation is reflected on the outer surface of the sample. Total reflectance attenuated spectrometry is a new and widely used technique that uses the principle of total internal reflection. For ATR, a wave of evanescent light is attenuated due to the resonances of the molecular vibrations located at the interface between the sample and a high refractive index crystal. For the analysis of spectra derived from FTIR,

different groups of molecular limits can be unequivocally distinguished at different and well defined wavelengths of an absorbance spectrum for characteristic maxima of the band (local maxima in the spectrum). Changes in chemical groups can therefore be related to changes in rheological properties and allow a better understanding of the chemical-mechanical coupling (Hofko et al. 2017). The ATR can be distinguished in multiple ATR and single point ATR (Fig. 4.12). In the first case, the light beam is reflected more than once in the crystal (multiple), therefore "hitting" the tested sample in multiple positions, while in the second case the beam is reflected only once by the sample and only in a single position (Mastoras 2019).

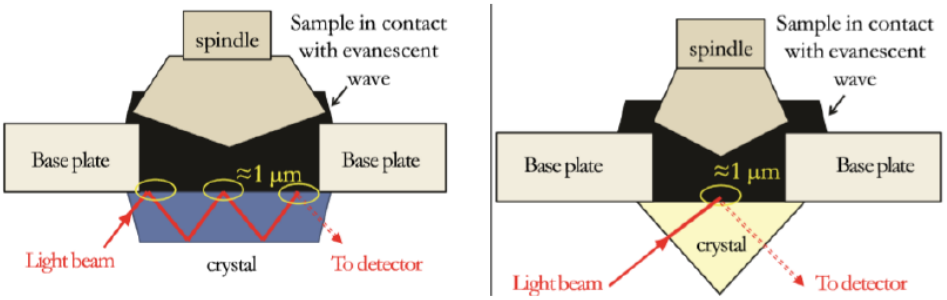

Figure 4.12 - FTIR/ATR spectrometer. Multiple FTIR/ATR and Single point FTIR/ATR.

The wave enters the material, the sample will absorb particular frequencies and the beam loses energy at that specific frequency. The resulting attenuated radiation is collected by a detector and an interferogram is derived. The diagram is expressed in terms of absorbance or transmittance on the vertical axis with respect to the wave number on the horizontal axis. Absorbance (A) and transmittance (T) are related by the equation:

$$A = log_{10}\frac{1}{T}$$

The absorbance is equal to the difference of the logarithms of the intensity of the entering light beam and the intensity of the transmitted one.

$$A = log_{10}I_0 - log_{10}I = log_{10}\frac{I_0}{I} = -log_{10}T$$

Where,

A = absorbance;

T = transmittance;

I_0 = intensity of the light beam entering the sample;

I = intensity of the light beam transmitted by the sample.

FTIR spectrometer test method

The laboratory of TU Delft provided the Spectrum 100 FTIR spectrometer of Perkin Elmer (Fig. 4.13). For this research, the single beam mode (single point-ATR) was used, in which radiation enters the sample only once. The wavelength region was set between 600 and 4000 cm^{-1}. A background check was required each time prior to the sample test, as a relative scale for absorption intensity was required. Specimen scanning was performed immediately after background check with 20 individual scans and a resolution of 4 cm^{-1}. The average value of the 20 individual scans on the sample provides the final interferogram.

Figure 4.13 - Spectrum 100 FTIR spectrometer Perkin Elmer with a single-point-ATR fixture.

Three replicates were tested for each material and conditioning time in order to obtain a more reliable result. The final spectra are the average of the three tests, while the indices of interest have been calculated for each replica individually to report the average value with its standard deviation. The amount of material required for the test is very small, so a small amount of filler or bituminous binder was taken with a spatula. After placing the material on the crystal, a spindle drop down to improve the contact between the material and the crystal. The monitor shows the force gauge, set around 140.

The first FTIR tests on the filler samples showed a high degree of uncertainty, due to the fact that the spectra of the three repetitions diverged excessively from each other, this due to the incoherent nature of the filler. In fact, in the study of bitumen and mastics, this problem did not arise.

The first indices obtained for the fillers were highly unreliable, for this reason an attempt was made to better compress the filler on the FTIR plate using a sheet of silicone paper between the sample and the spindle. Following this change, the filler spectra were much more overlapping and the error bars decreased significantly.

The following pictures (Fig. 4.14) show the preparation steps before running the FTIR test.

Figure 4.14 - Preparation of the filler (left) and mastic (right) on the FTIR.

Analysis method of infrared spectra on filler

For each filler analyzed, the software returns the raw spectrum that will have to be processed in order to carry out the correct chemical analyzes. The three repetitions sometimes have significantly different values, as compaction of the filler under the spindle also by means of silicone paper is difficult. The three spectra are originally presented in the following form (Fig. 4.15).

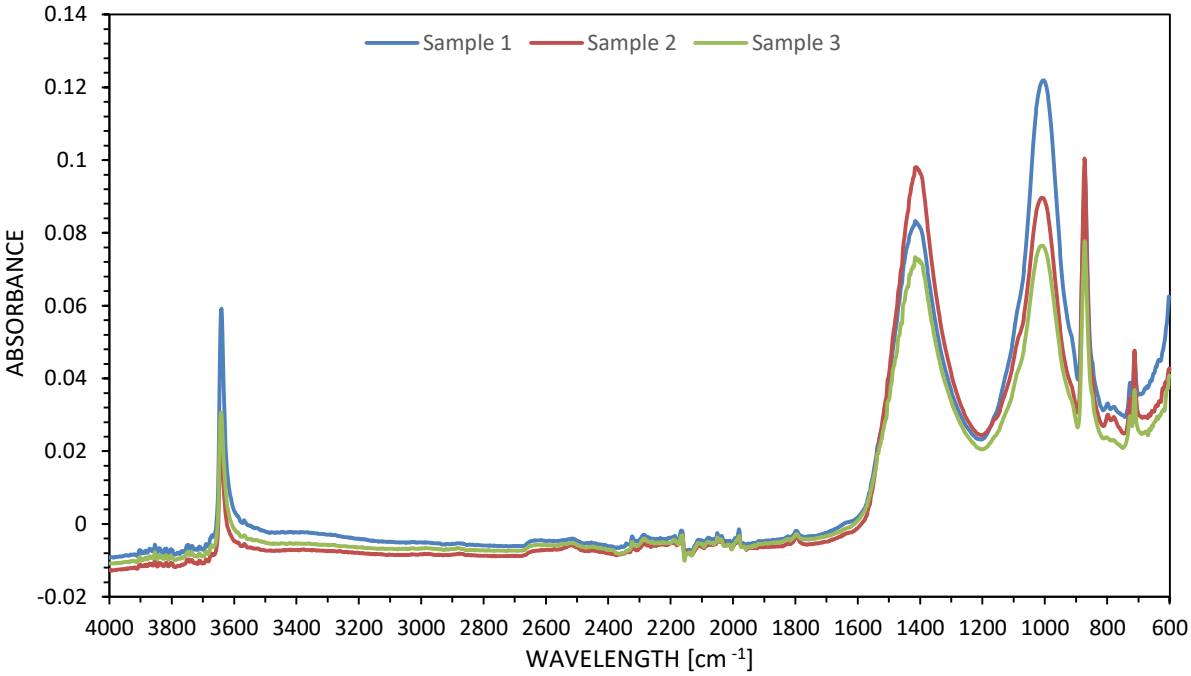

Figure 4.15 – Three raw spectra of filler sample.

Regarding fillers, the post processing consists first of all in translating the absorbance values to all positive values, superimposing the absorbances recorded at 4000 cm^{-1} of the three samples at the origin of the axes. At this point, an automatic baseline correction is performed through the software to initialize the sections with low absorbance to zero values and better identify the peaks of the various compounds to be analyzed. The three elaborate spectra are therefore presented in the following form (Fig. 4.16).

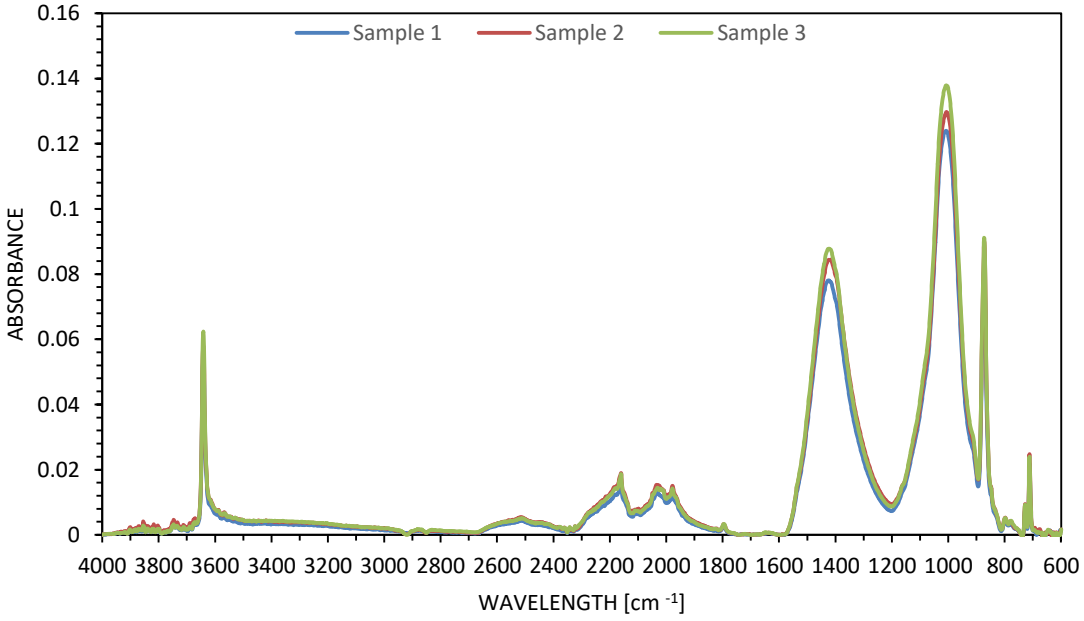

Figure 4.16 –Three elaborate spectra of filler sample.

As for the graphic display, we want to compare the six fillers and the five different conditions, then the three samples are averaged (Fig. 4.17). For the measurement of the peaks to obtain the indices of interest have been calculated for each replica individually to be reported as an average value with its standard deviation. To quantify the action of aging and moisture on the fillers and to be able to perform a chemical analysis on the degradation of hydrated lime, the wavelength ranges (Fig. 4.17) corresponding to the peaks and areas of the following compounds are taken into consideration:

- Calcium Hydroxide [$Ca(OH)_2$]: 3642 cm^{-1}
- Calcium Carbonate [CaCO3]: 1390 cm^{-1}
- Sulfoxide [S = O]: 1066 - 924 cm^{-1}
- Calcium Oxide [CaO]: 866 cm^{-1}

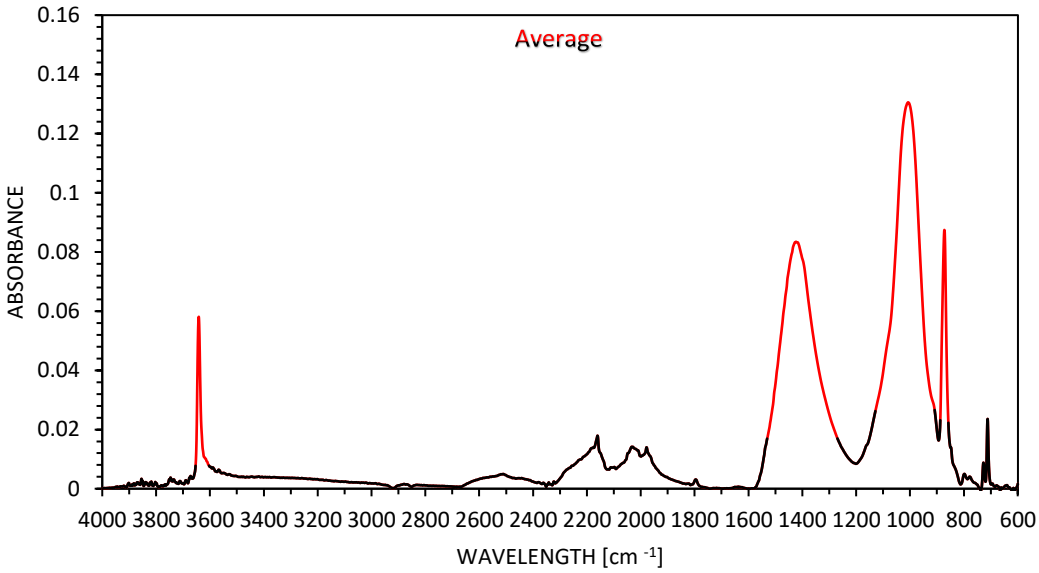

Figure 4.17 - Average of the spectra with the peaks of calcium hydroxide, calcium carbonate, calcium oxide and sulfoxides to be used in red.

Calcium hydroxide, calcium carbonate and calcium oxide are compared by the peak values. In a comparison between the various types of filler, the indices obtained are used to quantify the components of hydrated lime and limestone by comparing them with the parameters provided by *Sibelco* described in the Sub-Section 4.2. On the other hand, by comparing the fillers with different aging conditions, the indices obtained are useful for studying the degradation process of hydrated lime (carbonation), as described in the Sub-Section 2.3.2

The sulfoxide index is calculated as an area underlying the spectrum. Hofko et al. (2017) employed and studied various methods using the original or normalized spectrum, a

bandwidth or a calculation based on the integration of indices from an absolute or tangential basis. In the case of fillers, where the aliphatic group of bitumen is not present, the spectrum is not normalized. The baseline is corrected by the software so that you can use the absolute one and not have to trace the tangent. As far as sulfoxides are concerned, area integration was carried out by approximating the area below the infrared spectrum as a sequence of trapezoids. For this reason, we refer to the IBR (Integration-Baseline-Raw) calculation method (Hofko et al. 2017).

$$IBR = \int_{w_{l,i}}^{w_{u,i}} a\,(w)dw = SI = \int_{924}^{1066} a(w)dw$$

Where,

a(w): absorbance value at wavenumber w;
$w_{u,I}$ = 1066: upper wavenumber limit for structural group;
$w_{l,I}$ = 924: lower wavenumber limit for structural group.

Analysis method of infrared spectra on bitumen and mastic

Also in the case of bitumen and mastics, the recommendations provided by Hofko et al. (2017) were considered in this study, for the post-processing of the raw FTIR / ATR data and the derivation of the indices. According to Hofko et al. (2017) in case of normalization of the spectra before the analysis, the asymmetric stretching vibration of the aliphatic structures 2923 cm-1 was taken as the basis for normalization. For normalization, the absorbance value of this band was set to 1 and the full spectrum was multiplied by a ratio factor. Normalization is based on the following equation:

$$a_{norm}(w) = a(w) \cdot \frac{1}{a(2923cm^{-1})}$$

Where:

$a_{norm}(w)$ = normalized absorbance spectrum as a function of wave number w;
a(w) = original absorbance spectrum;
$a(2923cm^{-1})$ = original absorbance value at the reference band at wave number 2923 cm^{-1}.

This approach is based on the idea to remove any variation in the absorbance spectra due to a variation of the IR beam penetration between samples. The post normalization process is

carried out automatically by software. Added to this is the translation to positive values and the modification of the baseline as in the case of fillers. The final spectra of bitumen or mastics will come in the following form (Fig.4.18)

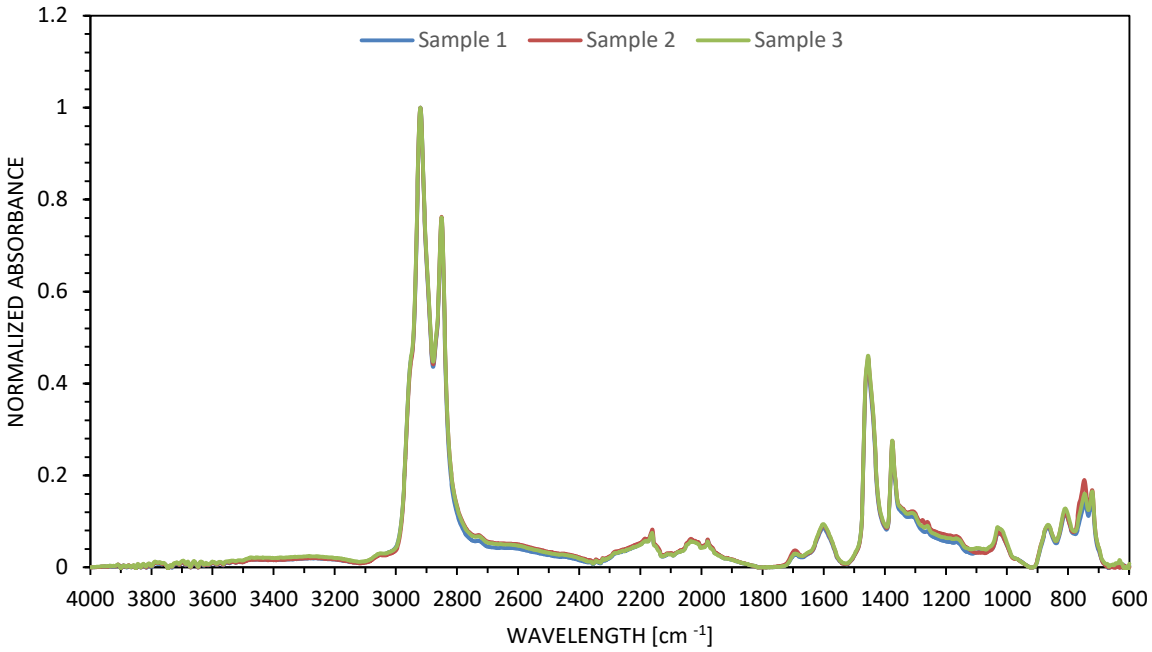

Figure 4.18 - Three elaborate spectra of bitumen sample.

To quantify the action of aging and moisture on mastics and evaluate the chemical effect of fillers on bitumen, the wavelength intervals corresponding to the areas of the following compounds are taken into consideration (Fig. 4.19):

- Carbonyl [C = O]: 1746 - 1666 cm^{-1}
- Sulfoxide [S = O]: 1066 - 924 cm^{-1}

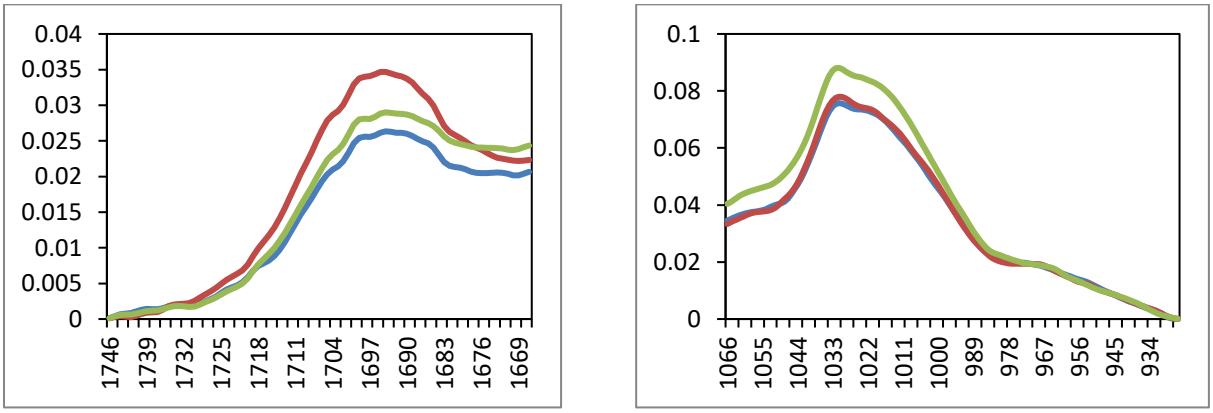

Figure 4.19 - Absorbance peak of the carbonyl group (left) and the sulfoxide group (right).

In this study, to calculate the Carbonyl and Sulfoxide indices, we worked with normalized spectra, an absolute baseline and with the integration of areas (IBN method). The integration of areas was performed by approximating the area below the infrared spectrum as a sequence of trapezoids. The following equations were employed for the calculation of the indexes.

$$CI = \int_{1666}^{1746} a(w)dw$$

$$SI = \int_{924}^{1066} a(w)dw$$

Where,

a(w): absorbance value at wavenumber w;

The utilization of Eq. for the derivation of the CI yields also a non-zero value for the unaged materials, regardless if there is a peak or not at the region around the wave number 1700 cm^{-1}. As Hofko et al. (2017) mention in their study, this is, of course, an artificial effect and the CI of the unaged materials should be reported as zero, if visual inspection of the infrared spectrum verifies that there is no peak at the carbonyls' group region.

4.5.2 DYNAMIC SHEAR RHEOMETER (DSR)

Dynamic Shear Rheometers (Fig. 4.20) are generally used to determine the rheological properties of viscoelastic materials, such as bituminous binders. In pavement engineering, DSR's are mainly used to evaluate the complex shear modulus (G*) and the phase angle (δ) of bitumen or bituminous binders at different temperatures and frequencies.

Bitumen is an viscoelastic material that acts as an elastic solid similar to glass at low temperatures and/or during rapid loading and as a viscous fluid (Newtonian) at high temperatures and /o during slow loading. As a viscoelastic material, bitumen has both elastic and viscous response components and shows a relationship dependent on temperature and time between the applied stresses and the resulting deformations. The rheology of bitumen is consequently defined by its stress-deformation-time-temperature response.

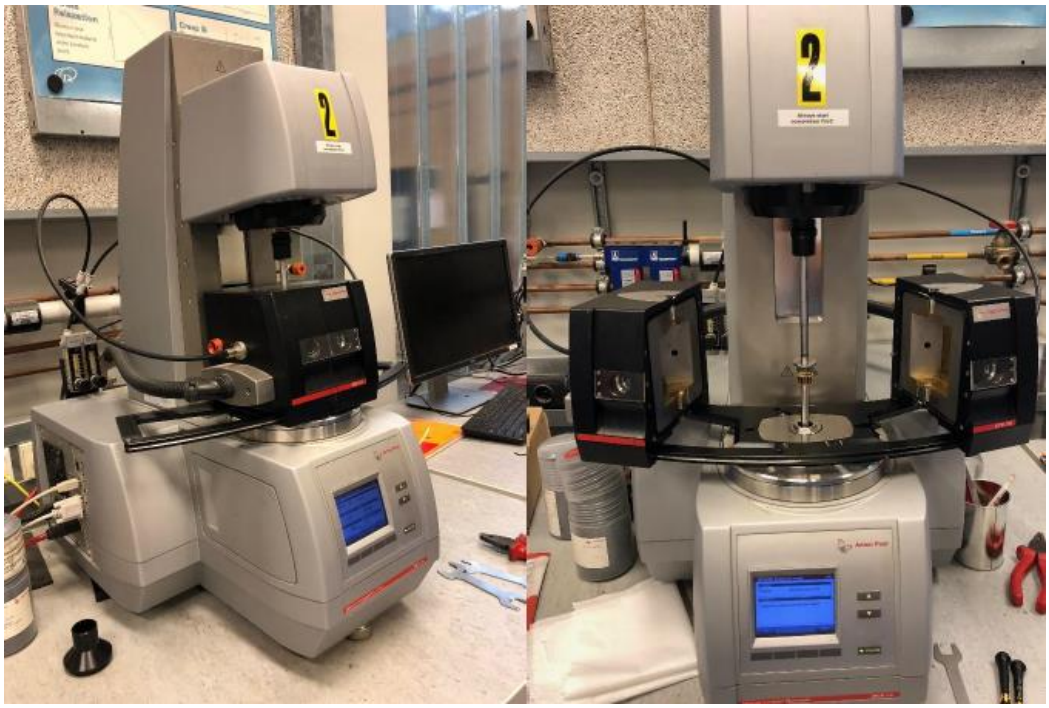

Figure 4.20 - DSR in the TU Delft laboratory with the chamber closed (left) and opened (right).

The standard test procedure involves the application of sinusoidal stresses or stresses on a sample inserted between the parallel plates (PP), also called test geometries, of the rheometer. The most frequently used test geometries are, for low to intermediate test temperatures an 8 mm diameter plate with a gap of 2 mm between the PP, while for higher temperatures, a 25 mm-flat diameter with a gap of 1 mm (Fig. 4.21) (Woldekidan 2011).

Figure 4.21 - 25 mm-diameter oscillating plate (left) 8 mm-diameter oscillating plate(right).

During dynamic measurements, the top plate of the DSR configuration oscillates while the bottom plate remains fixed. The test can be conducted in stress controlled mode or in

deformation controlled mode. In the first case, a sinusoidal stress is applied and the corresponding deformation is determined by measuring the displacement in response to the applied stress. In the second case, the amplitude of the stress is determined by measuring the torque in response to the applied deformation (Fig. 4.22).

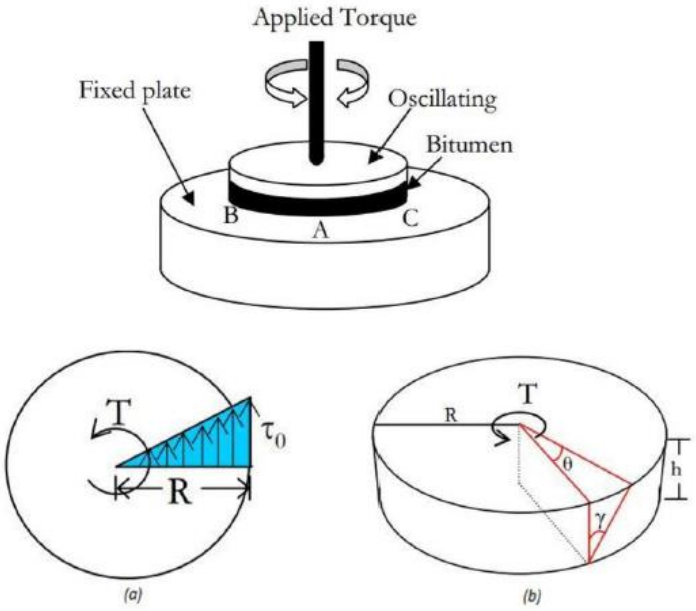

Figure 4.22 - DSR operating principal and maximum shear strain and stress location.

The maximum shear stress (τ_{max}) and the maximum shear strain (γ_{max}) occur at the edge of the specimen (Fig 4.22) and are calculated according to equations. (Van den Bergh 2011).

$$\tau_{max} = \frac{2 \cdot T}{\pi \cdot R^3}$$

$$\gamma_{max} = \frac{\theta \cdot R}{h}$$

Where,

τ_{max} = The maximum shear stress ([F]/[A])

T = The applied torque ([F]·[L])

R = The radius of the plates (specimen) ([L])

γ_{max} =The maximum shear strain

θ = The deflection angle (rad)

h = The specimen height/gap between the PP ([L])

The complex shear modulus is a measure of the resistance of the material against deformation when repeatedly sheared (Apostolidis 2015), and is calculated as the ratio of the maximum stress amplitude and the maximum strain amplitude (Eq.) (Van den Bergh 2011).

$$G^* = \frac{\tau_{max}}{\gamma_{max}}$$

The complex shear modulus G* can also be written as:

$$G^* = G' + iG'' = \sqrt{(G')^2 + (G'')^2}$$

Where *G'* is the storage modulus and describes the amount of energy stored and released elastically in each oscillation and is thus called the elastic modulus; *G''* is the loss modulus and describes the energy dissipation rate associated with the viscous effects (Fig. 4.23).

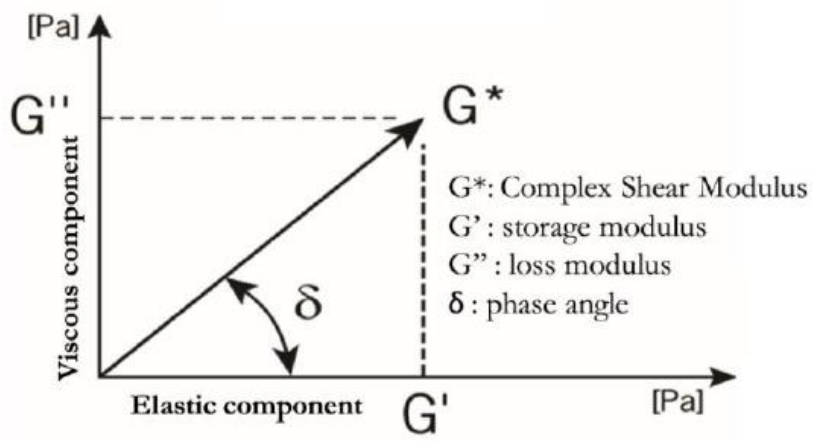

Figure 4.23 - Relationship between the complex shear modulus G, its components and the phase angle δ.*

The phase angle describes the phase lag between the stress and strain signals (Van den Bergh 2011). Purely elastic materials present a phase angle equal to 0° whereas purely viscous materials show a phase angle equal to 90°. For visco-elastic materials, lies in between the two extremes and its value depends on the testing temperature and frequency. The phase angle is calculated through equation (Van den Bergh 2011).

$$\delta = \omega \cdot \Delta t = 2 \cdot \pi \cdot f \cdot \Delta t = tan^{-1}\frac{G''}{G'}$$

Where,

δ = The phase angle (rad) or (^{o})

ω = The angular frequency (rad)

Δt = The time lag between the loading and response signals (sec.)

f = The frequency (Hz)

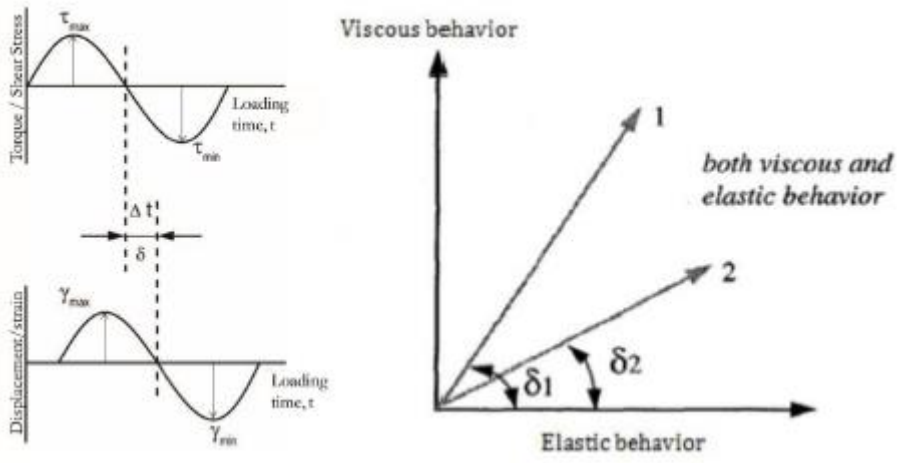

Figure 4.24 - Phase shift angle between sine curve of stress and strain (left). Phase angle as a function of different materials (right) according to Mastoras 2019..

Preliminary study on DSR configuration

The test geometry used for all the experiments was the PP (parallel plates) of 8 mm in diameter and 2 mm gap. To increase the accuracy of the data obtained, two replicates were tested for each condition and their mean was used for further studies. Before each test, the machine measurements were set, the forces were restored and the inertia was adjusted. Then the PP system is calibrated. A portion of bitumen or mastic was inserted between the two plates (Fig. 4.25). Once the 2.05 mm distance was reached, the excess bitumen was eliminated with a heated cutter and the climatic chamber closed. By adjusting the temperature from time to time, the space between the two plates has been reduced to the 2 mm required, then the test starts. A surveillance time of 600 seconds has been set, with a tolerance of +/- 0.2 ° C. The surveillance time is a parameter that helps the accuracy of the test: once the test temperature is reached, before the test starts, the temperature must not change (remain within the tolerance) for 600 seconds.

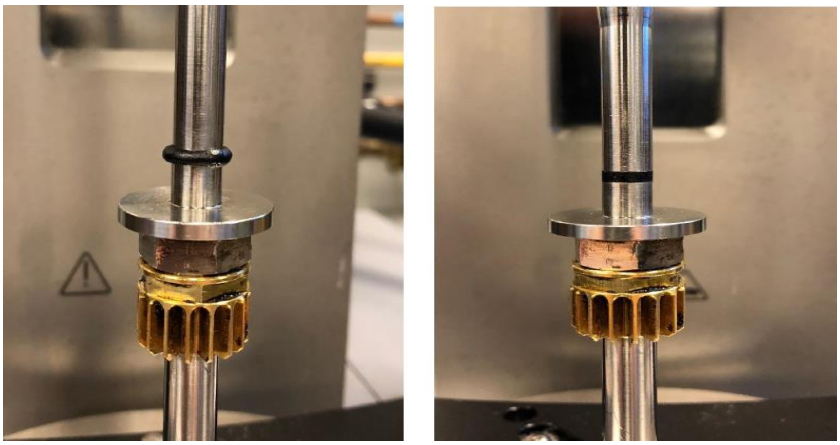

Figure 4.25 - Sample between 8 mm plates before trimming (left) at 2.05 mm gap and after (right) at 2 mm gap.

4.5.2.1 RELAXATION TEST

In order to study the changes in the relaxation properties of the bitumen and mastics due to oxidative ageing, relaxation DSR tests were performed. The relaxation tests were performed at 0 °C with 1% shear strain at the beginning, followed by a relaxation period of 100 seconds. The data collection frequency was 100 Hz. Total viscoelastic resistance to deformation at a constant stress level can be assessed by measuring the accumulated total deformation, after the material has had sufficient time to relax. Two replicated samples for each aging condition were tested using DSR.

The Figure 4.26 shows the relationship between shear stress and relaxation time of the neat bitumen.

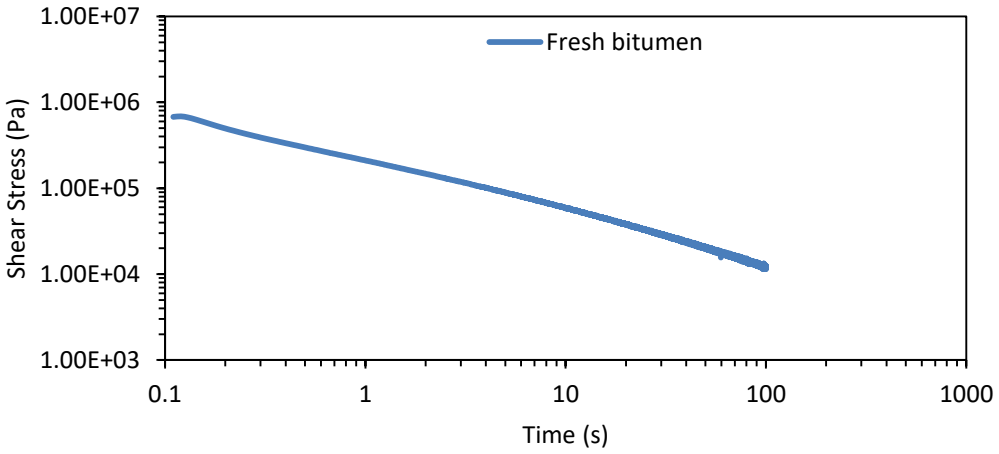

Figure 4.26 - Relaxation test of bitumen in a fresh state and in the four conditionings.

On the basis of the experimental results, three evaluation indices were used to analyze the changes in the relaxation properties of aged bitumen. Specifically, shear stress at 0 s and 100 s, and the ratio of shear stress at 0 s and 100 s based on study of Jing (2019).

All the indices will be described and analyzed in Sub-Section 6.2.1.

4.5.2.2 AMPLITUDE SWEEP TEST

The amplitude sweep test is normally used to distinguish the linear and nonlinear viscoelastic response of bitumen. The test is conducted at constant temperature and frequency with an increasing amplitude (stress / deformation). The relationship between stress and deformation for typical bituminous materials is shown in Figure 4.27. As the level of stress / deformation increases, the bituminous material passes through the linear viscoelastic phase to the nonlinear viscoelastic phase and therefore to the damage phase. In addition to the critical non-linear

viscoelastic point, the mechanical properties of bituminous materials change: the complex shear modulus decreases and the phase angle increases (Jing et al. 2019).

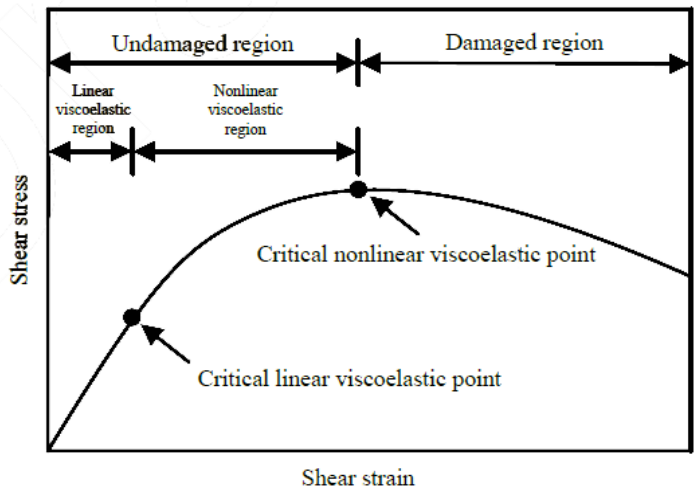

Figure 4.27 - Schematic of stress-strain curve for typical bituminous materials.

The critical linear viscoelasticity point is defined as the point that a 95% reduction in the initial complex shear modulus occurs (Fig. 4.28). After this point, the response of bitumen is in the nonlinear viscoelastic range, in which the complex shear modulus decreases and the phase angle increases, respectively. The critical nonlinear viscoelasticity point is defined as the point that the maximum shear stress occurs on the basis of the stress-strain curve. After this point, the response of bitumen is within the damage range, in which the shear stress decreases.

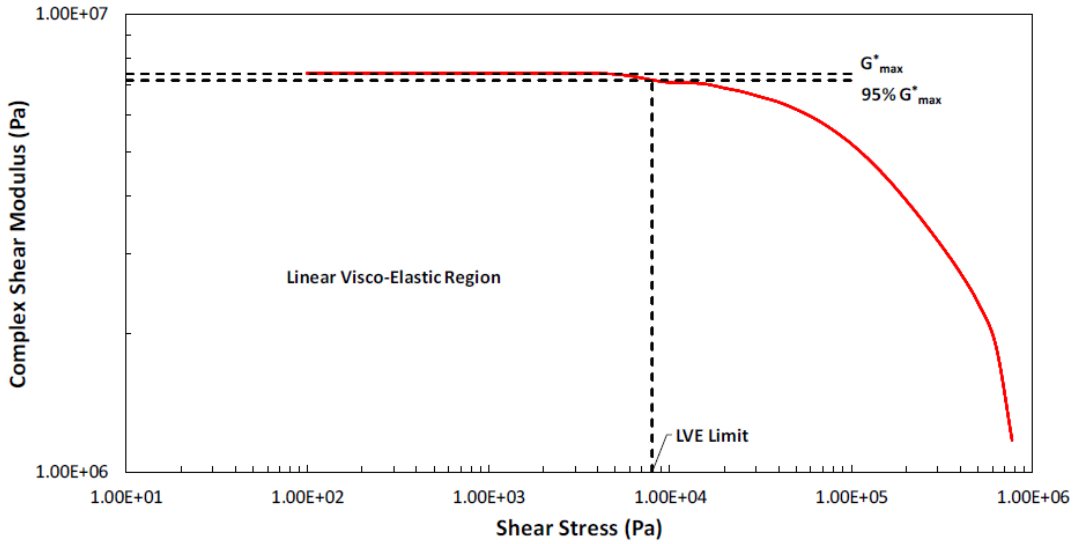

Figure 4.28 - Example of the determination of the LVE limit. Stress amplitude sweep.

The amplitude sweep test was performed on all materials (i.e. mastics and bitumen) at both the "fresh" and the aged state. The test was carried out at 20°C and frequency of 10 Hz. The above practice allowed to determine a governing LVE limit and select a stress level to be applied in the stress controlled frequency sweep tests, which would ensure that all materials are evaluated within their LVE region of response. It should be noted that different sets of stress levels were determined for the mastics and the bitumen. Table 4.13 summarizes the amplitude sweep test conditions.

Feature	Material	
	Mastic	**Bitumen**
Loading Mode	Stress-Controlled	Stress-Controlled
Stress Range (kPa)	0.1-1000	0.01-1000
Testing Points	41	41
Test Temperature (°C)	20	20
Test Frequency (Hz)	10	10
Test Geometry	8 mm Plate 2mm Gap	8 mm Plate 2mm Gap
Specimen Temperature Equilibrium	600 sec ±0.2°C Tolerance	600 sec ±0.2°C Tolerance

Table 4.13 - Amplitude sweep test conditions.

Fatigue analysis

The linear amplitude sweep test aims to evaluate the ability of bituminous materials to resist damage by using a cyclic load with increasing amplitudes in order to accelerate the damage. The characteristics of the damage accumulation rate in the material can be used to indicate the fatigue behaviour of bituminous materials. In order to perform the fatigue (damage) analysis, information regarding the undamaged material properties (represented by the parameter α) were determined on the basis of the results of frequency sweep tests. In order to determine parameter α, a best-fit straight line is applied to a plot with loading frequency on the horizontal axis and storage modulus on the vertical axis using the following equation.

$$\log G'(f) = \frac{1}{\alpha}\log f + \beta$$

Where f is the loading frequency, G' is the storage modulus, α and β are fitting parameters. The damage accumulation in the sample is calculated using:

$$D(t) \cong \sum_{i=1}^{n} [\pi\gamma_0^2(C_{i-1} - C_i)]^{\alpha/1+\alpha}(t_i - t_{i-1})^{1/1+\alpha}$$

Where:

$C(t) = \frac{|G^*|(t)}{|G^*|_{initial}} =$ integrity parameter;

γ_0 = applied strain (%);

G* = complex shear modulus in MPa;

α = 1/m, where m is the slope of logarithmic plot between storage modulus and applied frequency;

t = testing time in seconds.

The relationship between C(t) and D(t) is developed by the curve fitting method (Fig.) using the power law expressed in:

$$C(t) = C_0 - C_1 D^{C_2}$$

Where C_1 and C_2 are coefficients of curve fitting equations.

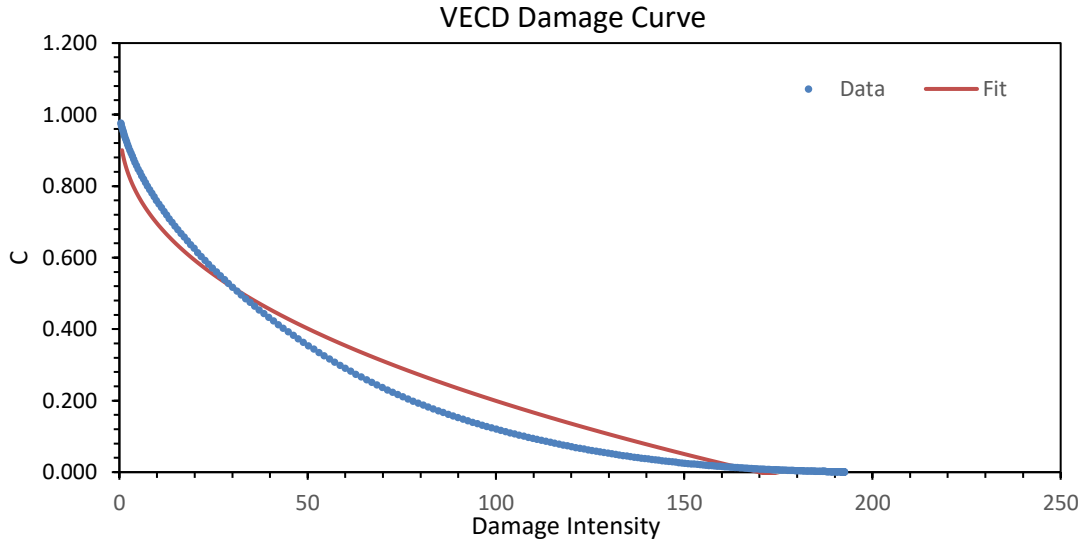

Figure 4.29 – Damage curve.

Further, damage value at failure point is being calculated. The value of D(t) at failure, D_f, is defined as the D(t) which corresponds to the reduction in initial |G*| at the peak shear stress, using:

$$D_f = \left(\frac{C_0 - C\ at\ peak\ stress}{C_1}\right)^{1/C_2}$$

Finally, the number of fatigue cycles (N_f) is evaluated using:

$$N_f = A(\gamma_{max})^B$$

Where A and B are regression parameters, and γ_{max} is the maximum expected binder strain for a given sample. A mastic having a high value of N_f indicates superior resistance to fatigue cracking. First, the test procedure includes a strain amplitude of 0.1% for the frequency range from 0.1 to 20 Hz to calculate B, which indicates undamaged material properties. Parameter B only depends on α and therefore is independent of the amplitude sweep test results. Second, parameter A is estimated based on the VECD concept and the test is conducted at a specified temperature using oscillatory shear loading in the strain controlled mode of 10 Hz frequency. Johnson and Bahia (2010) recommended using the damage accumulation (D_t) criterion corresponding to a 35% reduction of the initial loss shear modulus (G") to define A.

All the indices will be described and analyzed in Sub-Section 6.2.2.

4.5.2.3 FREQUENCY SWEEP TEST

Once the LVE regions for all materials are known, it is possible to study the fundamental rheological properties, such as complex shear modulus (G*) and phase angle (δ), by means of the frequency sweep test. To increase the accuracy of the obtained data, two replicates were tested for each material and their average was used to obtain the G* and δ isothermal curves to be post-processed. The test (Table 4.14) was carried out in the stress-control mode, at temperatures from 0°C to 40°C with 10°C increments and frequencies ranging from 0.02 to 20 Hz. 5 pt/dec was chosen as point density, 16 testing points totally. The applied sinusoidal stress level, per testing temperature and material, was set according to the amplitude sweep tests results (Table 4.15).

Feature	**Material**	
	Mastic	**Bitumen**
Loading Mode	Stress-Controlled	Stress-Controlled
Testing Points	16	16
Test Temperature (°C)	0, 10, 20, 30, 40	0, 10, 20, 30, 40
Test Frequency (Hz)	0.02, 0.03, 0.05, 0.08, 0.13, 0.20, 0.32, 0.50, 0.80, 1.26, 2.00, 3.17, 5.02, 7.96, 12.60, 20.00	0.02, 0.03, 0.05, 0.08, 0.13, 0.20, 0.32, 0.50, 0.80, 1.26, 2.00, 3.17, 5.02, 7.96, 12.60, 20.00
Test Geometry	8 mm Plate 2mm Gap	8 mm Plate 2mm Gap
Specimen Temperature	600 sec	600 sec

Equilibrium	±0.2°C Tolerance	±0.2°C Tolerance

Table 4.14 - Frequency sweep test conditions.

Temperature (°C)	Chosen Stress Level (Pa)	
	Mastic	Bitumen
0	100000	10000
10	50000	8000
20	7000	5000
30	2500	3000
40	2000	2000

Table 4.15 - Chosen stress levels applied in the frequency sweep tests.

When the test is over, the software provides plots of the complex shear modulus and phase angle as a function of the frequency and the temperature (Figure 4.30).

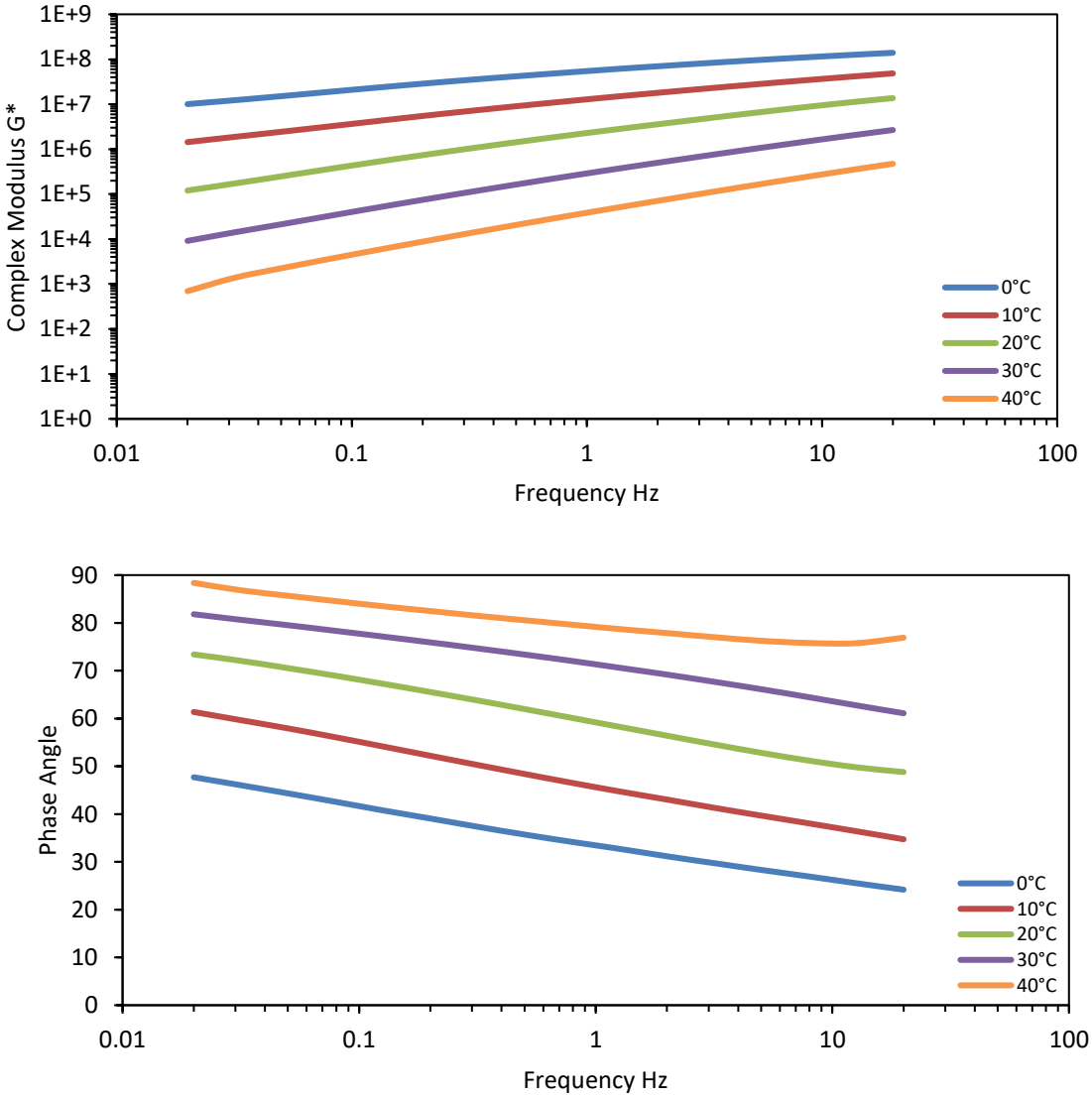

Figure 4.30 - Example of average isothermal plot: (Up) Complex shear modulus (Down) Phase angle.

Master curves of complex shear modulus and phase angle

Viscoelastic properties are often highly temperature dependent. Several studies have shown that moduluss G 'and G" recorded at different temperatures can be joined together in a single, continue, regular curve, called the master curve, by means of the principle of time-temperature equivalence, also known as the principle of *time-temperature superposition* (TTS) (Figure 4.31). This principle allows the horizontal displacement of the isothermal curves, along the frequency axis, at a predefined reference temperature. The extended frequency scale in a master curve is called the reduced frequency scale or simply the reduced frequency (Hunter et al. 2015). The amount of displacement required for each temperature is expressed through the displacement factors (α_T). Displacement factors depend only on temperature and, therefore, describe the temperature dependence of the viscoelastic behaviour of the material examined. By tracing the log (α_T) against temperature, it is possible to obtain a visual representation regarding the way in which the viscoelastic properties of the material change with temperature, since these values (log (α_T)) can be interpreted as the viscosity changes, always with respect to the viscosity at the reference temperature (Hunter et al. 2015).

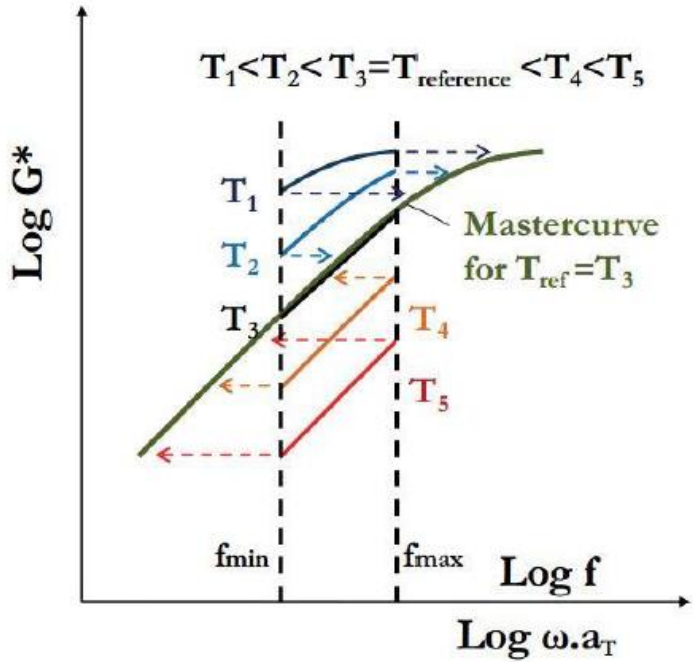

Figure 4.31 - Example of the generation of master-curve (TTS method).

For the derivation of the shift factors several techniques can be employed, ranging from manual shifting and determination of the shift factors, to the utilization of mathematical equations that describe the relationship between the shift factors and temperature. With respect to the latter, the most widely used mathematical expression is the Williams-Landel-Ferry (WLF) function.

$$\log(\alpha_T) = -\frac{C_1 \cdot (T - T_{REF})}{C_2 + T - T_{REF}}$$

Where,

α_T = The shift factor

T = The analysed temperature (°C)

T_{REF} = The reference temperature (°C)

C_1, C_2 = Coefficients

In this study, the WLF equation was used to obtain the shift factors and construct the various master-curves to a reference temperature of 20°C. Fig.4.32 illustrate an example of the fitting potential of the utilized equations in the case of fresh neat bitumen. The results indicate that the considered model can describe accurately enough the G*- δ master-curve. The remarks hold true for all materials considered in this study.

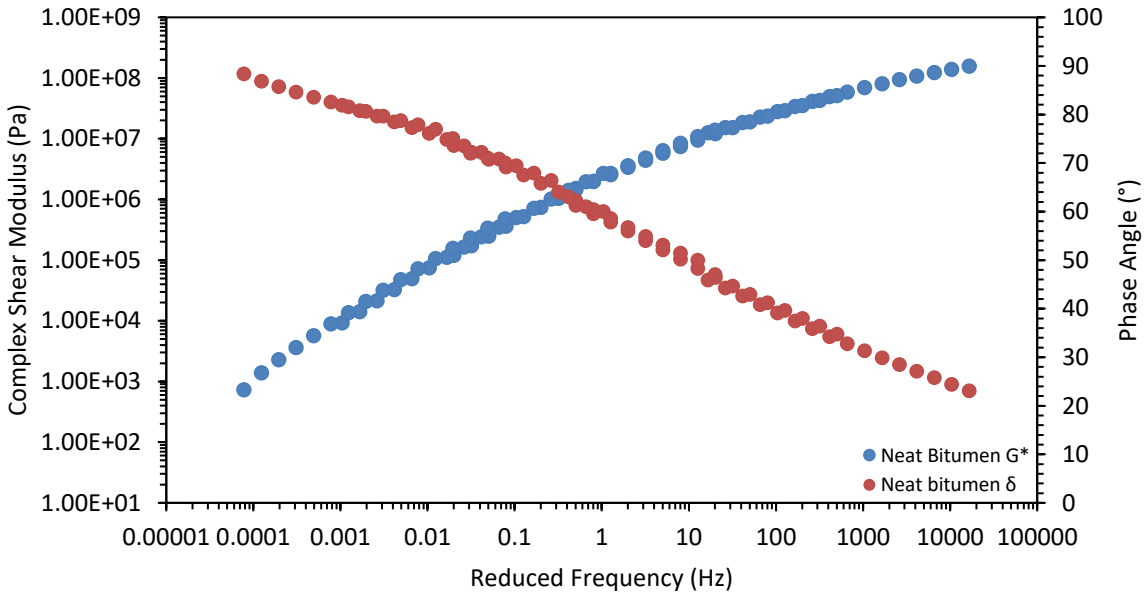

Figure 4.32 – Master curves of fresh bitumen according to WLF approach..

Black space plot

Black diagrams (Fig. 4.33) were plotted to present the rheological changes of bitumen and mastics with ageing. Black diagrams are graphs of the complex shear modulus versus the phase angle, in which the frequency and the temperature are eliminated, hence, the data can be presented in one plot without the need to apply the Time-Temperature Superposition (TTS) principle (Airey 2002). As ageing progresses, a shift of the Black diagram curves towards lower phase angles is observed; at the same time the shape of the curves changes to a straight line and the curvature reduces (Jing et al. 2019). These changes denote a tendency towards a

stiffer and less viscous material, which could result to failures such as brittle fracture at low temperatures.

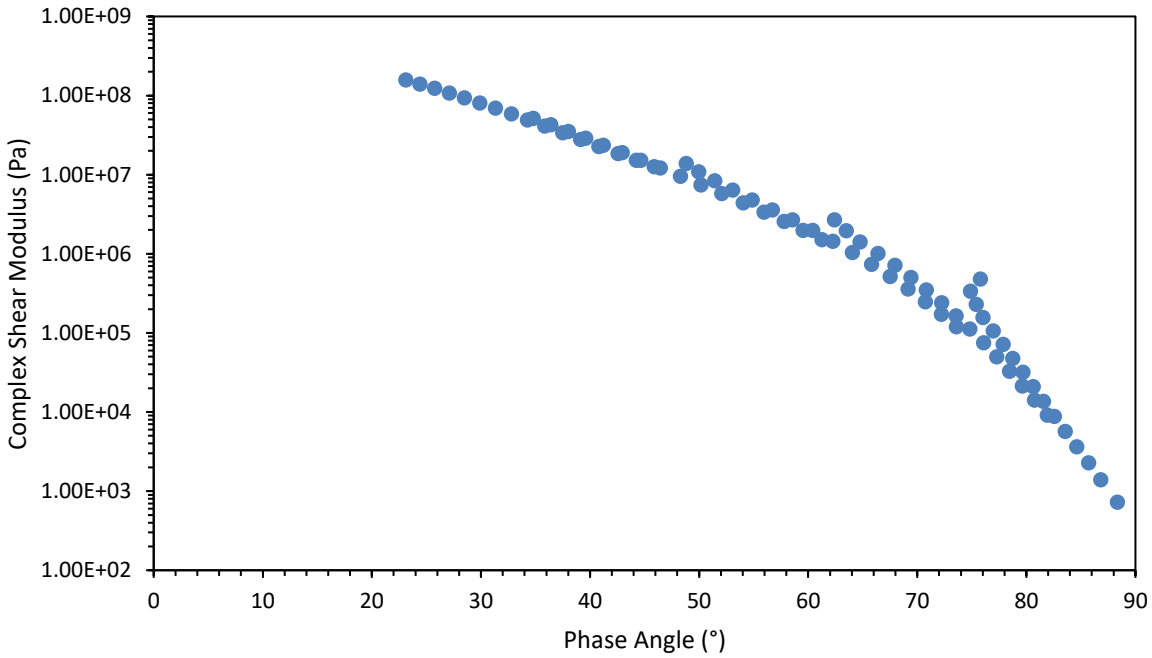

Figure 4.33 – Example (neat bitumen) of black space plot.

To understand deeper the effect of ageing on the Black diagrams, the crossover modulus is studied in this work. Crossover modulus is the complex shear modulus corresponding to the phase angle of 45°, which denotes that the storage shear modulus is equal to the loss shear modulus. When the phase angle is below 45°, the material has more solid behaviour; when it is higher than 45°, the materials have more fluid behaviour. The crossover modulus is a special point on the material's viscoelastic spectrum, which does not depend on the test frequency and temperature (Figure 4.34).

Lower crossover modulus denotes wider molecular mass distribution and higher polydispersity (Scarsella, Mastrofini, Barre, Espinat, & Fenistein, 1999).

All the indices will be described and analyzed in Sub-Section 6.2.3.

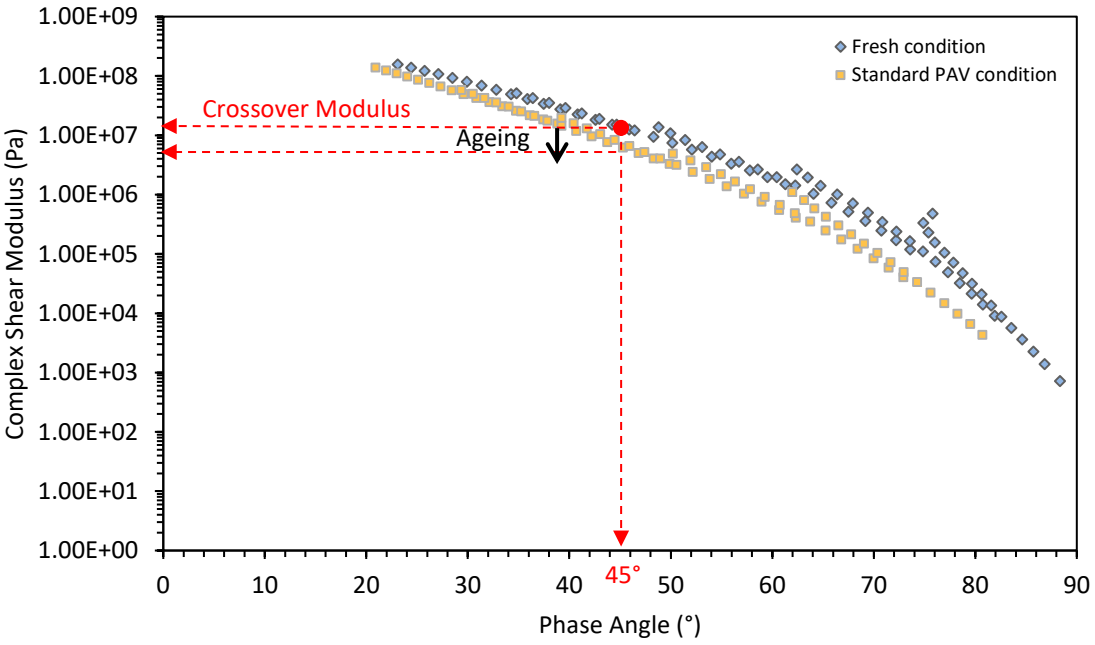

Figure 4.34 - Example to determine the crossover modulus in the black space plot.

In this study the frequency when the storage shear modulus is equal to the loss shear modulus (phase angle is 45°) at the reference temperature, explicitly the crossover frequency (Figure 4.35), was used to characterise the viscoelastic fluid to solid transitory behaviour. Lower crossover frequency suggests higher molecular mass (Liu, He, Ruymbeke, Keunings, & Bailly, 2006), longer relaxation time and higher softening point (Nivitha & Krishnan, 2016).

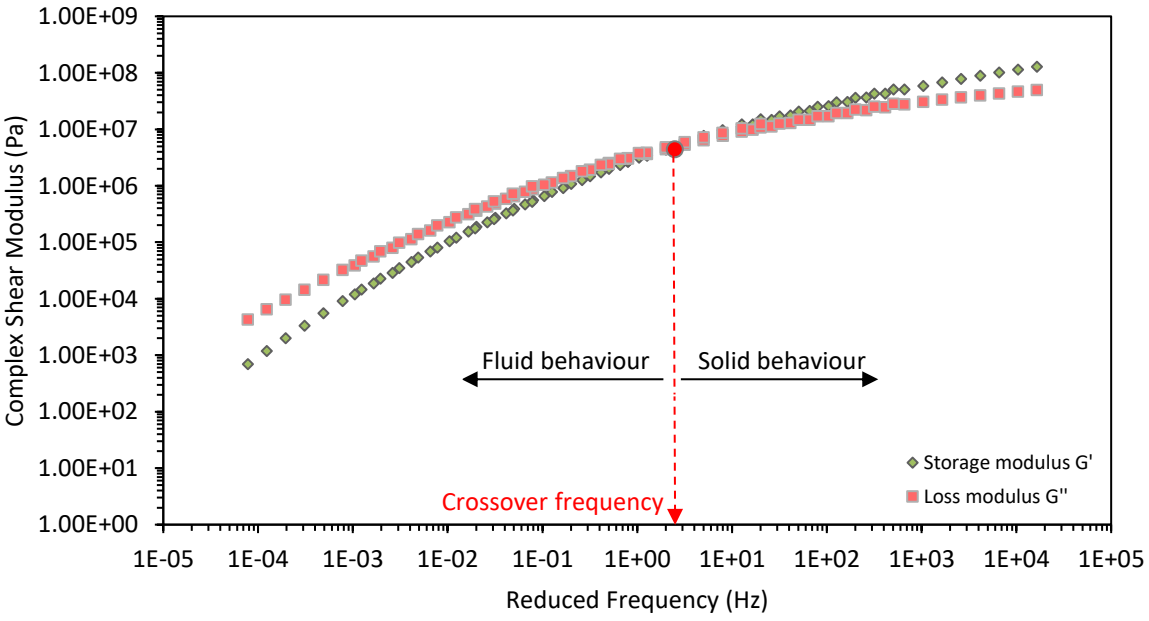

Figure 4.35 - Example to determine the crossover frequency in the black space plot.

CHAPTER 5 – MINERAL FILLERS TESTS RESULTS AND DISCUSSION

5.1 CHEMICAL EVALUATION

In this section, the results of the FTIR tests on the filler are presented and discussed. The main objective is to evaluate the chemical degradation processes of hydrated lime in mineral fillers after subjected to different aging protocols. The first study consists in the analysis of fillers in fresh conditions. The aim is to define, by means of the calcium hydroxide peaks of the FTIR spectra, the percentage of hydrated lime present inside the filler and to compare these values with those provided by *Sibelco.* From this indication it is therefore possible to draw a calibration curve useful for evaluating the hydrated lime of the samples even after aging. More in detail, the indices described in the Sub-Section 4.5.1.2 of the four conditioning were studied to quantify the carbonation process of limestone and possibly the hydration due to the presence of moisture.

5.1.1 HYDRATED LIME AT FRESH CONDITION

Starting from the processed spectra of the fillers in fresh conditions (Fig. 5.1), the hydrated lime peak is analyzed (at wavelength 3642 cm-1).

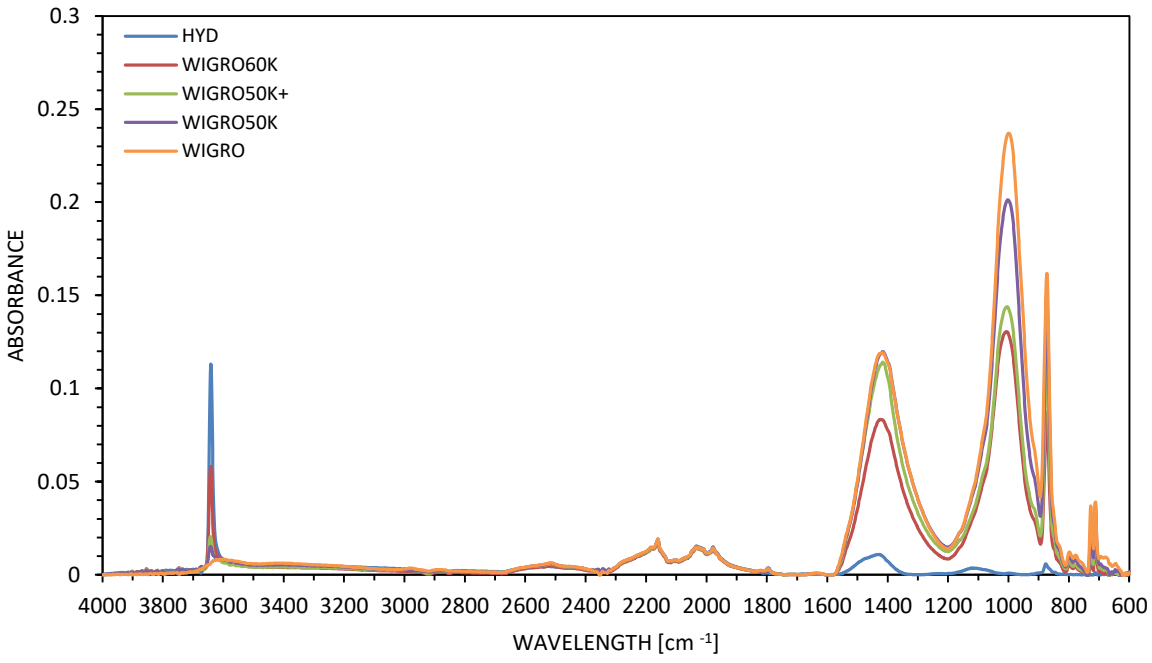

Figure 5.1 – FTIR spectra of fillers in fresh condition.

The absorbance peaks of calcium hydroxide for the various fillers are plotted (in Figure 5.2) in relation to the percentages of hydrated lime, as provided by *Sibelco*. Then a trendline is drawn, with $R^2 = 0.9588$. It can be observed that there is a linear relationship between the absorbance values of the FTIR and these can be used to study the presence of hydrated lime in the mineral filler.

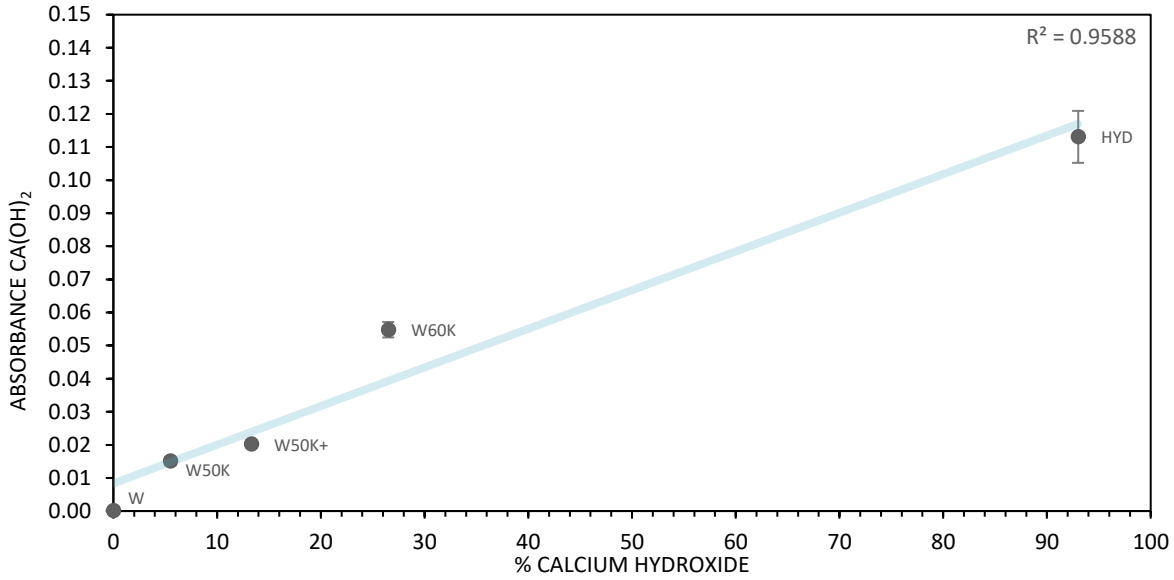

Figure 5.2 - Relationship between the calcium hydroxide peaks of FTIR and the percentage of hydrated lime.

For each filler, the absorbance peak of the hydrated lime is then compared in relation to the impurity peaks due to the presence of limestone (calcium carbonate) and quicklime (calcium oxide) (Fig. 5.3). Also in this case, following the trend line, it can be seen that there is a linear relationship, but with inverse proportionality: as the hydrated lime decreases in the mineral filler, there is an increase in calcium carbonate and calcium oxide.

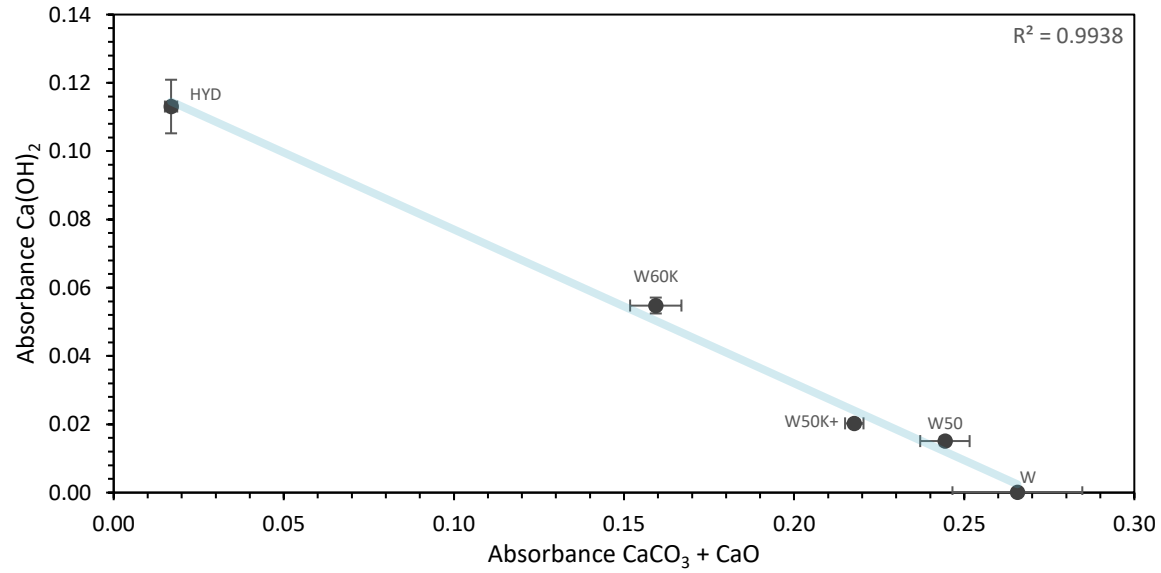

Figure 5.3 - Relation between the peaks of calcium hydroxide and those of calcium oxide + calcium carbonate obtained by FTIR.

By carrying out an analysis on the ratios between the absorbance peaks studied (Fig. 5.4), a ratio lower than 1 is observed that for the various fillers (W, W50K, W50K +, W60) which denotes a greater presence of limestone (calcium carbonate) in the filler, confirming the data provided by *Sibelco*. Also, there is a similar content of Calcium Carbonate and Calcium Oxide. As shown in the previous graph, an increase in hydrated lime corresponds to a decrease in calcium carbonate and calcium oxide therefore it is easy to understand that in comparison between relationships this trend translates into an exponential trendline. With regard to the HYD filler, there is a greater presence of calcium carbonate than calcium oxide.

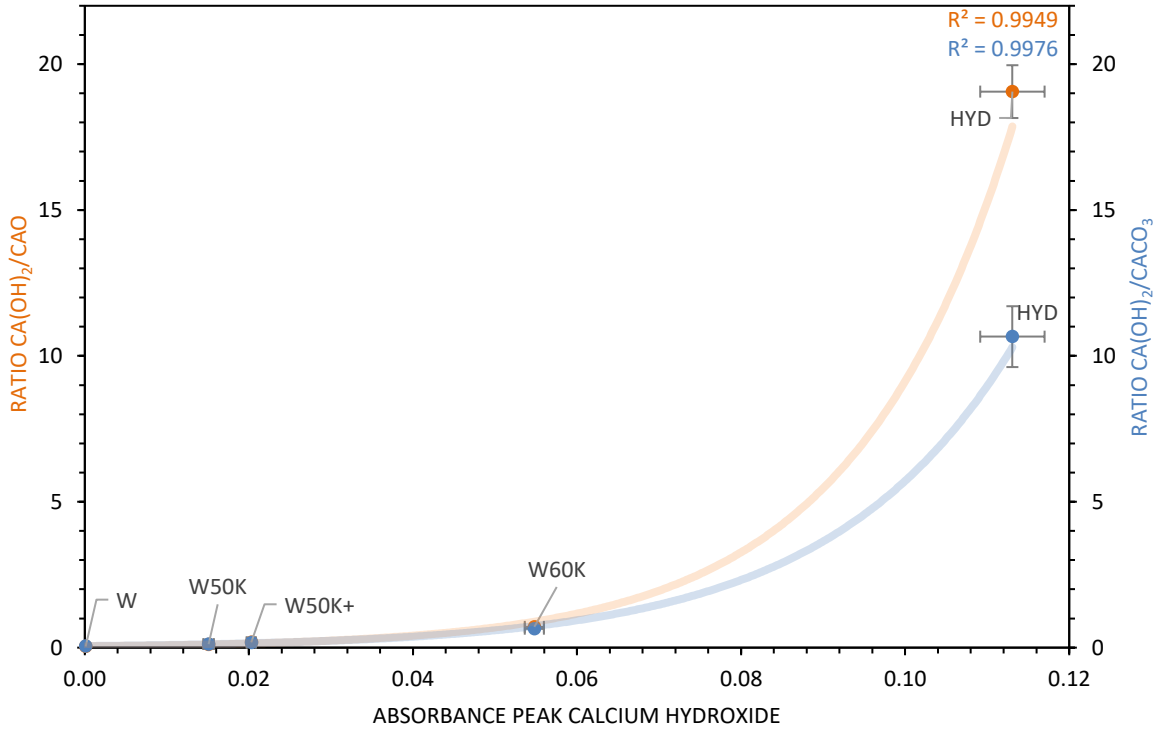

Figure 5.4 - Comparison between the ratios of the peaks of hydrated lime with those of calcium carbonate and calcium oxide.

5.1.2 DEGRADATION OF HYDRATED LIME AFTER AGING CONDITION

The various fillers were analyzed after being subjected to the four different aging protocols to evaluate the degradation effects of hydrated lime due to exposure to air, humidity or inert gas. As described in the Sub-Section, the exposure of hydrated lime to carbon dioxide present in the air causes a carbonation of the calcium hydroxide into calcium carbonate.

The possibility of the hydration phenomenon of quicklime (Calcium Oxide) is also assessed, in the presence of moisture.

From the trendline obtained in Figure 5.2, the calcium hydroxide peaks recorded by the FTIR after the four conditionings in PAV are inserted within the graph in order to compare them

with those in fresh conditions and establish the loss of hydrated lime within the filler. (Fig. 5.5).

The results show that a more substantial decrease of the hydrated lime content for the higher content fillers (HYD).

Since the carbonation process is a reaction that converts hydrated lime into calcium carbonate, fillers (W, W50K, W50K +) with already a high presence of calcium carbonate in nature will undergo this process less, and the peak values will be more constant under different conditions.

Comparing the various conditions, it is noted that aging with the inert gas N_2 is more limited, demonstrating the fact that the conversion of hydrated lime needs a ventilated environment with the presence of carbon dioxide to degrade into limestone.

For instance, it is noted that the peak of calcium hydroxide is reduced less in the presence of humidity compared to the same but dry conditions. This can be attributed to calcium oxide (quicklime) present in the filler which in the presence of humidity in the PAV hydrates and converts back to hydrated lime.

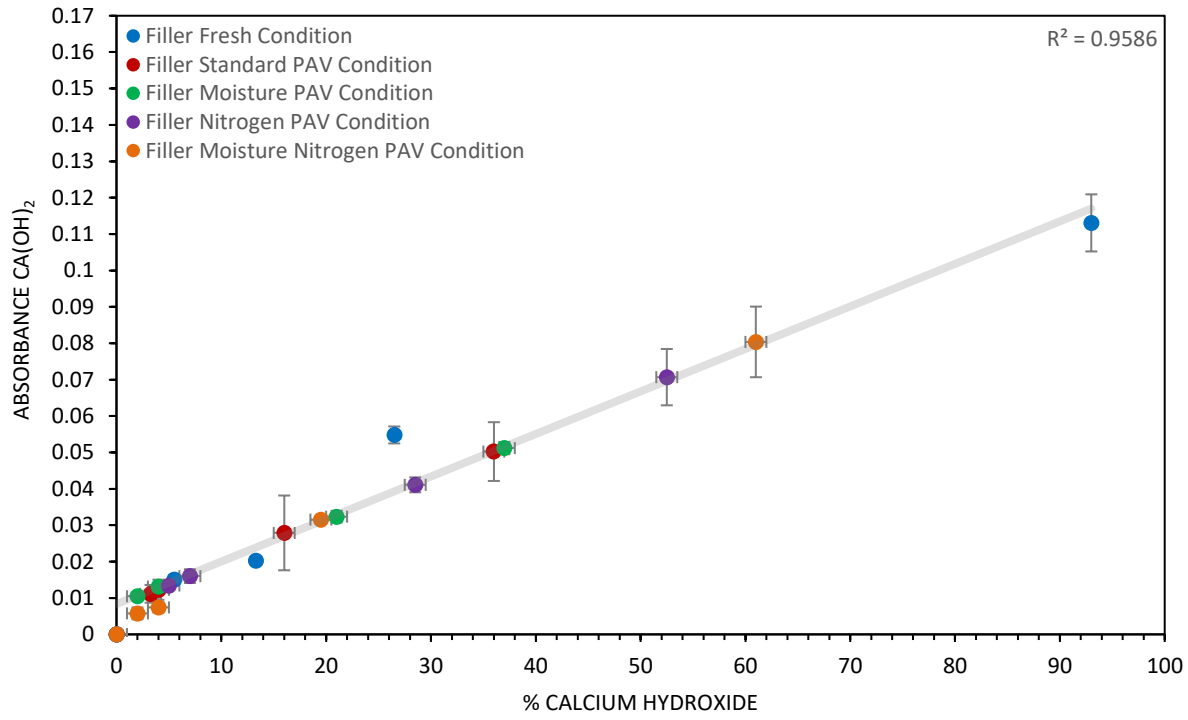

Figure 5.5 - Calcium hydroxide peaks under all conditions.

HYD

The assumption just made can be confirmed by studying in more detail the HYD filler (FTIR spectra in Figure 5.6) with a high content of hydrated lime for the various conditions.

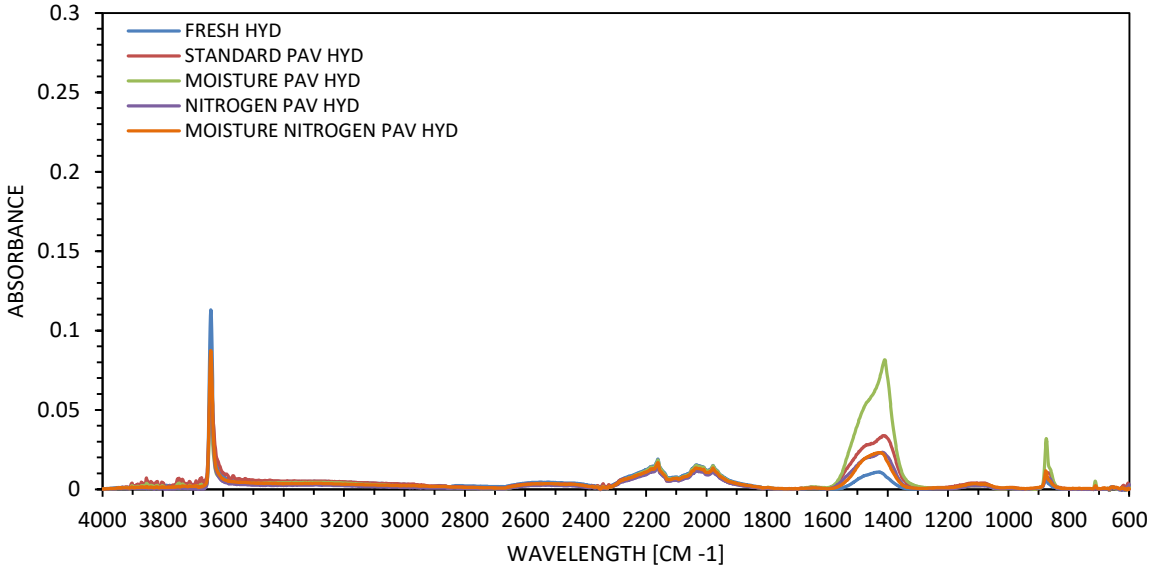

Figure 5.6 – FTIR spectra of HYD filler at different condition.

By comparing the absorbance peaks of calcium hydroxide with the ratio between calcium hydroxide and calcium carbonate useful for studying the carbonation process, a linear relationship can be found (Fig. 5.7). Also in this case it can be said that the reaction of hydrated lime is more limited in inert conditioning, while the presence of humidity contributes to safeguarding the contents of hydrated lime or converts the quicklime present in small percentages into hydrated lime.

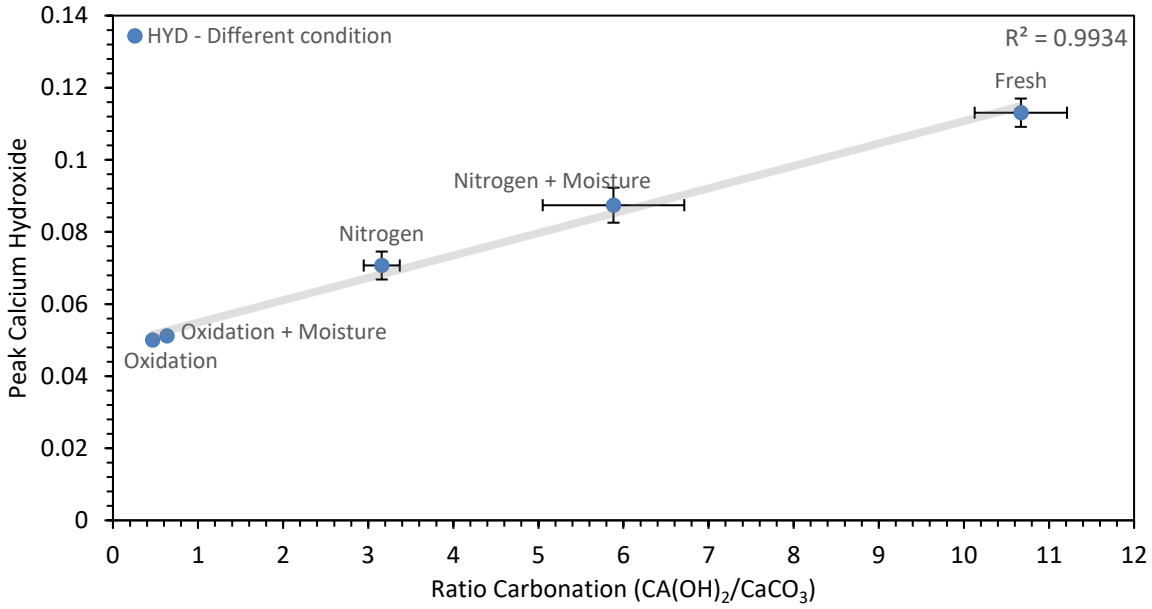

Figure 5.7 - Degradation of hydrated lime in different condition.

The values of absorbance peaks and ratios are shown below in histograms 5.8. Aging in air is more aggressive and the chemical composition of the mineral filler changes more substantially. On the other hand, humidity does not seem to have a degrading effect on hydrated lime.

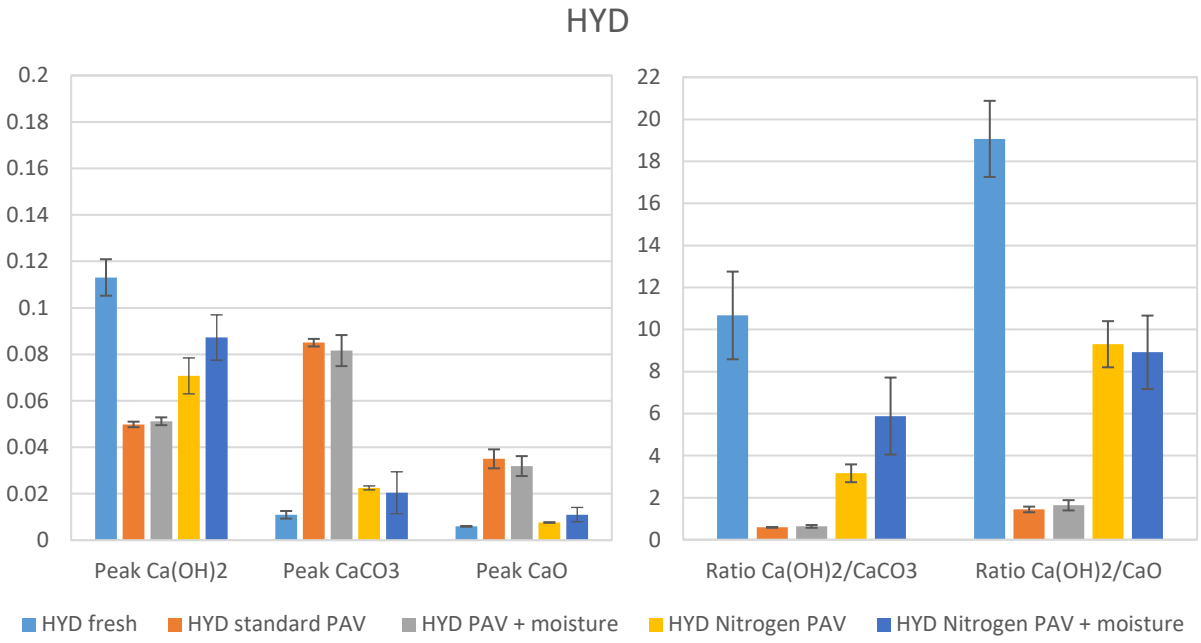

Figure 5.8 - The values of absorbance peaks and ratios of HYD filler

W60, W50K+, W50K, W

The absorbance peaks and the index ratios of the other fillers containing a lower content of hydrated lime do not show linear or exponential graphic correlations (like Figure 5.7 or 5.4).

Where there is no pure presence of hydrated lime, but greater limestone impurities are present as calcium carbonate and quicklime, it should be remembered however that the values are subject to errors also because when the FTIR laser impacts the sample it can indiscriminately hit a mineral particle of calcium hydroxide as of calcium carbonate, substantially changing the parameters.

The histograms (from Fig 5.9 to Fig.5.12) of the fillers W60K, W50K +, W50K, W are shown below with the peaks of calcium hydroxide, calcium carbonate, calcium oxide and the ratios under the five different conditions.

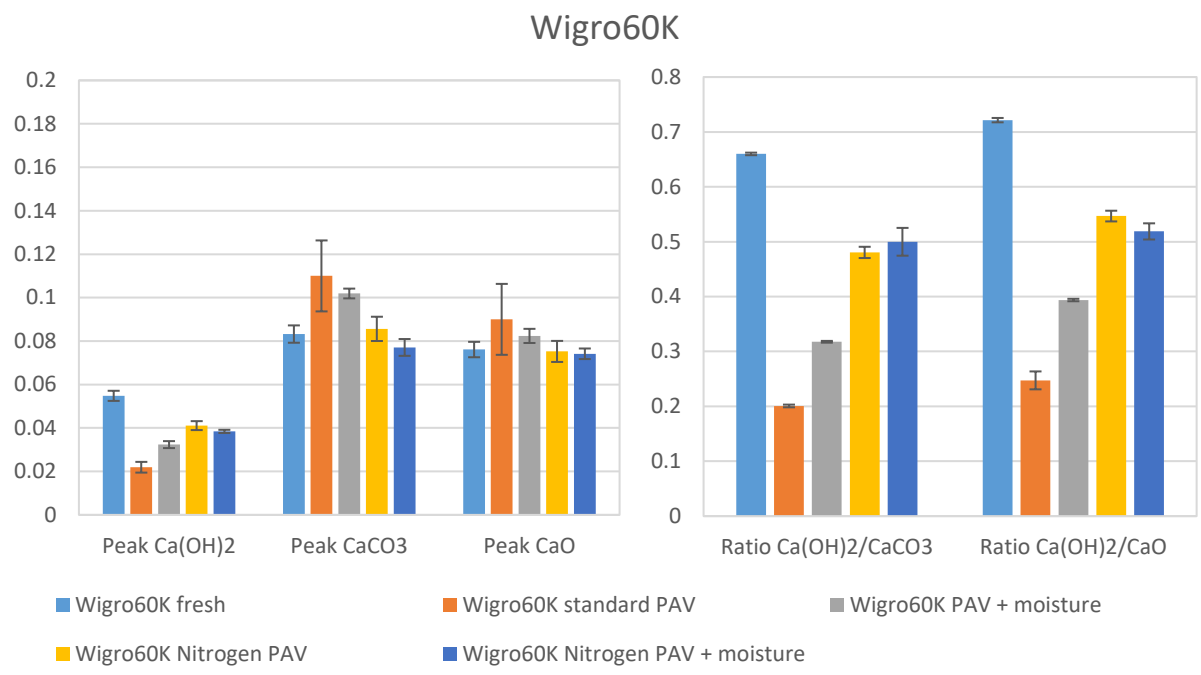

Figure 5.9 - The values of absorbance peaks and ratios of W60K filler

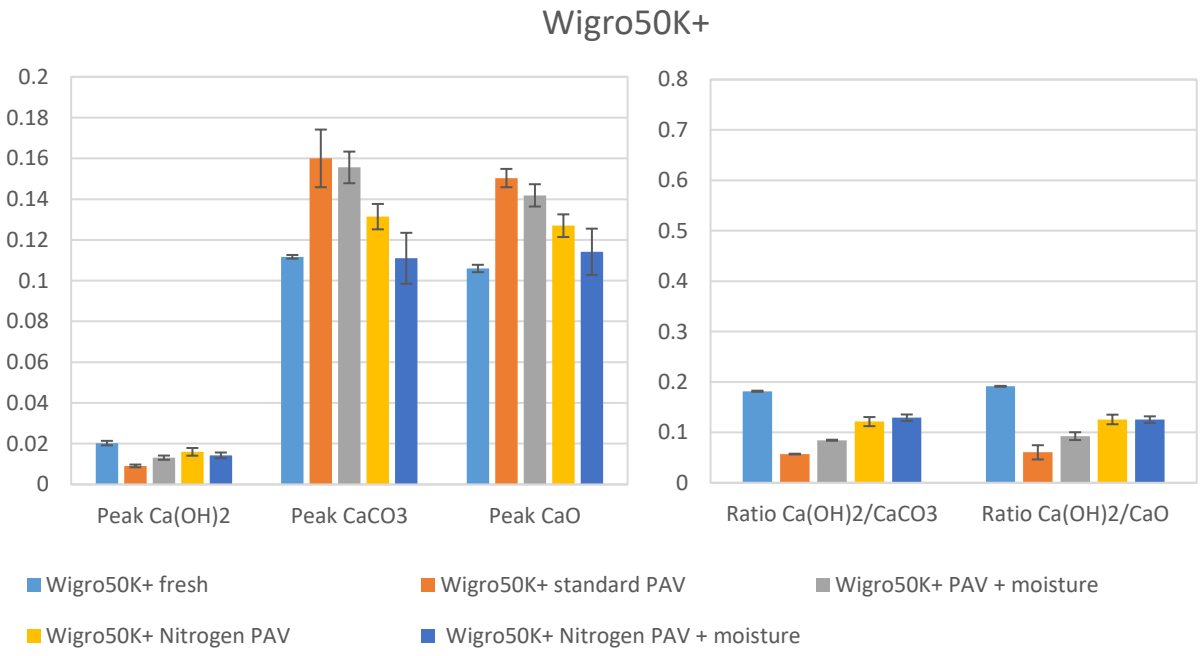

Figure 5.10 - The values of absorbance peaks and ratios of W50K+ filler

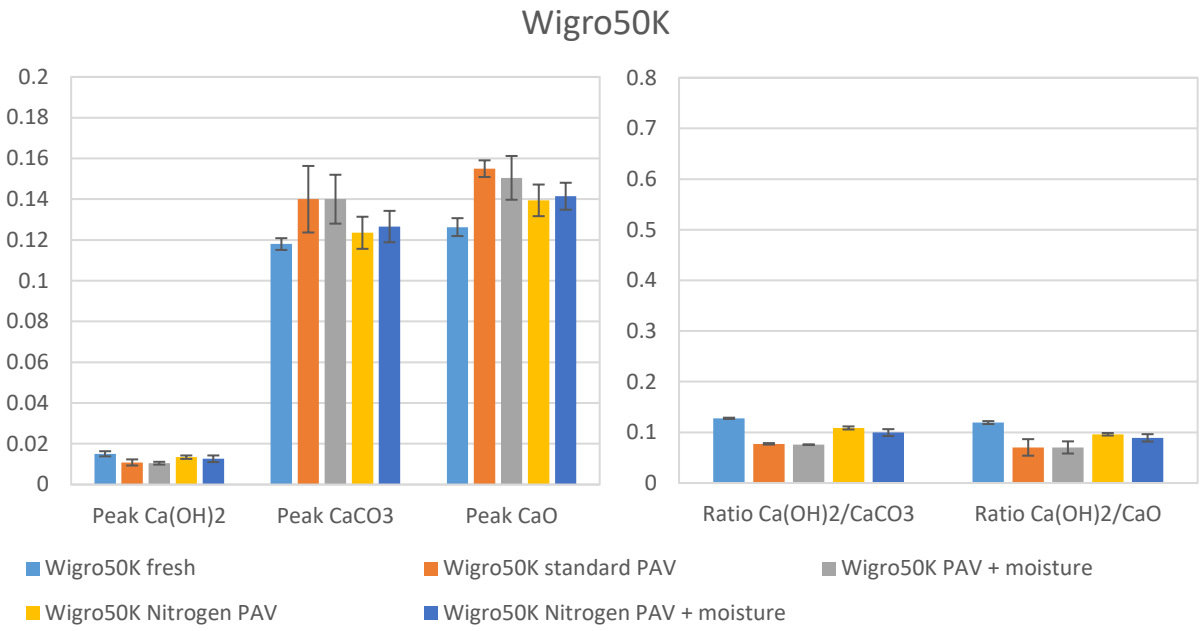

Figure 5.11 - The values of absorbance peaks and ratios of W50K filler

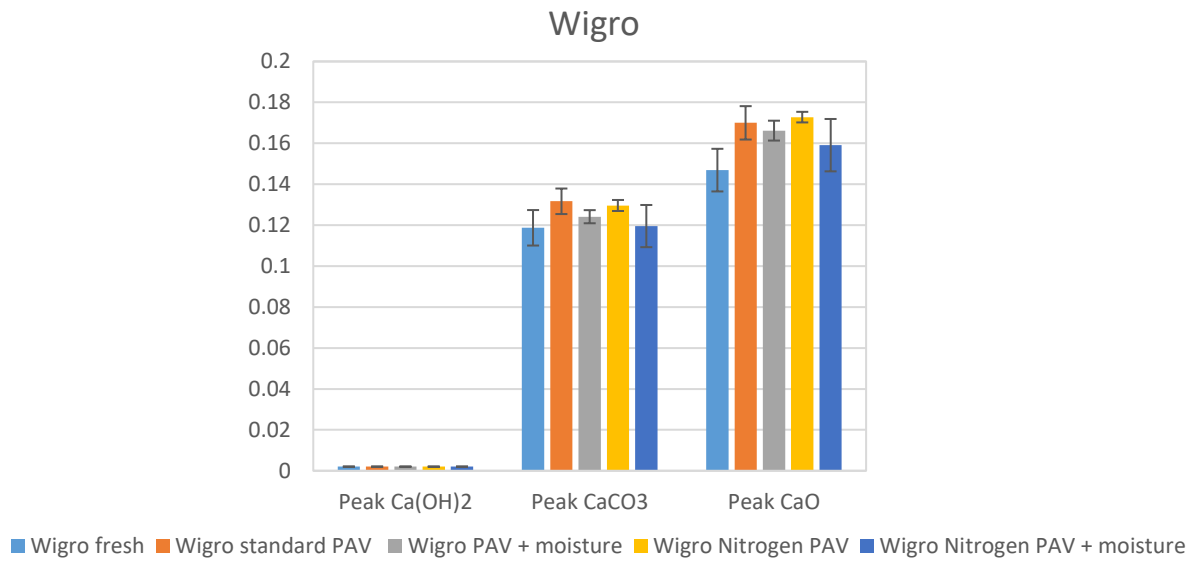

Figure 5.12 - The values of absorbance peaks and ratios of W filler

From the values obtained it can be seen that:

- The degradation of hydrated lime in the various fillers is more evident in aging in air at dry conditions;
- The conditioning with inert gas seems to have less influence on the chemical reactions inside the mineral filler;

- The presence of humidity in the conditioning helps to limit the reduction of the peaks of hydrated lime and at the same time the formation of those of calcium carbonate and calcium oxide. The values of the substantially greater ratios are proof of this.
- Overall, as can be expected, the degradation of lime is proportional to its content (the ratios between the various conditions differ more for HYD and W60K than for W50K).

HYDRATED LIME ON EXPOSURE TO AIR

As described in the Sub-Section 2.3.2, lime carbonation is a slow process due to contact with carbon dioxide present in the atmosphere. For this reason the hydrated lime filler was exposed to the air in a climatic chamber at 10 °C for two weeks, then tested again with the FTIR. The average of the three tests before and after two weeks are shown in the graph 5.13 below.

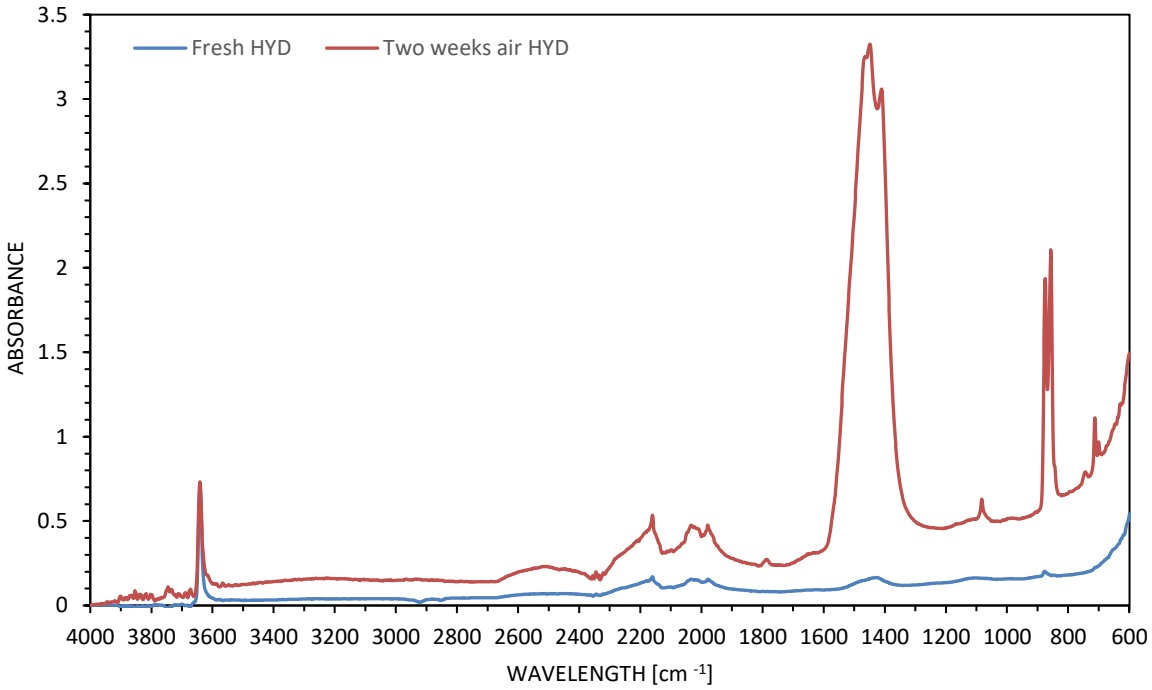

Figure 5.13 - FTIR spectra of the HYD filler in fresh condition and in air exposure (2 weeks) condition.

From the graph we can obtain the indices of the ratios between hydrated lime and calcium carbonate or calcium oxide as in the previous cases (Fig 5.14).

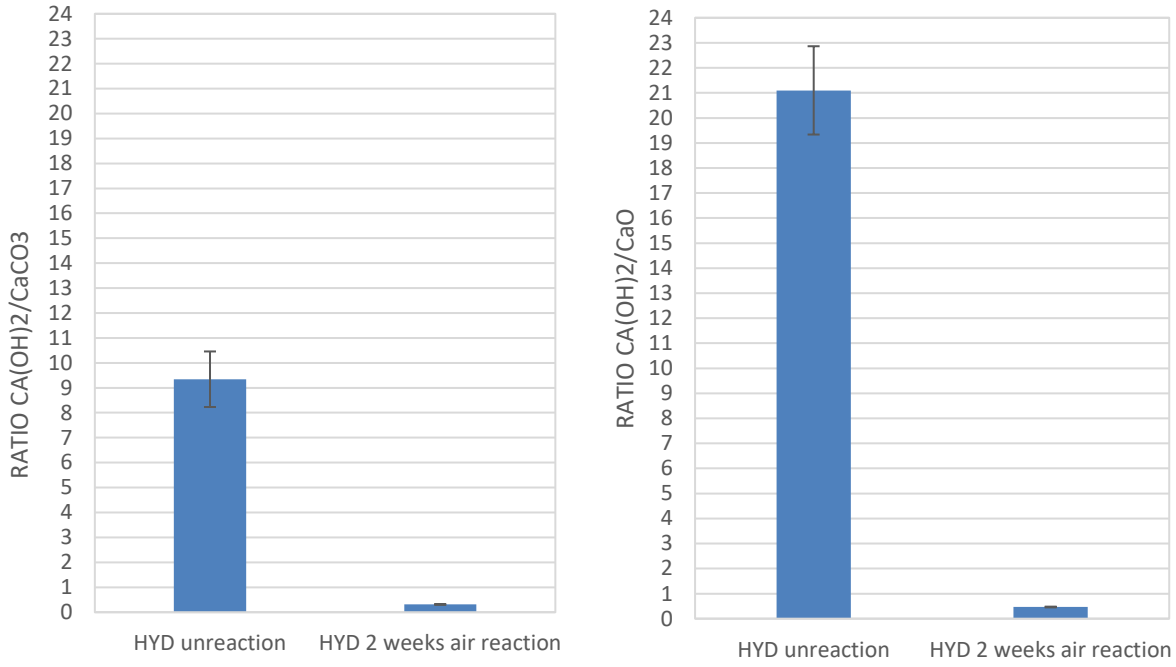

Figure 5.14 - Ratios between hydrated lime and calcium carbonate or calcium oxide.

It is noted very clearly that long-term exposure to air produces a significant change in the mineral. Compared with the four simulated aging phenomena (20h of exposure) it is observed that the carbonation phenomenon is mainly linked to the exposure time, in comparison to temperature or humidity conditions.

5.1.3 SULFOXIDE INDEX

In addition to the indices on hydrated lime and limestone to assess the phenomenon of carbonation of mineral fillers, the sulfoxide index is also analyzed with the area calculation method seen in the Sub-Section 4.5.1.

From these values (Fig. 5.15) it is possible to conduct some reflections on the chemical characteristics of the fillers and make a subsequent comparison with the same values obtained in the mastics composed with bitumen.

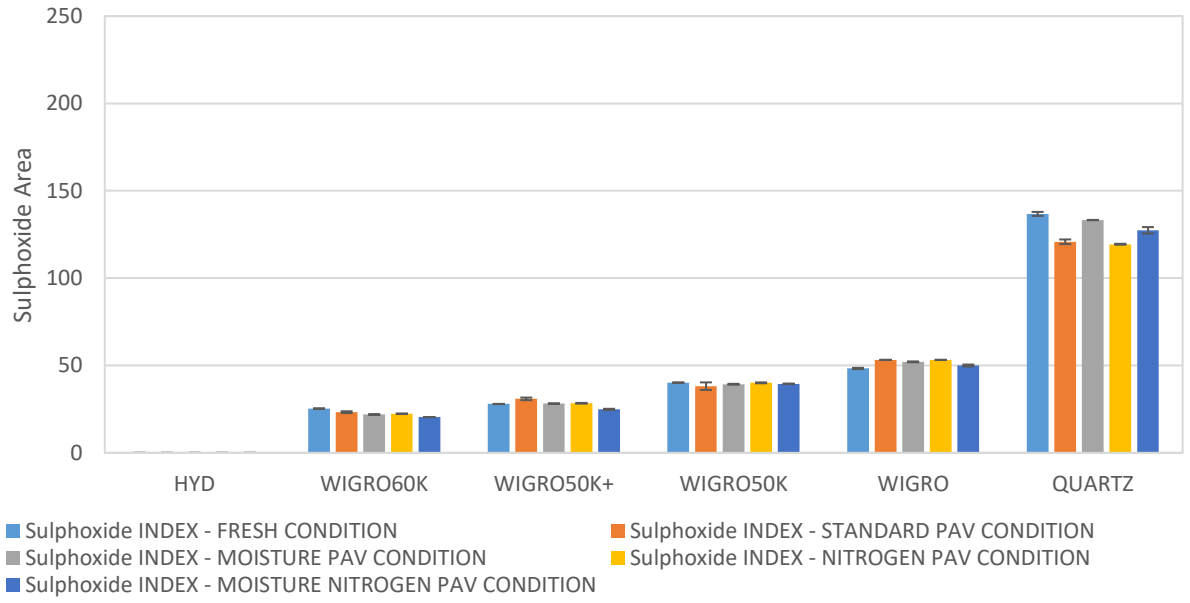

Figure 5.15 – Sulphoxide index

The peak area of the sulfoxides obtained by the FTIR is greater in the case of the mineral filler made up of silicates, quartz: a chemically inert filler for which the main analyzes will be mainly rheological. For "active" fillers composed of calcite, the values of the sulfoxides are clearly lower, with zero values in the case of mineral composed of hydrated lime gradually growing when the main components of the filler become calcium carbonate. From the analyzes in the Sub-Section 6.1.1 it will be found that these parameters are linked to the chemical characteristics of the filler and not of the bitumen. As for the various conditionings, aging and humidity do not affect these parameters therefore they are not very useful to study the phenomenon of degradation.

CHAPTER 6 – BITUMEN AND MASTICS TESTS RESULTS AND DISCUSSION

6.1 CHEMICAL EVALUATION

This section gives the chemical evaluation of the bitumen and the mastics. Infrared spectra were discussed, both before and after the various conditions, focusing on the previously described carbonyl and sulfoxide indices. As in the case of fillers, the post-processing of the FTIR data and the analysis of the spectra is carried out according to the guidelines provided by Hofko et al. (2017).

6.1.1 CARBONYL AND SULFOXIDE INDEX

In Appendix A the normalized infrared spectra of all materials are reported, while below are discussed the indices of the carbonyl (C = O) and sulfoxide (S = O) obtained with the method proposed in Sub-Section 4.5.1.2.

Fig. 6.1 presents one of the samples under examination, it can be deduced that the FTIR spectrum of a mastic is a "mixture" of the individual spectrum of its constituent material, which are attributed to both bitumen and mineral filler.

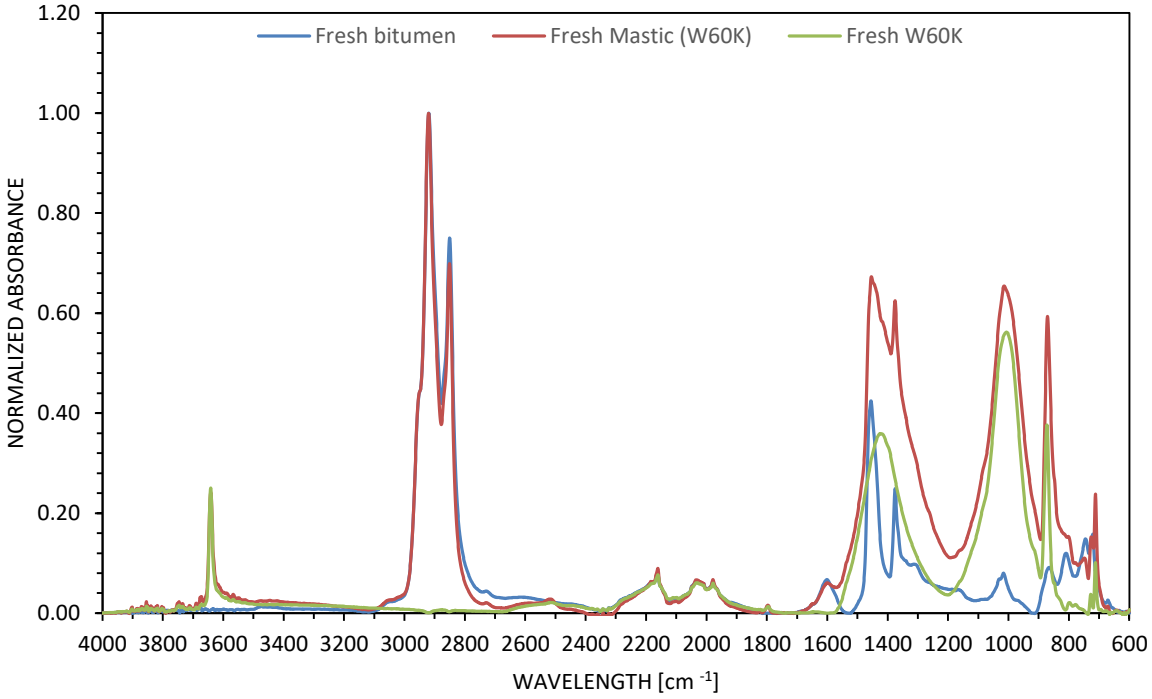

Figure 6.1 - Comparison of the FTIR spectra of bitumen, filler and corresponding mastic.

The area of the "fresh" sulphoxides of the mastics (ie ~ 1030 cm^{-1}) is strongly influenced by the presence of mineral fillers. This correlation can be found by comparing the areas of the sulphoxides of the mastics with the respective fillers seen previously (Fig. 6.2).

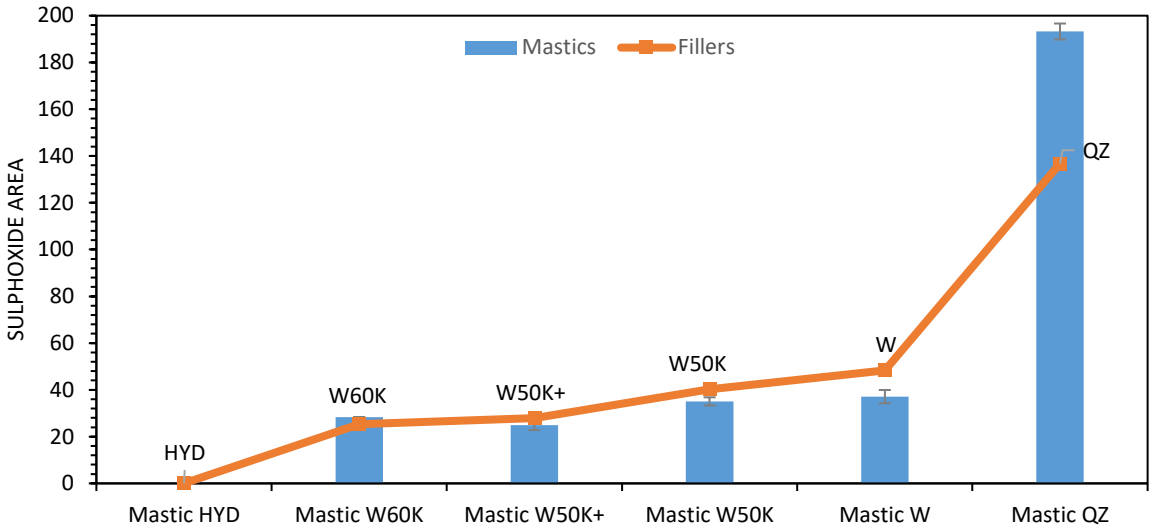

Figure 6.2 - Correlation between the areas of the sulphoxides of the mastics with the respective fillers.

As can be seen in Fig. 6.3, for some materials the infrared spectra corresponding to their "fresh" state show a higher peak than the respective of the aged state. This is in contradiction with what is normally expected and observed, i.e. the formation of S=O bonds in the bituminous microstructure after aging is translated through an increase in the sulphoxide peak. The reason behind these results is the presence of mineral fillers in mastics and, more specifically, the interference of the infrared ray, loaded in the sample, with solid particles. The effect of aging on the bitumen microstructure, in terms of sulphoxide formation, is present, but is hindered by the simultaneous contribution of mineral matter to the spectrum of aged mastic. The absorbance value recorded, during the measurements, depends very much on whether the infrared ray "hits" a particle of mineral charge, neat bitumen or a combination of the two. The latter is also corroborated by the variability of absorbance observed among the three replicates tested for each mastic.

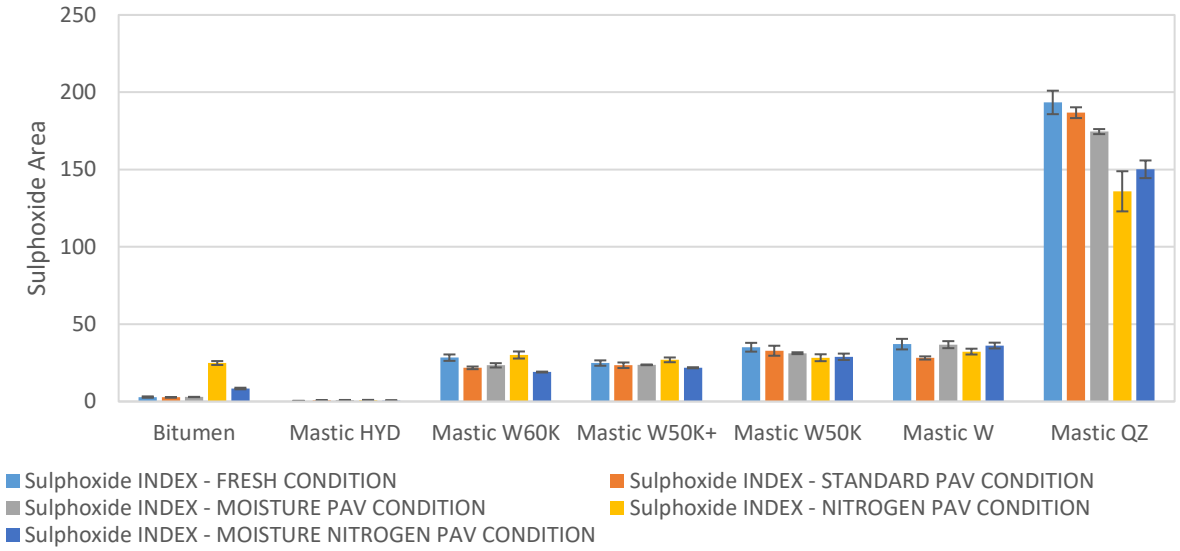

Figure 6.3 – Sulphoxide Index

The above qualitative analysis of infrared spectra implies that is not a reliable index for assessing the aging of mastics, from a chemical point of view, since it would produce irrational results.

On the other hand, the IC calculation seems a more reliable and solid way to trace the effect of aging on the various mastics and neat bitumen, in the case of exposure to air and not to inert gas, through the formation of bonds C=O in the matrices of the binders. The carbonyl area has the same shape as "fresh" neat bitumen, which does not imply any effect of the mineral matter on these wave numbers. This reaction is attributable exclusively to the bituminous phase. With aging, the increase in carbonyls, due to the formation of C = O bonds, is traced through visible peaks around the wave number 1700 cm-1. The CI was calculated according the method discussed in Sub-Section 4.5.1. The results are presented in Fig. 6.4.

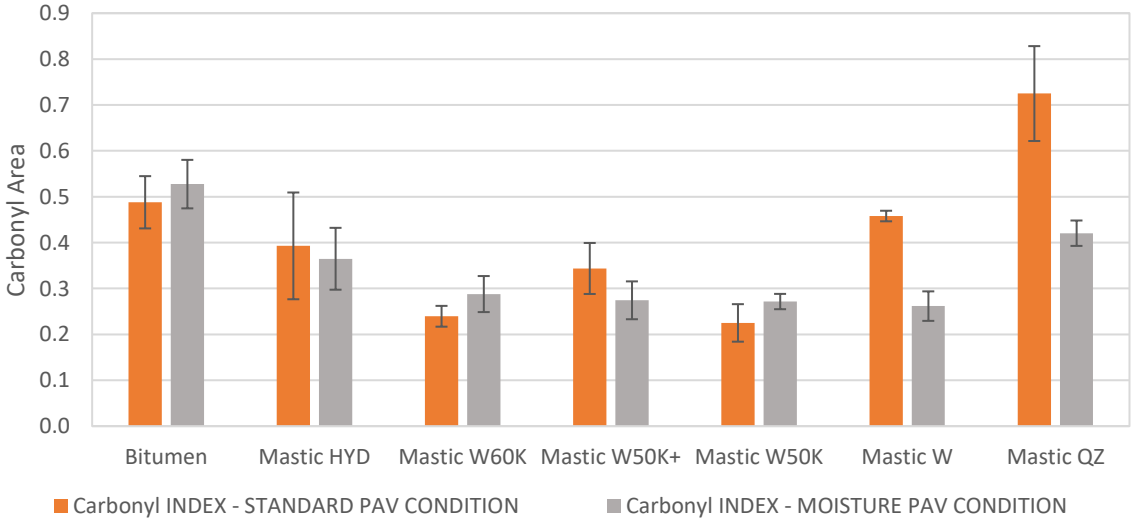

Figure 6.4 – Carbonyl Index

The results in Fig. 6.4 Show that there can be a correlation in the IC between the materials, from a statistical point of view, and the quantity of lime hydrated inside the mixture.

Analytically, the mastics W60K, W50K and W50K seem to have undergone less severe aging than neat bitumen, of the HYD mastic with a high percentage of hydrated lime or W and QZ with zero presence, as shown by their lowest CI. It is assumed that the presence of hydrated lime inside the mastic, as long as it is not excessive, leads to a limitation of chemical aging and a possible increase in performance over time. The presence of humidity in aging seems to confirm this trend, even if there is no linear correlation between the two conditions.

It can be globally stated that the presence of mineral fillers that should develop both physical and chemical interactions with bitumen, therefore not quartz, show a lower CI compared to the aging of neat bitumen, limiting the catalysis of the oxidation of bitumen in mastics. The formation of less carbonyls is believed to be the result of the lengthening of the oxygen diffusion path caused by the physical presence of the mineral filler's particles in the mastic.

Curtis et al. (1993) stated that the aging of bitumen in the presence of mineral substances causes a delay in its accumulation of viscosity, compared to the aging of neat bitumen, aged in identical conditions. The researchers believed that the difference in viscosity development was the result of the adsorption of polar functional groups from the bitumen onto the particles of mineral substances, which prevented the formation of viscosity build-ups.

The CI results verify the existence of the "anti-aging" mechanism.

Taking into account that these parameters will not be useful for rheological studies in the case of conditioning with inert gas, a subsequent comparison will be made between the following chemical indices and the rheological results on mastics.

6.1.2 HYDRATED LIME IN THE MASTICS

From the FTIR tests as for the fillers, the calcium hydroxide peaks are extrapolated to 3642 cm^{-1} to evaluate the presence of hydrated lime in the mastic at the various conditions.

Starting from the fresh conditions, it is taken into account the fact that the filler in the mastic is in a 1:1 ratio by weight with the bitumen, for this reason the hydrated lime content present will be halved.

From the absorbance values of the mastics with HYD, W60K, W50K+, W50K and W obtained for the fresh condition, the trendline is traced to evaluate the presence of hydrated

lime in the various mastics for the four stages of aging. Fig. 6.5 shows the graph with all the mastic for all conditions.

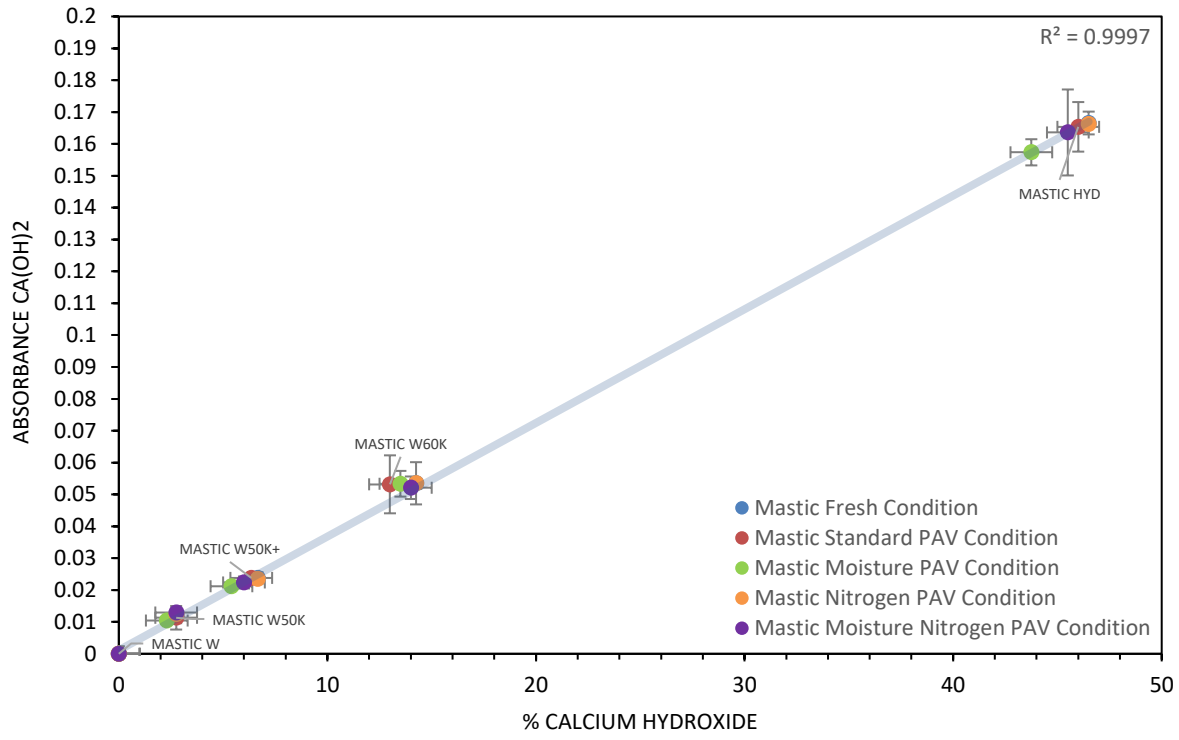

Figure 6.5 - Correlation between the presence of hydrated lime and calcium hydroxide peaks of the various mastics under different conditions.

As with fillers, the linearity between the absorbance values for the various mastics is evident. However, unlike the previous case (Fig. 5.5) It is noted that for the same material for the various aging conditions there is a decrease in the negligible peak of calcium hydroxide. This can be explained by the fact that the presence of the bituminous matrix inside the mastic covers and covers the mineral particles of the filler containing hydrated lime. The carbon dioxide present in the air in this way is unable to attack the surface of the mineral fillers causing the slow carbonation of the lime in carbonate. For this reason, bitumen allows to keep the chemical parameters of hydrated lime unchanged over time.

6.1.3 NITROGEN IN THE BITUMEN

Special mention must be made for the FTIR test of neat bitumen aged in conditions of inert gas N_2. As shown in the graph below (Fig.6.6) it is noted that the absorbance spectrum of the bitumen exposed to nitrogen has significantly changed.

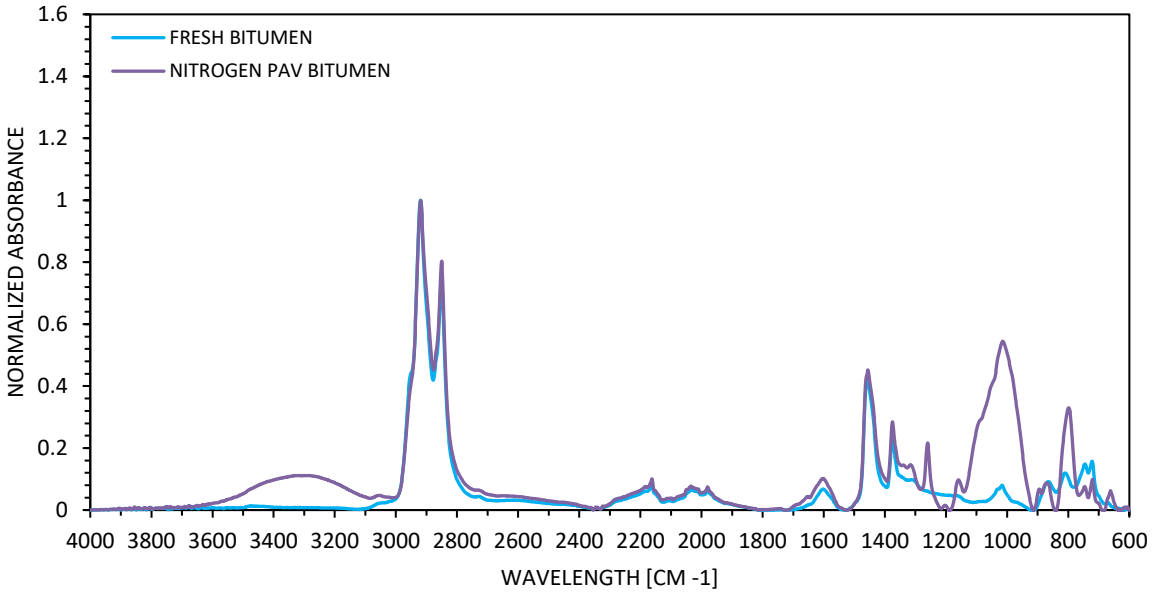

Figure 6.6 - FTIR spectrum of bitumen in fresh condition and after conditioning with nitrogen.

The bend, stretch and peaks recorded in the range 3300-3500 cm^{-1} and 900-1600 cm^{-1} according to the chemical studies carried out are the result of chemical bonds formed between the N_2 nitrogen present in the PAV and the C-H groups of the SARA fractionation present in the bituminous matrix (Fig. 6.6).

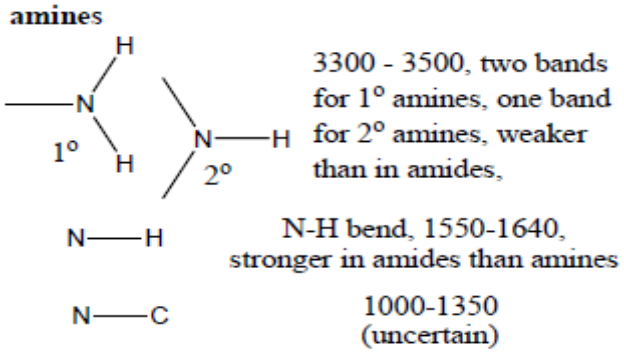

Figure 6.6 - Chemical bonds formed between the N_2 and the C-H groups.

This chemical transformation is scanned only in the case of neat bitumen, demonstrating that the inert gas in this respect does not react with the mineral fillers of the filler to form amines.

In the subsequent rheological studies (e.g. relaxation test), for the case of conditioning with inert gas there will be extremely different parameters between neat bitumen and mastic. This leads to the consideration that the mineral filler acts as a limiter in the formation of amines inside the mastic, maintaining the post-aging chemical and rheological properties.

6.2 RHEOLOGICAL EVALUATION

In this section, the rheological data of the mastics and neat bitumen were reported and discussed, using dynamic mechanical tests (frequency sweep, fatigue and relaxation) to study the effect of various conditions on the viscoelastic characteristics of bitumen.

6.2.1 RELAXATION

The stress relaxation capacity of bitumen can be considered an indicator of the loss of durability of bitumen due to aging. Stress relaxation is essentially an indicator of bitumen cracking, such as a decrease in the ability to relax stress (induced by traffic or heat load) due to aging (Othman et al. 1995, Daniel et al. 1998, Raad et al. 2001) eventually lead to the breaking of the pavement.

Jing et al. (2019) stated that the stress relaxation test was more suitable for characterizing bitumen aging. Aged bitumen had higher residual stresses and longer relaxation times. Hence, aged bitumen was more susceptible to the accumulation of stress and therefore to cracking.

Based on the experimental results, some evaluation indices were used to analyze the changes in the relaxation properties of bitumen and aged mastics. In particular, the relationship between the initial (0 s) and final (100 s) shear stresses was analyzed. In addition, the impact of certain factors, such as the presence of moisture, on the aging of the mixture was investigated.

In appendix B all 35 relaxation tests are reported (comparing materials and comparing conditions). From the graphs (From Fig. B6 to Fig. B12) it can be seen that the relaxation curve rises in the event of aging with air (with or without the presence of humidity), thus indicating that, at the same time of relaxation, the stress of shear the bitumen or mastics increases with aging. In other words, the relaxation form increases with aging.

To further analyze the relaxation properties of aged bitumen, the absolute values of the shear stress at 0 s and 100 s are shown in the Figure 6.7, which indicates the state of stress of the bitumen at the initial and final moment of relaxation.

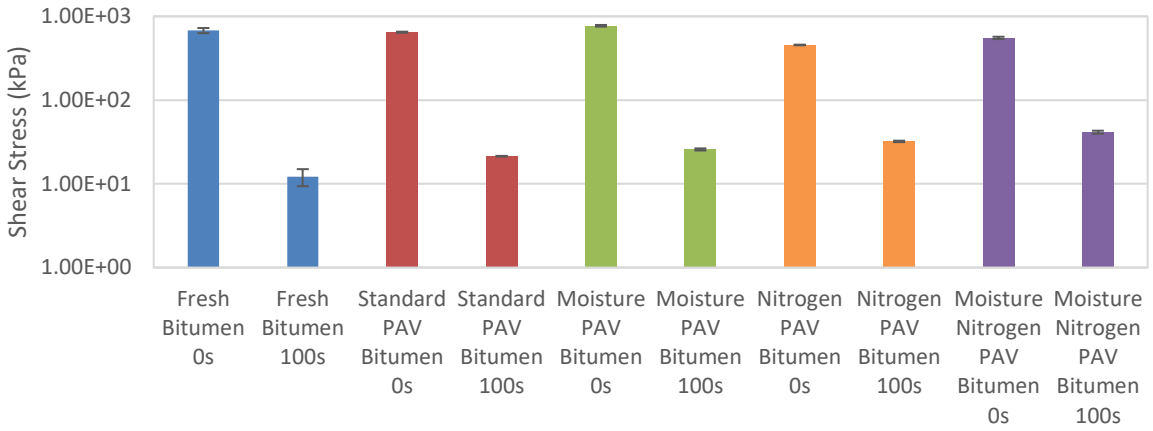

Figure 6.7 - Absolute values of the shear stress at 0 s and 100 s of neat bitumen.

In the Figure 6.7, the initial shear stress (shear stress at 0 s) of bitumen samples subjected to different aging conditions are in the order of 1000 kPa. After a relaxation period of 100 s, the shear stress of conditioned bitumen is 2 to 4 times higher than that of fresh bitumen. Hence, residual shear stresses after the same relaxation time are higher for conditioned bitumen (Fig. 6.7).

The Figure 6.8 shows that the relationship between residual shear stress (at 100 s) and initial stress (at 0 s) describes the relaxation rate at a specific time. Higher ratios indicate that bitumen can accumulate higher stresses after the same load number.

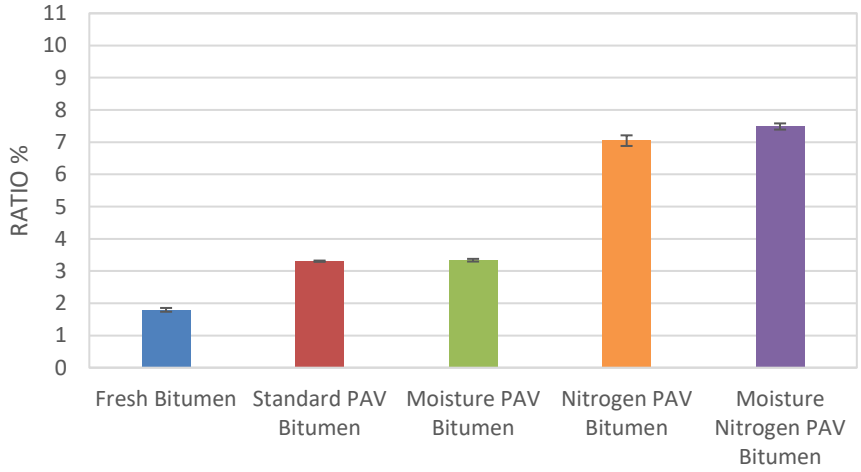

Figure 6.8 - Relationship between residual shear stress (at 100 s) and initial stress (at 0 s) of neat bitume).

The results show that the shear stress ratio in the case of neat bitumen increases with aging. In other words, the results show that aged bitumen leads to higher stress ratios, suggesting that it can accumulate higher stresses after the same load number. Due to the continuous traffic load, the bitumen relaxation time must be short in order to prevent the accumulation of stress in the pavement.

The results of the neat bitumen with inert gas conditioning are somewhat unusual. The high stress ratio can be attributed to a modification of the chemical/physical structure of the bitumen after reaction with nitrogen. In fact, as previously discussed, conditioning only causes amine groups to form only in the case of neat bitumen (and not mastics). This formation, as in the case of carbonyl groups for oxidative aging, can also have a rheological impact.

For mastics, the situation is somewhat different (Fig. 6.9).

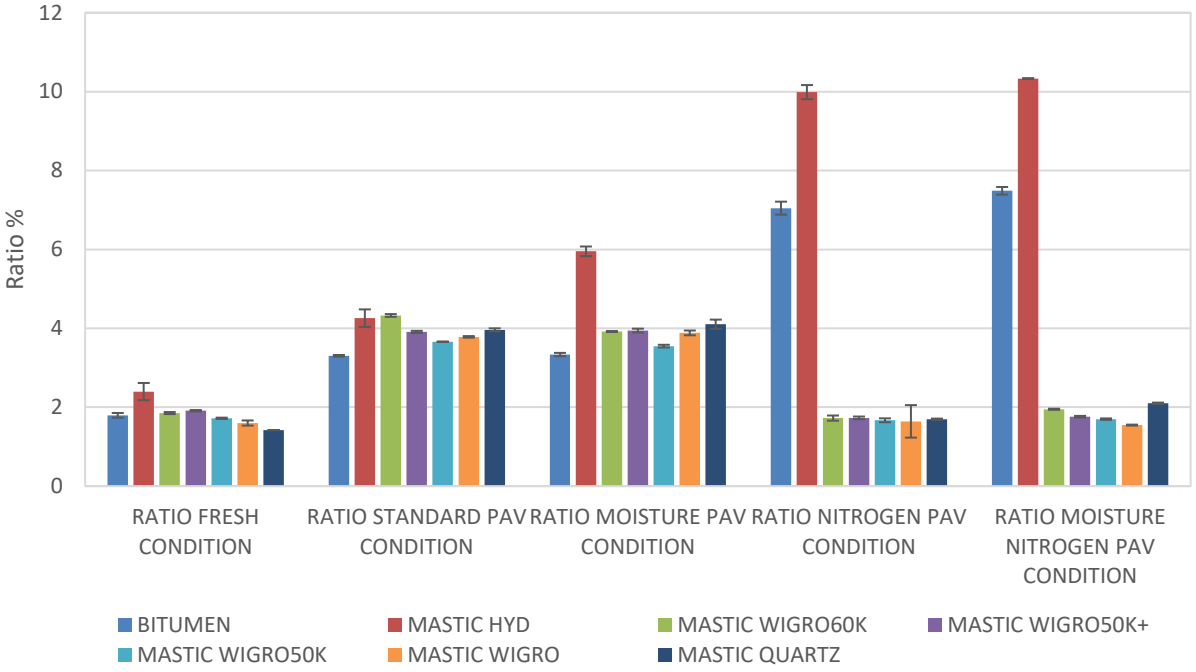

Figure 6.9 - Relationship between residual shear stress (at 100 s) and initial stress (at 0 s) for all mastic.

Aged HYD mastics, compared to fresh HYD mastics, show higher residual shear stresses after relaxation and are more susceptible to the accumulation of stress and therefore to cracking. The values, even in fresh conditions, are significantly higher than in the neat bitumen since the presence of hydrated lime causes a greater hardening of the mixture and therefore a greater susceptibility to cracking. In this case the presence of moisture seems to negatively affect the relaxation properties.

For fresh conditions the other mastics containing a lower percentage of hydrated lime (and therefore greater presence of calcium carbonate) or silicates (quartz) behave almost like bitumen.

In conditions of aging in air, in tendency with bitumen, aged samples show higher residual shear stresses after relaxation and are more susceptible to the accumulation of stress. Also in

this case the presence of mineral filler contributes to a greater hardening of the mixture and therefore to higher parameters compared to only bitumen.

For aging conditions in inert gas, however, a collapse of the relaxation parameters is observed. We had noticed that on a chemical level there was a strong influence of nitrogen in the bituminous matrix through the formation of amines. This was not visible in the spectrum of the mastics. Apparently, in mastics containing carbonates or silicates, nitrogen has an inactive role and the relaxation values remain unchanged compared to fresh conditions.

With the exception of the mastic with HYD, the presence of moisture in aging does not clearly affect the susceptibility to accumulation of stress.

6.2.2 LINEAR AMPLITUDE SWEEP

The amplitude test is normally used to distinguish the linear and nonlinear viscoelastic response of bitumen. The test is conducted at constant temperature and frequency with an increasing amplitude (strain / deformation). As the level of strain / deformation increases, the bituminous material passes through the linear viscoelastic phase to the nonlinear viscoelastic phase and therefore to the damage phase. In addition to the critical non-linear viscoelastic point, the mechanical properties of bituminous materials change: the complex shear modulus decreases and the phase angle increases.

The stress-strain curves of the studied fresh and conditioned bitumen are shown in Figure 6.10.

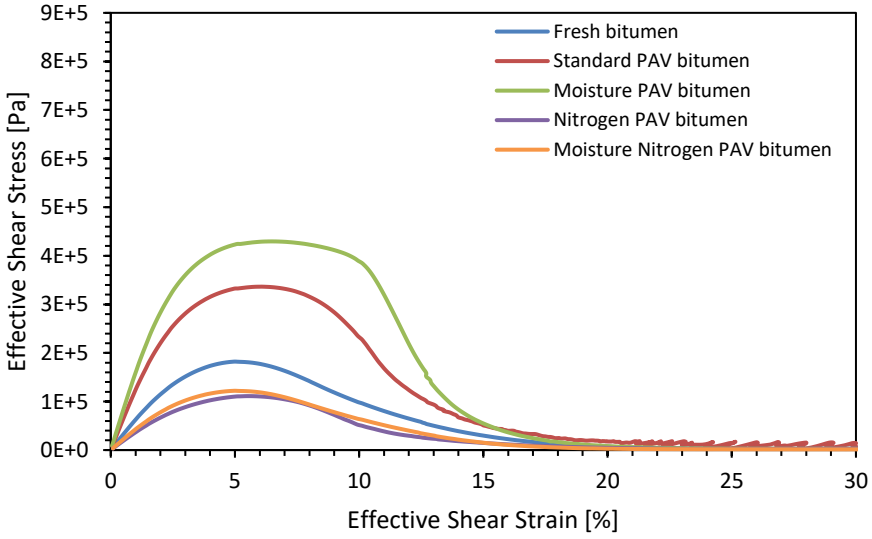

Figure 6.10 - Stress-strain curves of bitumen at different condition.

The figure 6.10 shows that the shear stress increases with the shear strain and reaches a maximum value at about 5-6% shear strain. For the strain controlled mode, the shear stress increases linearly with the shear strain at the beginning. So the shear stress increases more and more slowly, which indicates that the bitumen response is in the nonlinear viscoelastic range. As soon as the applied strain increases to a certain level, the shear stress of the materials reaches the maximum and subsequently decreases continuously due to the accumulation of damage.

Based on the stress-strain curve in Figure 6.10, the result of complex shear modulus for the stress control mode was calculated and shown in Figure 6.11.

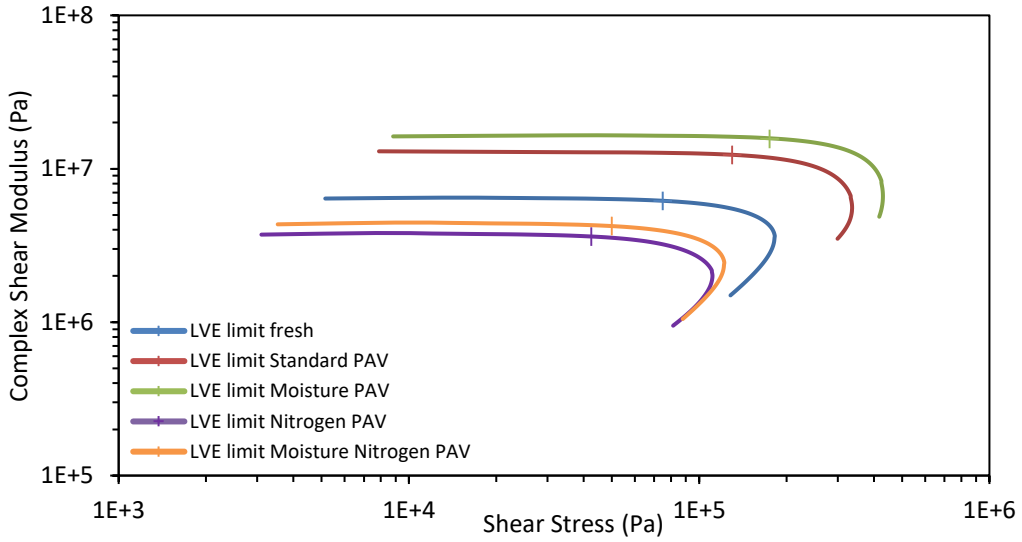

Figure 6.11 - Complex shear modulus of neat bitumen at different conditions condition under the stress-controlled mode.

As described in Sub-Section 3.5.2.2, the critical linear viscoelasticity point is defined as the point that a 95% reduction in the initial complex shear modulus occurs. After this point, the response of bitumen is in the nonlinear viscoelastic range, in which the complex shear modulus decreases and the phase angle increases, respectively. The changes of the critical linear viscoelasticity point in fresh conditions and after aging for bitumen and for all types of mastic are shown in the Figure 6.12.

The critical nonlinear viscoelasticity point is defined as the point that the maximum shear stress occurs on the basis of the stress-strain curve in Figure. After this point, the response of bitumen is within the damage range, in which the shear stress decreases. The changes of the critical nonlinear viscoelasticity in fresh conditions and after aging for bitumen and for all types of mastic are shown in the Figure 6.13.

In Appendix C there are all the graphs obtained from the LAS test useful for obtaining the linear VE and non-linear VE points.

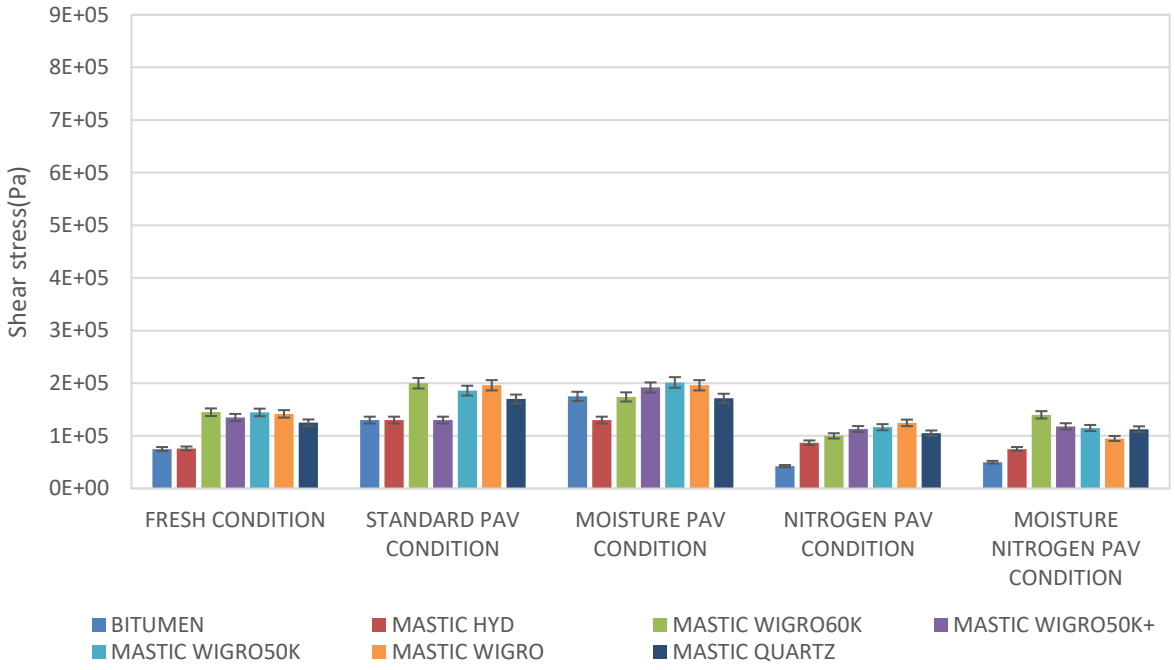

Figure 6.12 - Critical linear viscoelastic points of each fresh and aged sample under shear stress control modes.

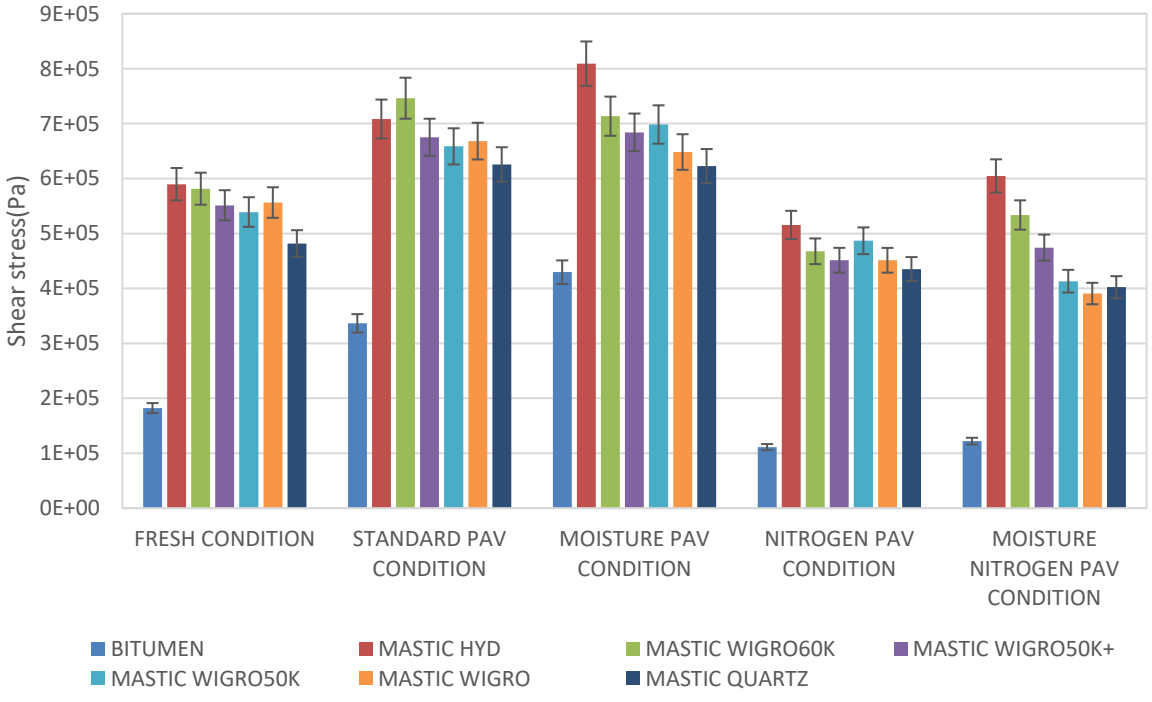

Figure 6.13 - Critical nonlinear viscoelastic points of each fresh and aged sample under shear stress control modes.

The results show that aging definitely has an effect on the linear viscoelastic limits of the material. A comparison between mastics and bitumen at fresh and aged standard conditions (dry air) reveals that the aged material has higher linear limits for stress. The reason for these

phenomena is that the hardening of the bitumen caused by aging makes the material capable of withstanding greater stress with less deformation. In the case of aging in inert gas, the values remain almost unchanged with respect to the fresh conditions, therefore this conditioning does not influence the mixture in the study of viscoelasticity. Furthermore, for both conditions, the presence of humidity does not seem to affect the values in a linear way, demonstrating that the linear and non-linear critical point are parameters which are not useful for understanding the differences in aging with or without moisture.

Mastic with HYD has a low critical LE point around the values of neat bitumen while the non-critical LE point value is very high, exceeding that of the other mastic; this means that its linear viscoelastic region is very small as it is an extremely rigid and more fragile mixture.

The other mastics (with a lower or no presence of hydrated lime) have higher values of critical and non-critical points, which means that they endure greater stress before reaching the area of damage.

Fatigue cycles

The linear amplitude test also aims to evaluate the ability of bituminous materials to resist damage by using a cyclic load with increasing amplitudes in order to accelerate the damage. The characteristics of the damage accumulation rate in the material can be used to indicate the fatigue behavior of bituminous materials.

From the procedure described in Sub-Section 4.5.2. we obtain the results of the fatigue tests, shown in Figure 6.14-15-16-17.

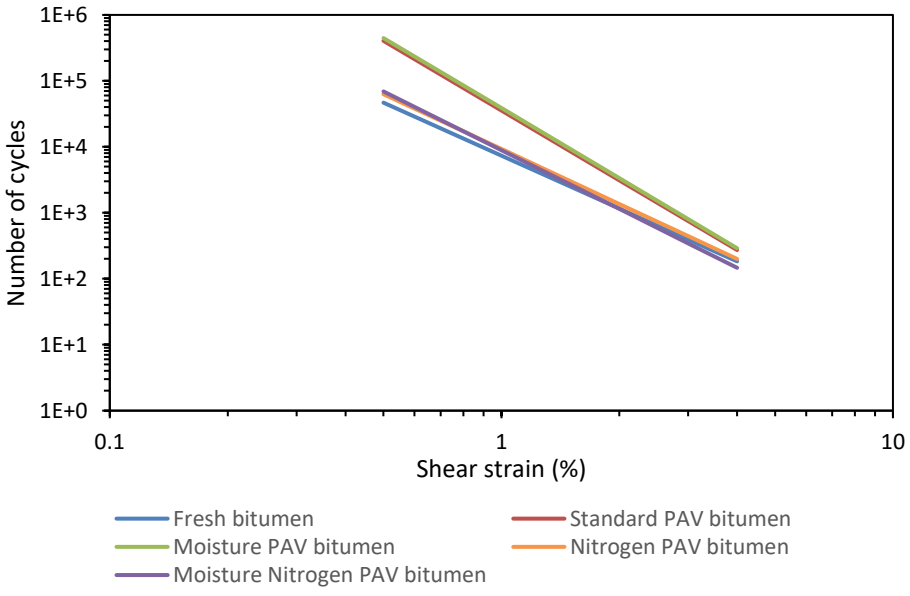

Figure 6.14 – Fatigue results of bitumen.

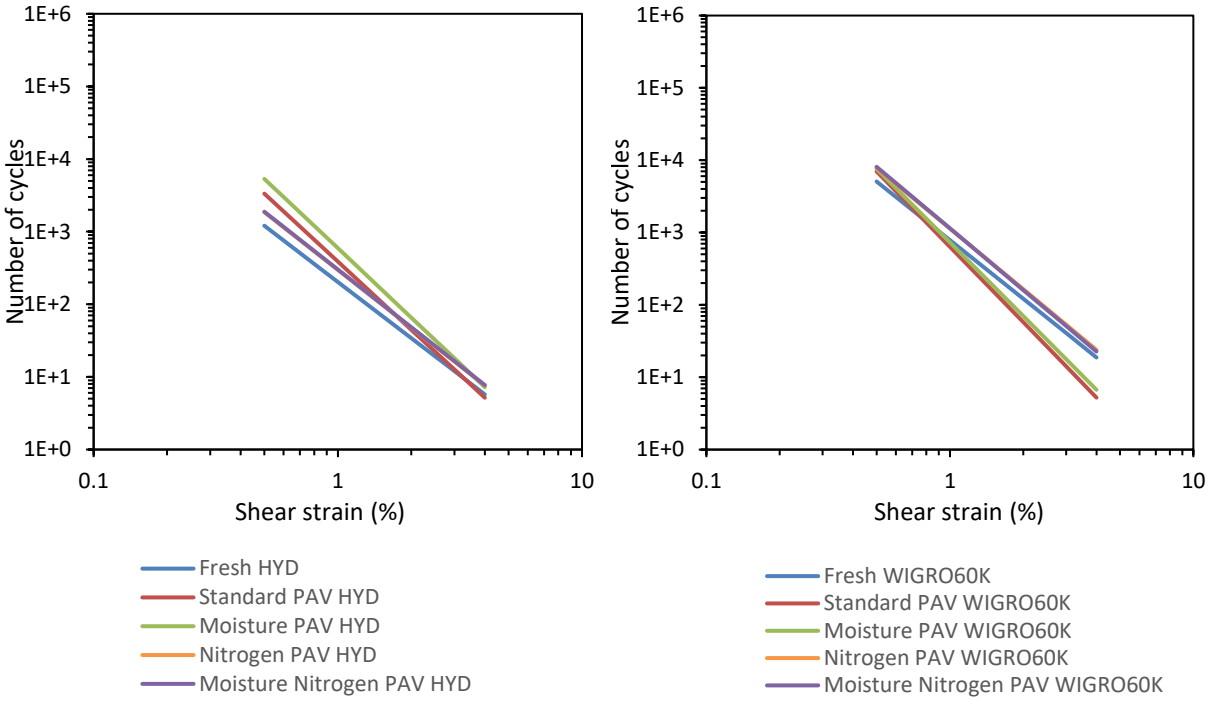

Figure 6.15 – Fatigue results of Mastic HYD (left) and Mastic W60K (right).

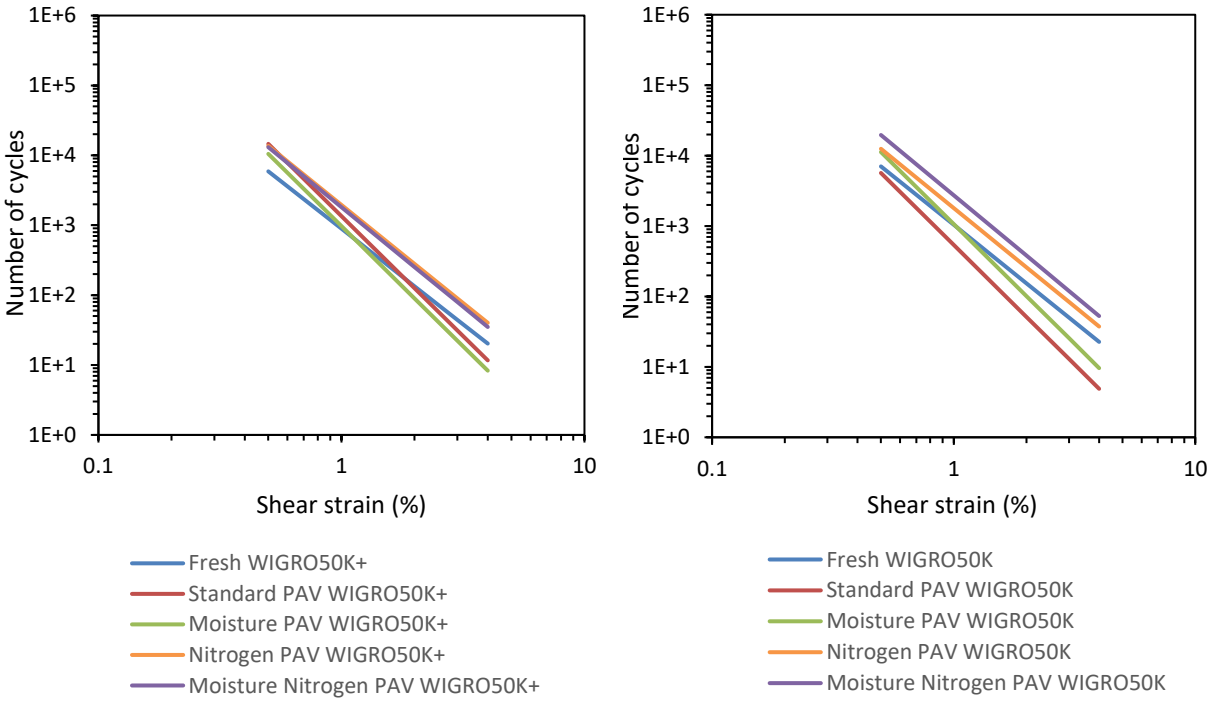

Figure 6.16 - Fatigue results of Mastic W50K+ (left) and Mastic W50K (right).

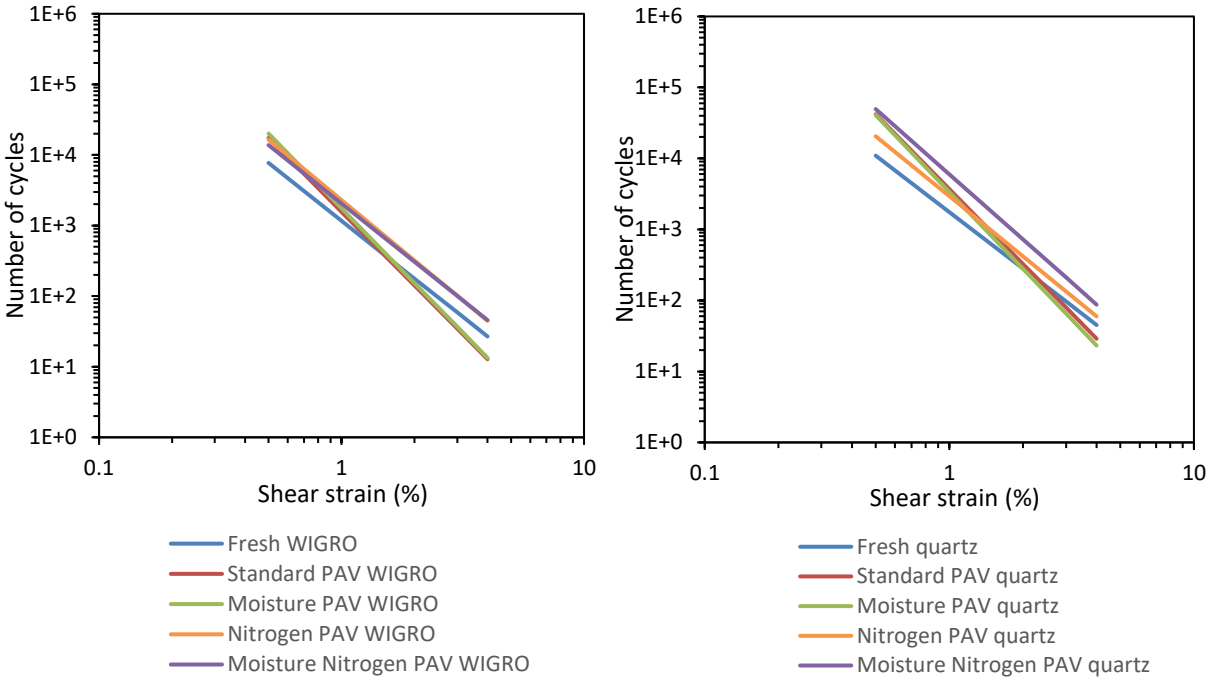

Figure 6.17 -- Fatigue results of Mastic W (left) and Mastic QZ (right).

Interestingly, based on the standard fatigue analysis criteria, ageing appears to have a positive effect on bitumen fatigue life. The fact that aging seems to increase the fatigue life of bitumen is in conflict with the common opinion that a pavement becomes susceptible to fatigue failure due to aging (Airey and Rahimzadeh 2004, Ouyang et al. 2006, Liu et al. 2014, Villegas-Villegas et al. 2018). One reason could be that the fatigue damage of a pavement due to aging is not only due to the cohesive damage inside the bitumen but also to the loss of adhesion between the aggregate and the bitumen. Aging increases the fatigue life of the bitumen itself but can reduce the adhesive adhesion strength with the aggregates.

As for the various types of mastics, LAS analysis suggests that, after aging, fatigue resistance improves at low load levels and decreases at higher load levels. Since the material becomes stiffener due to aging, it can undertake more load cycles at low strain levels, on the contrary, it can withstand less load cycles at high strain levels due to greater fragility. The study, however, is carried out well below 1 million cycles, therefore it is not appropriate to extrapolate from this data the useful life of a pavement, whose repeated loads are between 1 and 100 million.

The comparison can also be performed between the different types of material with the same condition, to define which mastic performs best with fatigue. In the figure 6.18 below only the

fresh condition is shown, as even in the four aging conditions the performance comparisons between the mastics remain unchanged.

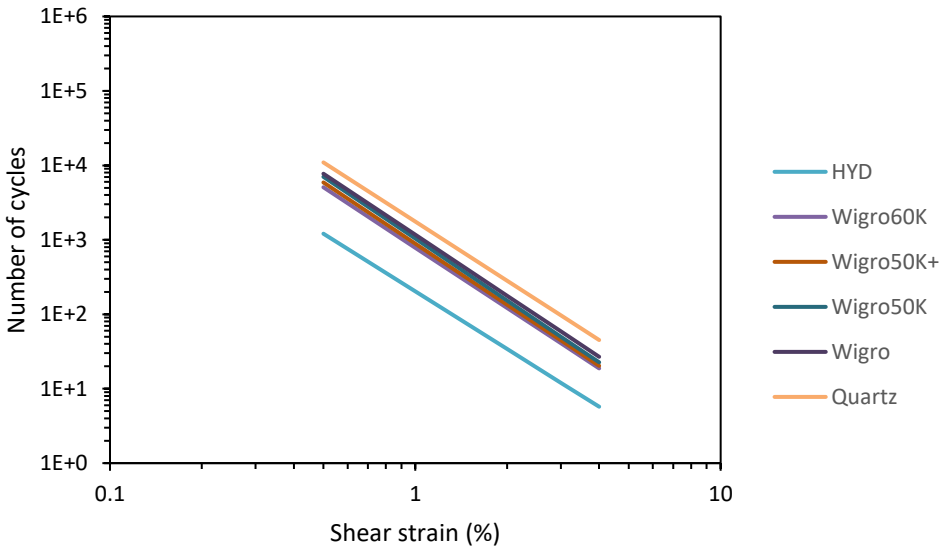

Figure 6.18 - Fatigue results of different Mastic at fresh condition.

The observations are immediate: the excessive presence of hydrated lime contributes to making the mixture extremely rigid, therefore with the same strain, greater stresses occur inside. Based on fatigue tests the best answer is therefore given by mastics composed of silicate or limestone fillers with low or no hydrated lime content.

6.2.3 FREQUENCY SWEEP

In this section the rheological evaluations of the materials analyzed through the frequency test are reported and discussed. The master curves of the complex shear modulus and the phase angle are plotted, for each material, under fresh conditions and after the conditioning phases.

Master curves comparison of neat bitumen under different conditioning processes

Two replicates for each condition were considered for the frequency scan tests. The effect of aging is generally seen as an increase in the complex shear modulus and a reduction in the phase angle.

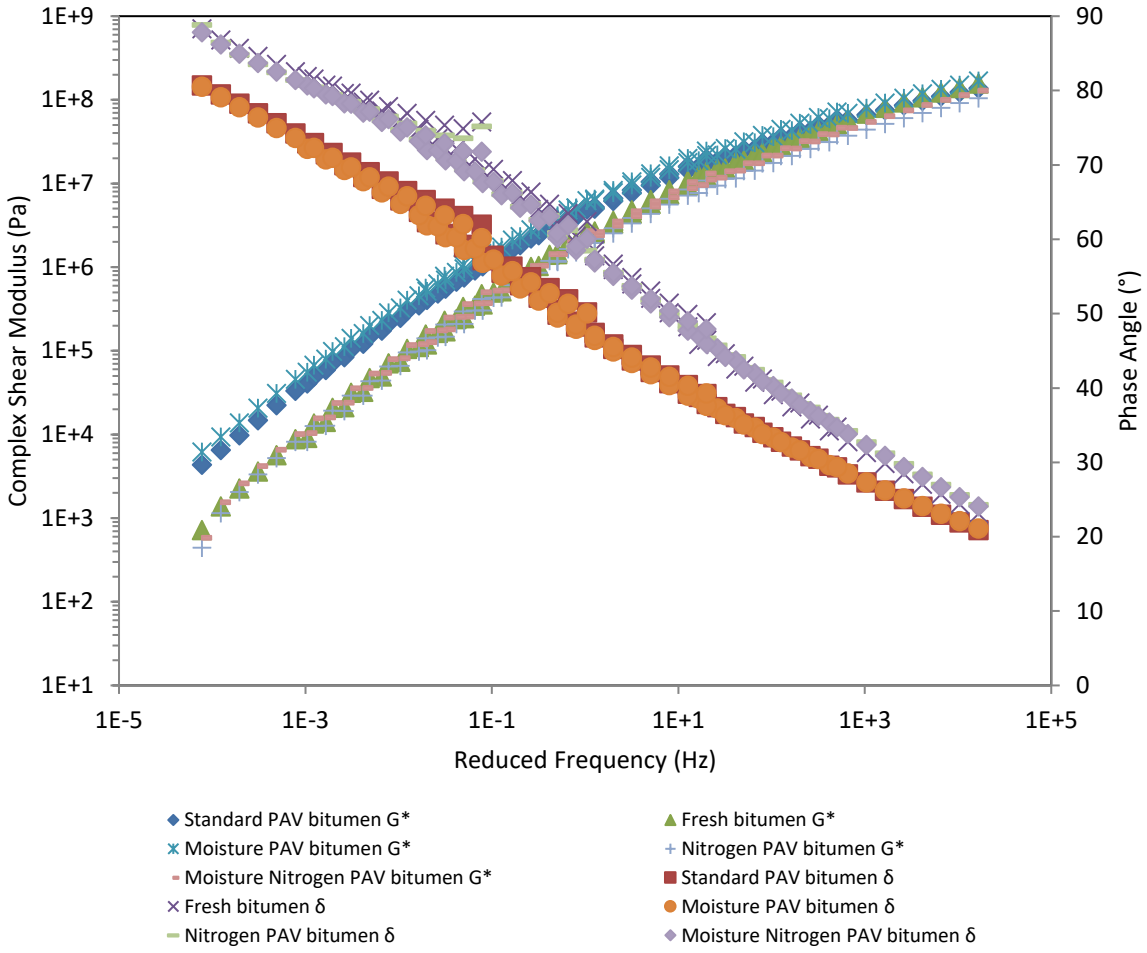

Figure 6.19 – Master curves comparison of neat bitumen under different conditioning processes

In this case the Figure 6.19 shows the rheological parameters of the neat bitumen during all the conditioning phases. It is clear that at high frequency or low temperature, the complex shear modulus is not excessively influenced by aging, the presence of water or inert gas and all the master curves converge at approximately the same value (glassy modulus).

On the other hand, at low frequency or high temperatures, a slight increase in values can be noted, from fresh samples to those conditioned in dry or humid air. The stiffening of the material is also confirmed by the reduction of the phase angle master curve: The bitumen after conditioning becomes more elastic.

From the results obtained, conditioning with inert gas does not seem very useful to quantify the aging state through the complex modulus and the phase angle.

Instead, although the impermeable nature of bitumen and the small amount of humidity in the conditioning do not allow to see evident changes in the rheological behavior of the material, it is quite clear that water influences the properties of bitumen.

Master curves comparison of all mastics under different conditioning processes

Although mineral fillers have different physical and chemical properties, such as the quantity of hydrated lime, the content of Rigden voids or a specific surface area, the different conditioning procedures adopted for this research do not show great differences between the different mastics in terms of rheological parameters.

The figures D7.1, D8.1, D9.1, D10.1, D11.1, D12.1 in Appendix D, show the main curves of the complex shear modulus and phase angle of mastics with different fillers, respectively HYD, W60K, W50K +, W50K, W, QZ. The post aging behavior is similar to that studied in bitumen: increase in the complex shear modulus at low frequencies or high temperatures, asymptotic tendency at high frequencies and decrease in the master curves of the phase angle.

Master curves comparison of all analysed materials under the same conditioning process

Figure 6.20 shows the master curves of all the unconditioned materials.

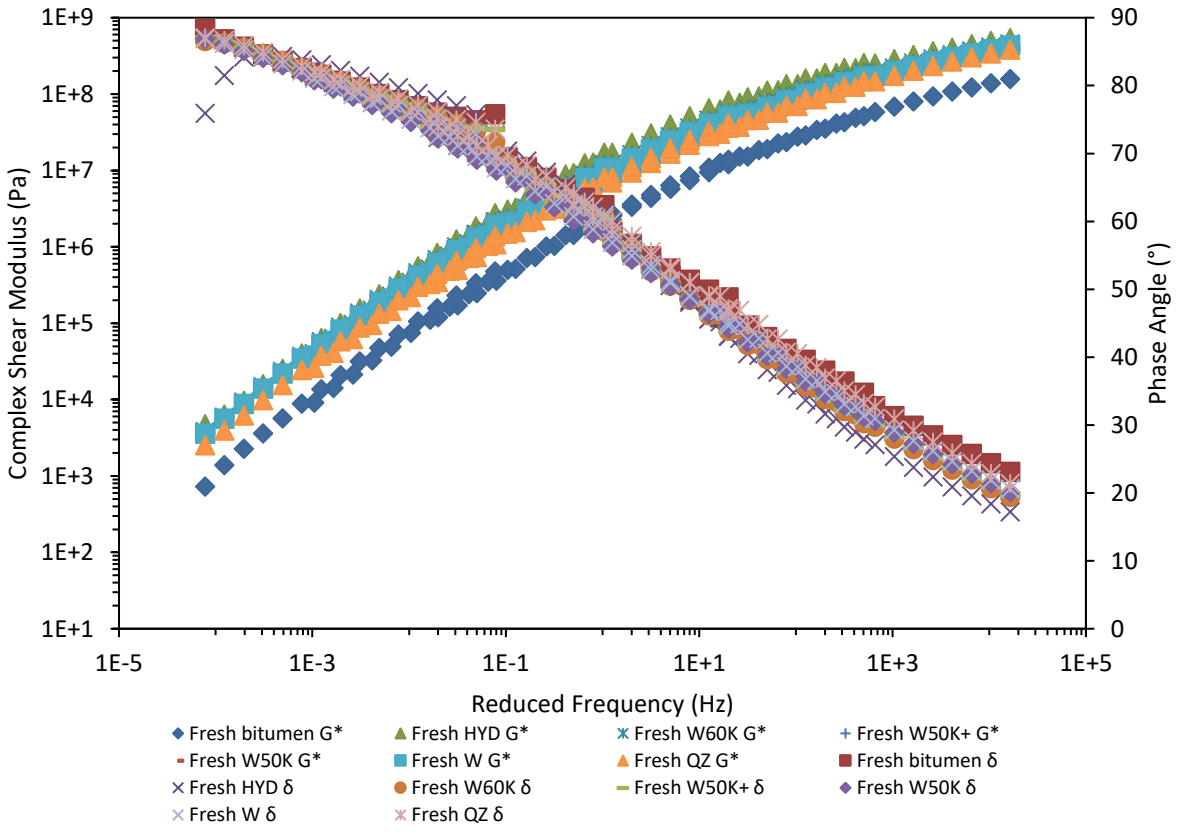

Figure 6.20 - Master curves comparison of all analysed materials under the same conditioning process

It is well-known that the addition of mineral filler in bitumen entails a stiff behaviour and a relatively more elastic response of the resulting mastic (Hunter 2015). Indeed mastics have a higher complex shear modulus than neat bitumen at the whole frequency domain. The greatest difference between the phase angle values of mastics and neat bitumen is observed at

intermediate to high frequencies, where the mineral fillers' stiffening effect is corroborated by the simultaneous effect of low testing temperatures, whereas at lower frequencies and/or higher temperatures the effect of the mineral fillers is hindered by the viscous behaviour of the binder.

Furthermore, mastic HYD with higher presence of hydrated lime seems to be stiffest with respect to others mastics. The latter is confirmed also by the phase angle master curves, especially at higher frequencies and/or lower temperatures, where the HYD mastic shows the lowest value. Correlation between Rigden voids (RV) value of mineral fillers and stiffening effects have been found and reported in literature (Leuseur 2010), the higher the RV value, the smaller the volume of free bitumen, the higher the stiffening of the binder. Indeed, Rigden air voids increase when the hydrated lime content increases, with typical values in the 45-50% range for 25wt.% hydrated lime in the mixed filler.

As previously mentioned, aging in dry air or with the presence of moisture slightly influences the rheological responses of mastics and bitumen. However, at all condition, from the comparison of the complex modulus and the phase angle between the mastics it is observed that the differences remain unchanged with those of fresh conditions and therefore the considerations on the material and on the properties and stiffness of the mastics also can apply in aging conditions. The master curves with the same condition (Fig. D1, D2, D3, D4, D5) are available in Appendix D.

Black diagrams

Black diagrams, Figure D6.2, D7.2, D8.2, D9.2, D10.2, D11.2, D12.2 in Appendix D, were drawn to present the rheological changes of bitumen and mastics with aging. Unlike the previous Master Curves the black diagrams are graphs of the complex shear modulus with respect to the phase angle, in which the frequency and the temperature are eliminated, therefore the data can be presented in a diagram without the need to apply the principle of time-temperature superposition (TTS). Taking as an example the black diagram of the neat bitumen (Fig 6.21) (but this also applies to mastics) as aging progresses, we observe a displacement of the curves of the black diagram towards lower phase angles; at the same time the shape of the curves changes in a straight line and the curvature is reduced. These changes denote a trend towards a stiffer and less viscous material, which could result in breakdowns such as a brittle fracture at low temperatures.

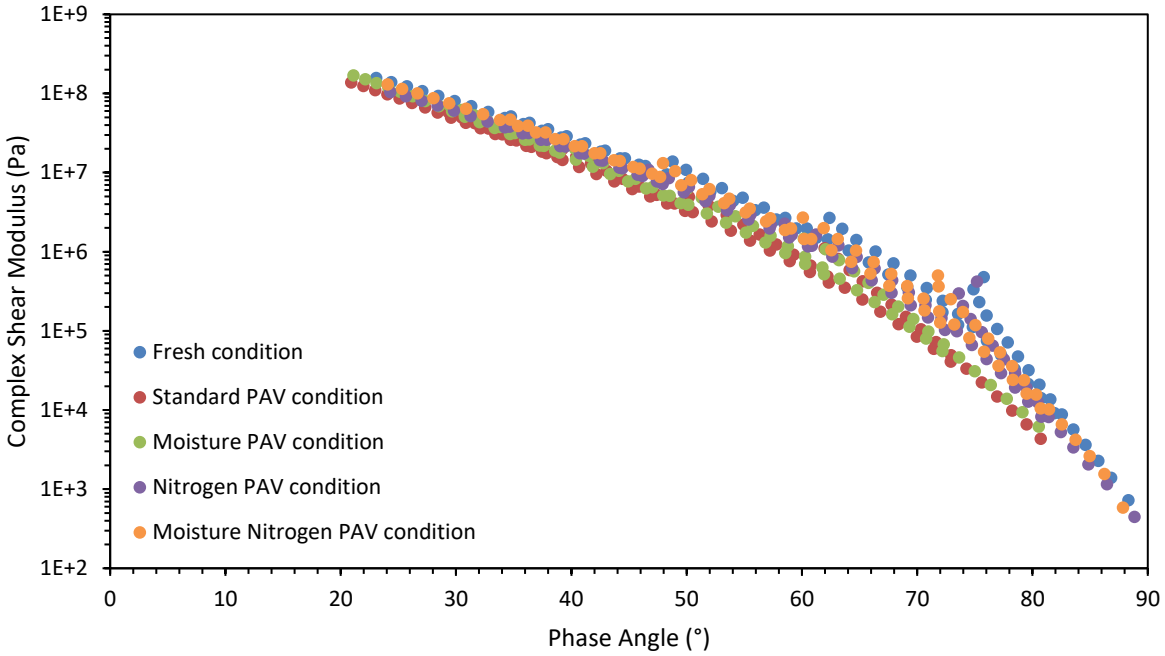

Figure 6.21 – Black diagram of neat bitumen

To better understand the effect of aging on black diagrams, the crossover modulus is studied in this work. The crossover modulus is the complex shear modulus corresponding to the 45 ° phase angle, which indicates that the storage shear modulus is the same as the loss shear modulus. When the phase angle is less than 45°, the material has a more solid behavior; when it is above 45°, the materials have a more fluid behavior. As shown in the Figure 6.21, multiple data points appear in the region with a phase angle of less than 45° after aging, indicating that bitumen has a more solid behavior (elastic response) and a less fluid behavior (viscous response) due to aging.

The crossover modulus is a special point on the material's viscoelastic spectrum, which does not depend on the frequency and temperature of the test. However, aging has a significant influence on the crossover modulus, as the crossover modulus decreases with aging (Jing et al. 2019).

The values of the crossover modulus for all materials under different conditions are shown in Fig 6.22.

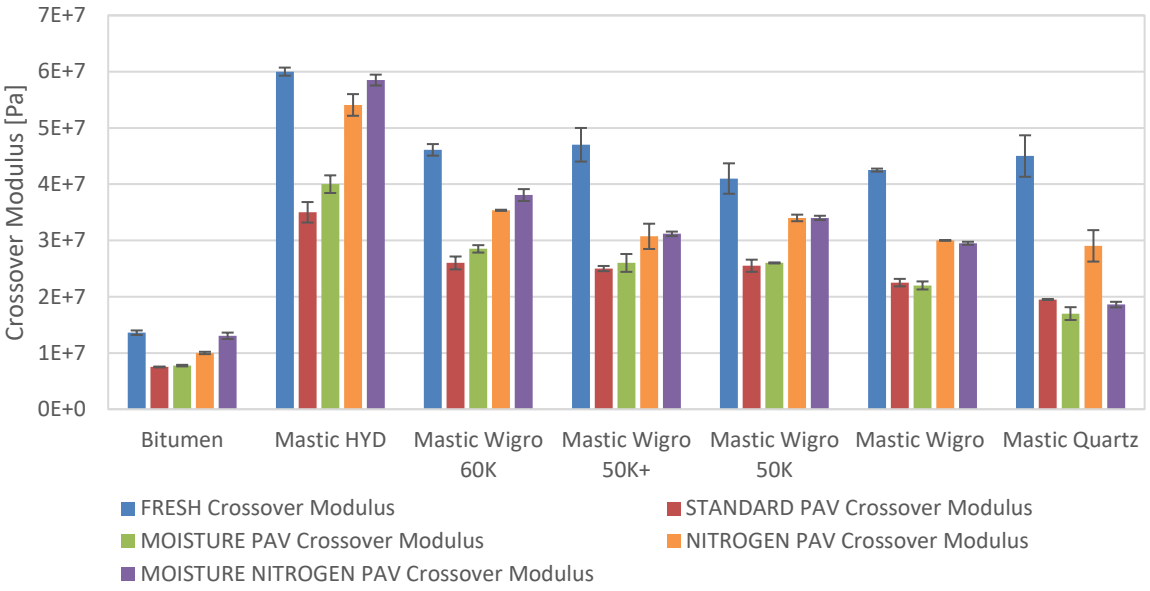

Figure 6.22 - Crossover modulus for all materials under different conditions.

As expected, for all materials, compared to the fresh conditions in aging conditions there is a decrease in the crossover modulus. For all mastics, except W and QZ with the presence of zero hydrated lime, in conditions of moisture, the crossover modulus values are higher; therefore, it is possible that the hydrated lime limits the aging process in the presence of humidity.

A further rheological index for evaluating the aging of bitumen and mixtures is given by the Crossover Frequency, as seen in Sub-Section 4.5.2.3. This index is obtained from the intersection of Storage Modulus *G'* and Loss Modulus *G''*. Jing et al. (2019) describes that the frequency (Hz) obtained from the intersection of the two modules indicates the passage from the fluid to the solid state of the sample (as seen in Figure 4.35). The aging of the sample involves a lowering of the frequency value with consequent increase of the solid behavior area, in other words the mixture is stiffer.

In Figure 6.23 shows the change in Frequency of the bitumen under examination from the fresh state to that aged in PAV.

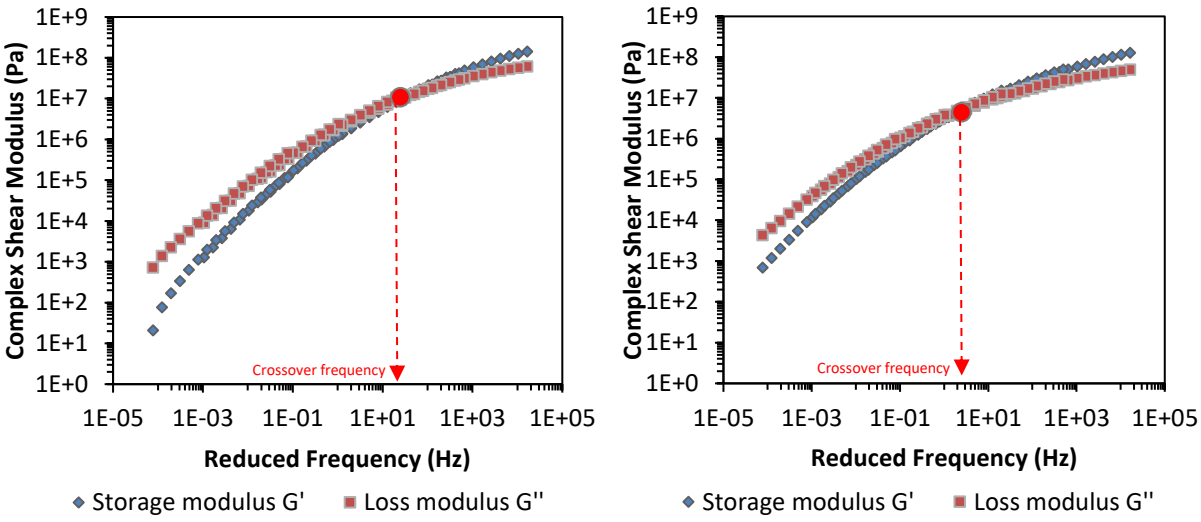

Figure 6.23 - Crossover frequency value for fresh neat bitumen (left) and standard PAV bitumen (right).

The Crossover Frequency values are obtained for each sample in a fresh state and under different conditions (Fig. 6.24).

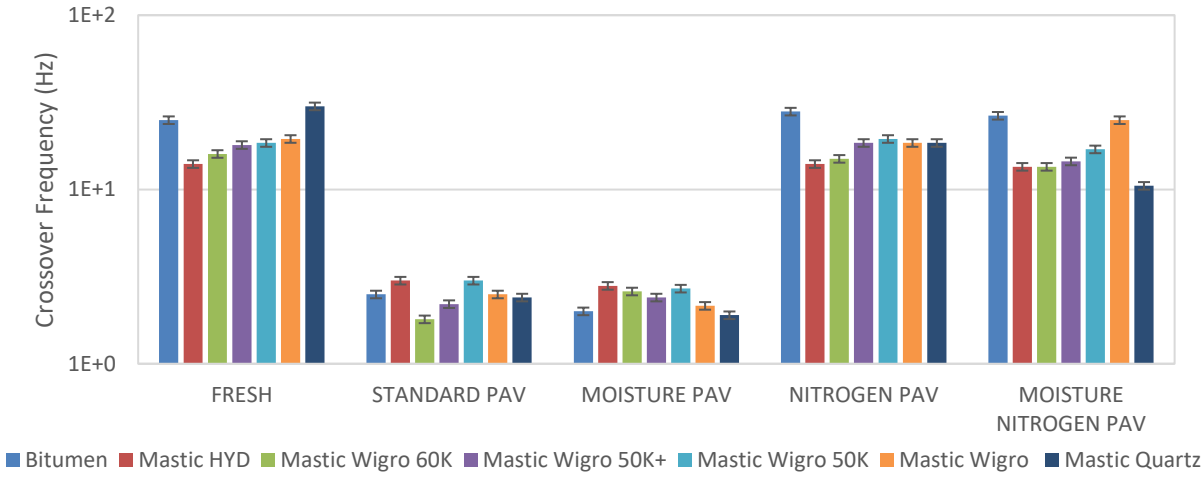

The decrease in the crossover frequency in conditions of aging in air or in the presence of humidity confirms the above. From the analyzes on the frequencies, it is also possible to confirm what has already been said for the previous studies regarding the ridgen voids (RV) and the softening point for mastics containing hydrated lime. In fact, in a fresh state the linear lowering of the crossover frequency with the increase of the percentage of hydrated lime in the mastic shows how the filler affects the stiffening of the mixture.

In the proposed study, an attempt was also made to compare the crossover modulus with the crossover frequency to verify a linear correlation as in the study of Jing et al (2019). However, the comparison did not show any linear correlation between the various conditionings with and without humidity, demonstrating the studies by Ma et al. (2011).

In order to quantify the effect of aging on the bitumen crossover modulus, an ageing index is proposed and expressed as the ratio of the crossover modulus of the fresh bitumen over the crossover modulus of the aged. The AI values of all the samples were obtained and plotted in the Figure 6.23.

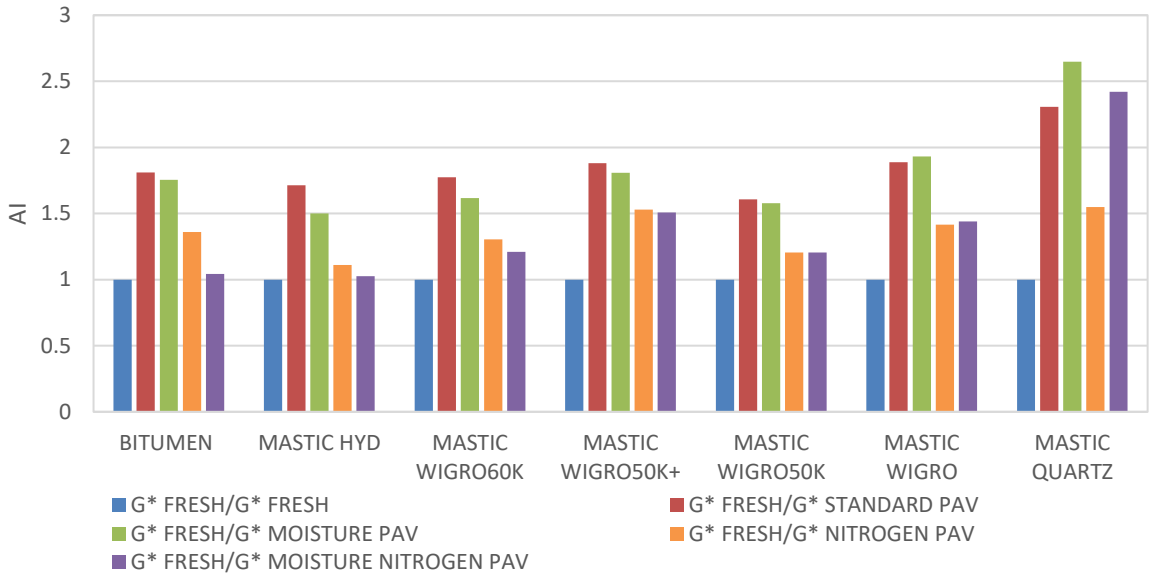

Figure 6.23 - AI (ageing index) of all the samples at different condition.

The results show that the AI increases with aging. From this conclusion some important observations can be drawn about the presence of hydrated lime in mastics aged with or without moisture.

The AI values of the mastic W and QZ, with a percentage of hydrated lime equal to zero, are higher than those of the other mastic containing hydrated lime. In other words, hydrated lime helps to limit the aging of the mastic. Furthermore, it can be noted that the AI indices are higher in the case of presence of humidity only for the mastics W and QZ, therefore the presence of hydrated lime has a positive contribution on the effects of moisture, demonstrating what was said in Sub-Section 2.3.3.

Aging is less pronounced in the case of conditioning with Nitrogen but this observation on the quantity of hydrated lime in the mastic and on the presence of humidity is also found in this case.

CHAPTER 7 – CONCLUSIONS

Changes in the rheological response and chemical composition of different materials after a specific conditioning process were investigated by means of DSR and FTIR measurements. Materials such as mineral fillers with different percentage of hydrated lime, bitumen and mastics have been studied. The conditioning protocol consisted of using the Pressure Aging Vessel in four different ways: with dry air, with moist air, with only nitrogen and with nitrogen and humidity. The main aim of the study was to investigate the effect of aging coupled with moisture, for all materials. Parallel to this, regarding fillers, a study is carried out on the phenomenon of carbonation of hydrated lime following the conditionings. In addition, correlations were found between the chemical properties of the mineral filler and the related mastics with the rheological performance following conditioning. Main conclusions of this research are listed below:

- Neat bitumen shows the lowest complex shear modulus master curves with respect to mastics; fillers increase the stiffness of the binder over all frequencies; stiffness increases proportionally with hydrated lime content.
- Crossover modulus decrease with aging: bitumen is more aged than all mastics, also the presence of hydrated lime in the mastic optimizes performance in wet conditions.
- The crossover frequencies drop with the stiffening of the mixture: even this analysis showed that the presence of hydrated lime stiffens the mixture. Oxidative aging causes the mixture to stiffen and is more prone to craking. However, this index is not useful for evaluating the phenomenon of aging and the influence of humidity.
- The Aging Index confirms the considerations made by the analysis of the Crossover Modulus: hydrated lime helps to limit the aging of the mastic. Furthermore, the presence of hydrated lime helps to increase resistance to damage caused by moisture.
- From the analyzes carried out with the LAS test we can conclude that aged materials have higher linear limits for stress. The reason for these phenomena is that the hardening of the bitumen caused by aging makes the material able to withstand greater stresses with less deformations. An excessive presence of hydrated lime in the mastic results in an extremely rigid and more fragile material. The other mastics with a lower or no presence of hydrated lime have higher LVE and non-LVE values, which means that they endure greater stress before reaching the damage area. This study is very

useful for evaluating the viscoelastic properties of mastics, however it is not suitable for studying the phenomenon of aging.

- According to the standard fatigue analysis criteria, from the values obtained it appears that aging has a positive effect on the duration of the bitumen fatigue. This observation contradicts the field observations and raises questions about the suitability of these criteria. It seems that fatigue tests can give a false impression of the effects of aging on the viscoelastic properties of bitumen.
- From the Relaxation test it is observed that aged bitumen and mastics show higher residual shear stresses after relaxation and are more susceptible to the accumulation of stress. Also in this case the presence of mineral filler contributes to a greater hardening of the mixture and therefore to higher parameters than neat bitumen. In this case the presence of humidity seems to negatively affect the relaxation properties. HYD mastic, even in fresh conditions, has significantly higher values than neat bitumen since the presence of hydrated lime causes a greater hardening of the mixture and therefore a greater susceptibility to cracking.
- From the chemical evaluations on mastics it is observed that the sulphoxide indices cannot be taken into account for the study of aging, due to the influence of different mineral particles in the FTIR spectrum. While the carbonyl indices are useful to highlight a correlation between the chemical changes of the mastic and the rheological ones.
- From the chemical evaluations on bitumen it is observed that nitrogen conditioning shows an unusual chemical modification: from the study carried out it was hypothesized that the bituminous matrix composed of hydrocarbons reacts with nitrogen molecules to form amide groups.
- From the chemical evaluations on the fillers, the carbonation process of the hydrated lime in calcium carbonate is confirmed. This chemical reaction is linked to the slow degradation of the calcium hydroxide particles on the surface of the filler exposed to carbon dioxide present in the air. For this reason, there was a greater carbonation in calcium carbonate for the sample exposed to long-term air (2 weeks), compared to those conditioned in PAV (20 hours).

  In addition, the parameters of calcium hydroxide or calcium carbonate recorded by the FTIR can be influenced by the position of the replicant in the filler taken with the spatula for the test. By taking the filler immediately on the surface, in direct contact

with the air, this is probable to have reacted more by converting to calcium carbonate than the filler in contact with the bottom of the can.

However, by making a comparison with the values provided by *Sibelco*, the FTIR test is useful for evaluating the quantities of hydrated lime, calcium carbonate and calcium oxide present in the fillers.

In conclusion, it can be said that in general, mineral fillers are active participants and play a role in the aging process of bitumen and they have a positive effect on the aging of mastics. The presence of hydrated lime inside the mastics can be an advantage, while remaining a limited percentage. Otherwise, the mastic is excessively rigid and more inclined to cracking phenomena. From the results obtained it is observed that the addition of hydrated lime to the mineral filler does not determine a greater effectiveness of the mixed mineral substance to mitigate only the aging of the mastic, however it seems to have positive effects as regards the increase in resistance to moisture damage . As a demonstration of this, it has been noted that in the chemical studies on fillers, hydrated lime has undergone a process of deterioration due to carbonation phenomena from exposure to air while the presence of water has not affected degradation.

The FTIR tests were quite reliable for the quantification of hydrated lime in mineral fillers. Among the DSR tests, the Frequency Sweep was certainly the most suitable for assessing the aging of mastics.

7.1 POSSIBLE FUTURE STUDIES

The conclusions obtained can be taken as a starting point for possible future studies.

The results obtained show that the characteristics of the conditionings do not allow a linear comparison in the study of aging linked to humidity. A future study could be carried out with conditionings with progressive increase of temperature, hours or presence of humidity inside the PAV. Regarding the presence of humidity, it is however necessary to carry out a preliminary study to evaluate the pressure increase inside the oven.

The study of stiffness and fatigue behavior of bitumen cannot directly characterize the degradation of its properties due to aging, since both rigidity and fatigue life increase with aging. The result of the fatigue test is in this case unreliable and it is necessary in future studies to carry out a different analytical approach.

As for a mainly chemical study, even with the use of a microscope, it would be interesting to carry out a more in-depth analysis of the bonds that occur between the hydrocarbons of the bitumen and the inert gas N_2.

Finally, a more in-depth study on the carbonation phenomenon of hydrated lime is recommended, with incremental steps on the exposure time to air.

REFERENCES

Abukarba E. & Muniandy R. *An Overview of the Use of Mineral Fillers in Asphalt Pavements*. Australian Journal of Basic and Applied Sciences, 10(9), pp 279-292, 2016.

Airey G.D., Rahimzadeh B. & Collop A.C. *Linear Viscoelastic Limits of Bituminous Binders*. Asphalt Paving Technology: Association of Asphalt Paving Technologists-Proceedings of the Technical Sessions, Vol. 71, pp 89-115, 2002.

Airey, G., Collop, A., Zoorob, S. and Elliott, R. (2008). The influence of aggregate, filler and bitumen on asphalt mixture moisture damage. *Construction and Building Materials*, 22(9), pp.2015-2024.

Apeagyei, A. K., Grenfell, J. R., & Airey, G. D. (2013). *Evaluation of moisture sorption and diffusion characteristic of asphalt mastics using manual and automated gravimetric sorption techniques*. Journal of Materials in Civil Engineering.

Apostolidis P. *Experimental and Numerical Investigation of Induction Heating in Asphalt Mixes*. Delft University of Technology, M.Sc. Thesis, 2015.

Aragão, F., Lee, J., Kim, Y. and Karki, P. (2010). Material-specific effects of hydrated lime on the properties and performance behavior of asphalt mixtures and asphaltic pavements. *Construction and Building Materials*, 24(4), pp.538-544.

Aragão F., Kim Y.-R. and J. Lee, *Research on Fatigue of Asphalt Mixtures and Pavements in Nebraska*, Report to NDOR Research Project Number P579, Lincoln (Nebraska, USA): University of Nebraska Lincoln,2008

Arambula, E., Caro, S. and Masad, E. (2010). Experimental Measurement and Numerical Simulation of Water Vapor Diffusion through Asphalt Pavement Materials. *Journal of Materials in Civil Engineering*, 22(6), pp.588-598.

Arnold, T., Rozario-Ranasinghe, M. and Youtcheff, J. (2006). Determination of Lime in Hot-Mix Asphalt. *Transportation Research Record: Journal of the Transportation Research Board*, 1962(1), pp.113-120.

Banja, A., Araújo, M., Castro, M., Moreira, R., Leite, L. and Lins, V. (2018). Optimal hydrated lime concentration in asphalt binder to improve photo degradation resistance. *REM - International Engineering Journal*, 71(2), pp.225-233.

Bari J. and Witczak M. W., *Evaluation of the Effect of Lime Modification on the Dynamic Modulus Stiffness of Hot-Mix Asphalt: Use with the New Mechanistic-Empirical Pavement Design Guide*, Transportation Research Record 1929, pp.10-19, 2005

Britishlime.org. (2020). *British Lime Association (BLA) part of the Mineral Products Association (MPA)*. [online] Available at: https://britishlime.org/education/lime_cycle.php.

Buttlar, W., Bozkurt, D., Al-Khateeb, G. and Waldhoff, A. (1999). Understanding Asphalt Mastic Behavior Through Micromechanics. *Transportation Research Record: Journal of the Transportation Research Board*, 1681(1), pp.157-169.

Caro, S., Masad, E., Bhasin, A. and Little, D. (2008). *Moisture susceptibility of asphalt mixtures, Part 1: mechanisms*. International Journal of Pavement Engineering, 9(2), pp.81-98.

Caro, S., Masad, E., Bhasin, A. and Little, D. (2008). *Moisture susceptibility of asphalt mixtures, Part 2: characterisation and modelling.* International Journal of Pavement Engineering, 9(2), pp.99-114.

Cazalla, O., Rodriguez-Navarro, C., Sebastian, E., Cultrone, G. and Torre, M. (2004). Aging of Lime Putty: Effects on Traditional Lime Mortar Carbonation. *Journal of the American Ceramic Society*, 83(5), pp.1070-1076.

C. V. Chachas, W. J. Liddle, D. E. Peterson and M. L. Wiley, *Use of hydrated lime in bituminous mixtures to decrease hardening of the asphalt cement*, Report PB 213 170, Salt Lake City (Utah, USA): Utah State Highway Department, 1971

Chaturabong, P. and Bahia, H. (2016). *Effect of moisture on the cohesion of asphalt mastics and bonding with surface of aggregates*. Road Materials and Pavement Design, 19(3), pp.741-753.

Cizer, Ö., Rodriguez-Navarro, C., Ruiz-Agudo, E., Elsen, J., Van Gemert, D. and Van Balen, K. (2012). Phase and morphology evolution of calcium carbonate precipitated by carbonation of hydrated lime. *Journal of Materials Science*, 47(16), pp.6151-6165.

Corbett L.C. *Composition of Asphalt Based on Generic Fractionation Using Solvent Deasphalteneing, Elution-Adsorption Chromatography and Densiometric Characterization*. Analytical Chemistry, Vol. 41, pp 576-579, 1969.

Das, A. and Singh, D. (2018). Effects of Regular and Nano Sized Hydrated Lime Fillers on Fatigue and Bond Strength Behavior of Asphalt Mastic. *Transportation Research Record: Journal of the Transportation Research Board*, 2672(28), pp.31-41.

Das, P., Baaj, H., Kringos, N. and Tighe, S. (2015). Coupling of oxidative ageing and moisture damage in asphalt mixtures. *Road Materials and Pavement Design*, 16(sup1), pp.265-279.

Erans, M., Nabavi, S. and Manović, V. (2020). Carbonation of lime-based materials under ambient conditions for direct air capture. *Journal of Cleaner Production*, 242, p.118330.

European Lime Association / Asphalt Task Force (2010). *Hydrated Lime: A Proven Additive For Durable Asphalt Pavements*.

Ghouse Baig M. and H. I. Al-Abdul Wahhab, *Mechanistic evaluation of hedmanite and lime modified asphalt concrete mixtures*, J. Materials in Civil Engineering 10(3), pp.153-160, 1998

Gundla A., Medina J., Gudipudi P. & Stevens R. *Investigation of Aging in Hydrated Lime and Portland Cement Modified Asphalt Concrete at Multiple Length Scales*. Journal of Materials in Civil Engineering, 2015.

Han, S., Dong, S., Liu, M., Han, X. and Liu, Y. (2019). Study on improvement of asphalt adhesion by hydrated lime based on surface free energy method. *Construction and Building Materials*, 227, p.116794.

Hintz, C., R. Velasquez, R. Associate, C. Johnson, S. Asphalt, and H. Bahia. *Modification and Validation of the Linear Amplitude Sweep Test for Binder Fatigue Specification*. Transportation Research Record: Journal of the Transportation Research Board, 2010. 2207: 99–106.

Hofko, B., Alavi, M., Grothe, H., Jones, D. and Harvey, J. (2017). Repeatability and sensitivity of FTIR ATR spectral analysis methods for bituminous binders. *Materials and Structures*, 50(3).

Huang, S., Claine Petersen, J., Robertson, R. and Branthaver, J. (2002). Effect of Hydrated Lime on Long-Term Oxidative Aging Characteristics of Asphalt. *Transportation Research Record: Journal of the Transportation Research Board*, 1810(1), pp.17-24.

Huang, S., Glaser, R. and Turner, F. (2012). Impact of Water on Asphalt Aging. *Transportation Research Record: Journal of the Transportation Research Board*, 2293(1), pp.63-72.

Huang, S., Turner, T. and Thomas, K. (2008). The influence of moisture on the aging characteristics of bitumen. *EUROPEAN ASPHALT PAVEMENT ASSOCIATION (EAPA)*.

Hunter R.N., Self A. & Read J. *The Shell Bitumen Handbook*, 6th Edition. 2015.

Ismael, M. and Ahmed, A. (2019). *Effect of Hydrated Lime on Moisture Susceptibility of Asphalt Mixtures*. Journal of Engineering, 25(3), pp.89-101.

Iwański, M. and Mazurek, G. (2013). Hydrated Lime as the Anti-aging Bitumen Agent. *Procedia Engineering*, 57, pp.424-432.

Iwański, M. and Mazurek, G. (2012). *Durability of Sma pavement with Hydrated Lime additive*. Kielce University of Technology, Poland.

Jing, R., Varveri, A., Liu, X., Scarpas, A. and Erkens, S. (2019). Rheological, fatigue and relaxation properties of aged bitumen. *International Journal of Pavement Engineering*, pp.1-10.

Jing, R., Varveri, A., Liu, X., Scarpas, A. and Erkens, S. (2019). Ageing effect on chemo-mechanics of bitumen. *Road Materials and Pavement Design*, pp.1-16.

Jing, R., Varveri, A., Liu, X., Scarpas, A. and Erkens, S. (2019). Fatigue Performance Evaluation of Aged Bitumen Using Linear Amplitude Sweep and Time Sweep Tests.

Jing, R., Varveri, A., Liu, X., Scarpas, A. and Erkens, S. (2019). *Ageing effect on the relaxation properties of bitumen*. Delft University of Technology, Delft, the Netherlands.

Kim, S., Shen, J., Lee, S., Kim, Y. and Kim, K. (2018). Examination of physical property degradation due to severe short-term ageing and effect of hydrated lime as antioxidant in asphalt mixture. *Road Materials and Pavement Design*, 20(7), pp.1638-1652.

Kollaros, G., Kalaitzaki, E. and Athanasopoulou, A. (2017). Using Hydrated Lime in Hot Mix Asphalt Mixtures in Road Construction. *American Journal of Engineering Research (AJER)*, pp.Volume-6, Issue-7, pp-261-266.

Legodi, M., de Waal, D., Potgieter, J. and Potgieter, S. (2001). Rapid determination of CaCO3 in mixtures utilising FT—IR spectroscopy. *Minerals Engineering*, 14(9), pp.1107-1111.

Lesueur, D. and Little, D. (1999). *Effect of Hydrated Lime on Rheology, Fracture, and Aging of Bitumen*. Transportation Research Record: Journal of the Transportation Research Board, 1661(1), pp.93-105.

Lesueur, D., Lázaro Blázquez, M., Andaluz Garcia, D. and Ruiz Rubio, A. (2017). *On the impact of the filler on the complex modulus of asphalt mixtures*. Road Materials and Pavement Design, 19(5), pp.1057-1071.

Lesueur D. *The Colloidal Structure of Bitumen: Consequences on the Rheology and on the Mechanisms of Bitumen Modification*. Advances in Colloid Interface Science, 145(1-2), pp 42-82, 2009.

Lesueur, D., Petit, J. and Ritter, H. (2012). The mechanisms of hydrated lime modification of asphalt mixtures: a state-of-the-art review. *Road Materials and Pavement Design*, 14(1), pp.1-16.

Lesueur, D., Ritter, H. and Petit, J. (2012). Increasing the durability of asphalt mixtures by hydrated lime addition: What evidence?. *European Roads Review*, (20).

Little, D. and Epps, J. (2001). The Benefits of Hydrated Lime In Hot Mix Asphalt. *National Lime Association*.

Little, D. and Petersen, J. (2005). Unique Effects of Hydrated Lime Filler on the Performance-Related Properties of Asphalt Cements: Physical and Chemical Interactions Revisited. *Journal of Materials in Civil Engineering, Vol. 17, No. 2*.

Liu, C., He, J., Ruymbeke, E., Keunings, R., & Bailly, C. (2006). *Evaluation of different methods for the determination of the plateau modulus and the entanglement molecular weight.* Polymer, 47, 4461–4479.

Ma, T., Huang, X., Mahmoud, E. and Garibaldy, E. (2011). Effect of moisture on the aging behavior of asphalt binder. *International Journal of Minerals, Metallurgy, and Materials*, 18(4), pp.460-466.

Marchi, F. (2019). *Effect Of Moisture Susceptibility On Different Bituminous Mastics*. M.Sc. Thesis. UNIBO.

Mastoras, F. (2019). *Effect Of Mineral Fillers On Ageing Of Bituminous Mixtures*. M.Sc. Thesis. TUDelft.

Mazzotta, F. (2012). *Studio Reologico Avanzato Di Bitumi Modificati Ed Additivati: Proposta Di Una Nuova Procedura Di Aging*. Master Thesis. UNIBO.

Mikhail, R., Brunauer, S. and Copeland, L. (1966). Kinetics of the thermal decomposition of calcium hydroxide. *Journal of Colloid and Interface Science*, 21(4), pp.394-404.

Mouillet, V., Séjourné, D., Delmotte, V., Ritter, H. and Lesueur, D. (2014). Method of quantification of hydrated lime in asphalt mixtures. *Construction and Building Materials*, 68, pp.348-354.

Nasrazadani, S. and Eureste, E. (2008). *Application of FTIR for Quantitative Analysis of Lime*. University of North Texas.

Nivitha, M. R., & Krishnan, J. M. (2016). *What is transition temperature for bitumen and how to measure it*. Transportation in Developing Economies, 2, 3.

Petersen J.C. *Chemical Composition of Asphalt as Related to Asphalt Durability: State of Art.* Transportation Research record 999, Transportation Research Board, Washington D.C., pp 13-30, 1984.

Petretto, F. (2012). *Le reologia dei leganti bituminosi stradali: studio delle proprietà meccaniche a seguito di processi di "aging" in laboratorio*. UNIBO.

Pierard, N. and Vanelstraete, A. (2008). The impact of moisture on the ageing of bituminous binders and asphalt mixtures. *EUROPEAN ASPHALT PAVEMENT ASSOCIATION (EAPA).*

Plancher H. & Petersen J.C. *Reduction of Oxidative Hardening of Asphalts by Treatment with Hydrated Lime-A Mechanistic Study*. Proceedings of the Association of Asphalt Paving Technologists, Vol. 45, pp 1-24, 1976.

Scarsella, M., Mastrofini, D., Barre, L., Espinat, D., & Fenistein, D. (1999). *Petroleum heavy ends stability: Evolution of residues macrostructure by ageing*. Energy & Fuels, 13, 739–747.

Schellenberg K. & Eulitz H.J. *Verbesserung von Asphalteigenschaften durch Einsatz von Kalkhydrat*. Bitumen1, pp 2-8, 1999.

Sengul, C., Aksoy, A., Iskender, E. and Ozen, H. (2012). Hydrated lime treatment of asphalt concrete to increase permanent deformation resistance. *Construction and Building Materials*, 30, pp.139-148.

Thomas, K. (2002). Impact of Water during the Laboratory Aging of Asphalt. *Road Materials and Pavement Design*, 3(3), pp.299-315.

Timoshenko S., *Strength of Materials*, 2 vol., 3rd edition, Malabar (Florida, USA): Krieger Publishing Company, 1976.

Van den Bergh W. *The Effect of Ageing on the Fatigue and Healing Properties of Bituminous Mortars*. Delft University of Technology, Ph.D. Thesis, 2011.

Vansteenkiste, S., De Visscher, J. and Vanelstraete, A. (2013). Impact of hydrated lime on the durability of SMA mixtures: laboratory and field evaluation. *Road Materials and Pavement Design*, 14(sup1), pp.162-174.

Varveri, A. (2017). *Moisture damage susceptibility of asphalt mixtures: Experimental characterization and modelling*. DOI:10.4233/uuid:9c25df0e-2df0-4d30-b9aa-d95a31fcaafd. Technische Universiteit Delft.

Varveri, A., Zhu, J., & Kringos, N. (2015). *Moisture damage in asphaltic mixtures*. Woodhead Publishing Series in Civil and Structural Engineering 2015, Pages 303-344.

Verhasselt A. and Puiatti D., *Effect of hydrated lime on ageing behaviour of bituminous mastics*, Proc. 3rd Eurasphalt & Eurobitume Congress, Vienna, vol.1, paper 108, pp.746-756, 2004.

Wu, J. (2009). *The influence of mineral aggregates and binder volumetrics on bitumen ageing*. Thesis submitted to the University of Nottingham for the degree of Doctor of Philosophy.

Woldekidan M.F. *Response Modelling of Bitumen, Bituminous Mastic and Mortar*. Delft University of Technology, Ph.D. Thesis, 2011.

Yilmaz, M. and Yalcin, E. (2015). The effects of using different bitumen modifiers and hydrated lime together on the properties of hot mix asphalts. *Road Materials and Pavement Design*, 17(2), pp.499-511.

Zhou, S. B., Liu, S., Xiang, Y. (2018). *Effects of Filler Characteristics on the Performance of Asphalt Mastic: A Statistical Analysis of the Laboratory Testing Results*. International Journal of Civil Engineering (2018) 16:1175–1183.

Zou, J., Isola, M., Roque, R., Chun, S., Koh, C. and Lopp, G. (2013). Effect of hydrated lime on fracture performance of asphalt mixture. *Construction and Building Materials*, 44, pp.302-308.

ACKNOWLEDGMENTS

This thesis is the conclusion of a course of study for the Master in Civil Engineering, with specialization in Road and Transport Engineering. At this point, I would like to express my sincere gratitude to the people who contributed to the realization and completion of this research.

First and foremost, I would like to express my gratitude to my TUDelft supervisor, Dr. Aikaterini Varveri, for hosting me, trusting me and offering me the opportunity to be involved in such an interesting research, as well as for her efforts, her availability and her continuous support throughout the duration of this study.

In addition, I would like to express my gratitude to Dr. Ruxin Jing for his assistance in the laboratory, for his numerous advices and for his constant presence and reliability whenever problems arose.

Furthermore, I would like to express my appreciation to the members of the TUDelft pavement department: in particular, to Prof. Sandra Erkens, who supported, in any case, the implementation of the proposed research methodology.

I would also like to thank my UNIBO supervisor, Dr. Claudio Lantieri for his commitment in organizing this important experience and for distance support during the development of this study.

I would also like to make a special mention to Prof. Valeria Vignali and Prof. Giulio Dondi for their skill in teaching and to have helped to get passionate about these issues, as well as the choice of my course of study.

I would obviously like to thank my parents, Paola and Otello, and my sister Sara for their support, from all points of view. Without them, none of this would have been possible.

I also want to thank my friends Francesco, Nicolas, Gioele, Riccardo, Giacomo, Luca, Pierpaolo, Lisa, Carlotta, Alice, Sofia, Martina for putting up with me and supporting me at all times. It is also thanks to having chosen the right friends that I managed to get this far.

I would also like to thank Giorgia and Davide, who have undertaken this experience with me at TUDelft and thanks to them, they have made it unforgettable.

APPENDIX A – FTIR SPECTRA

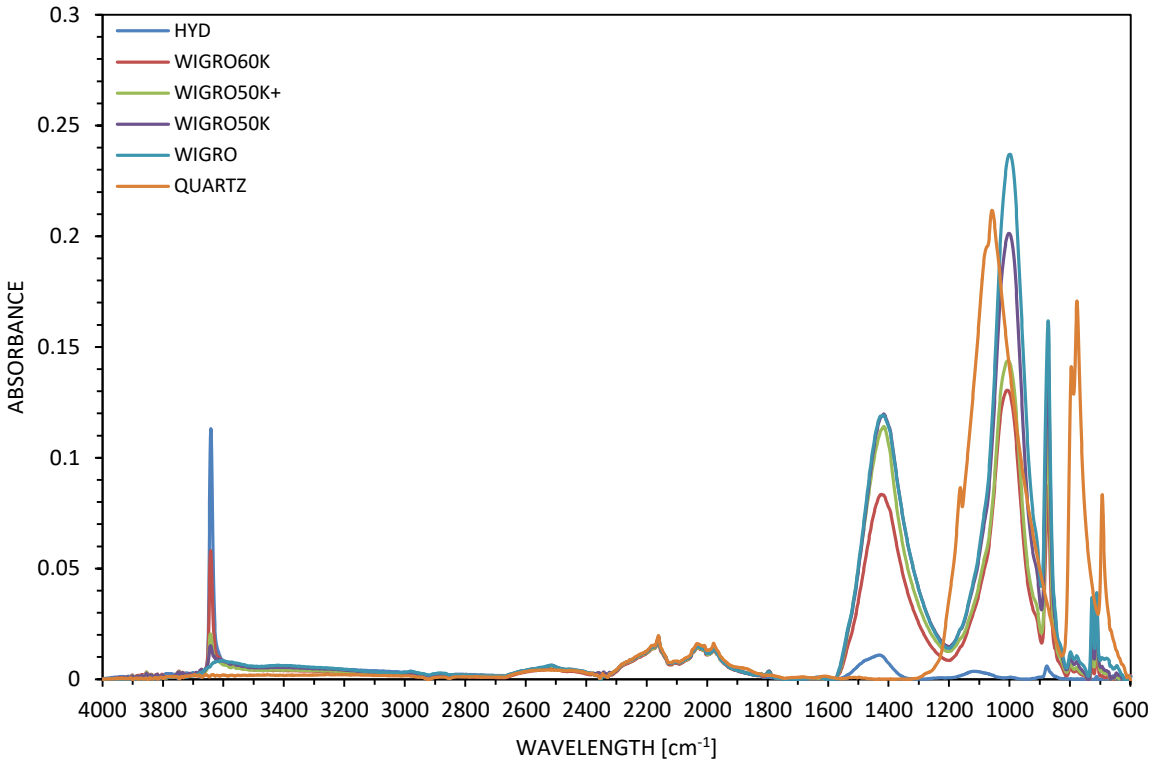

Figure A1 – FTIR spectra of six fillers at fresh condition.

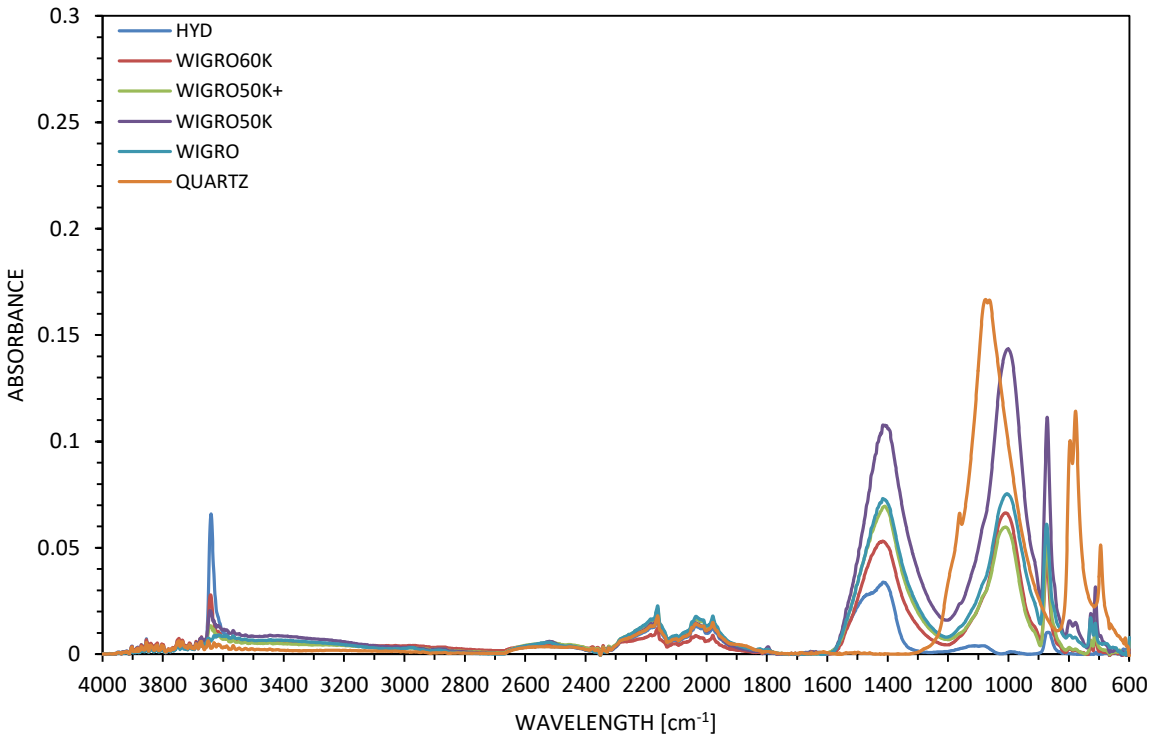

Figure A2 – FTIR spectra of six fillers at standard PAV condition.

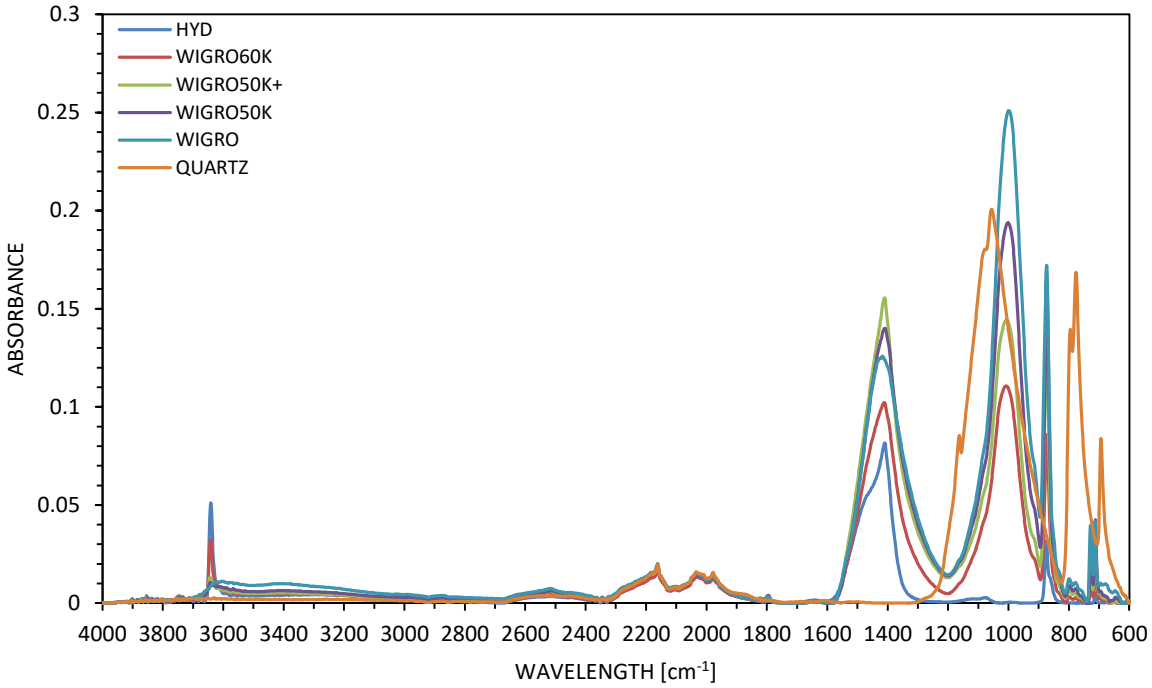

Figure A3 - FTIR spectra of six fillers at moisture PAV condition.

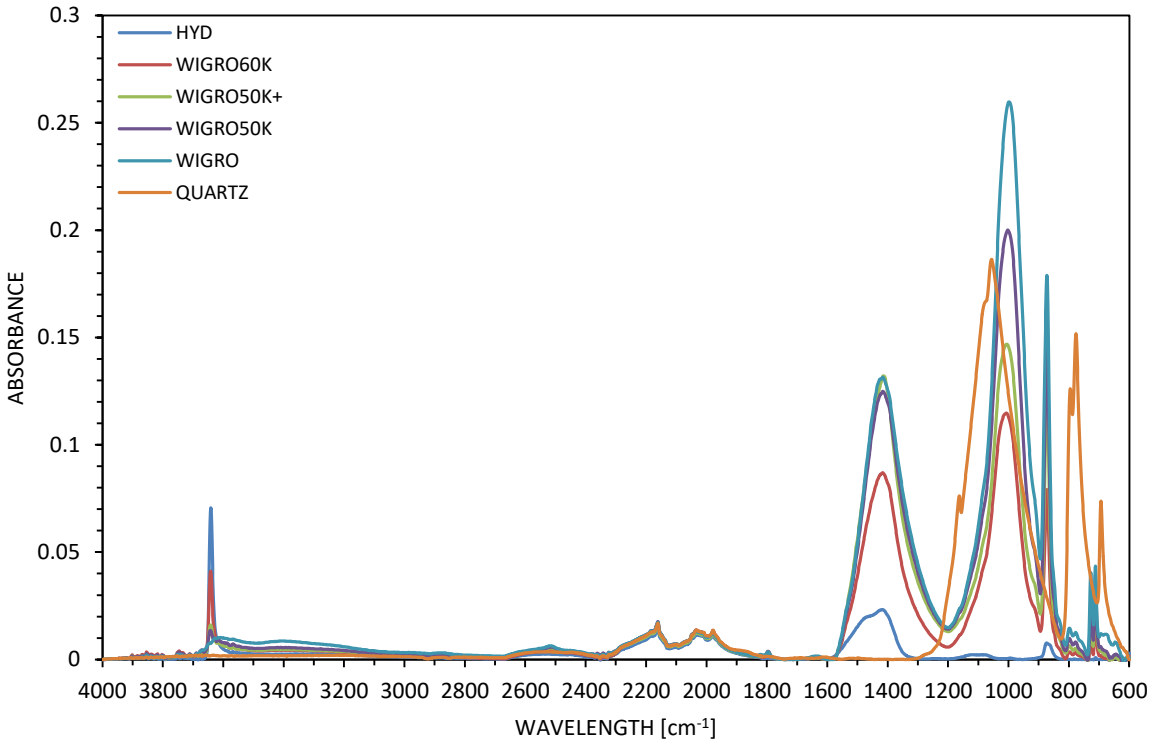

Figure A4 - FTIR spectra of six fillers at nitrogen PAV condition.

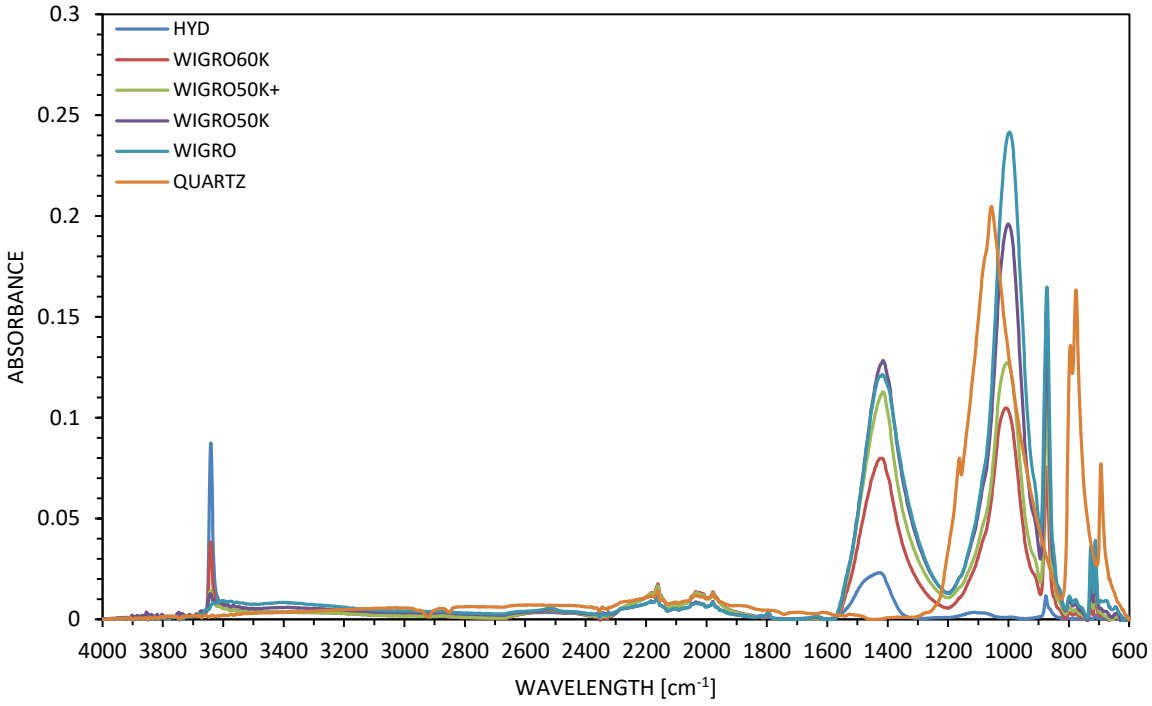

Figure A5 - FTIR spectra of six fillers at moisture nitrogen PAV condition.

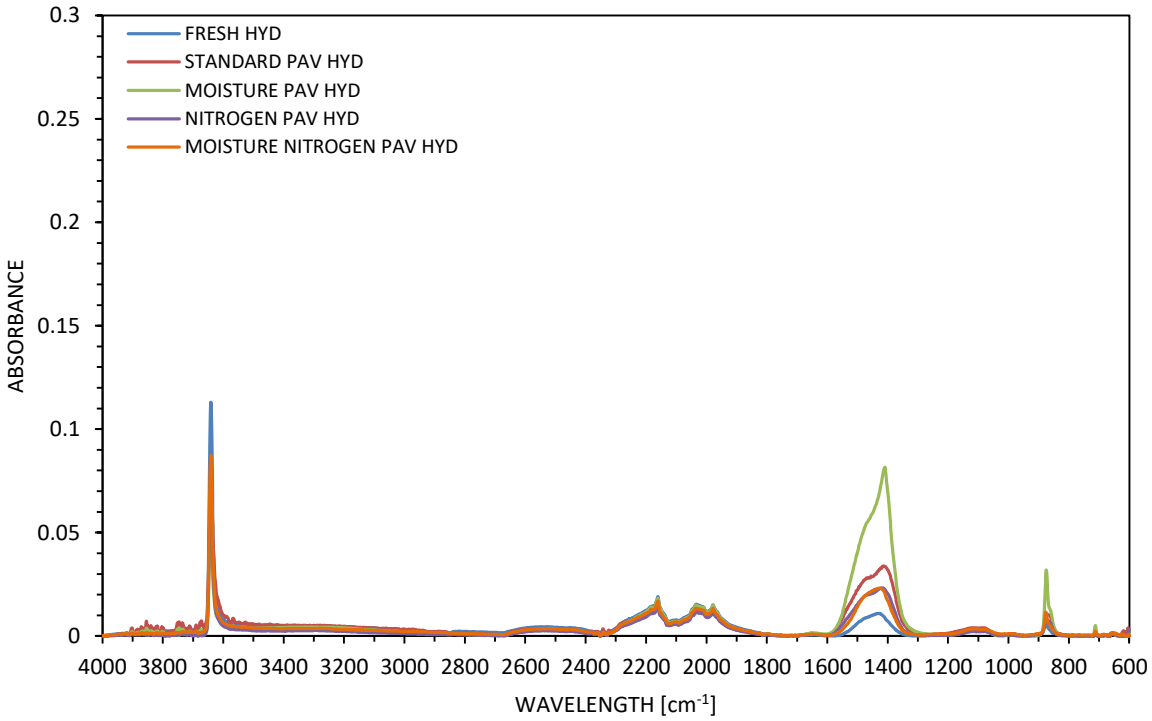

Figure A6 - FTIR spectra of HYD filler at different conditions.

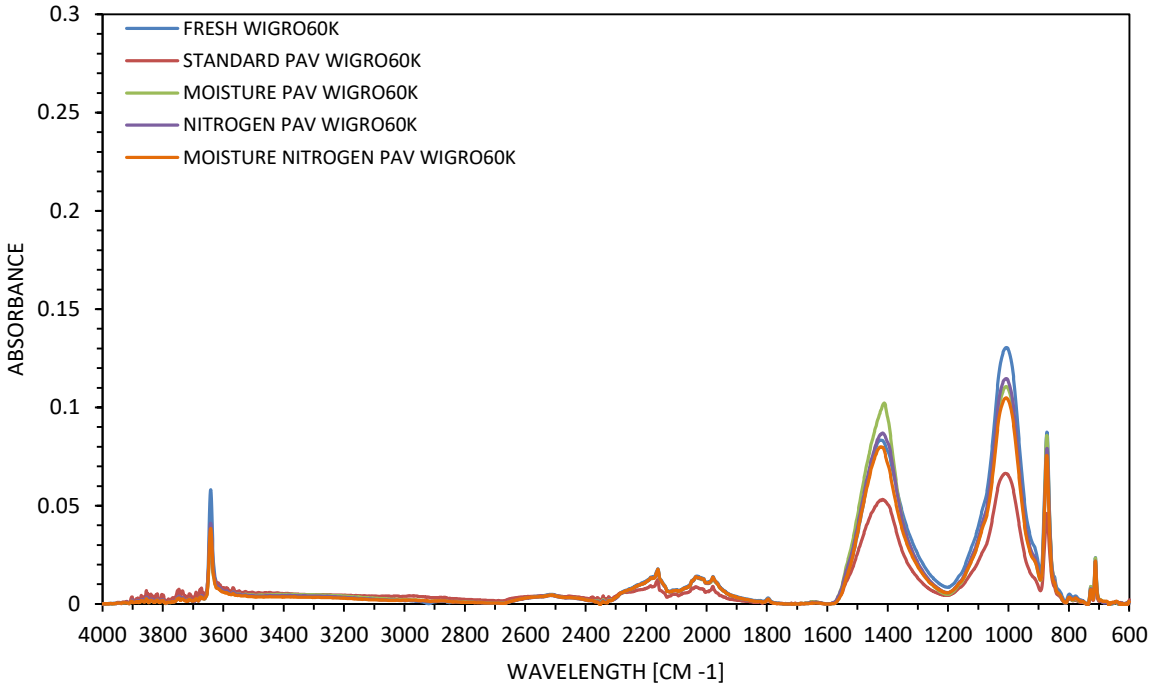

Figure A7 - FTIR spectra of W60K filler at different conditions.

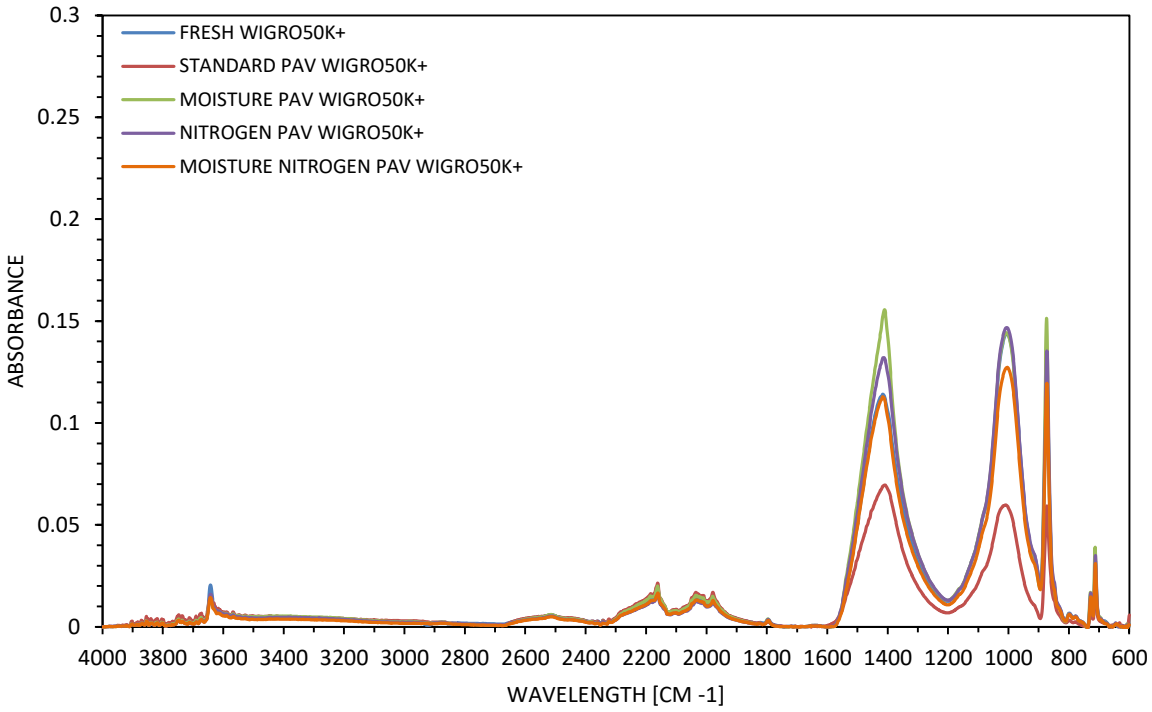

Figure A8 - FTIR spectra of W50K+ filler at different conditions.

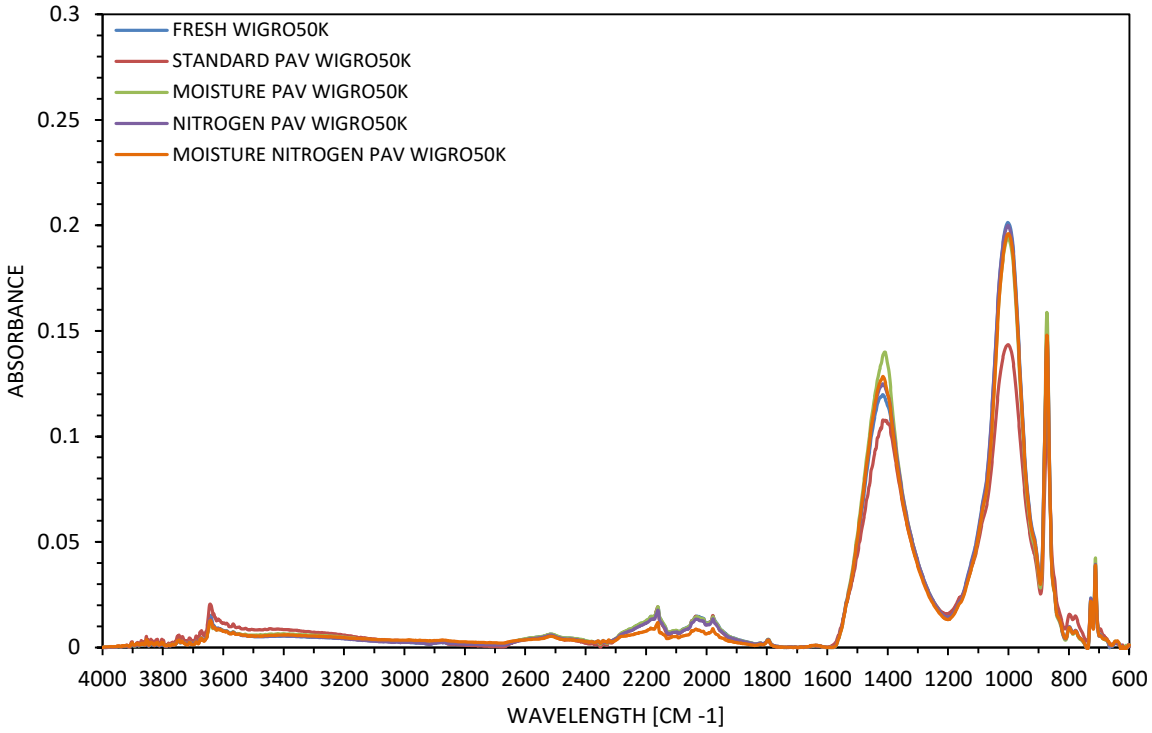

Figure A9 - FTIR spectra of W50K filler at different conditions.

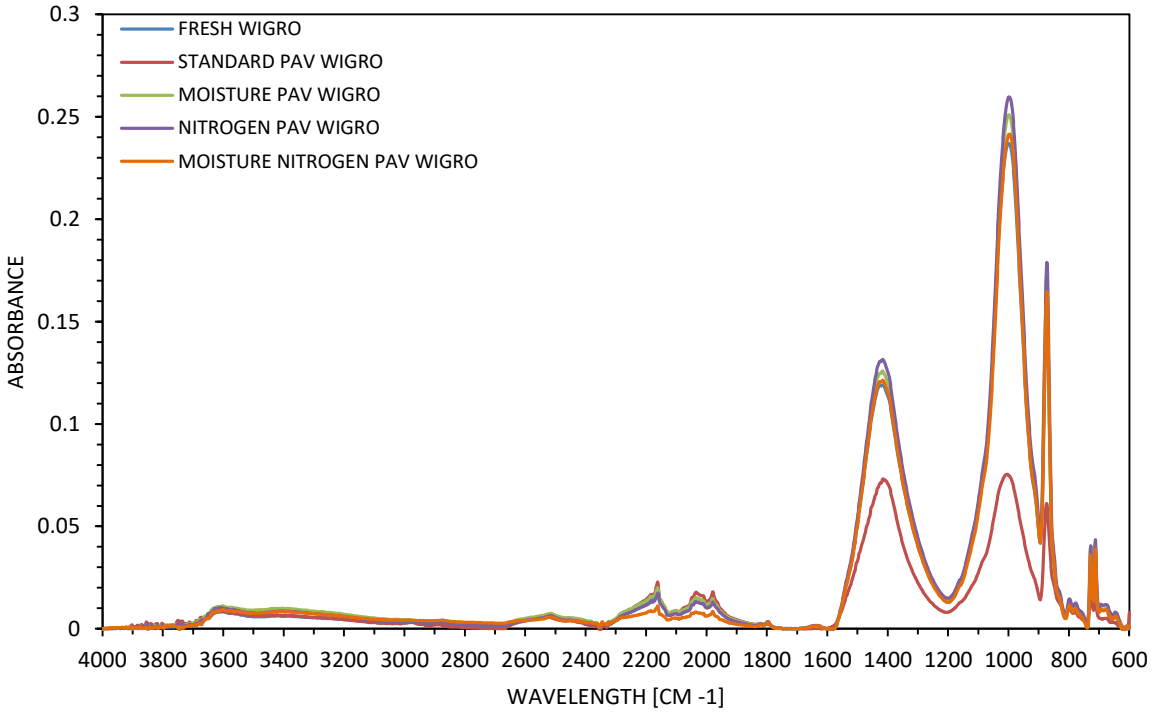

Figure A10 - FTIR spectra of W filler at different conditions.

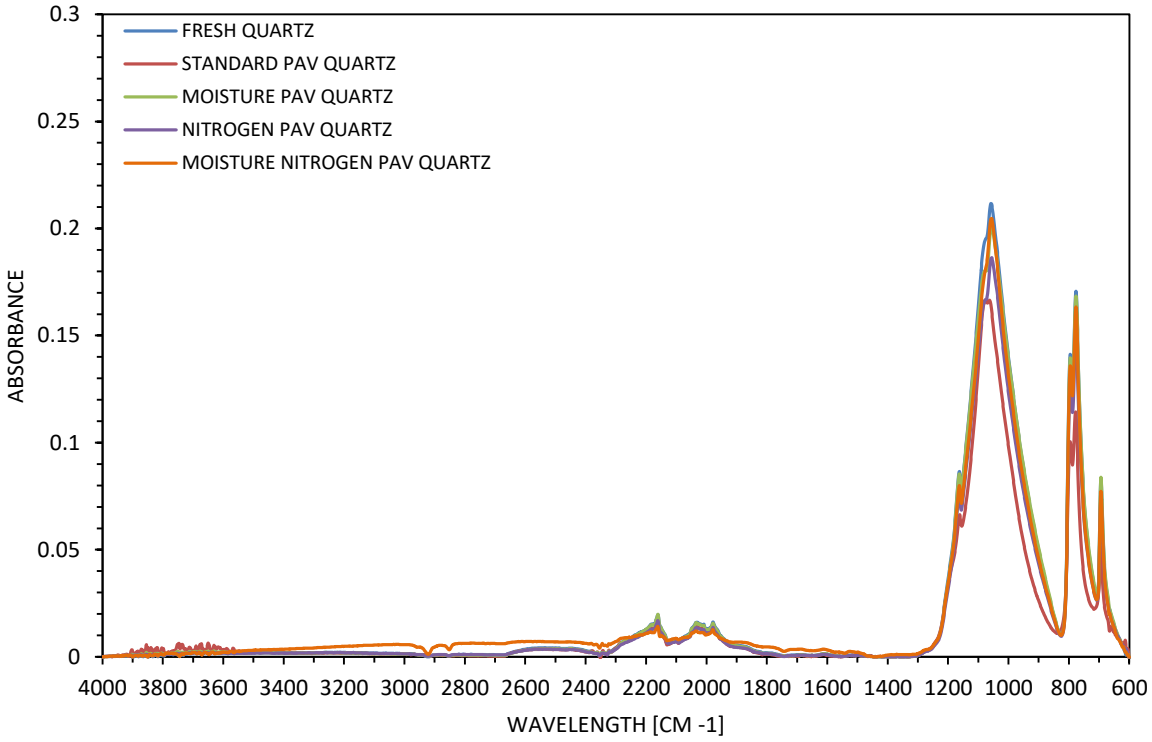

Figure A11 - FTIR spectra of QZ filler at different conditions.

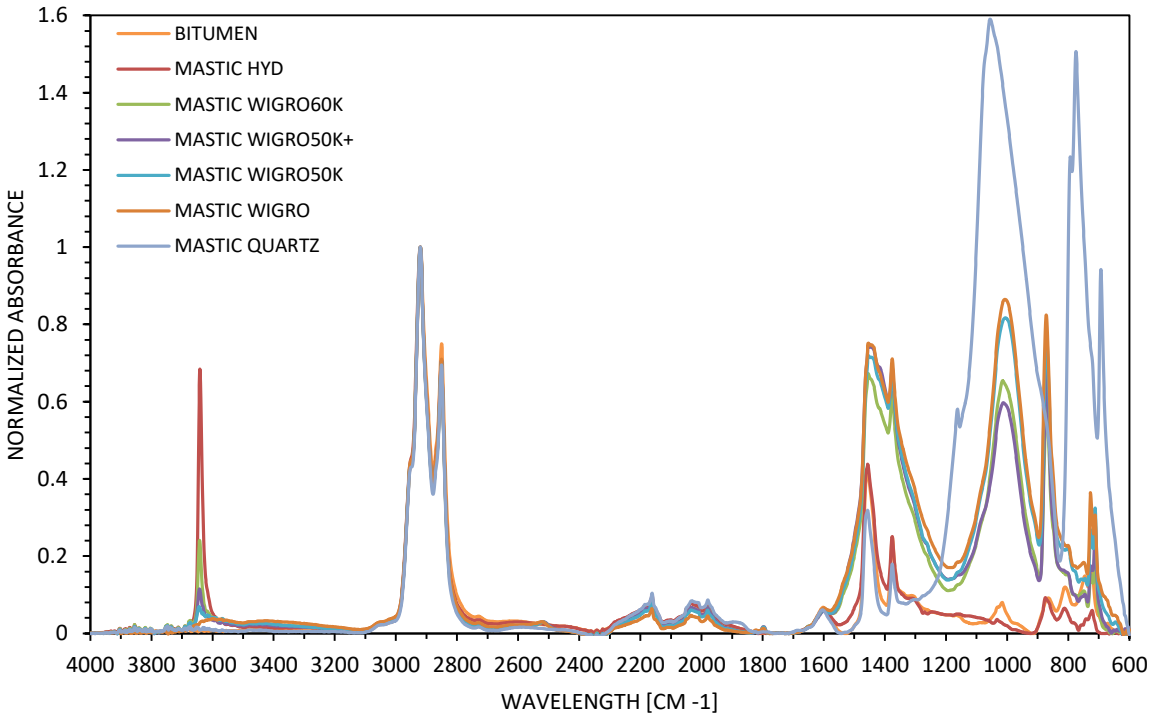

Figure A12 - FTIR spectra of neat bitumen and six mastics at fresh condition.

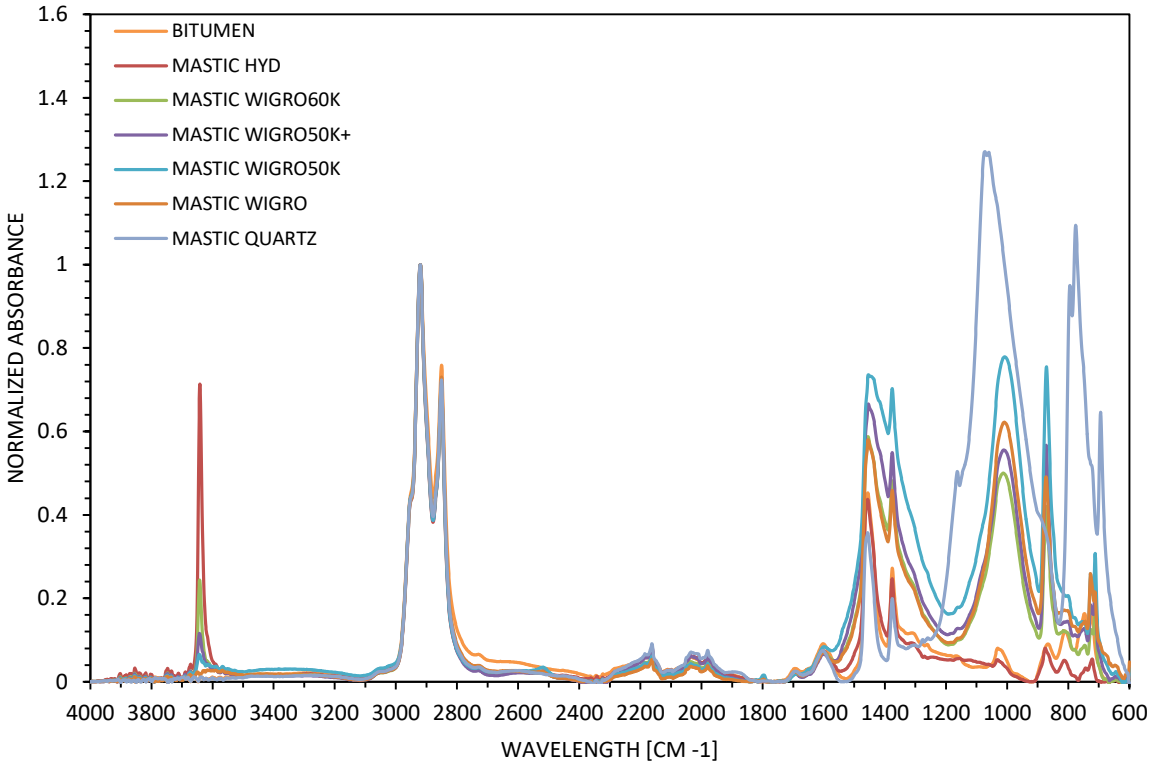

Figure A13 - FTIR spectra of neat bitumen and six mastics at standard PAV condition.

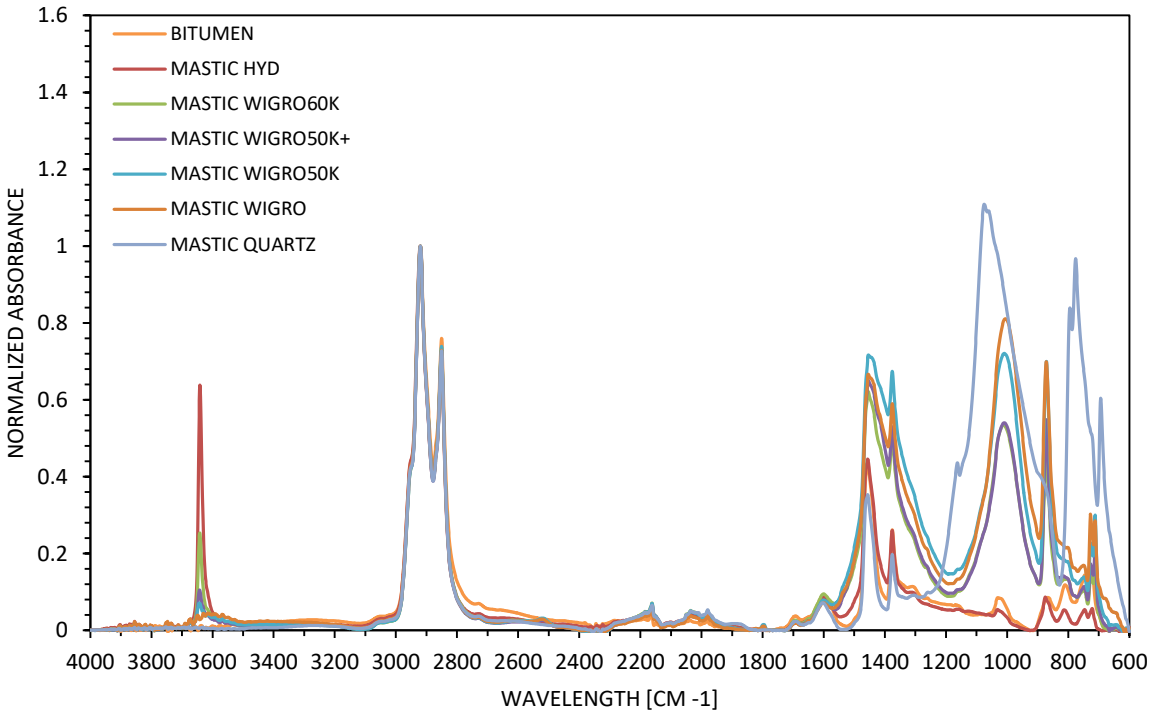

Figure A14 - FTIR spectra of neat bitumen and six mastics at moisture PAV condition.

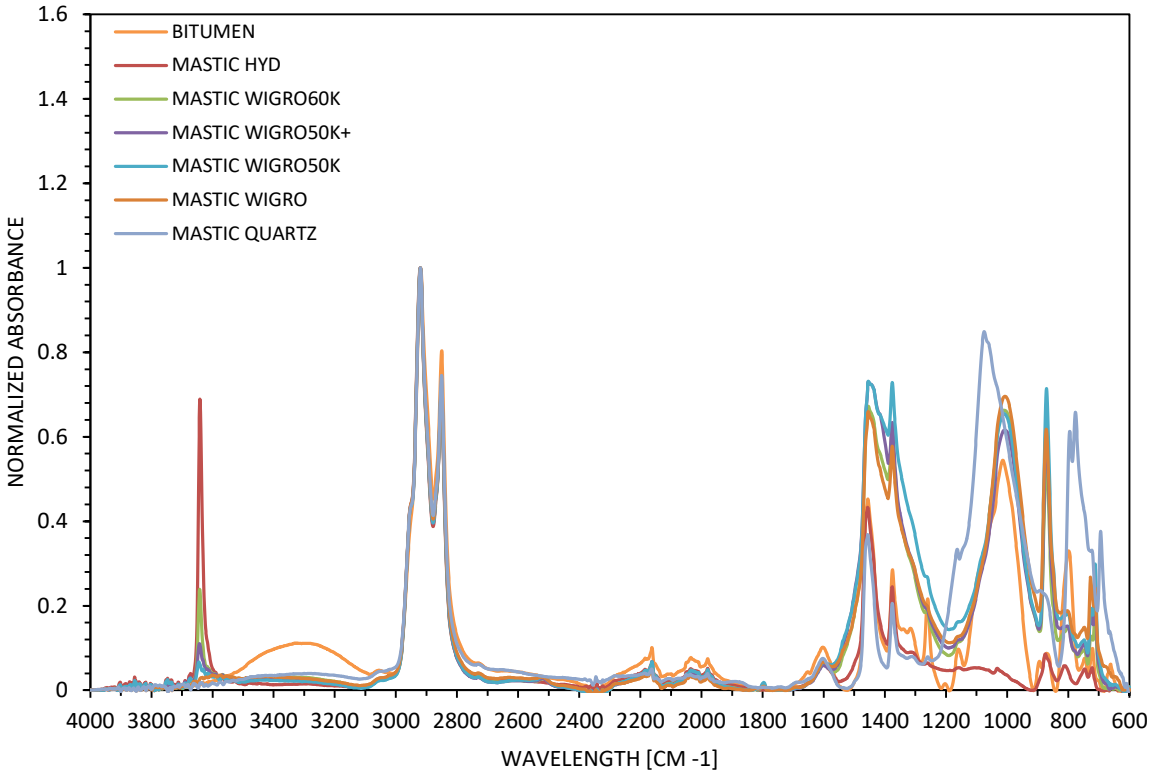

Figure A15 - FTIR spectra of neat bitumen and six mastics at nitrogen PAV condition.

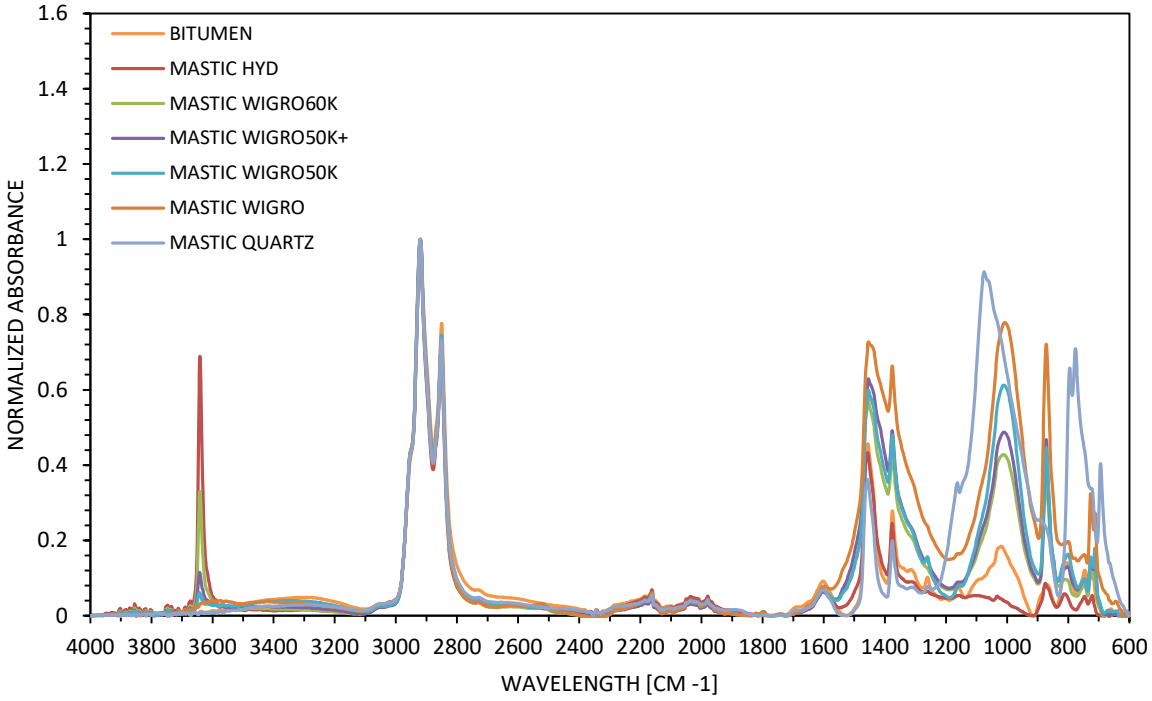

Figure A16 - FTIR spectra of neat bitumen and six mastics at moisture nitrogen PAV condition.

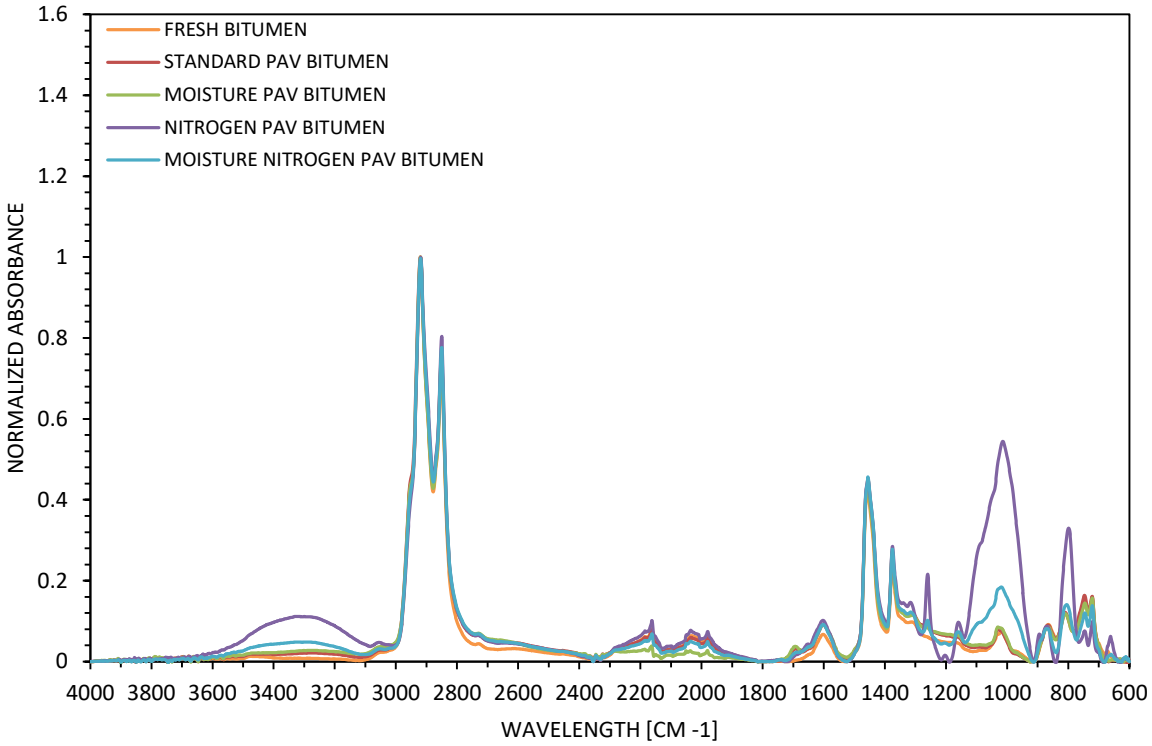

Figure A17 - FTIR spectra of neat bitumen at different conditions.

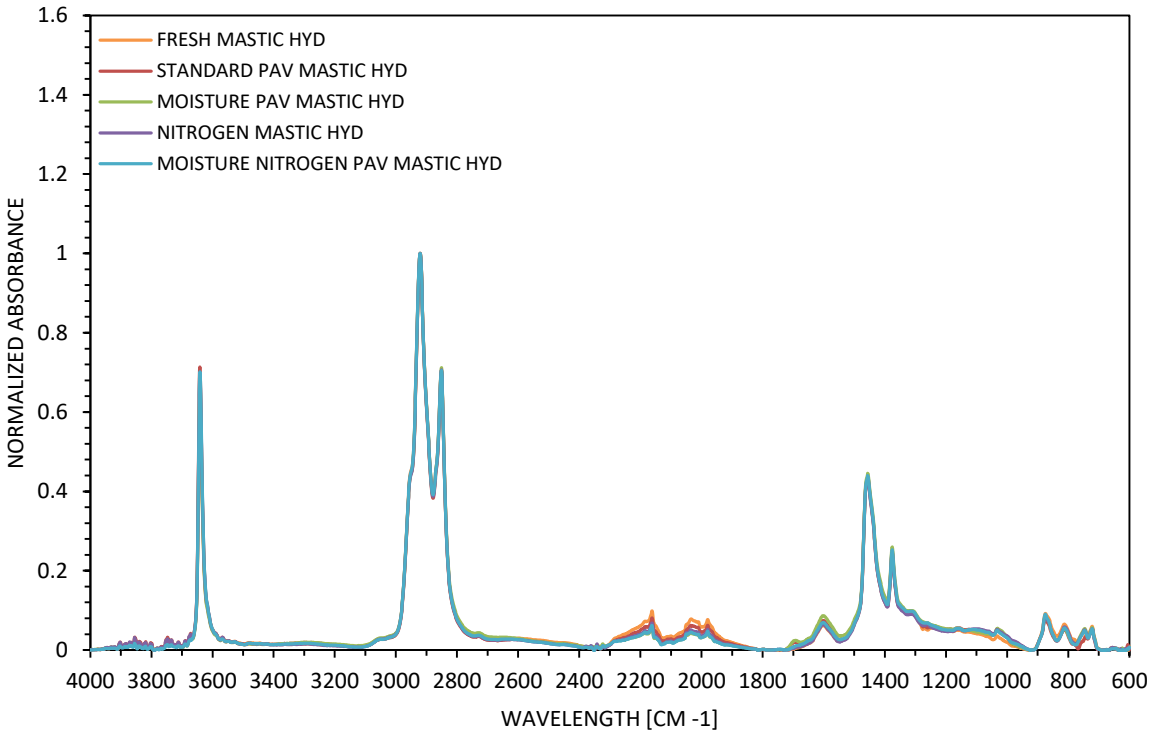

Figure A18 - FTIR spectra of HYD mastic at different conditions.

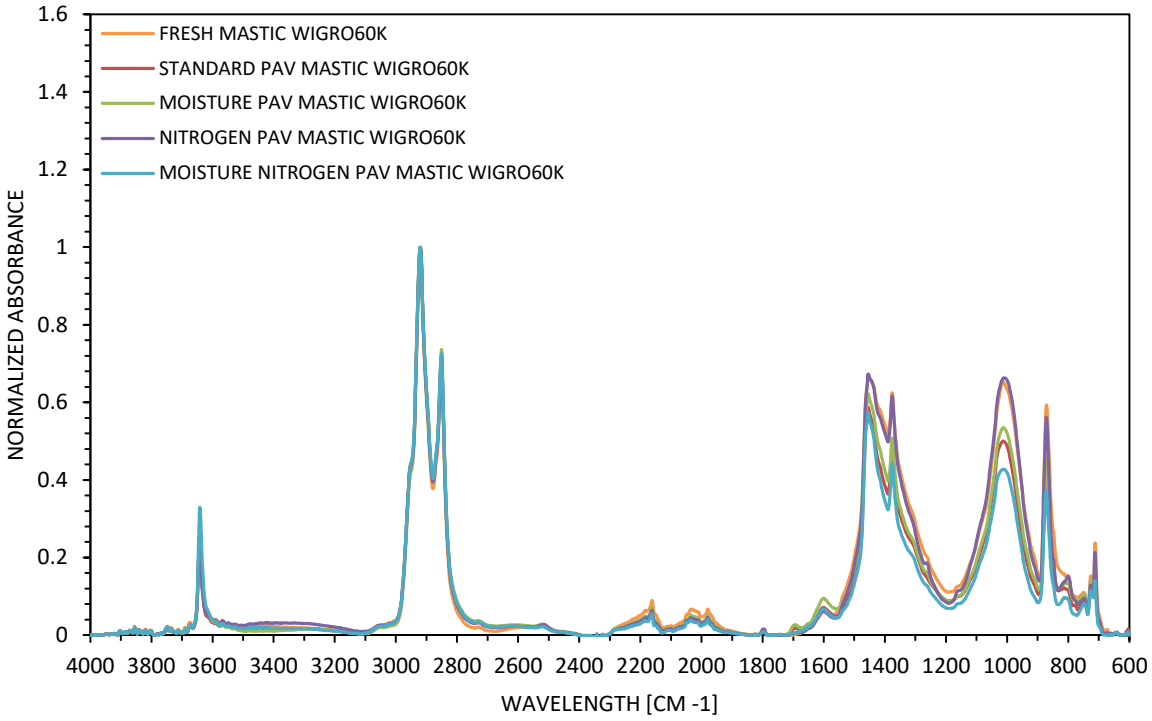

Figure A19 - FTIR spectra of W60K mastic at different conditions.

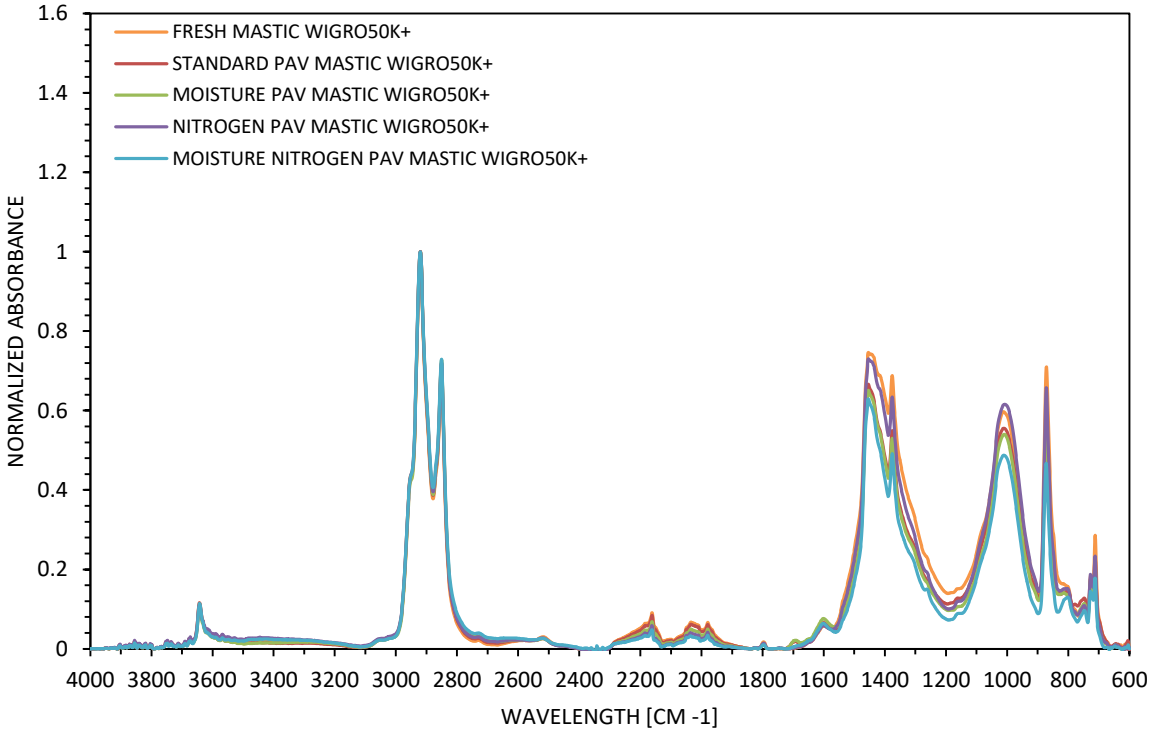

Figure A20 - FTIR spectra of W50K+ mastic at different conditions.

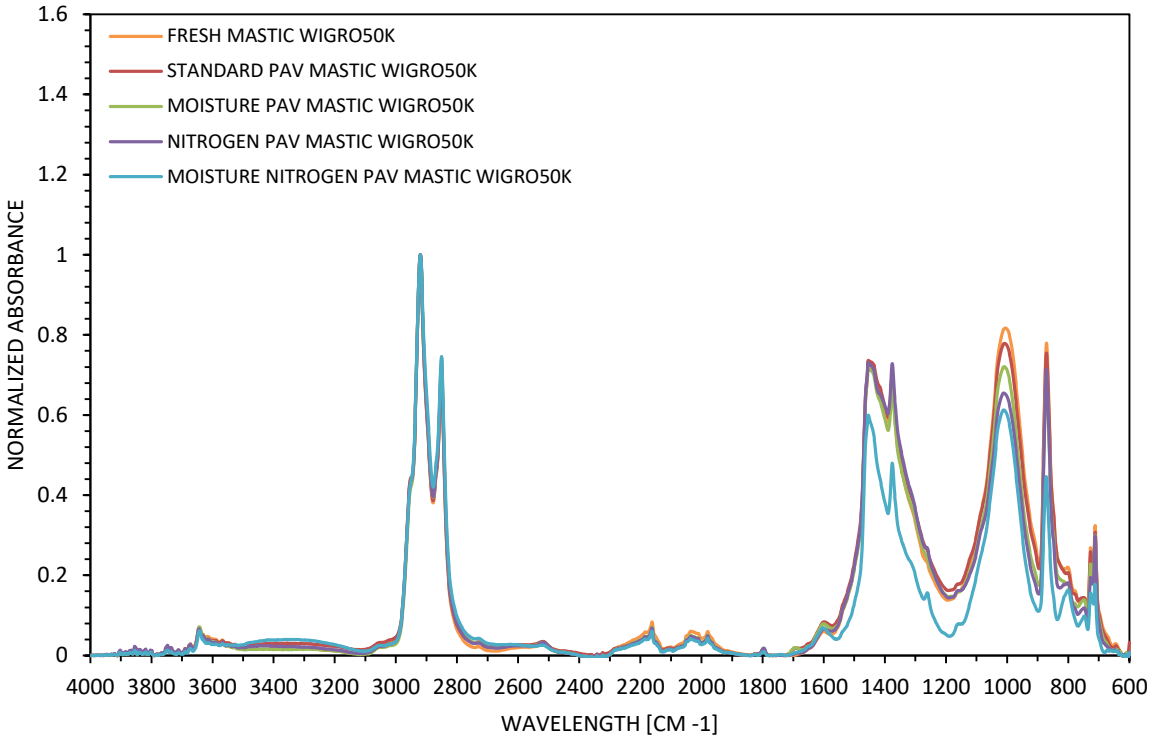

Figure A21 - FTIR spectra of W50K mastic at different conditions.

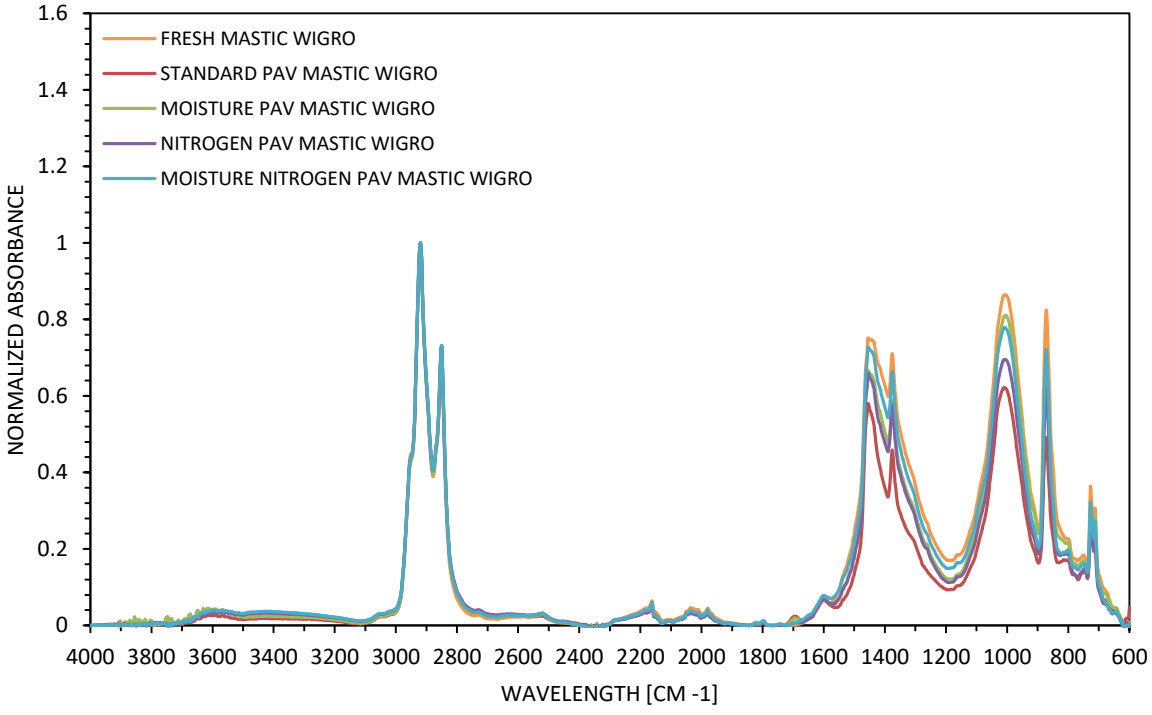

Figure A22 - FTIR spectra of W mastic at different conditions.

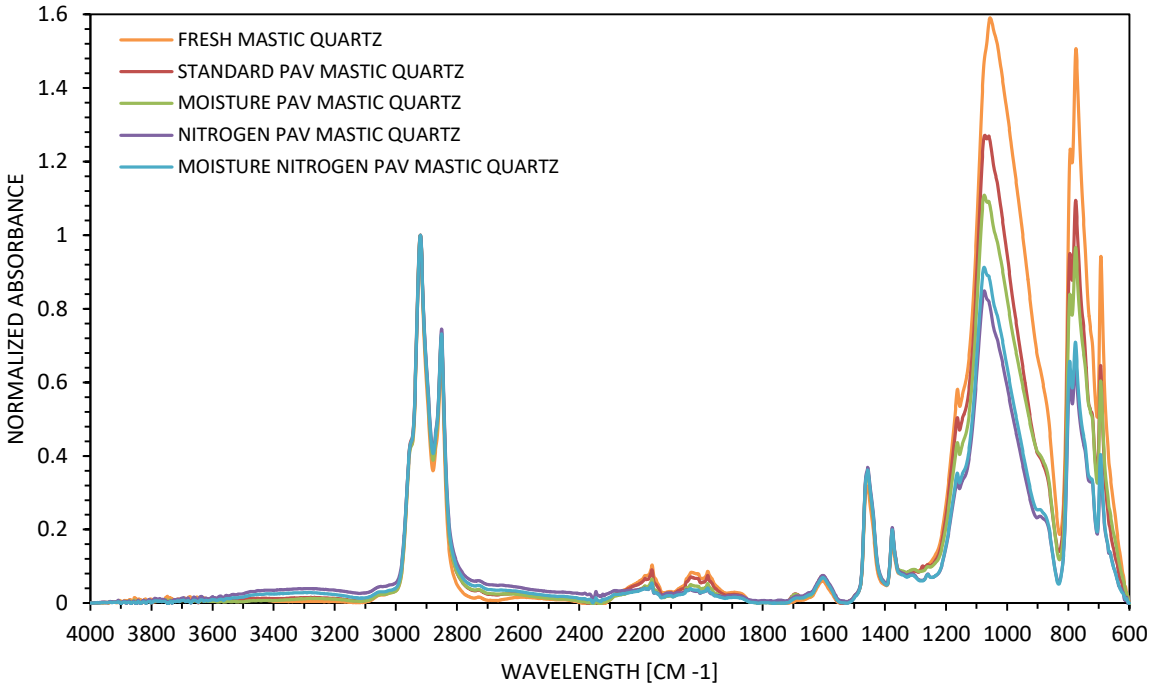

Figure A23 - FTIR spectra of QZ mastic at different conditions.

APPENDIX B – RELAXATION

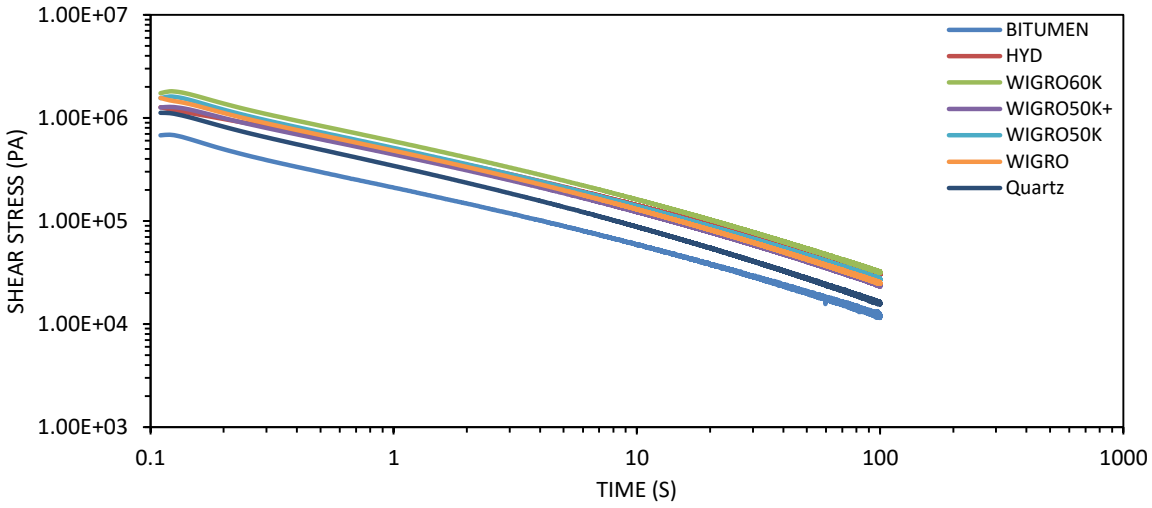

Figure B1 –Relaxation test for neat bitumen and six mastics at fresh condition.

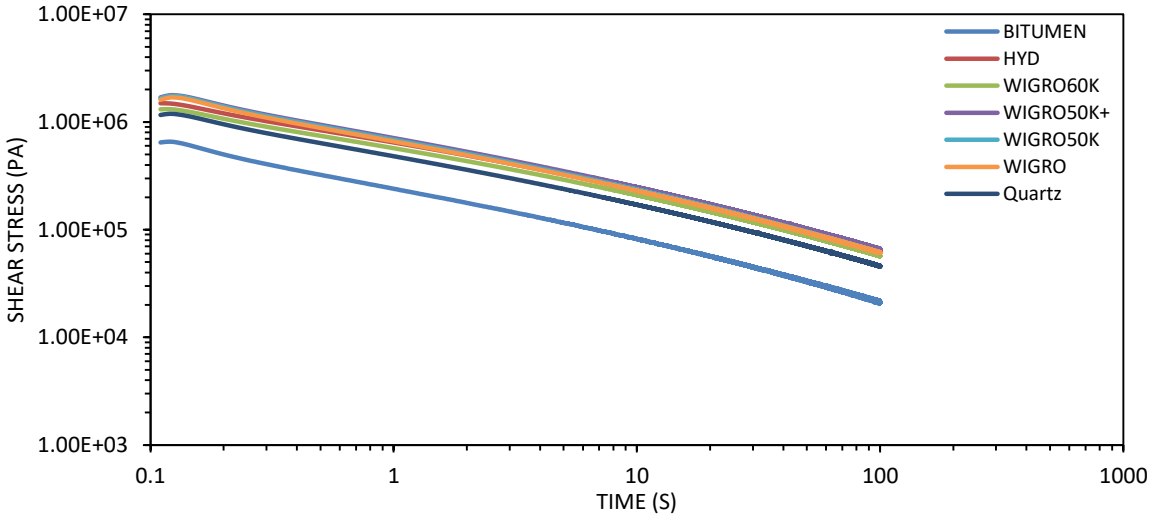

Figure B2 - Relaxation test for neat bitumen and six mastics at standard PAV condition.

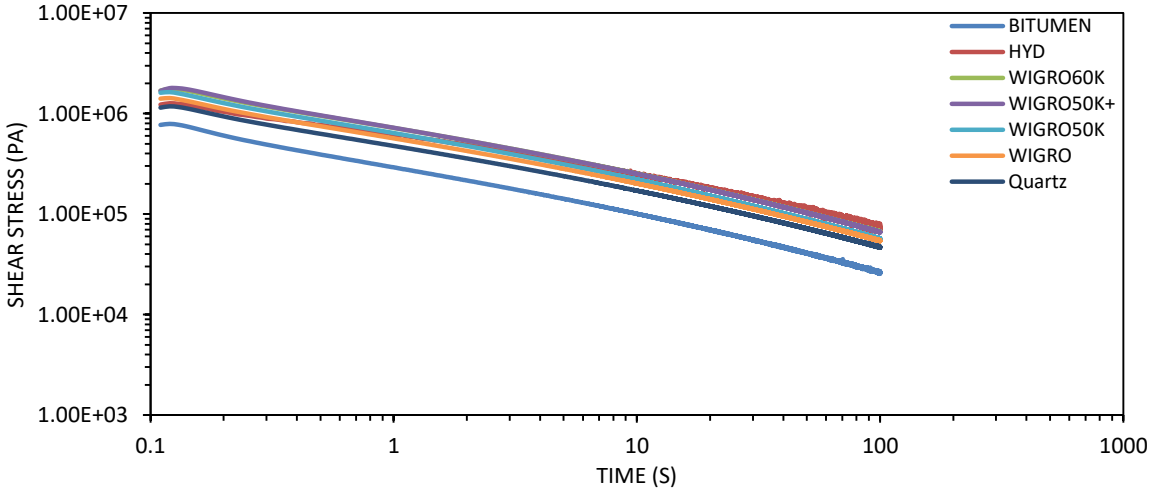

Figure B3 - Relaxation test for neat bitumen and six mastics at moisture PAV condition.

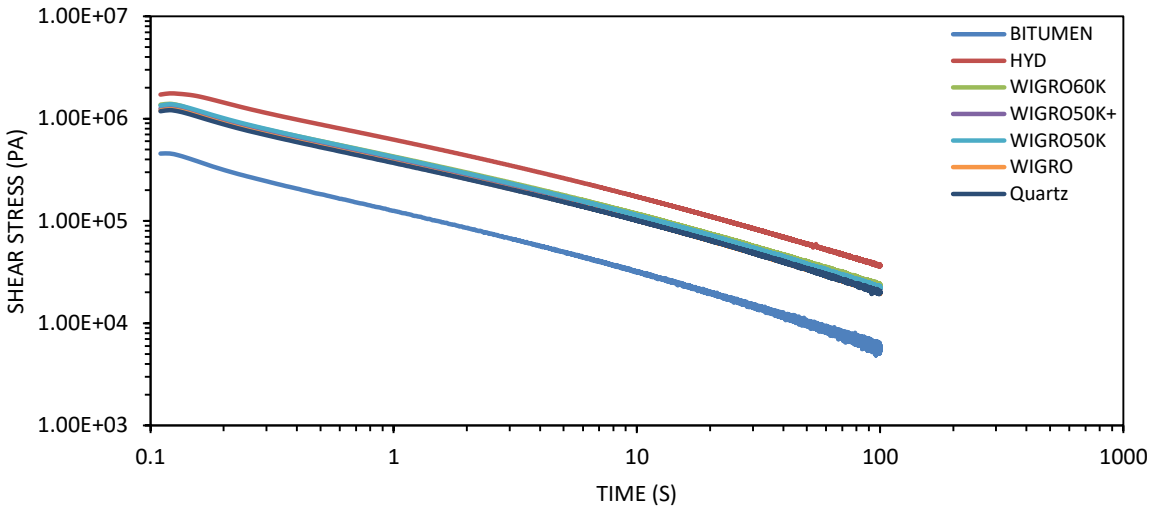

Figure B4 - Relaxation test for neat bitumen and six mastics at nitrogen PAV condition.

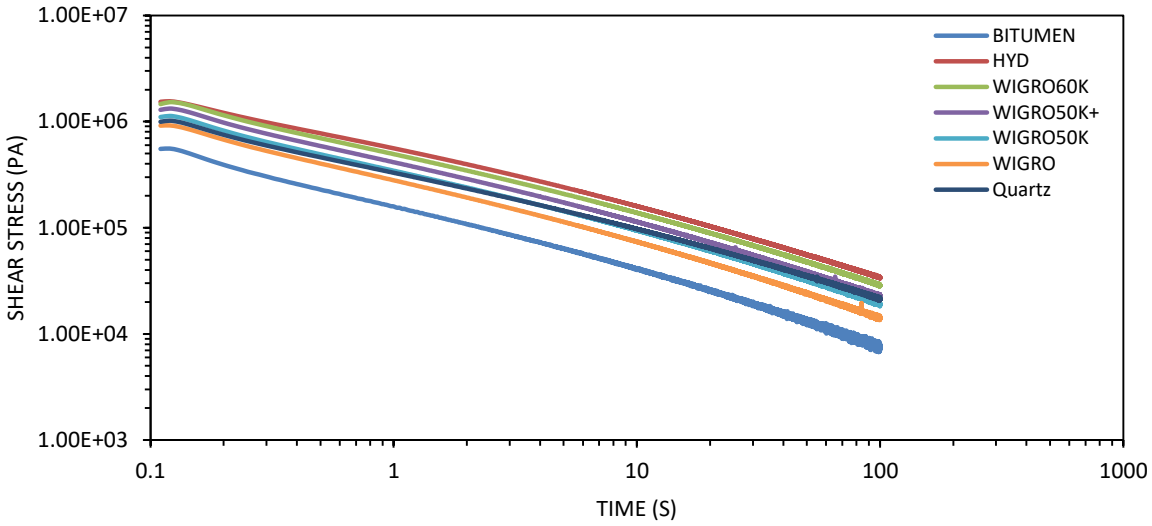

Figure B5 - Relaxation test for neat bitumen and six mastic at moisture nitrogen PAV condition.

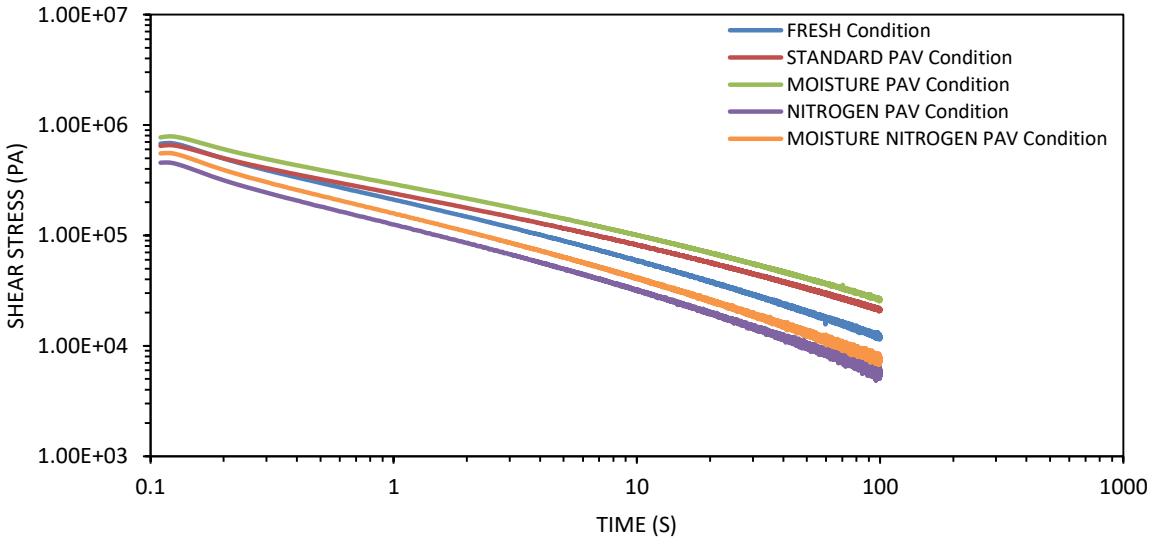

Figure B6 - Relaxation test for neat bitumen at different conditions.

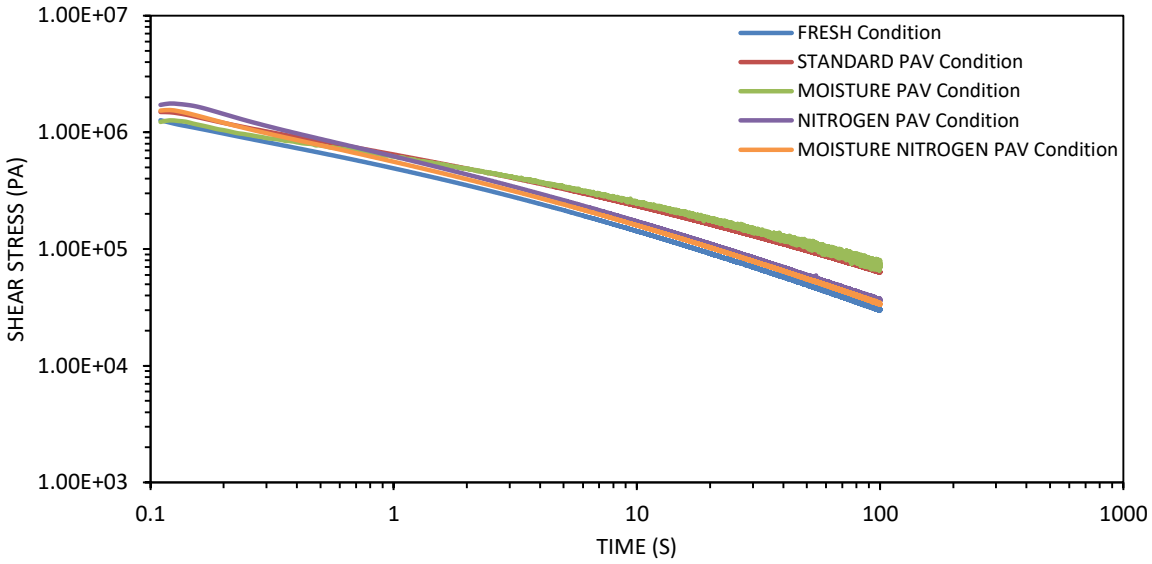

Figure B7 - Relaxation test for HYD mastic at different conditions.

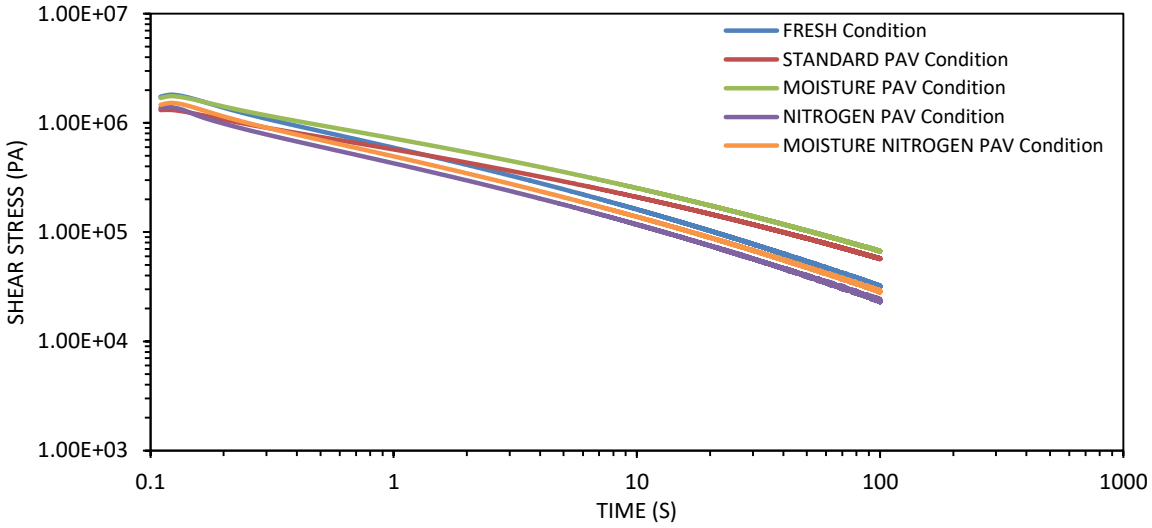

Figure B8 - Relaxation test for W60K mastic at different conditions.

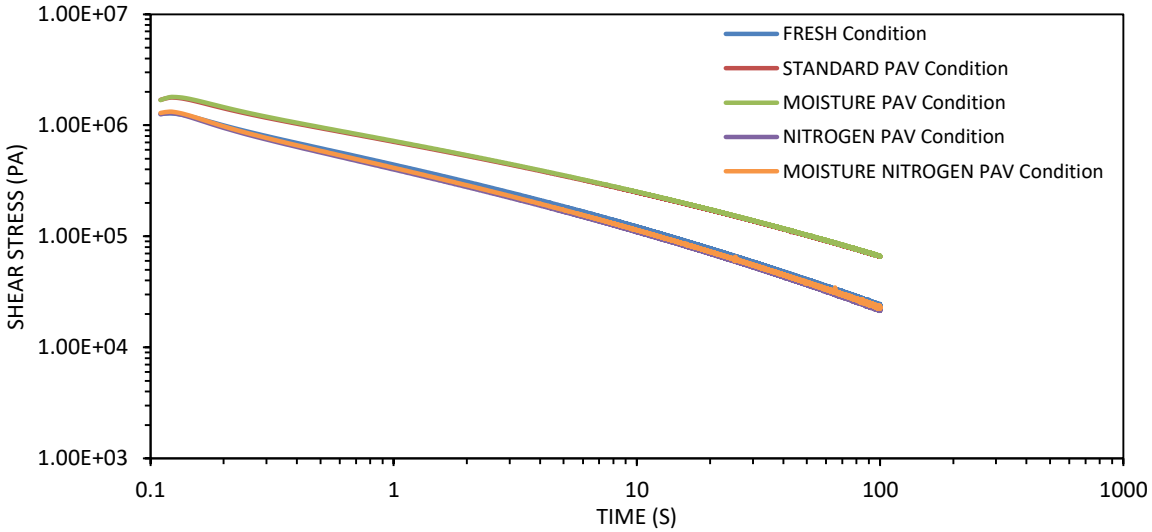

Figure B9 - Relaxation test for W50K+ mastic at different conditions.

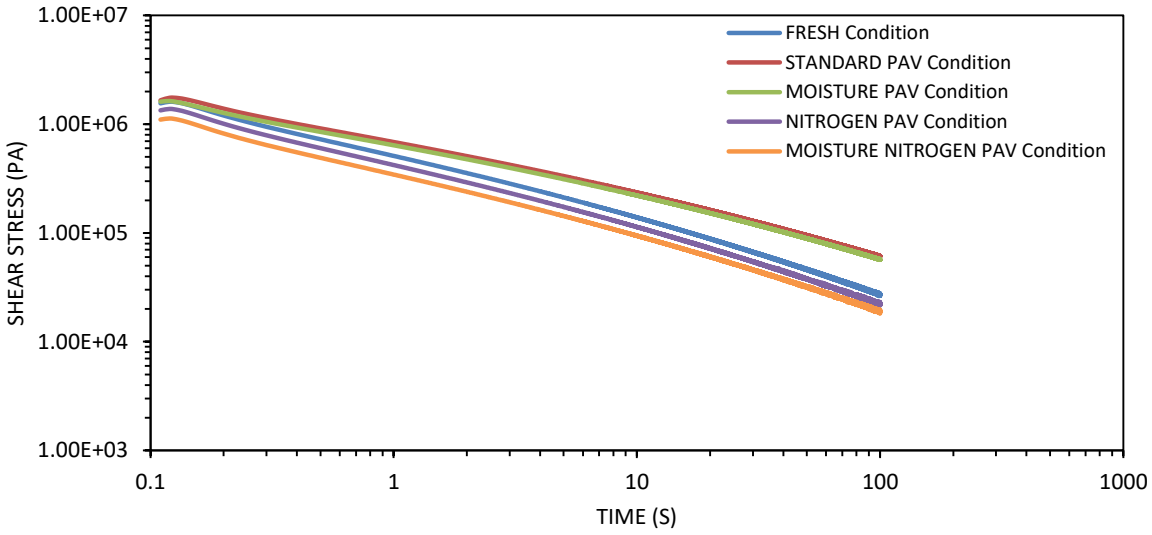

Figure B10 - Relaxation test for W50K mastic at different conditions.

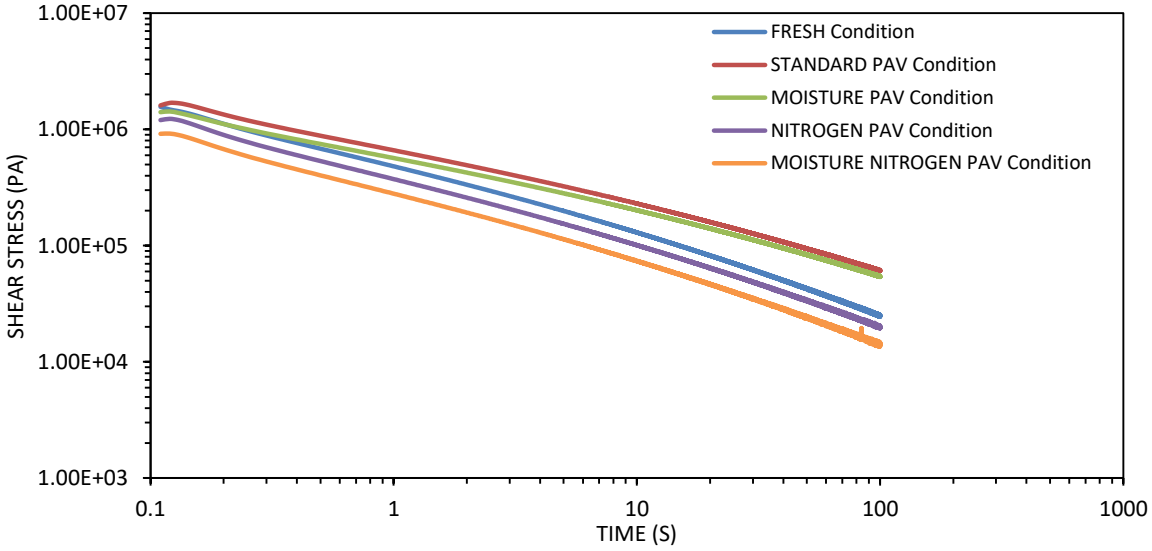

Figure B11 - Relaxation test for W mastic at different conditions.

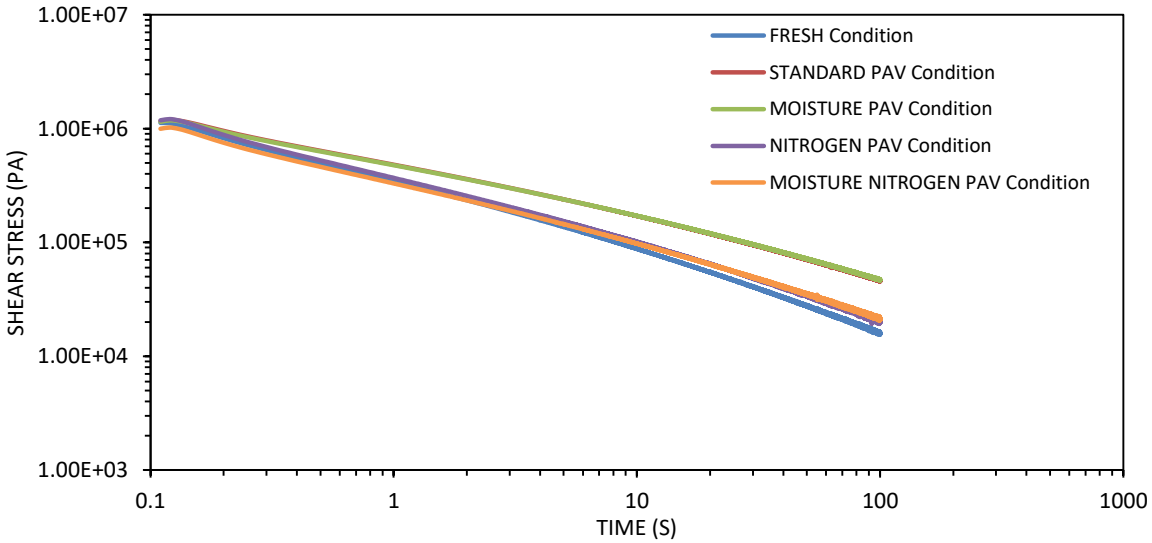

Figure B12 - Relaxation test for QZ mastic at different conditions.

APPENDIX C – LINEAR AMPLITUDE SWEEP

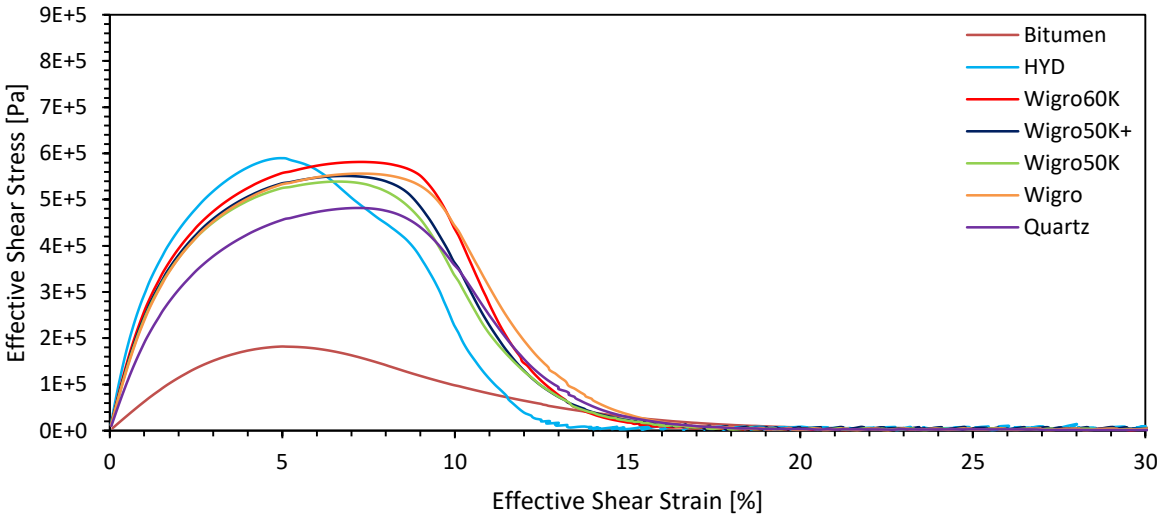

Figure C1.1 - Stress-strain curve of neat bitumen and six mastics at fresh condition under the strain-controlled mode.

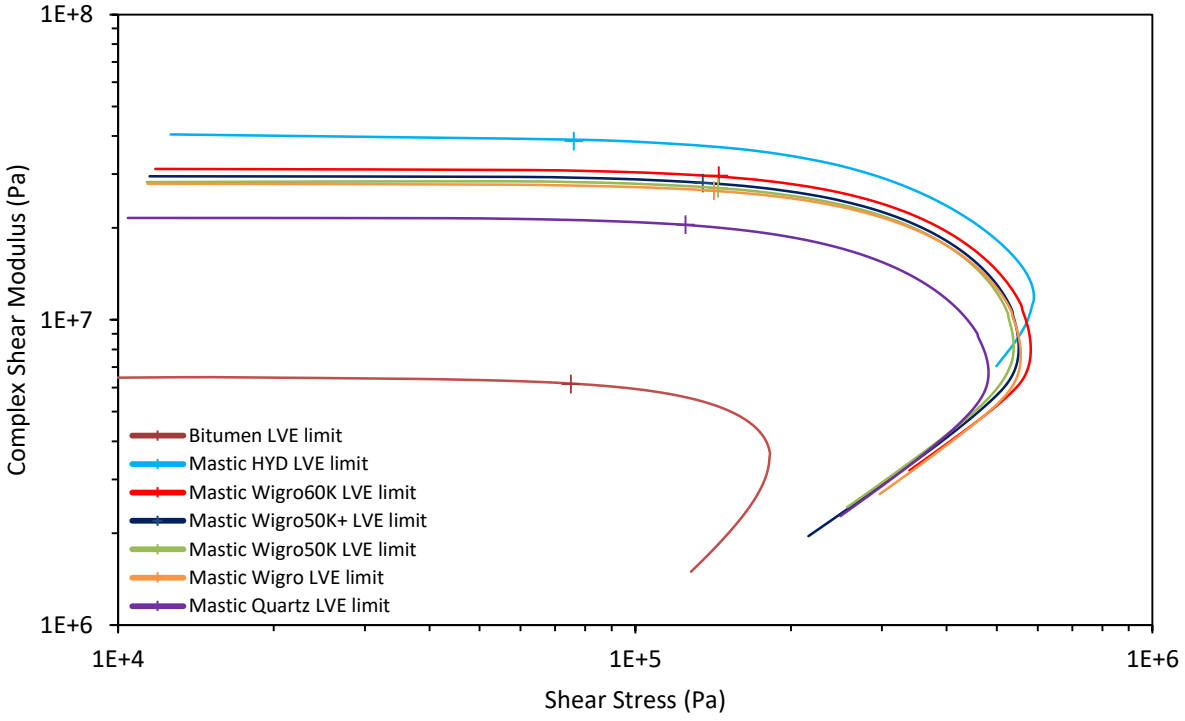

Figure C1.2 - Complex shear modulus of neat bitumen and six mastics at fresh condition under the strain-controlled mode.

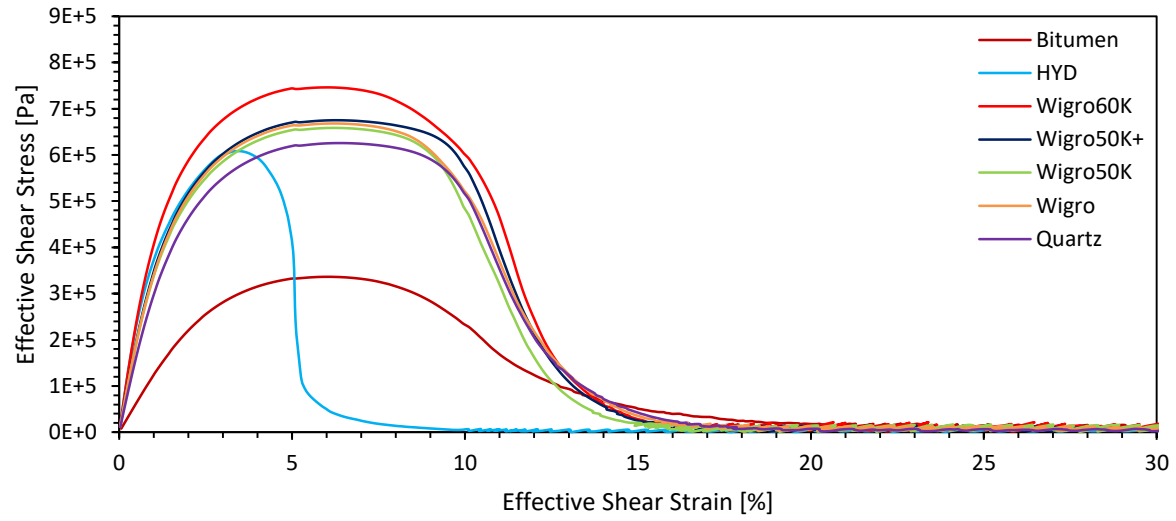

Figure C2.1 - Stress-strain curve of neat bitumen and six mastics at standard PAV condition under the strain-controlled mode.

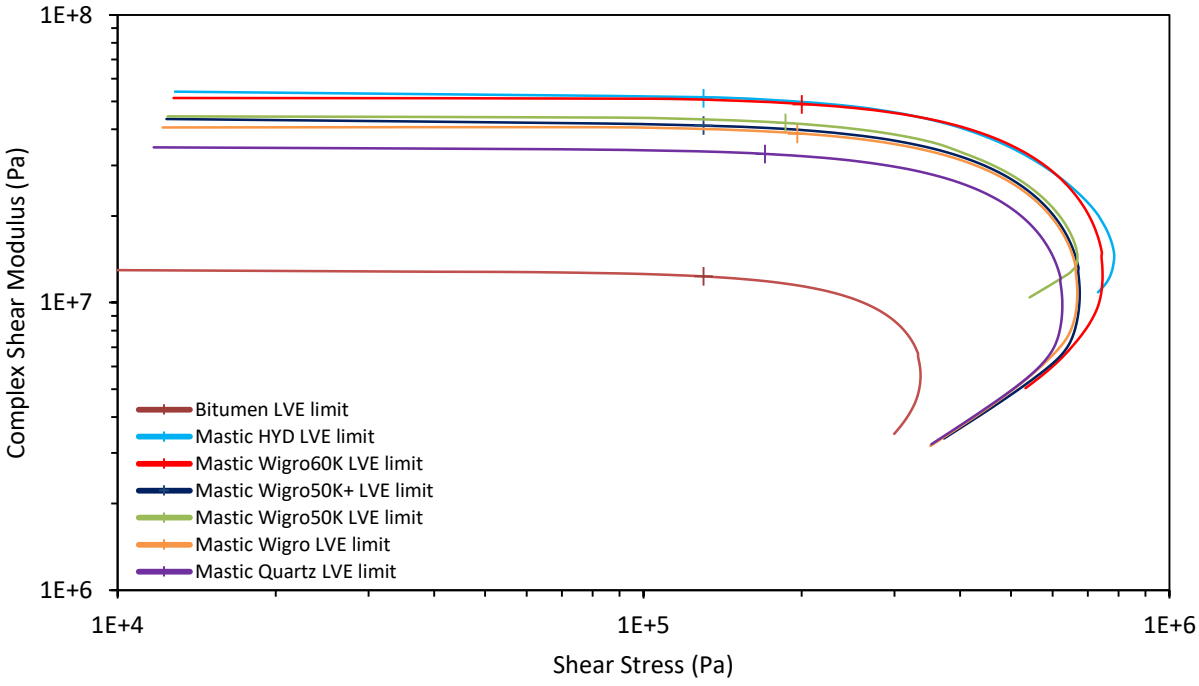

Figure C2.2 - Complex shear modulus of neat bitumen and six mastics at standard PAV condition under the strain-controlled mode.

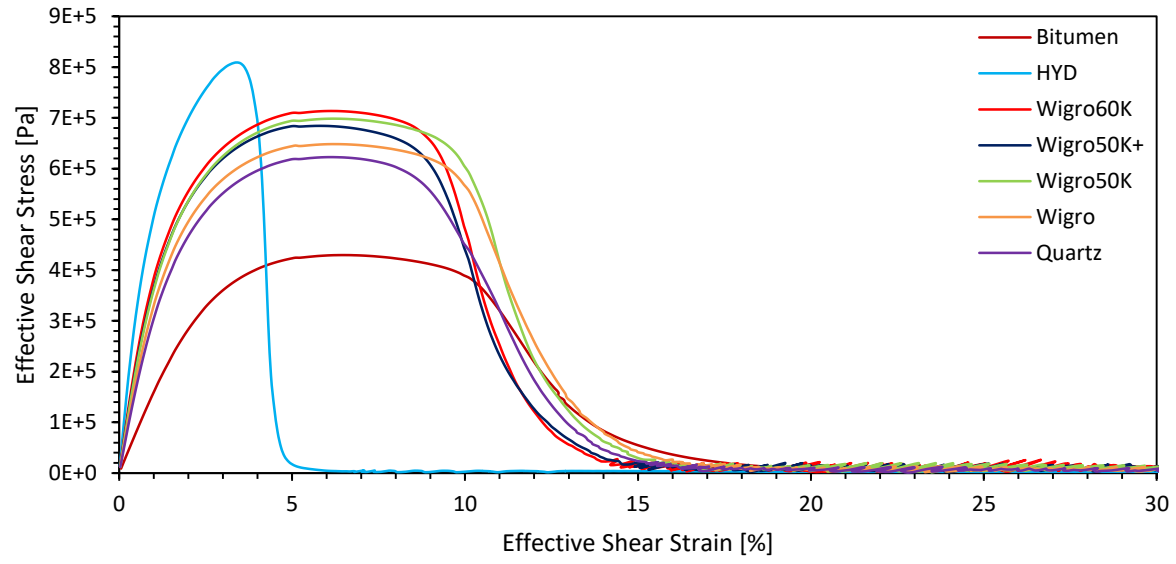

Figure C3.1 - Stress-strain curve of neat bitumen and six mastics at moisture PAV condition under the strain-controlled mode.

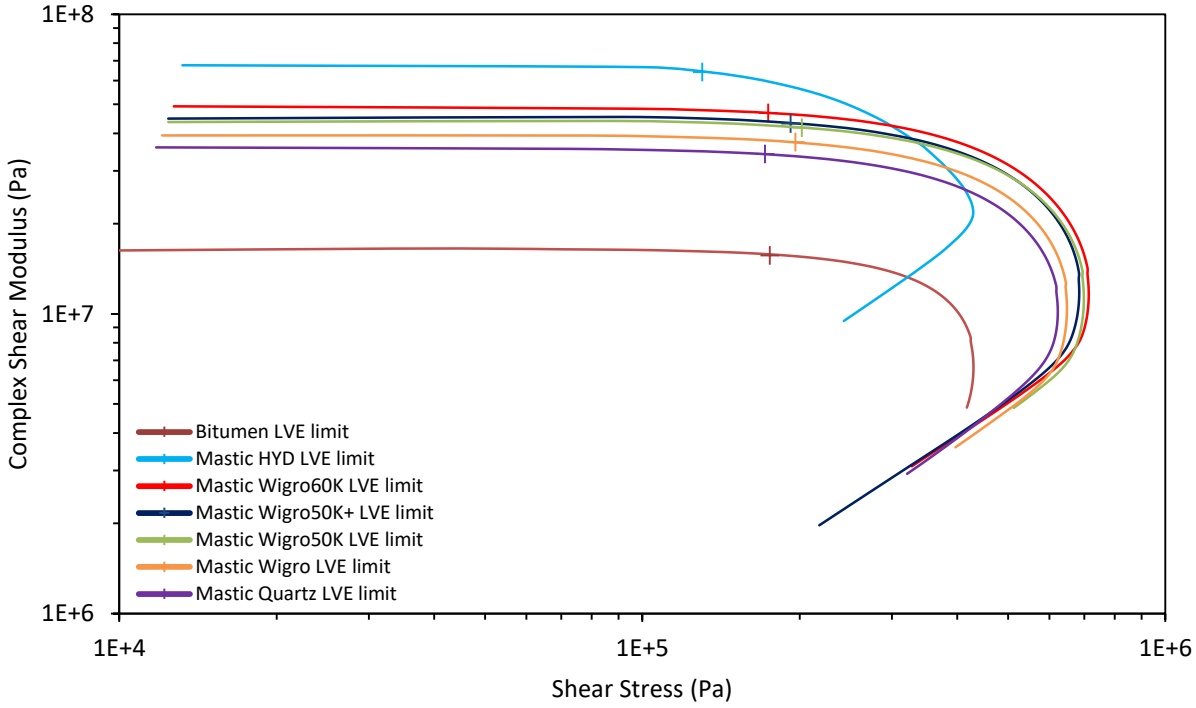

Figure C3.2 - Complex shear modulus of neat bitumen and six mastics at moisture PAV condition under the strain-controlled mode.

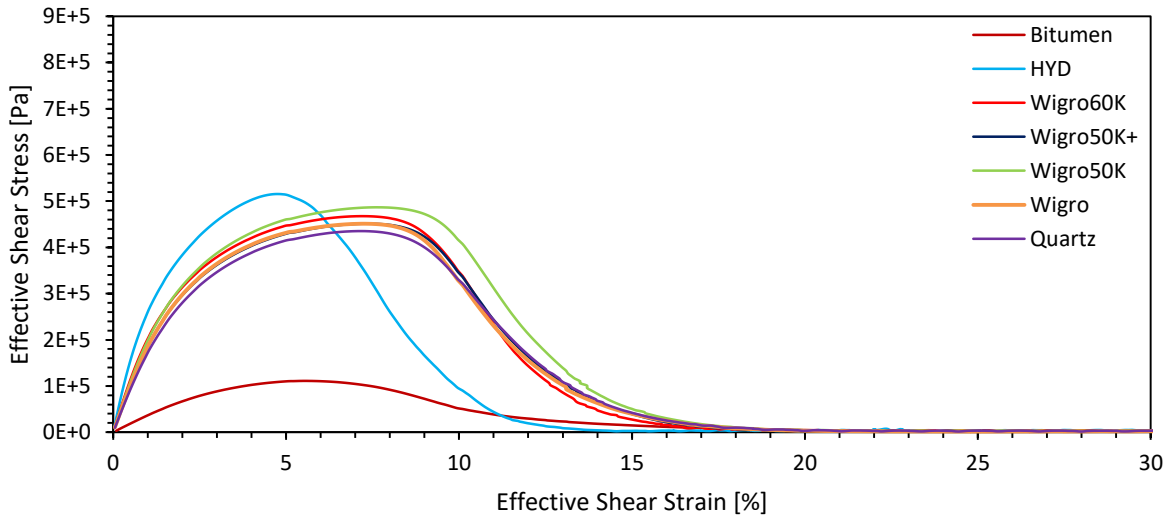

Figure C4.1 - Stress-strain curve of neat bitumen and six mastics at nitrogen PAV condition under the strain-controlled mode.

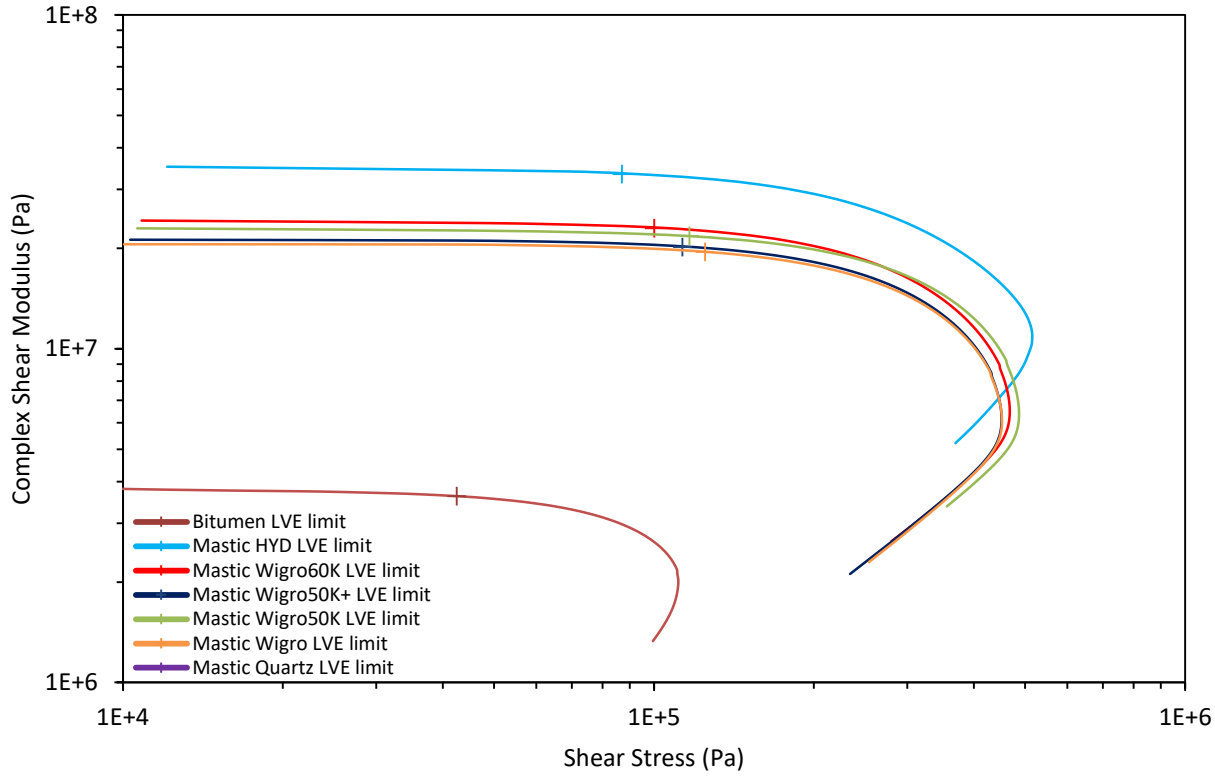

Figure C4.2 - Complex shear modulus of neat bitumen and six mastics at nitrogen PAV condition under the strain-controlled mode.

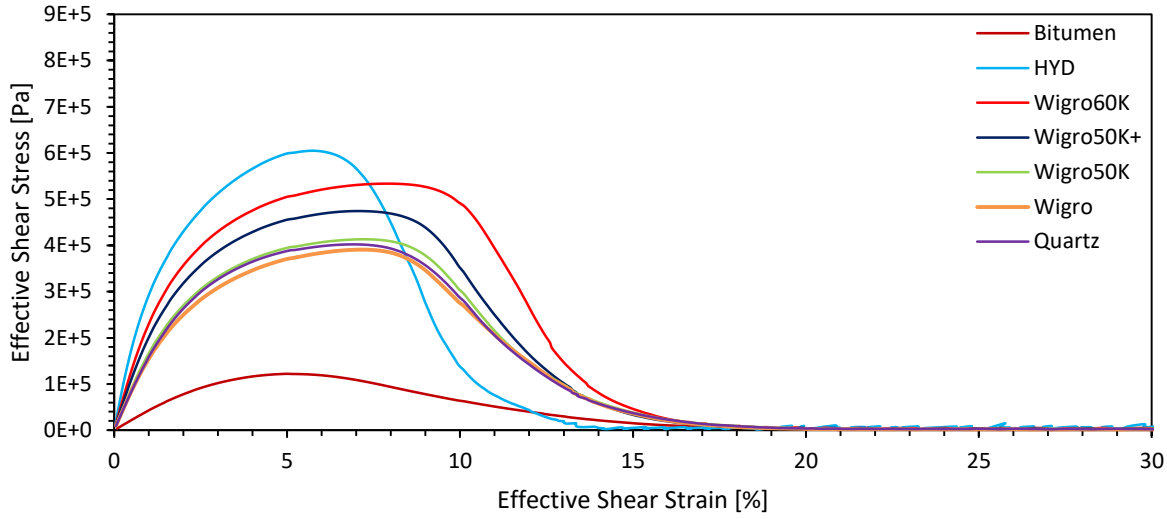

Figure C5.1 - Stress-strain curve of neat bitumen and six mastics at moisture nitrogen PAV condition under the strain-controlled mode.

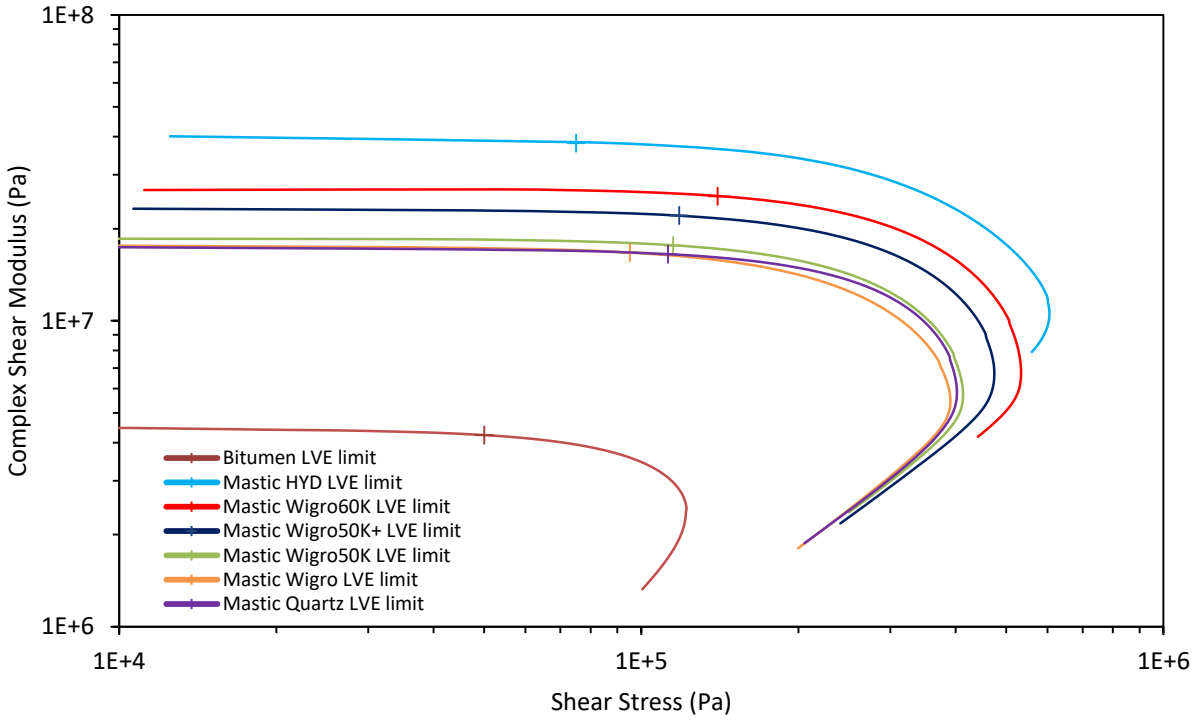

Figure C5.2 - Complex shear modulus of neat bitumen and six mastics at moisture nitrogen PAV condition under the strain-controlled mode.

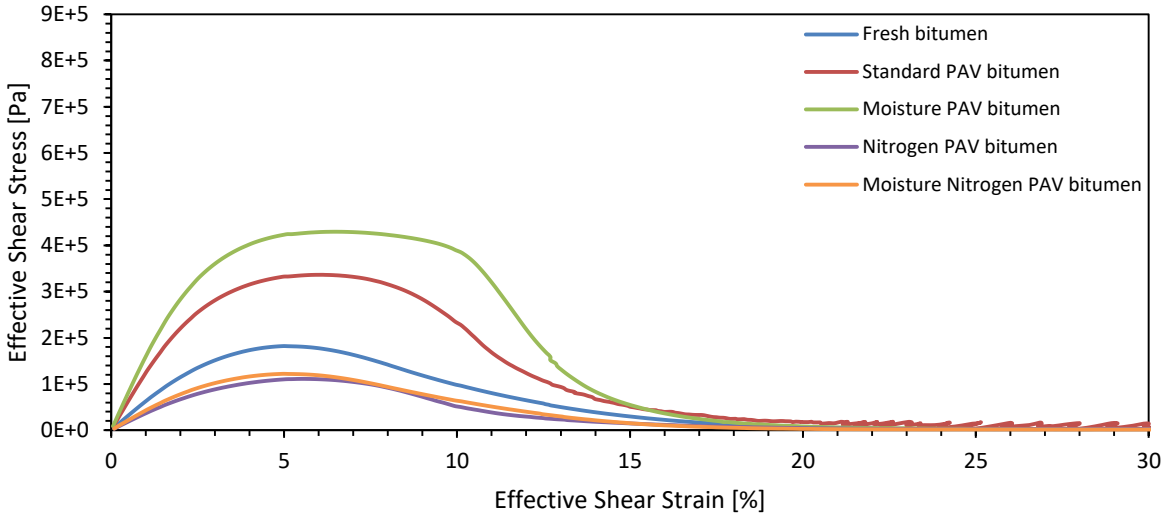

Figure C6.1 - Stress-strain curve of neat bitumen at different conditions under the strain-controlled mode.

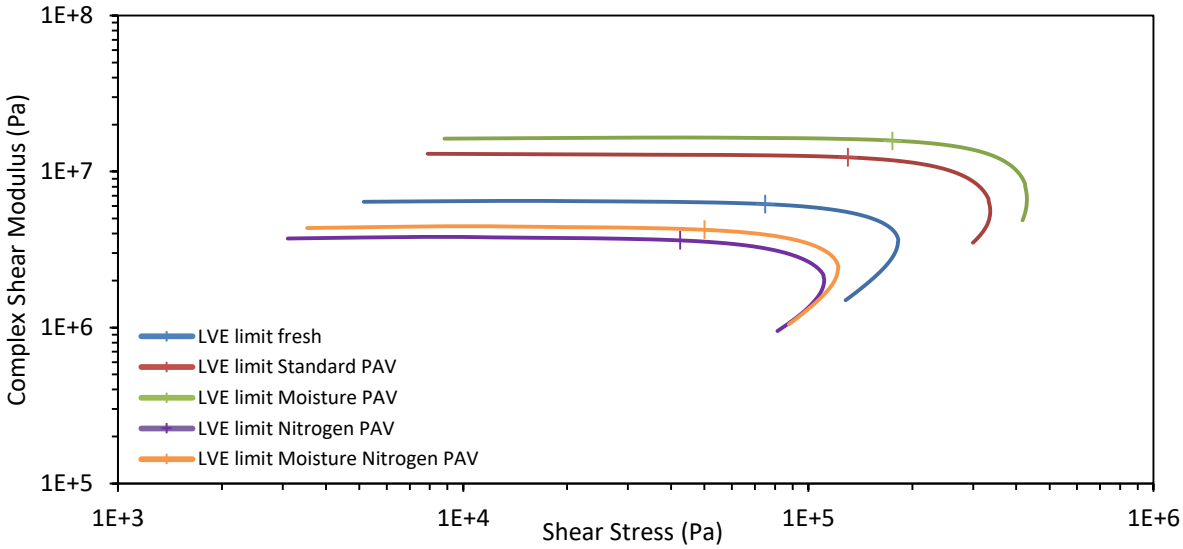

Figure C6.2 - Complex shear modulus of neat bitumen at different conditions condition under the strain-controlled mode.

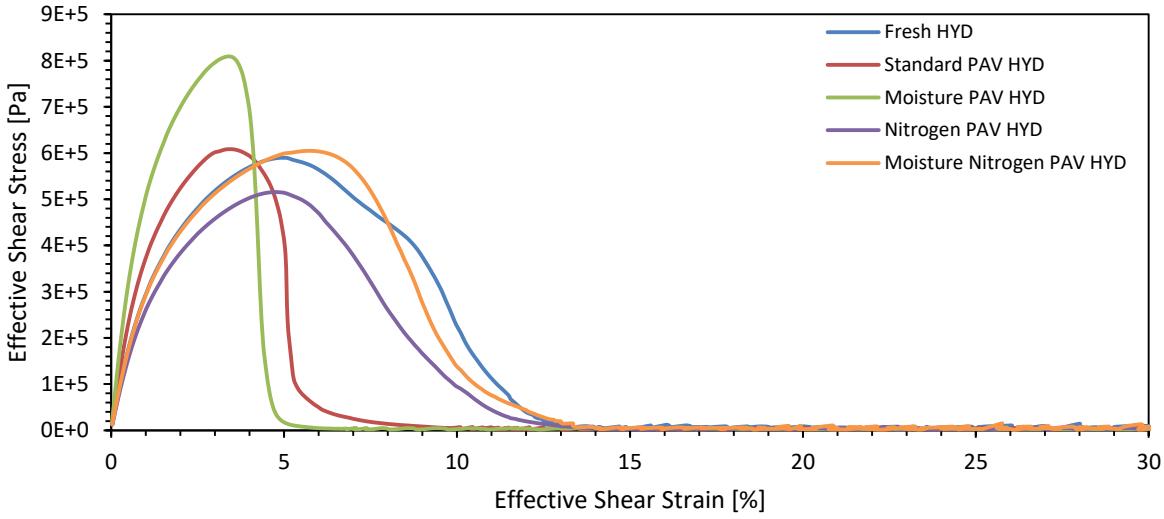

Figure C7.1 - Stress-strain curve of HYD mastic at different conditions under the strain-controlled mode.

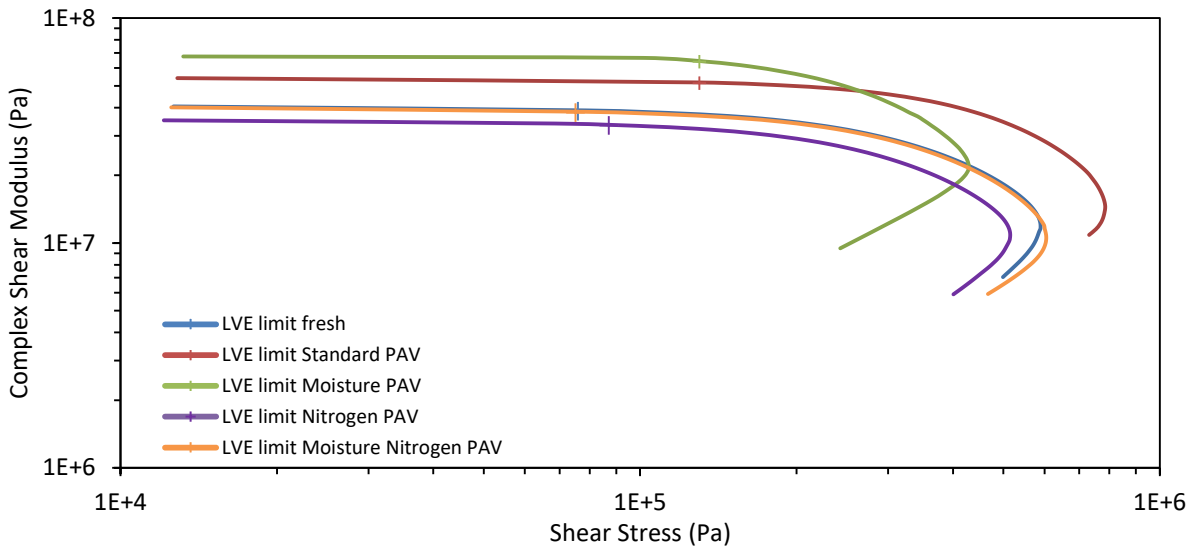

Figure C7.2 - Complex shear modulus of HYD mastic at different conditions condition under the strain-controlled mode.

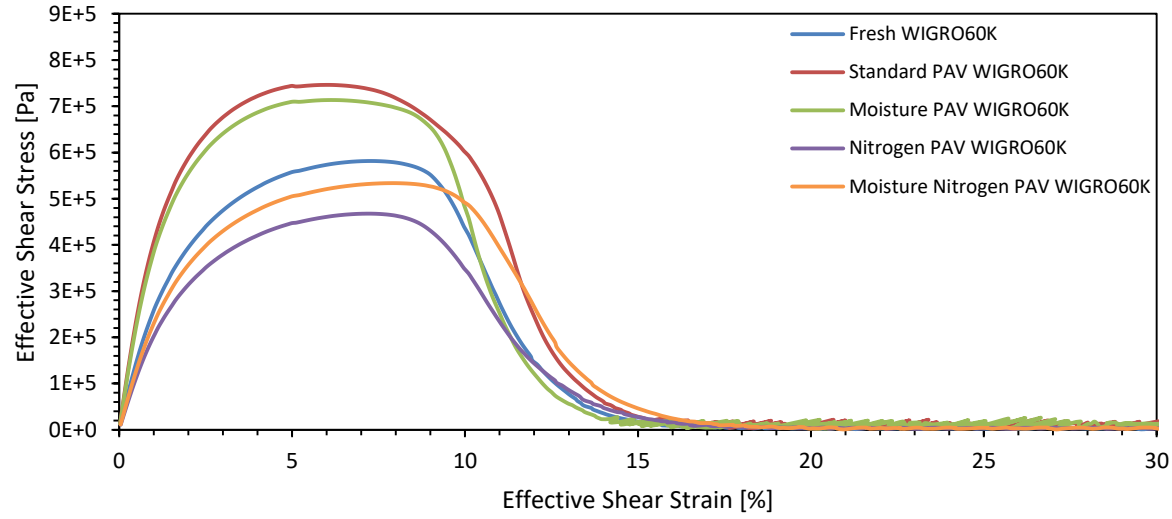

Figure C8.1 - Stress-strain curve of W60K mastic at different conditions under the strain-controlled mode.

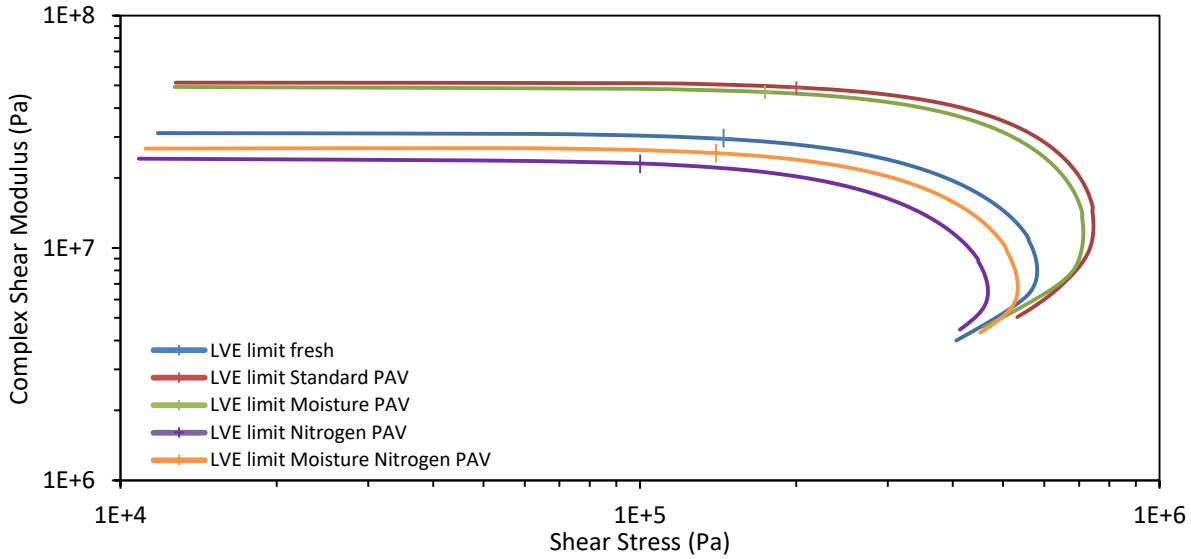

Figure C8.2 - Complex shear modulus of W60K mastic at different conditions condition under the strain-controlled mode.

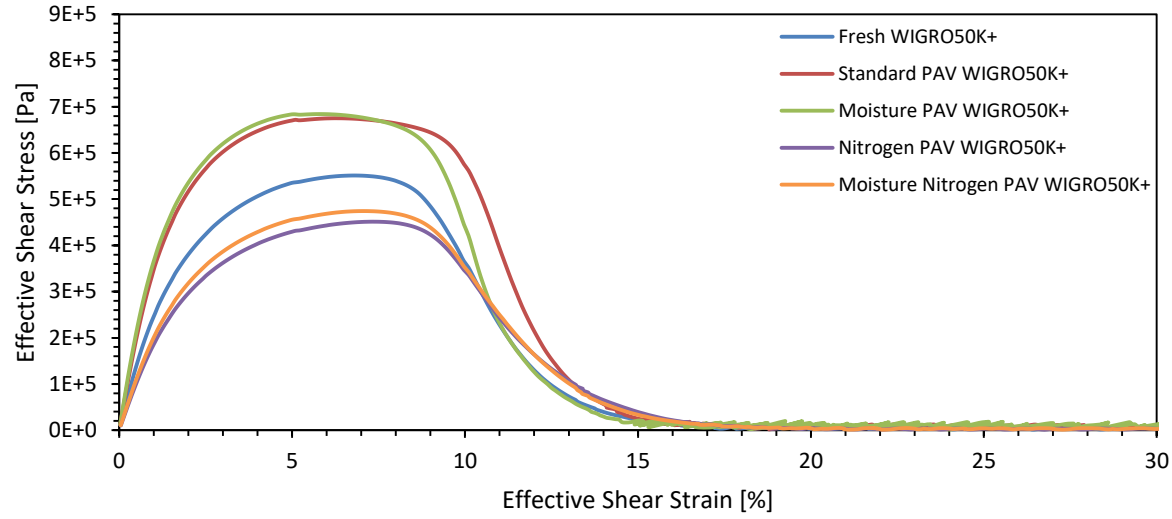

Figure C9.1 - Stress-strain curve of W50K+ mastic at different conditions under the strain-controlled mode.

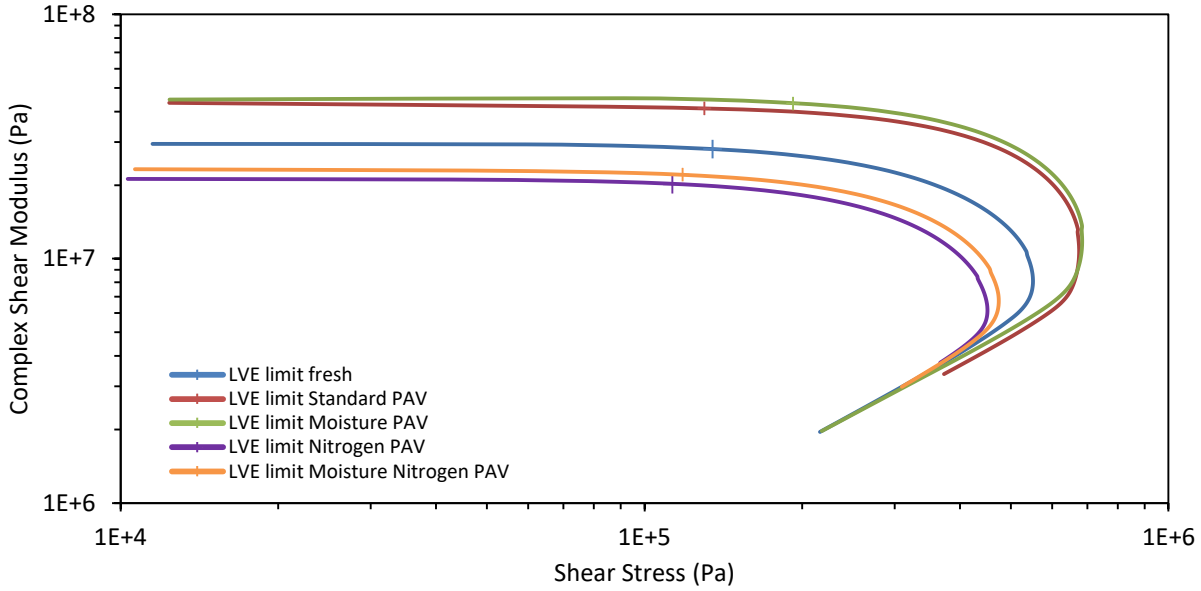

Figure C9.2 - Complex shear modulus of W50K+ mastic at different conditions condition under the strain-controlled mode.

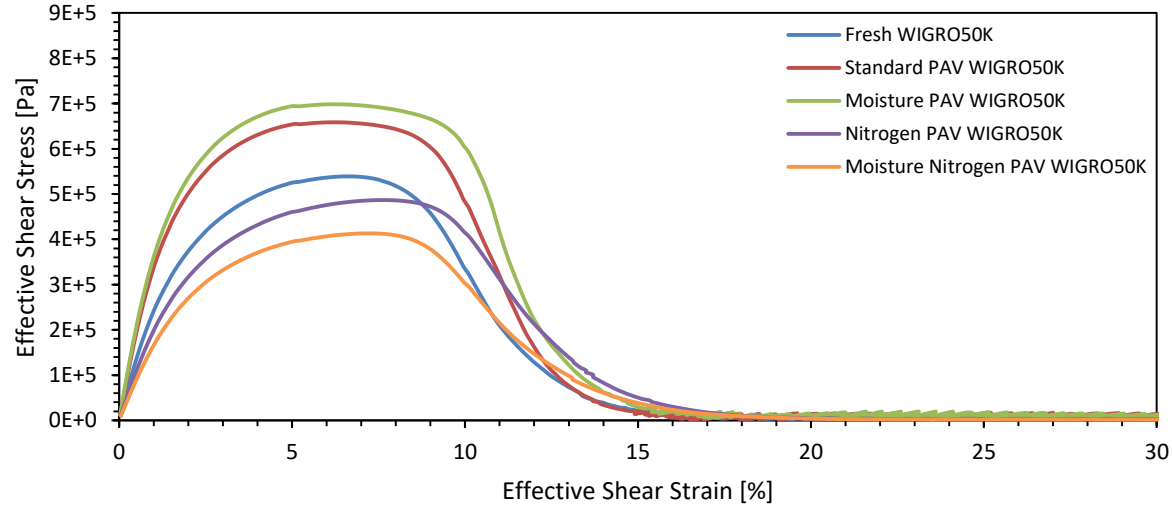

Figure C10.1 - Stress-strain curve of W50K mastic at different conditions under the strain-controlled mode.

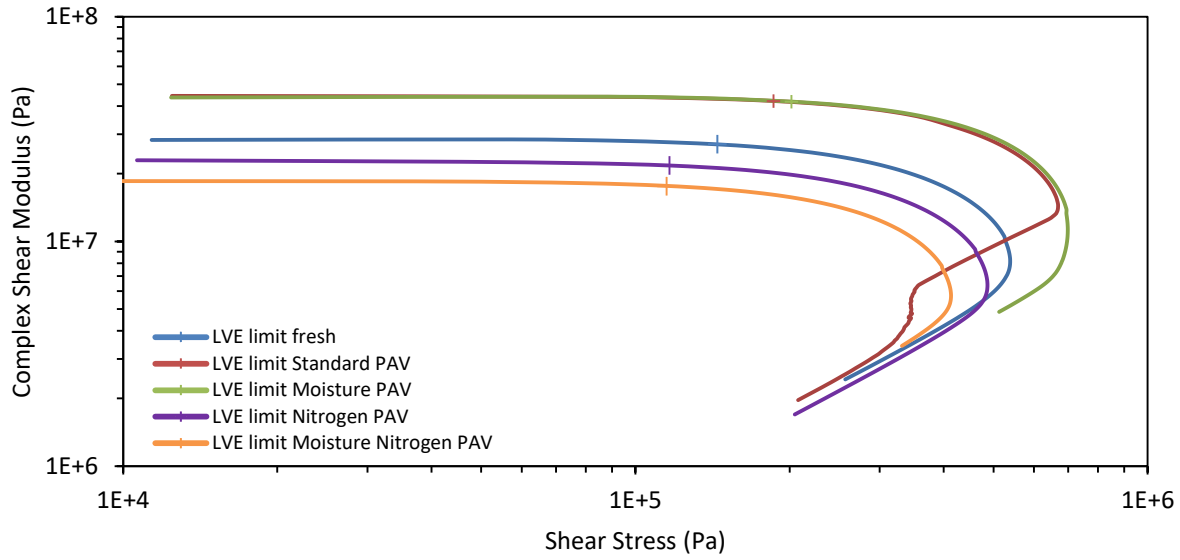

Figure C10.2 - Complex shear modulus of W50K mastic at different conditions condition under the strain-controlled mode.

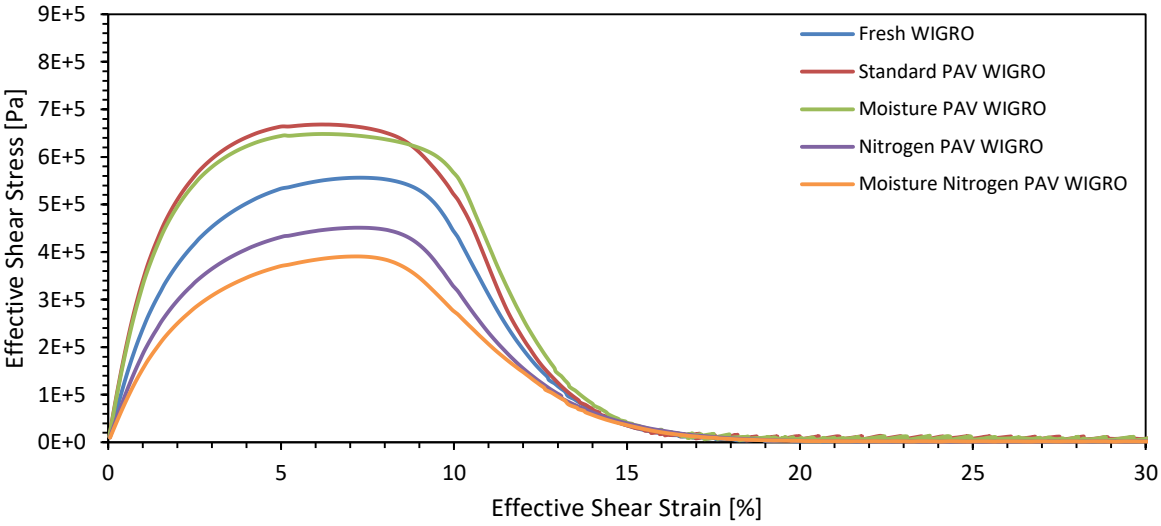

Figure C11.1 - Stress-strain curve of W mastic at different conditions under the strain-controlled mode.

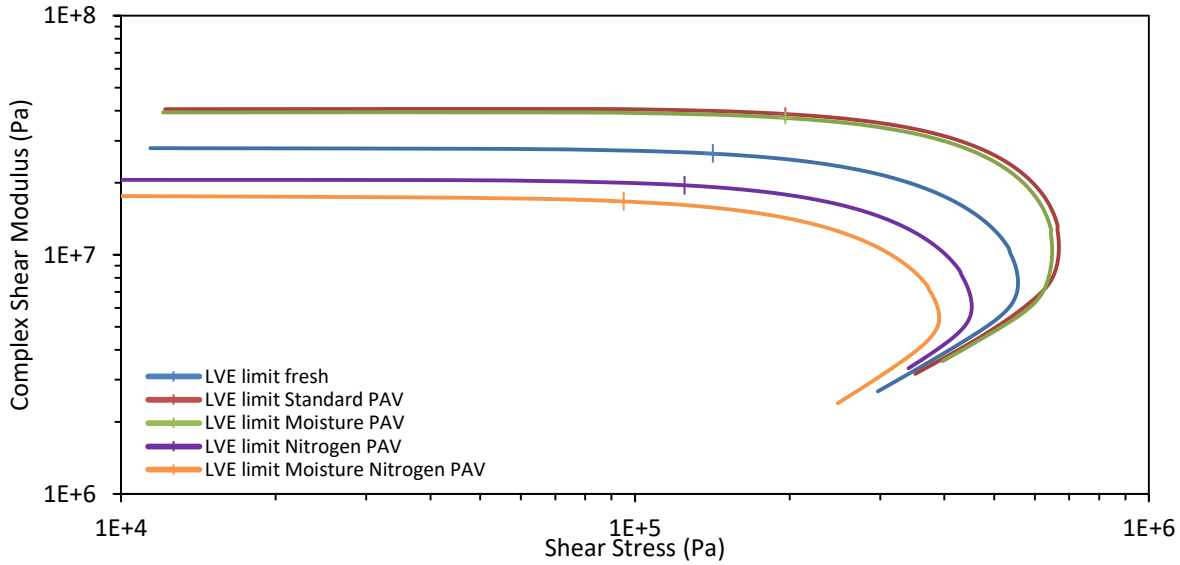

Figure C11.2 - Complex shear modulus of W mastic at different conditions condition under the strain-controlled mode.

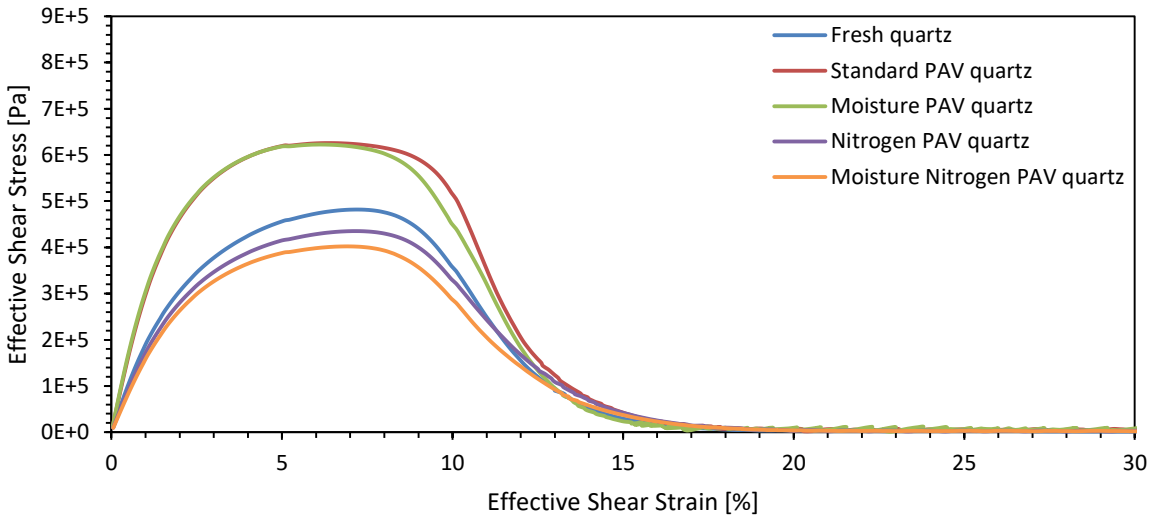

Figure C12.1 - Stress-strain curve of QZ mastic at different conditions under the strain-controlled mode.

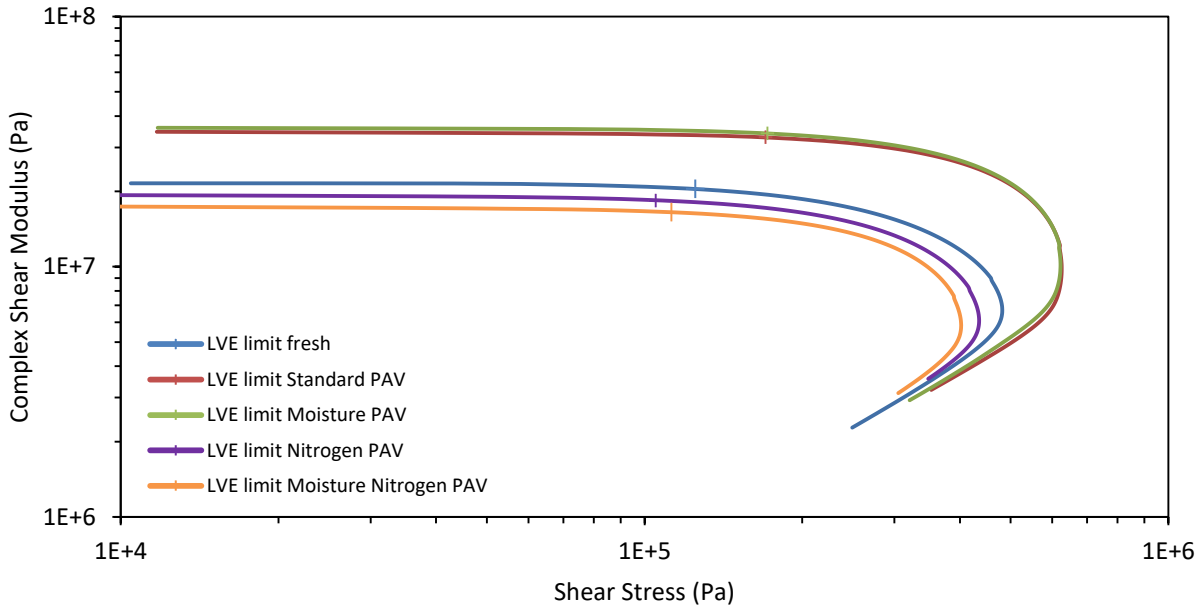

Figure C12.2 - Complex shear modulus of QZ mastic at different conditions condition under the strain-controlled mode.

APPENDIX D – FREQUENCY SWEEP

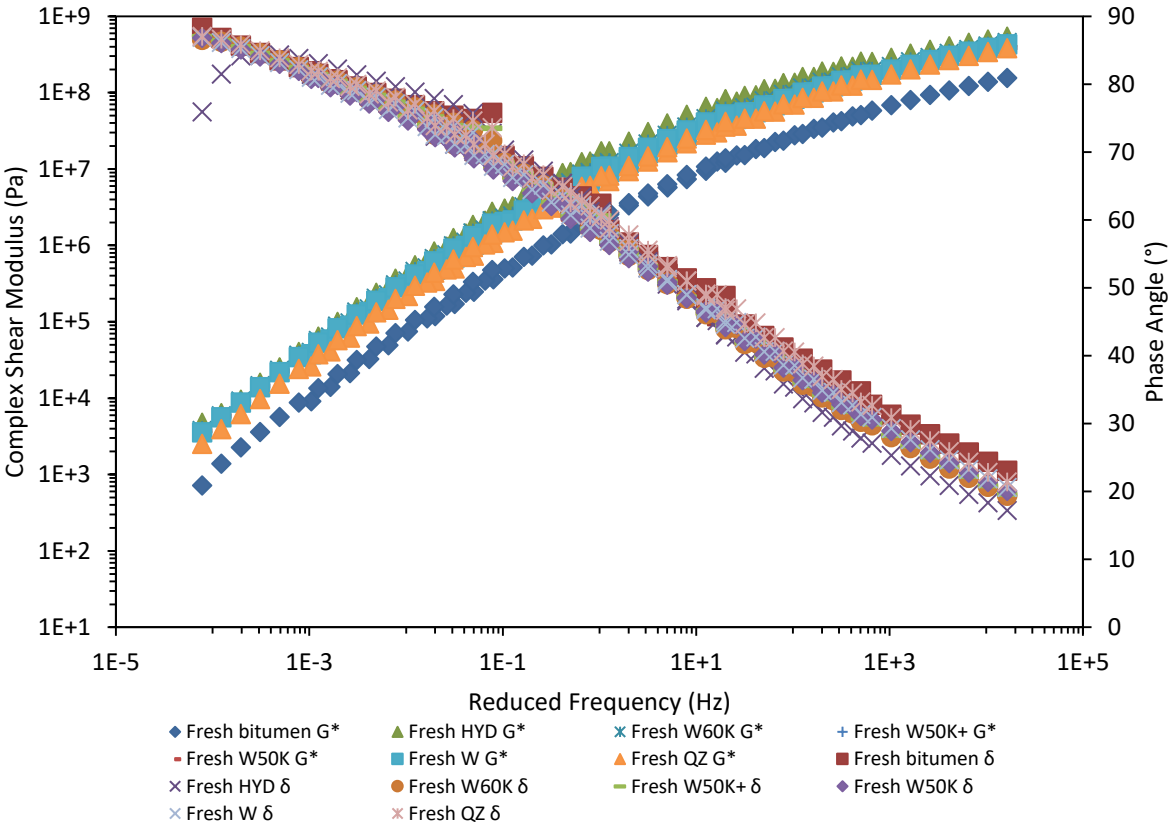

Figure D1 - Master curves comparison of all analysed materials under the fresh condition.

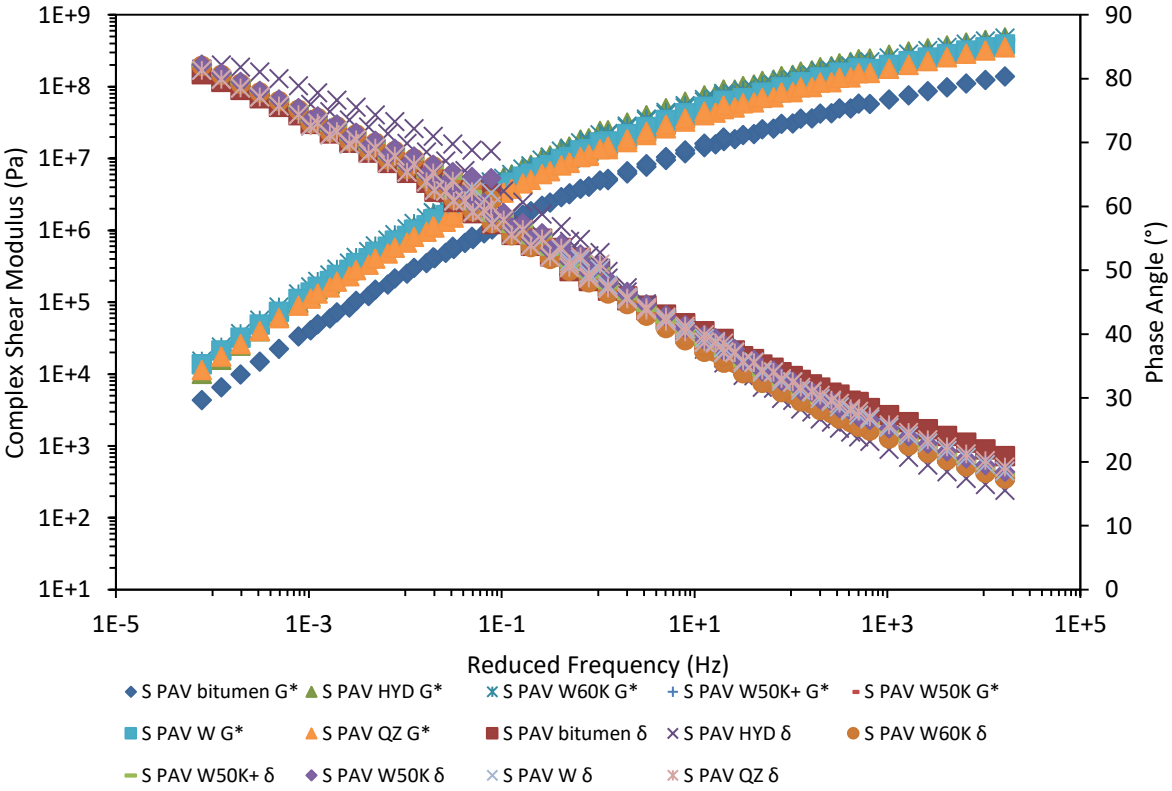

Figure D2 - Master curves comparison of all analysed materials under standard PAV conditioning process.

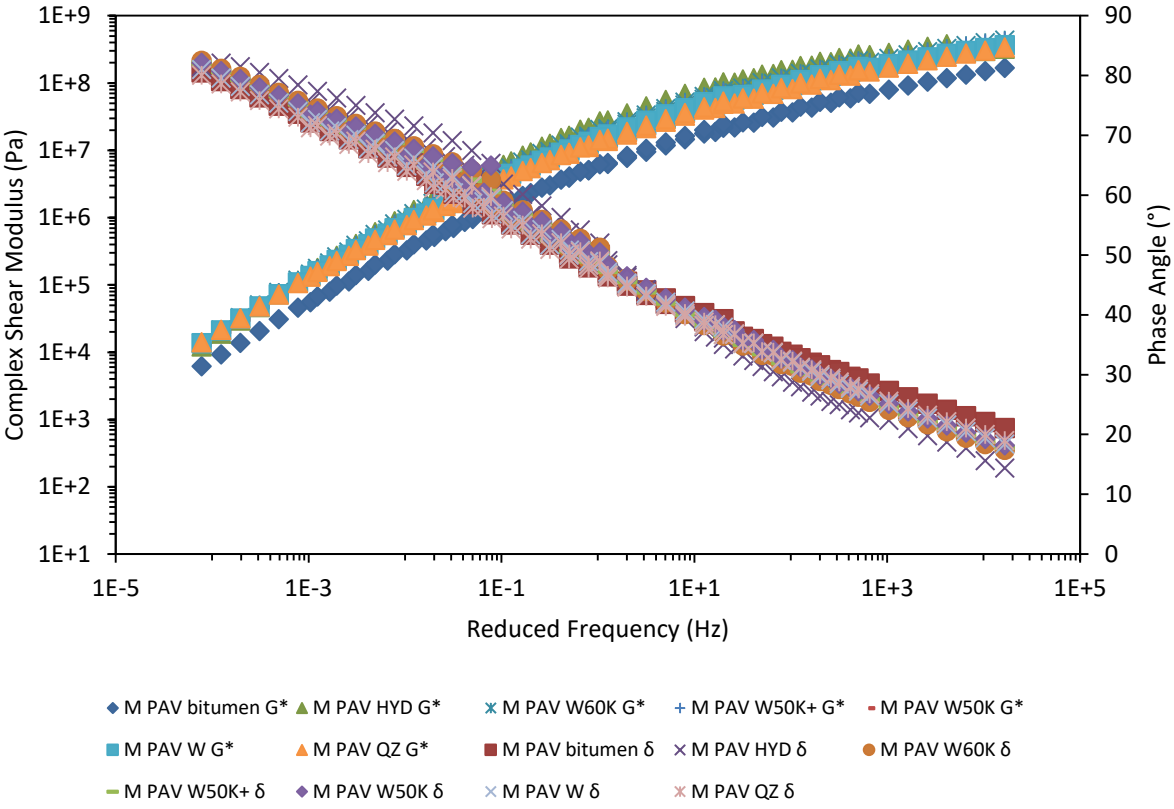

Figure D3 - Master curves comparison of all analysed materials under moisture PAV conditioning process

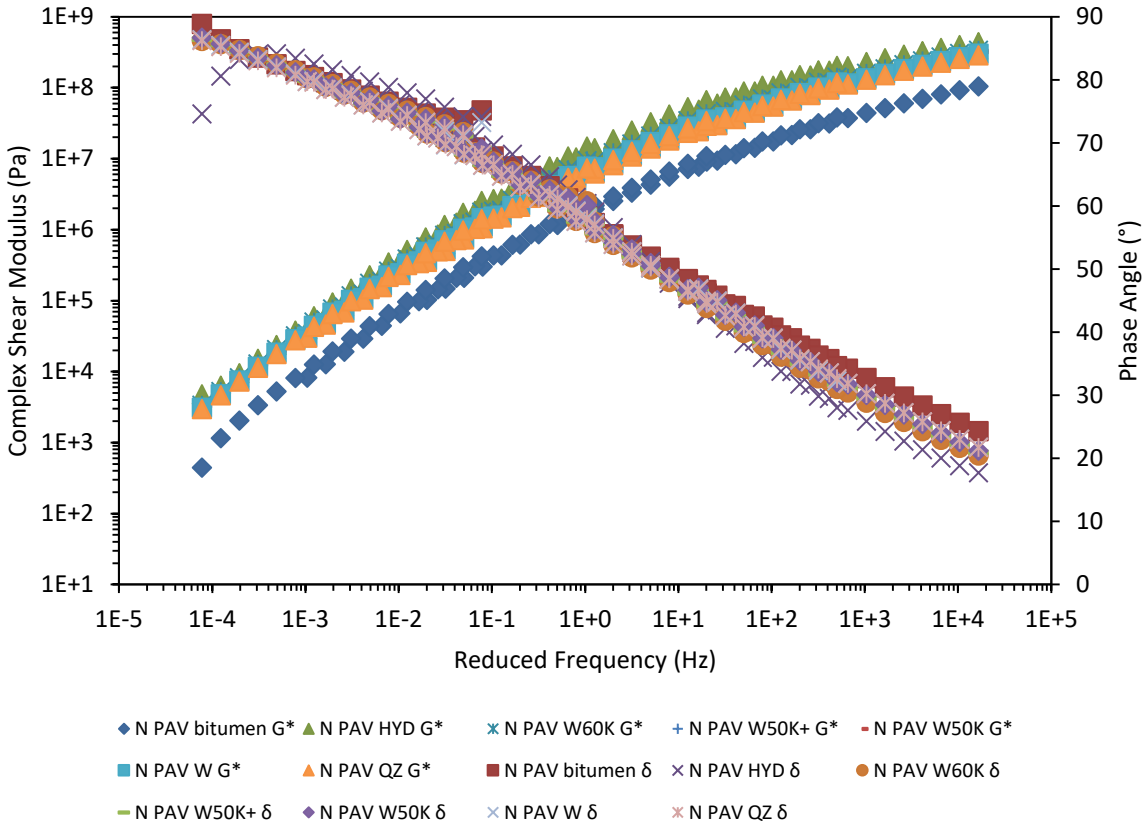

Figure D4 - Master curves comparison of all analysed materials under nitrogen PAV conditioning process.

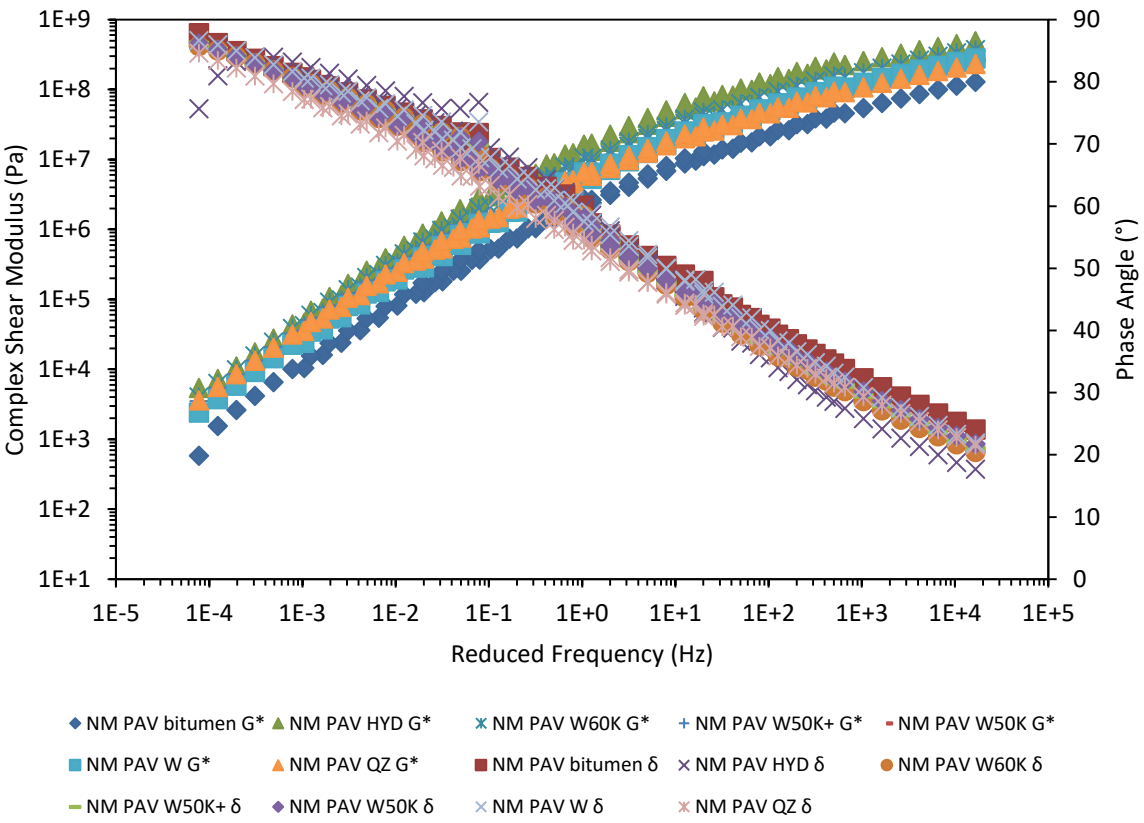

Figure D5 - Master curves comparison of all analysed materials under moisture nitrogen PAV conditioning process

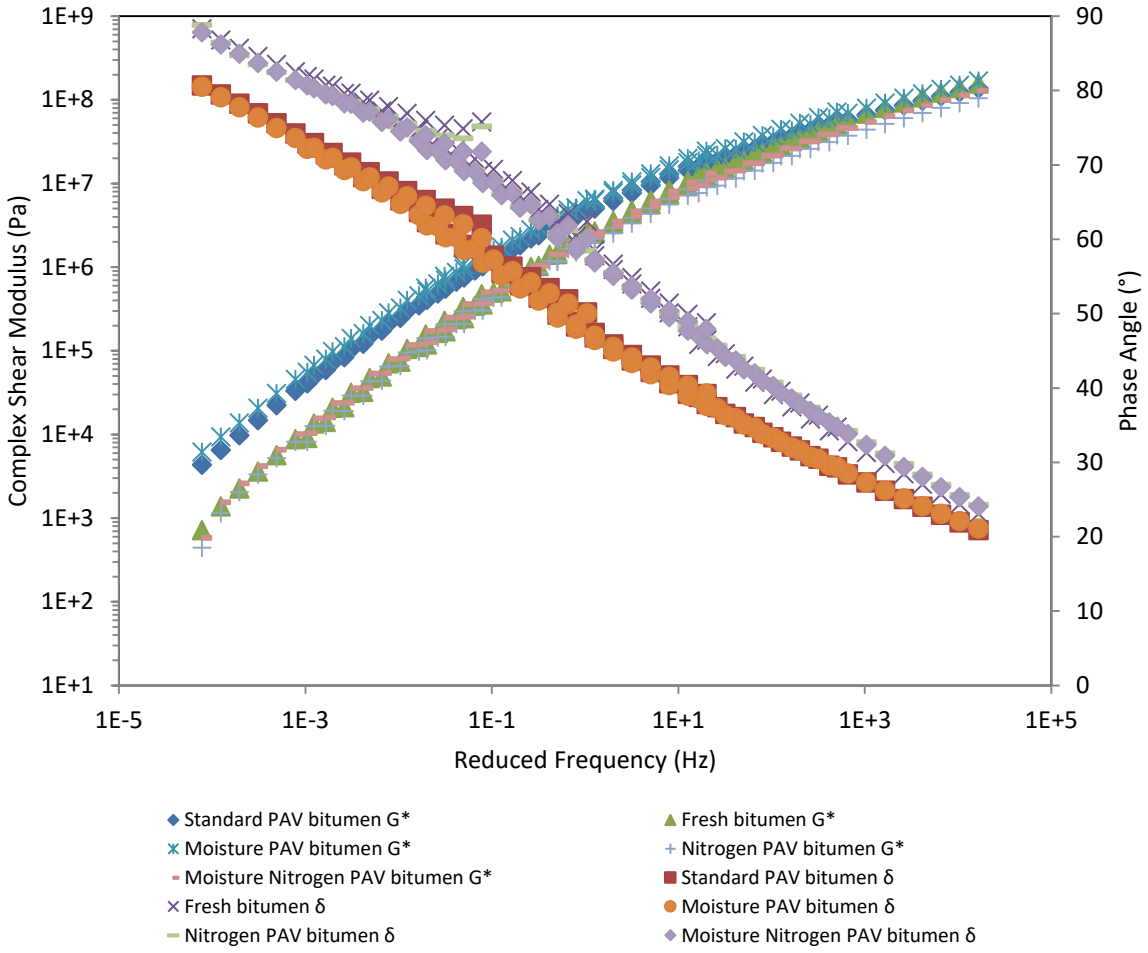

Figure D6.1 – Master curves comparison of neat bitumen under different conditioning processes.

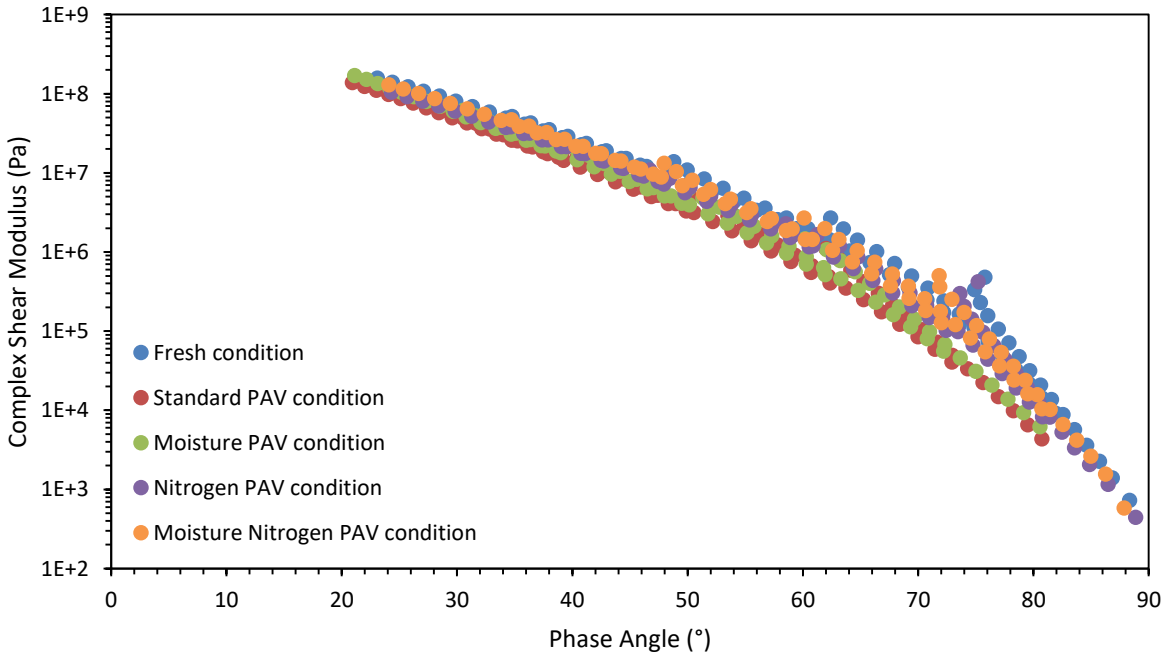

Figure D6.2 – Black diagram comparison of neat bitumen under different conditioning processes.

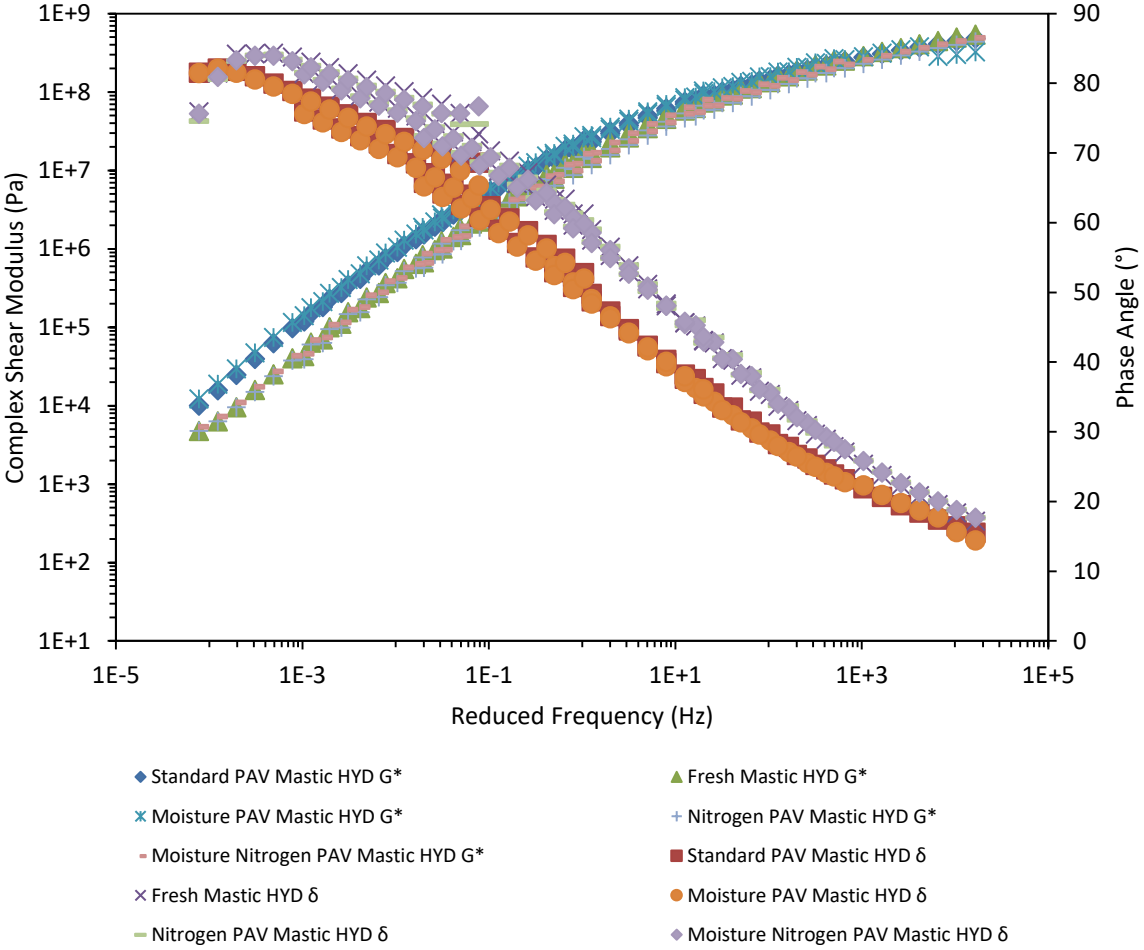

Figure D7.1 – Master curves comparison of HYD mastic under different conditioning processes.

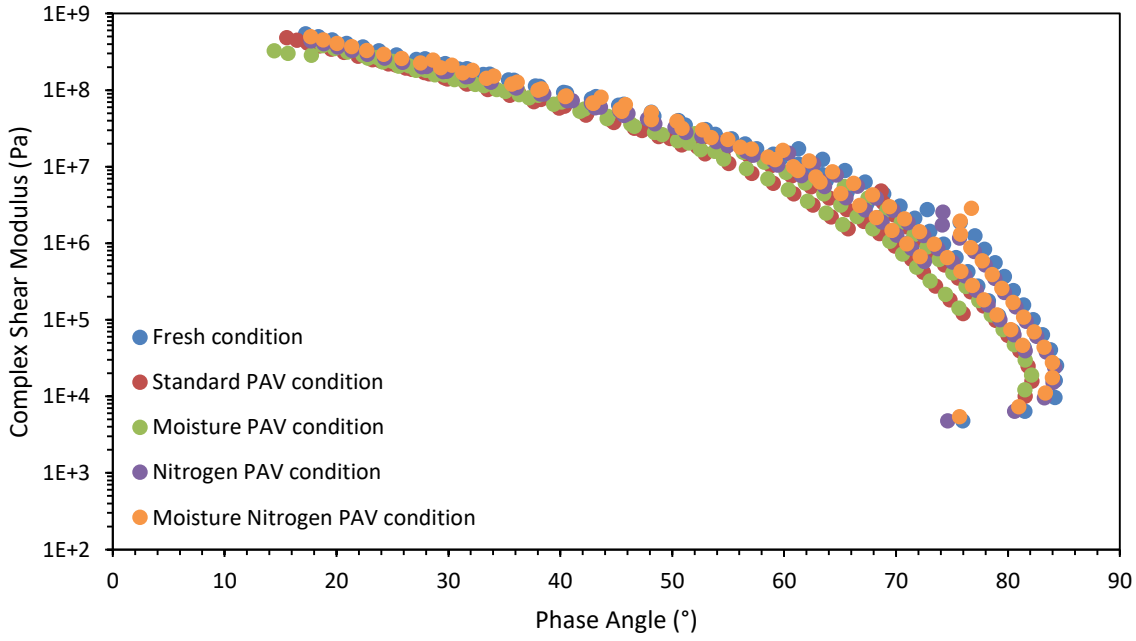

Figure D7.2 – Black diagram comparison of HYD mastic under different conditioning processes.

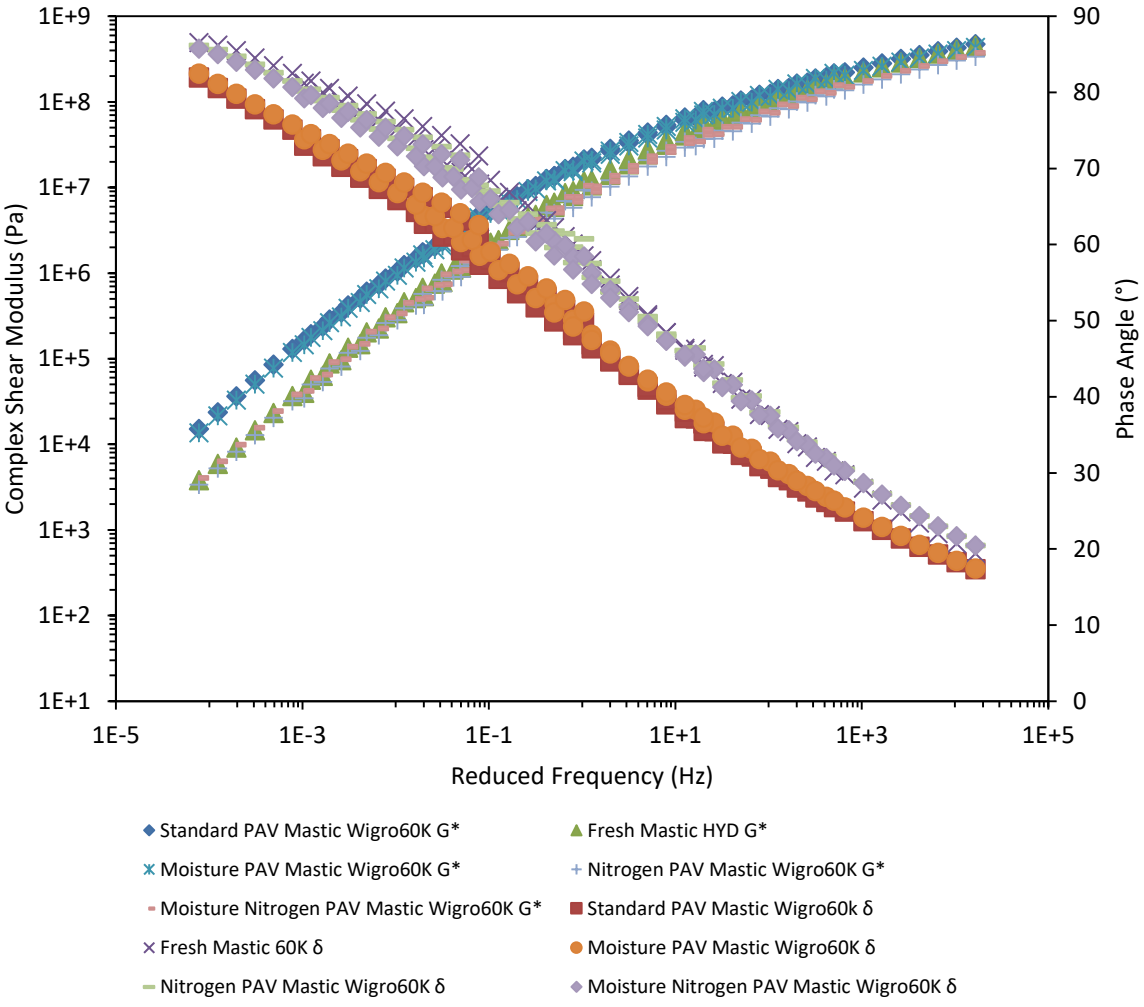

Figure D8.1 – Master curves comparison of W60K mastic under different conditioning processes.

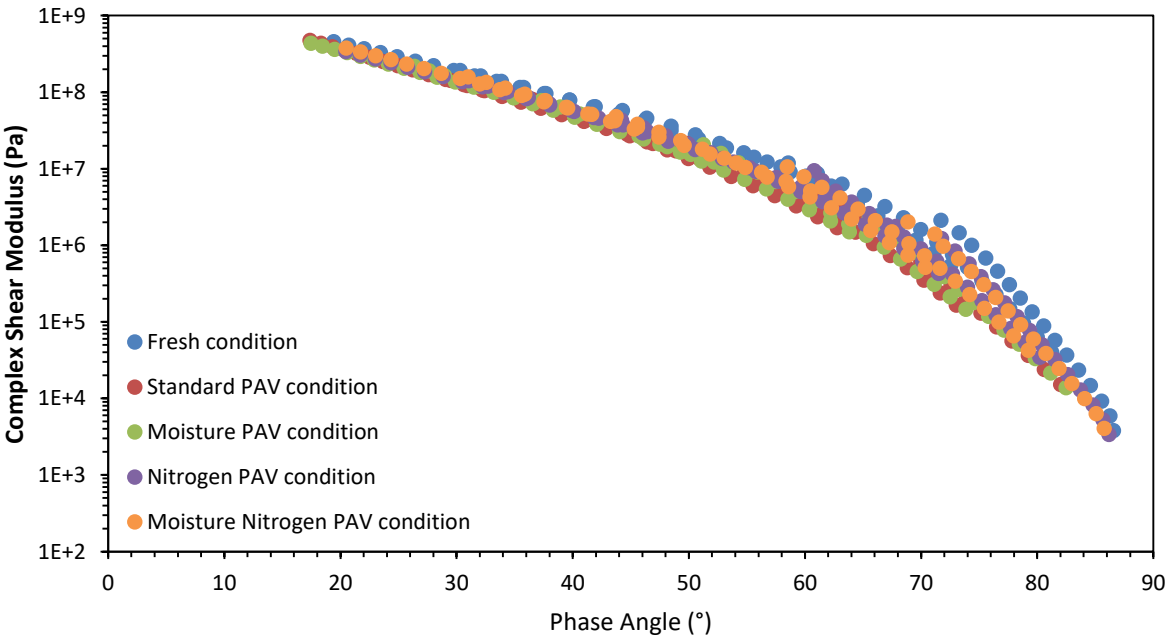

Figure D8.2 – Black diagram comparison of W60K mastic under different conditioning processes.

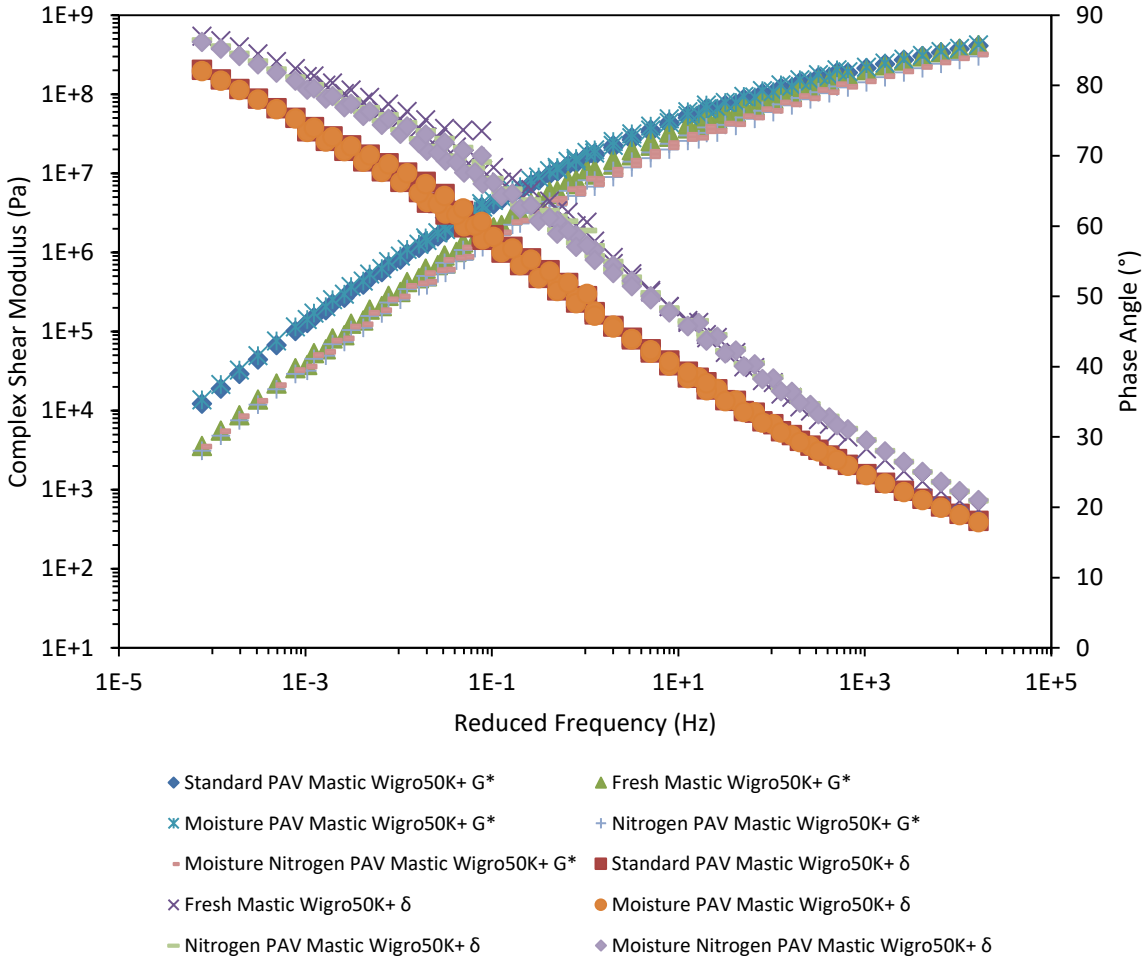

Figure D9.1 – Master curves comparison of W50K+ mastic under different conditioning processes.

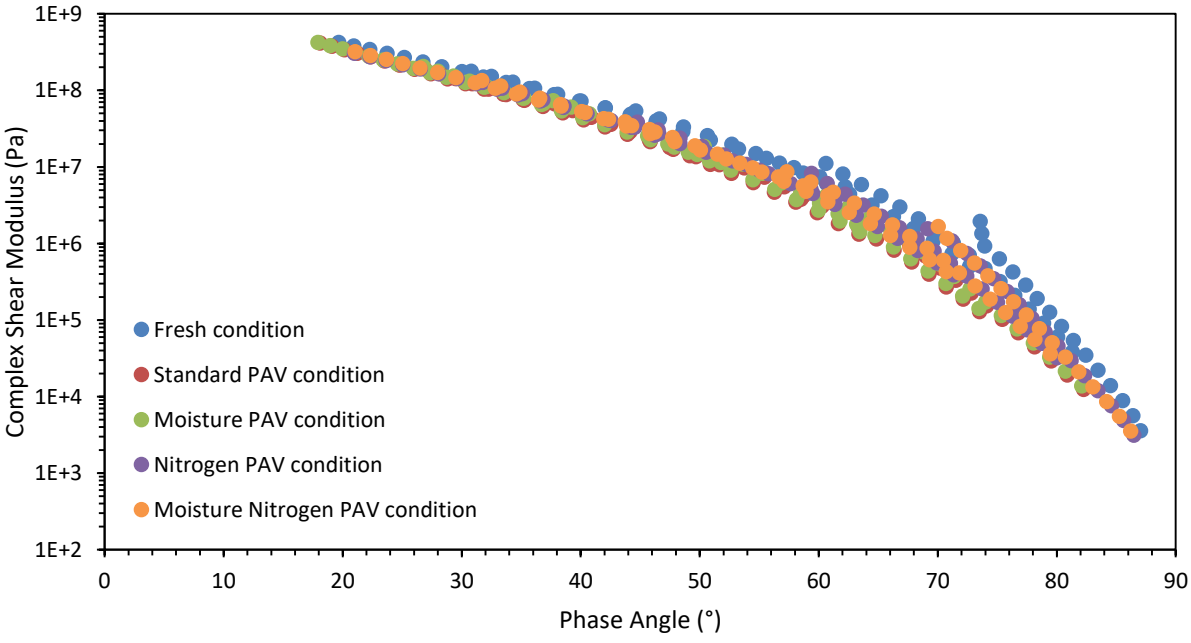

Figure D9.2 – Black diagram comparison of W50K+ mastic under different conditioning processes.

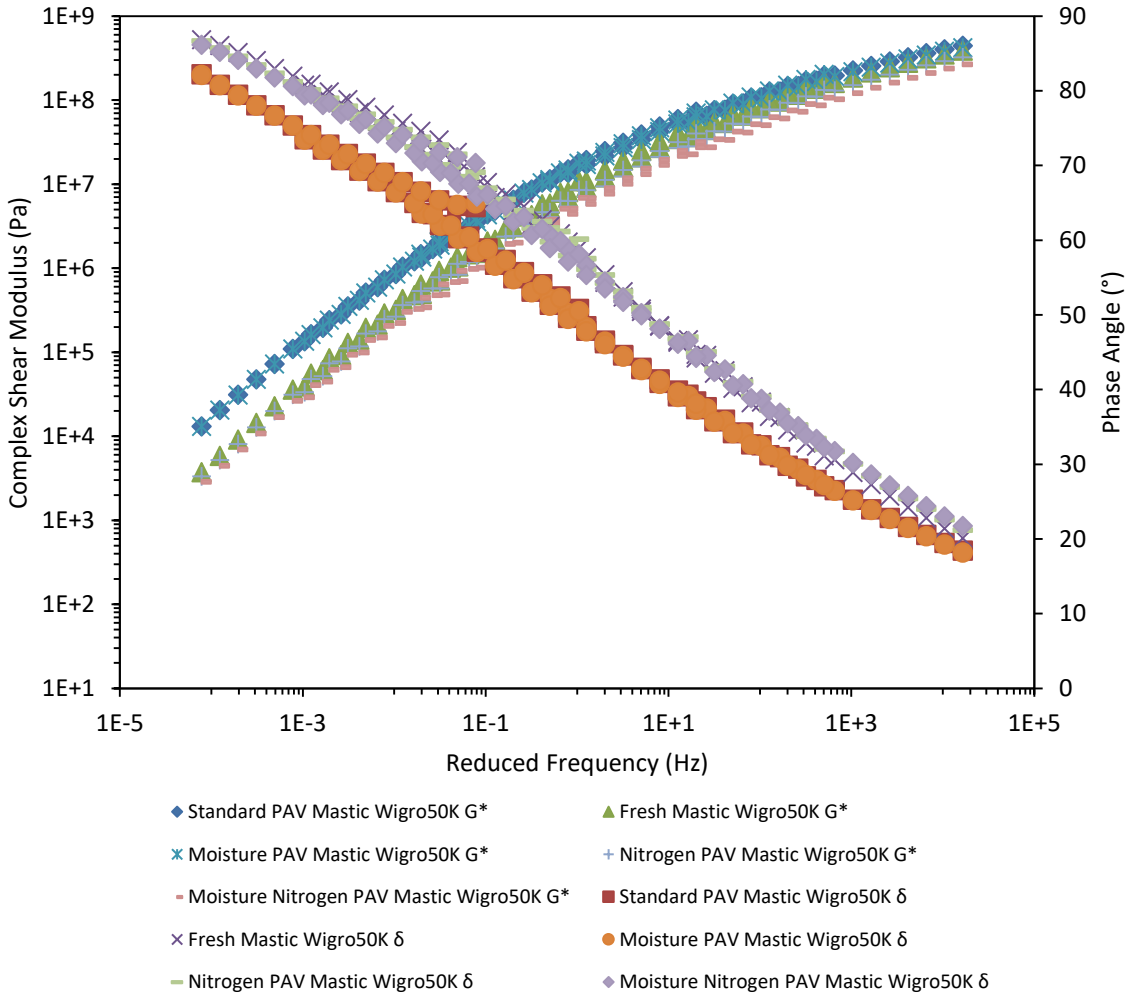

Figure D10.1 – Master curves comparison of W50K mastic under different conditioning processes.

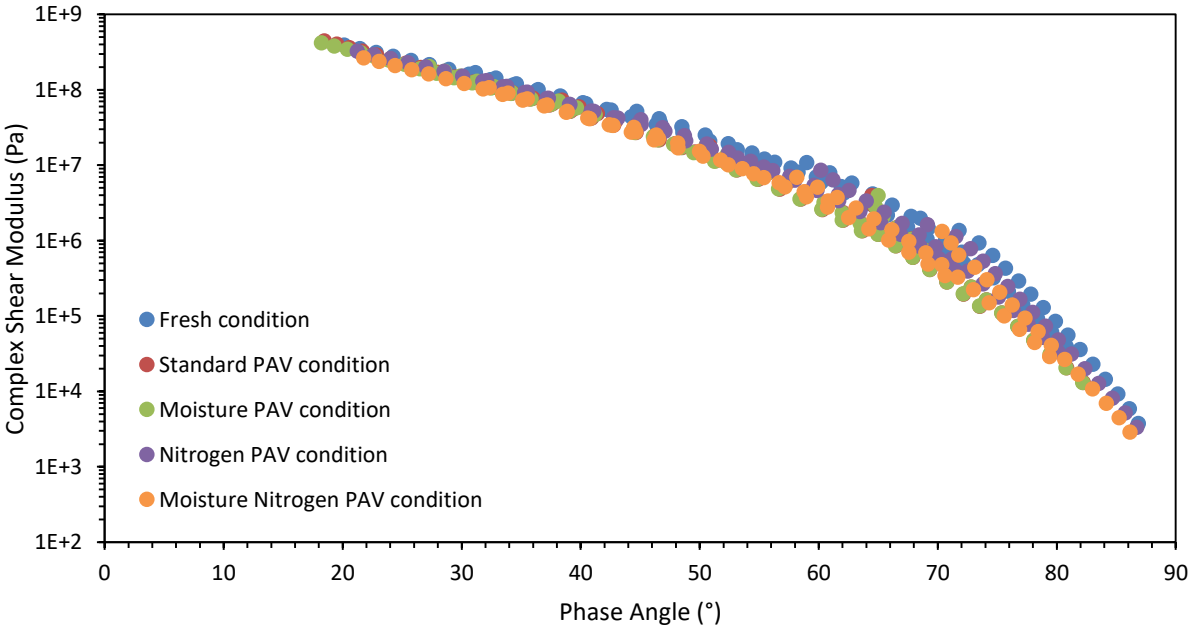

Figure D10.2 – Black diagram comparison of W50K mastic under different conditioning processes.

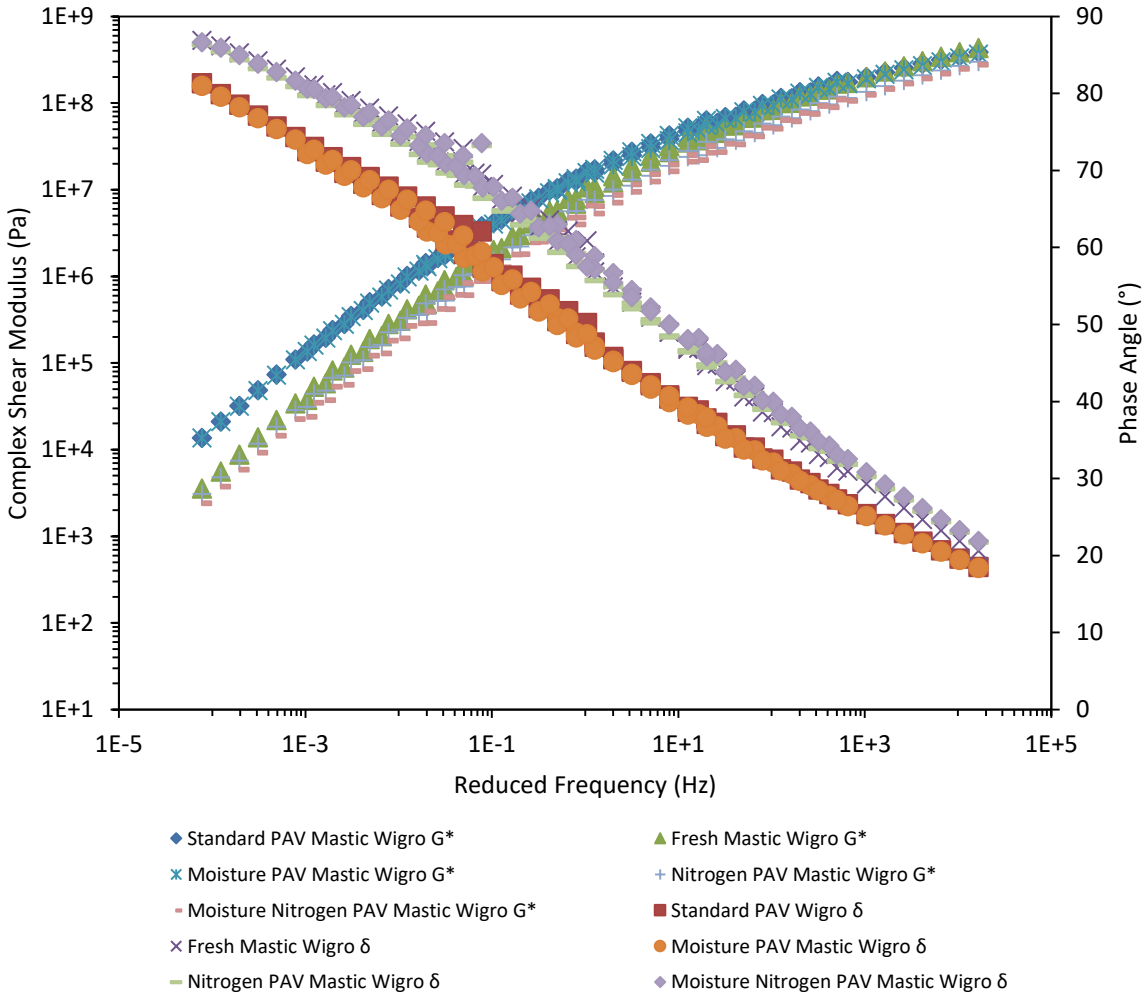

Figure D11.1 – Master curves comparison of W mastic under different conditioning processes.

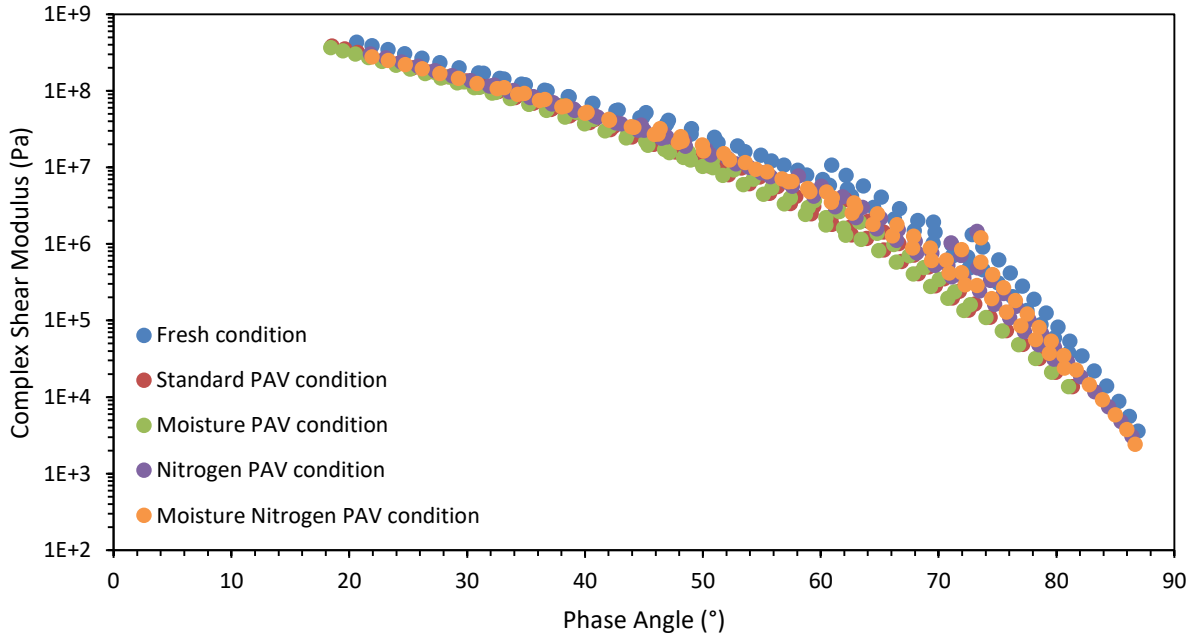

Figure D11.2 – Black diagram comparison of W mastic under different conditioning processes.

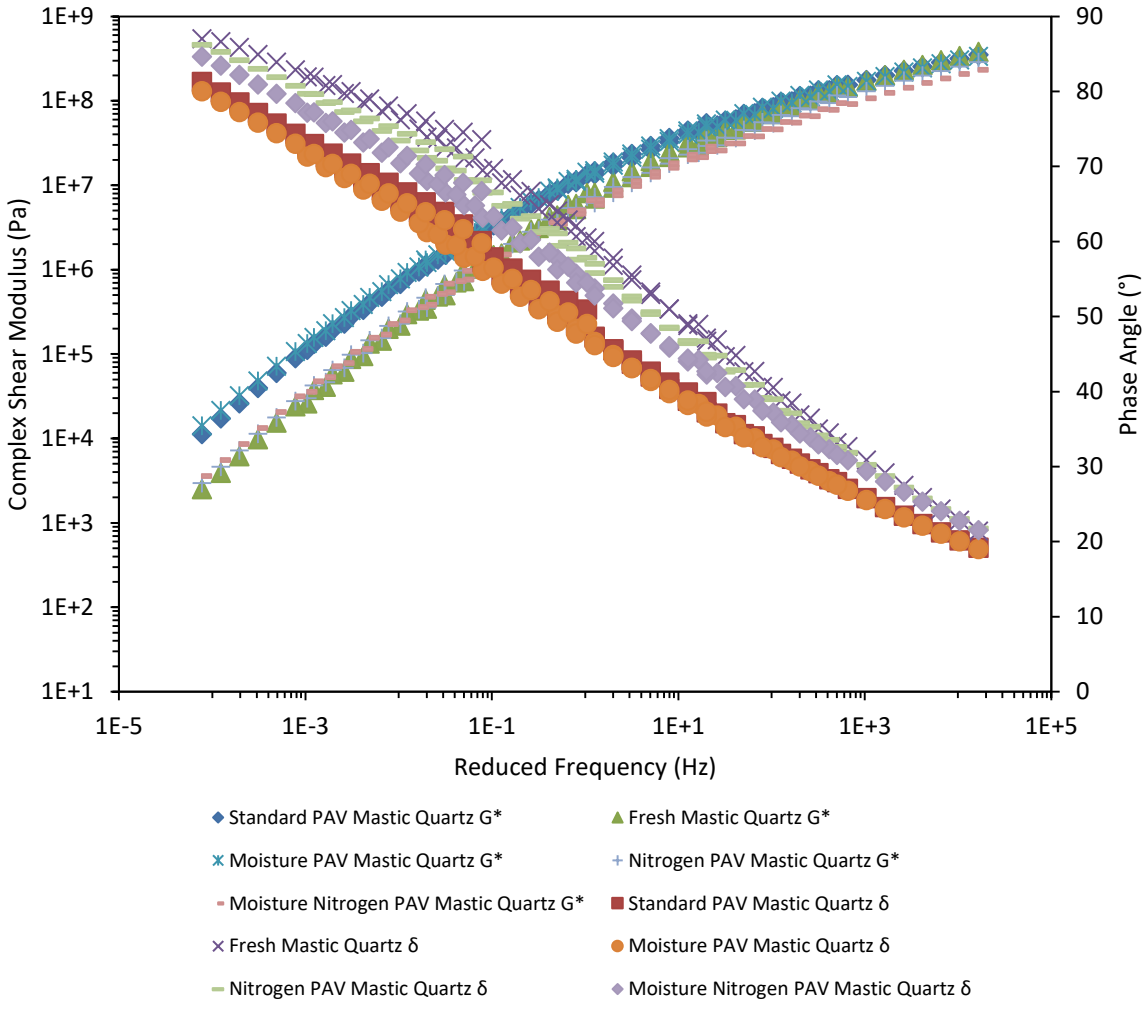

Figure D12.1 – Master curves comparison of QZ mastic under different conditioning processes.

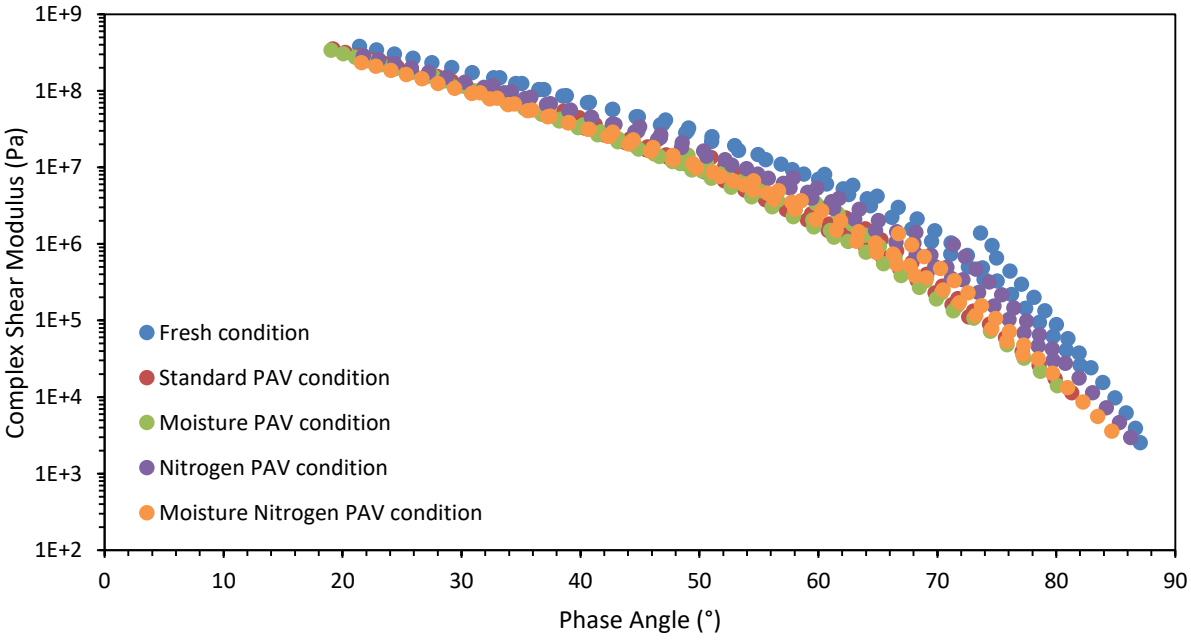

Figure D11.2 – Black diagram comparison of QZ mastic under different conditioning processes.